

# Towards the Development of a Benzylpiperazine Specific Molecular Imprinted Polymer



Kathleen M Wright B.Sc (Hons)

Discipline of Chemistry, The University of Newcastle

Callaghan, NSW 2308, Australia

A thesis submitted for the degree of

*Doctor of Philosophy (Chemistry)*

March, 2010

---

This work contains no material which has been accepted for the award of any other degree or diploma in any university or other tertiary institution and, to the best of my knowledge and belief, contains no material previously published or written by another person, except where due reference has been made in the text. I give consent to this copy of my thesis, when deposited in the University Library, being made available for loan and photocopying subject to the provisions of the Copyright Act 1968.

Signature: ..... Date: .....

To

My Family and Peter

for all your love, support, encouragement and understanding.

## Acknowledgements

Firstly I would like to thank my supervisors Dr. Clovia Holdsworth, Dr Michael Bowyer and Prof. Adam McCluskey for their unlimited wealth of knowledge, guidance, help, and encouragement throughout my PhD. They have helped me develop and hone my research and laboratory skills into what I hope is a better chemist.

I would like to acknowledge financial support from ARC - LP - APAI.

I would like to thank Dave Phelan for his assistance with obtaining SEM images for all my samples I know they were quite troublesome.

A number of other people deserve many thanks for their assistance and input throughout my PhD. The first are the other postgrads, Jenny, Carrie, Kate, Tim, Sunsan and Sorwaporn, that have been in the office over the time. I would like to thank you all for your friendship and helpfulness that you have given me, for keeping the office amusing with the antics that went on and for your support. I would also like to acknowledge Chris Gordon for all his help in organic synthesis matters.

To everyone else in the Chemistry Building who I have had the pleasure of working with and who has helped me over the years, a big thank you for all your assistance and help.

Finally I would like to thank my family, Peter and his family for their love, continued support and encouragement throughout my entire PhD, they were always there when I needed them the most.

# Contents

List of Figures	vii
List of Tables	xii
Abbreviations	xiii
<b>1 Introduction</b>	<b>1</b>
1.1 Benzylpiperazine . . . . .	2
1.2 Molecular Imprinting . . . . .	4
1.2.1 Introduction to Molecular Imprinting . . . . .	4
1.2.2 History of Molecular Imprinting . . . . .	5
1.2.3 The Imprinting Process . . . . .	6
1.2.3.1 Covalent Molecular Imprinting . . . . .	7
1.2.3.2 Non-Covalent Molecular Imprinting . . . . .	10
1.2.4 Optimisation of Molecularly Imprinted Polymers . . . . .	12
1.2.4.1 Optimisation of Template-Functional Monomer Interactions . . . . .	13
1.2.4.2 Optimisation of the Cross-linking Agent . . . . .	17
1.2.4.3 Porogen Selection for Polymerisation . . . . .	19
1.2.4.4 Temperature Effects . . . . .	20
1.2.5 Evaluation of Binding Capabilities . . . . .	20
1.2.5.1 Evaluation by Batch methods . . . . .	21
1.2.5.2 Evaluation by Chromatography . . . . .	25
1.2.6 Characterisation of Polymers . . . . .	26
1.2.6.1 Surface Area and Porosity . . . . .	26

1.2.6.2	Swelling Measurements . . . . .	27
1.2.6.3	Further Characterisation . . . . .	28
1.3	Project Outline . . . . .	29
<b>2</b>	<b>Materials and Methods</b>	<b>31</b>
2.1	Reagents . . . . .	31
2.2	Monomer Synthesis . . . . .	32
2.2.1	Preparation of <i>N,O</i> -bismethacryloyl Ethanolamine (NOBE)	32
2.2.2	Preparation of 7-Hydroxy-4-methylcoumarin Acrylate (HMCA)	33
2.2.3	Preparation of Benzylpiperazine(4-Vinylphenyl) Carbamate (TM adduct) . . . . .	34
2.2.3.1	Step 1: Preparation of 4-Vinylphenol . . . . .	34
2.2.3.2	Step 2: Preparation of 4-Vinylphenyl Chlorothio- formate . . . . .	34
2.2.3.3	Step 3: Preparation of Benzylpiperazine(4-Vinylphenyl) Carbamate . . . . .	35
2.3	Molecular Modelling . . . . .	36
2.4	NMR Spectroscopic Analysis . . . . .	36
2.5	Polymer Synthesis . . . . .	36
2.5.1	Non-covalent MIPs . . . . .	36
2.5.2	Covalent MIPs . . . . .	37
2.6	Batch Binding Experiments . . . . .	37
2.7	Selectivity and Cross-reactivity Studies . . . . .	38
2.8	Characterisation . . . . .	39
2.8.1	Swelling Measurements . . . . .	39
2.8.2	Scanning Electron Microscopy (SEM) . . . . .	39
2.8.3	Porosity and Surface Area . . . . .	39
<b>3</b>	<b>Pre-synthesis: Template-Monomer Interaction Studies</b>	<b>40</b>
3.1	Introduction . . . . .	40
3.2	Results and Discussion . . . . .	43
3.2.1	Computer Generated Molecular Modelling Data . . . . .	43
3.2.1.1	Selection of Monomers . . . . .	43
3.2.2	NMR Analysis . . . . .	51

3.2.2.1	Template-Functional Monomer Investigations . . .	51
3.2.2.2	Optimisation of the Cross-linker . . . . .	59
3.3	Conclusions . . . . .	63
<b>4</b>	<b>Preparation of Benzylpiperazine MIPs: The Self-assembly (non-covalent) Approach</b>	<b>64</b>
4.1	Introduction . . . . .	64
4.2	Results and Discussion . . . . .	66
4.2.1	Selection of Cross-linker . . . . .	66
4.2.2	Preparation of BZP Imprinted Polymers: Physical Characterisation . . . . .	69
4.2.3	Polymer Absorption of BZP: Evaluation of Imprinting Effect	73
4.2.4	Determination of Optimal Time of Contact . . . . .	85
4.2.5	Saturation Curve and Analysis . . . . .	89
4.3	Conclusion . . . . .	97
<b>5</b>	<b>Preparation of Benzylpiperazine MIPs: The Semi-covalent Approach</b>	<b>99</b>
5.1	Introduction . . . . .	99
5.2	Results and Discussion . . . . .	101
5.2.1	Synthesis of Benzylpiperazine (4-vinylphenyl) carbamate and Semi-covalent MIPs . . . . .	101
5.2.2	Preparation of Semi-covalent MIPs . . . . .	102
5.2.3	Physical Characterisation of the MIPs . . . . .	103
5.2.4	Polymer Absorption of BZP: Evaluation of Imprinting Effect	104
5.2.5	Determination of Optimal Time of Contact . . . . .	107
5.2.6	Saturation Curve and Analysis . . . . .	110
5.3	Conclusion . . . . .	116
<b>6</b>	<b>Semi-Covalent versus Non-covalent BZP MIPs: A Comparative Assessment</b>	<b>118</b>
6.1	Introduction . . . . .	118
6.2	Polymer Synthesis . . . . .	120
6.3	Binding Affinity . . . . .	121

---

6.4	Physical Characterisation . . . . .	124
6.5	Binding Dynamics . . . . .	125
6.6	Conclusion . . . . .	131
<b>7</b>	<b>Cross-Reactivity and Selectivity Studies</b>	<b>132</b>
7.1	Introduction . . . . .	132
7.2	Results and Discussion . . . . .	134
7.2.1	Cross-reactivity Studies . . . . .	134
7.2.1.1	Non-Covalent Imprinted Polymers . . . . .	134
7.2.1.2	Covalent Imprinted Polymers . . . . .	143
7.2.2	Selectivity Studies . . . . .	147
7.2.2.1	Non-Covalent Polymers . . . . .	147
7.2.2.2	Covalent Polymers . . . . .	153
7.3	Conclusions . . . . .	158
<b>8</b>	<b>Summary and Recommendations</b>	<b>162</b>
8.1	Summary of Results . . . . .	162
8.2	The Next Step . . . . .	165
	<b>References</b>	<b>167</b>

# List of Figures

1.1	Structure of benzylpiperazine ( <b>1</b> ) and its related analogues . . . . .	3
1.2	Schematic of the imprinting process . . . . .	7
1.3	Reversible covalent imprinting using the boronate ester . . . . .	8
1.4	Covalent imprinting with ketals . . . . .	9
1.5	Covalent imprinting with Schiff's base . . . . .	9
1.6	Template monomer of cholesteryl(4-vinyl)phenyl carbonate . . . . .	10
1.7	Templates and template monomers using the carbonyl sacrificial spacer technique: . . . . .	11
1.8	Proposed mechanism of template-functional monomer interaction	12
1.9	Chemical structure of common cross-linkers . . . . .	19
1.10	Appearance of MIP binding isotherm . . . . .	23
1.11	Binding isotherm ( <b>A</b> ) and corresponding Scatchard plot ( <b>B</b> ) . . . . .	25
1.12	Langmuir plot for a Neu5AC-MIPs. . . . .	25
2.1	Synthesis of <i>N,O</i> -bismethacryloyl ethanolamine (NOBE). . . . .	33
2.2	Synthesis of 7-hydroxy-4-methylcoumarin acrylate (HMCA). . . . .	33
2.3	Synthesis of 4-vinylphenol from 4-acetoxystyrene. . . . .	34
2.4	Synthesis of 4-vinylphenyl chlorothioformate. . . . .	35
2.5	Synthesis of Benzylpiperazine(4-vinylphenyl)carbamate. . . . .	35
3.1	Chemical structure of BZP . . . . .	41
3.2	A library of potential functional monomers . . . . .	44
3.3	Computer generated molecular modelling images of BZP:MAA 1:1 ( <b>A</b> ), 1:2 ( <b>B</b> ) and 1:3 ( <b>C</b> ) . . . . .	46

## LIST OF FIGURES

---

3.4	Computer generated molecular modelling images of BZP:AA 1:1 (A), 1:2 (B) and 1:3 (C) . . . . .	48
3.5	Computer generated molecular modelling images of BZP:HEM 1:1 (A) and 1:4 (B) . . . . .	49
3.6	Computer generated molecular modelling image of BZP:IA 1:1 (A) and 1:2 (B) . . . . .	49
3.7	Computer generated molecular modelling images of BZP with 4-vinyl pyridine (4-VP) (A) and styrene (STY) (B) . . . . .	50
3.8	Molecular modelling images of BZP:HMCA . . . . .	51
3.9	NMR analysis of BZP with MAA . . . . .	53
3.10	NMR analysis of BZP with IA . . . . .	55
3.11	NMR analysis of BZP with AA . . . . .	56
3.12	NMR analysis of BZP with HMCA . . . . .	57
3.13	NMR titration of BZP with NOBE . . . . .	58
3.14	NMR titration of BZP with NOBE, MAA and EGDMA . . . . .	59
3.15	NMR titration of BZP with EGDMA, TRIM, DVB and MAA . . . . .	60
3.16	Computer generated molecular modelling image for BZP:EGDMA . . . . .	60
3.17	Computer generated molecular modelling image for BZP:TRIM . . . . .	61
3.18	Computer generated molecular modelling image for BZP:DVB . . . . .	62
4.1	BZP binding results for EGDMA, TRIM and DVB polymers . . . . .	67
4.2	SEM images for NC-MAA-EGDMA-2A . . . . .	70
4.3	SEM images for the polymers prepared for the three functional monomers . . . . .	71
4.4	SEM images for two different ratios . . . . .	71
4.5	SEM images for NC-MAA-2A MIPs . . . . .	72
4.6	SEM images for NC-MAA-EGDMA-2 MIPs . . . . .	72
4.7	Swelling results . . . . .	74
4.8	BZP binding results for BZP:AA polymer formulations prepared in AN . . . . .	75
4.9	BZP binding results for BZP:MAA polymer formulations prepared in AN . . . . .	76

## LIST OF FIGURES

---

4.10	BZP binding results for BZP:IA polymer formulations prepared in AN . . . . .	77
4.11	BZP binding results for BZP:AA polymer formulations prepared in CHCl <sub>3</sub> . . . . .	78
4.12	BZP binding results for BZP:MAA polymer formulations prepared in CHCl <sub>3</sub> . . . . .	79
4.13	Imprinting factors calculated from the rebinding studies for MAA prepared polymers: . . . . .	82
4.14	Imprinting factors calculated from the rebinding studies for IA prepared polymers: . . . . .	83
4.15	Imprinting factors calculated from the rebinding studies for the AA prepared polymers: . . . . .	84
4.16	Rebinding results for BZP:MAA formulations . . . . .	86
4.17	Time rebinding results for BZP:MAA 1:1 (A) and 1:2 (B) CHCl <sub>3</sub> EGDMA . . . . .	87
4.18	Time rebinding results for BZP:MAA 1:1 (A) and 1:2 (B) CHCl <sub>3</sub> TRIM . . . . .	88
4.19	Binding isotherm data . . . . .	90
4.20	Scatchard plots . . . . .	93
4.21	Langmuir linear plots . . . . .	95
5.1	Chemical structure of BZP TM adduct with proposed sacrificial spacer and functional monomer. . . . .	101
5.2	Synthetic scheme for the preparation of TM adduct . . . . .	102
5.3	Proposed mechanism of BZP rebinding . . . . .	103
5.4	SEM images for the covalent EGDMA polymers prepared in CHCl <sub>3</sub> . . . . .	104
5.5	SEM images for the covalent TRIM polymers prepared in CHCl <sub>3</sub> . . . . .	105
5.6	Swelling results for the EGDMA and TRIM covalent polymers . . . . .	105
5.7	Rebinding results for semi-covalent BZP polymers prepared with EGDMA and TRIM in CHCl <sub>3</sub> . . . . .	106
5.8	Time rebinding results for covalent BZP polymers . . . . .	108
5.9	Rebinding results for covalent BZP polymer prepared with TRIM in water . . . . .	110

## LIST OF FIGURES

---

5.10	Binding isotherm data . . . . .	111
5.11	Scatchard plots produced for the semi-covalent polyers . . . . .	113
5.12	Langmuir regression plots produced for the semi-covalent polyers .	114
6.1	BZP binding capacities and imprinting factors for 30 mg of the 1:1 BZP:MAA NC MIPs and the SC MIPs . . . . .	122
6.2	SEM images . . . . .	124
6.3	Swelling results for non-covalent and semi-covalent BZP imprinted polymers . . . . .	126
6.4	Binding isotherm for NC EGDMA and NC TRIM ( <b>A</b> ) and SC EGDMA and SC TRIM ( <b>B</b> ) . . . . .	128
6.5	Langmuir regression plot for NC EGDMA and NC TRIM ( <b>A</b> ) and SC EGDMA and SC TRIM ( <b>B</b> ) . . . . .	129
6.6	Scatchard regression plot for NC EGDMA and NC TRIM ( <b>A</b> ) and SC EGDMA and SC TRIM ( <b>B</b> ) . . . . .	130
7.1	Chemical structures of three common drugs of abuse, . . . . .	133
7.2	Cross-reactivity studies of NC EGDMA1 . . . . .	135
7.3	Cross-reactivity studies of NC EGDMA2 . . . . .	136
7.4	Cross-reactivity studies of NC TRIM1 . . . . .	137
7.5	Cross-reactivity studies of NC TRIM2 . . . . .	138
7.6	Molecular modelling images of BZP ( <b>A</b> ) and PHP ( <b>B</b> ) . . . . .	140
7.7	Molecular modelling image of PHP with 1 MAA unit. . . . .	140
7.8	Molecular modelling images of BZP ( <b>A</b> ) and MO ( <b>B</b> ) . . . . .	141
7.9	Molecular modelling image of MO with 1 MAA unit. . . . .	141
7.10	Molecular modelling images of BZP ( <b>A</b> ) and CO ( <b>B</b> ) . . . . .	142
7.11	Molecular modelling image of CO with 1 MAA unit . . . . .	143
7.12	Molecular modelling images of BZP ( <b>A</b> ) and EPH ( <b>B</b> ) . . . . .	144
7.13	Molecular modelling image of EPH with 1 MAA unit . . . . .	144
7.14	Cross-reactivity studies of the EGDMA prepared semi-covalent im- printed polymers . . . . .	145
7.15	Non-competitive cross reactive study of TRIM prepared covalent imprinted polymers . . . . .	146
7.16	Molecular modelling image of 1 phenol unit with the analytes . .	148

## LIST OF FIGURES

---

7.17	Molecular modelling image of 1 phenol unit with the analytes . . .	149
7.18	Selectivity studies of NC EGDMA1 . . . . .	151
7.19	Selectivity studies of NC EGDMA2 . . . . .	152
7.20	Selectivity studies of NC TRIM1 . . . . .	154
7.21	Selectivity studies of NC TRIM2 . . . . .	155
7.22	Competitive studies of BZP semi-covalent imprinted polymers with BZP and morphine. . . . .	156
7.23	Competitive study of BZP semi-covalent imprinted polymers with BZP and cocaine. . . . .	157
7.24	Competitive study of BZP semi-covalent imprinted polymers with BZP and ephedrine. . . . .	158

# List of Tables

3.1	Calculated $\Delta E$ values for the template-monomer clusters from molecular modelling studies. All calculations were performed in triplicate.	45
4.1	Binding constants ( $K_d$ and number of binding sites ( $n$ )) extracted from the binding isotherm, Scatchard plot and Langmuir plot for the BZP:MAA 1:1 and 1:2, EGDMA and TRIM polymers prepared in $\text{CHCl}_3$ .	91
4.2	Summary of absorption and time rebinding results for BZP:MAA non-covalent imprinted polymers	98
5.1	Binding constants, $K_d$ and number of binding sites ( $n$ ), extracted from the binding isotherm, Scatchard plot and Langmuir plot for the semi-covalent EGDMA and TRIM polymers prepared in $\text{CHCl}_3$ .	112
6.1	Binding constants ( $K_d$ and number of binding sites ( $n$ )) extracted from the binding isotherm for NC EGDMA, NC TRIM, SC EGDMA and SC TRIM	127
7.1	Selectivity factors calculated from the $\Delta B$ values for the cross-reactivity study with the NC and SC polymers	160
7.2	Selectivity factors calculated from the $\Delta B$ values for the selectivity study with the NC and SC polymers	160

# Abbreviations

$^{13}\text{C}$ NMR	Carbon NMR
$^1\text{H}$ NMR	Proton NMR
4VP	4-vinyl pyridine
6-MAM	6-monoacetylmorphine
AA	Acrylic acid
AAm	Acrylamide
AFM	Atomic force microscopy
AIBN	2,2' Azob(isisobutyronitrile)
AN	Acetonitrile
ATS	Amphetamine type substances
BET	Brunauer Emmett and Teller
BJH	Barret, Joyner and Halenda
BZP	Benzylpiperazine
$\text{CHCl}_3$	Chloroform
CNS	Central nervous system
CO	Cocaine
DEA	Drug Enforcement Administration
DMSO	Dimehtyl sulfoxide
DSC	Differenttial scanning couliometry
DVB	Divinyl benzene
EGDMA	Ethylene glycol dimethacrylate
EPH	Ephedrine
EtOAc	Ethyl acetate
FM	Functional monmer

---

FT-IR	Furier transform-infrared
GC-MS	Gas chromatography - mass spectrometry
H <sub>3</sub> PO <sub>4</sub>	Phosphoic acid
HCl	Hydrochloric acid
HEM	2-Hydroxyethyl methacrylate
HMCA	7-Hydroxy-4-methylcoumarin acrylate
HPLC	High presure liquid chromatography
IA	Itaconic acid
KCl	Potassium chloride
KH <sub>2</sub> PO <sub>4</sub>	Dihydrogen phosphate
KOH	Potassium hydroxide
LOD	Level of detection
LSD	Lysergic acid diethylamide
MAA	Mathacrylic acid
MAAm	Methacrylamide
mCPP	1-(3-Chlorophenyl)piperazine
MDA	3,4-Methylenedioxyamphetamine
MDBP	1-(3,4-Methylenedioxyphenyl)piperazine
MDMA	3,4-Methylenedioxy-N-methylamphetamine
MDMA	3,4-Methylenedioxymethamphetamine
MIP	Molecular imprinted polymer
MISPE	Molecular imprinted solid phase extraction
MO	Morphine
mTFMPP	1-(3-Trifluoromethylphenyl)piperazine
NaHCO <sub>3</sub>	Sodium carbonate
NaOH	Sodium hydroxide
NC	Non-covalent
NDPSC	National Drugs and Poisons Scheduling Committee
NIP	Non-imprinted polymers
NMR	Nuclear magnetic resonance
NOBE	N,O-bis-methacryloyl ethanolamine
OMNiMIP	One monomer molecularly imprinted polymer
PETA	Pentaerythritol triacrylate
PHP	Phenylpiperazine
pMeOPP	1-(4-Methoxyphenyl)piperazine
SC	Semi-covalent

---

SEM	Scanning electron microscopy
SNS	Sympathic nervous system
STY	Styrene
SUSDP	Standard for the Uniform of Scheduling of Drugs and Poisons
T	Template
T:FM	Template:functional monomer ratio
TEGDMA	Tetraethylene glycol dimethacrylate
TGA	Therapeutic Goods Administration
TGA	Thermal gravitational analysis
TRIM	Trimethylolpropane trimethacrylate
UV-Vis	Ultra violet - visable spectroscopy
VOC	Volatile organic compound
XL	Cross-linker

## Abstract

Molecular imprinting has proved to be an effective technique for the creation of artificial recognition sites within a polymer matrix. These synthetic receptors known as MIPs, are cheap, are relatively simple to prepare and can be tailor made for potentially any target including large molecular-weight molecules. Two approaches, non-covalent (self assembly) and semi-covalent, have been employed to prepare MIPs for benzylpiperazine (BZP), a dominant bioactive compound in a new class of piperazine-base designer drugs. To the best of my knowledge, this is the first report on the synthesis of BZP MIPs via either approach.

Non-covalent MIPs were prepared in 1:1, 1:2 and 1:4 template:monomer ratios employing itaconic acid (IA), methacrylic acid (MAA) and acrylic acid (AA), identified through molecular modelling and NMR spectroscopy studies as favourable functional monomers, with two cross-linkers, ethyleneglycol dimethacrylate (EGDMA) and trimethylolpropane trimethacrylate (TRIM), shown to exhibit the lowest affinity to BZP, and using acetonitrile (AN) and chloroform ( $\text{CHCl}_3$ ) as porogens. Of the 30 polymer formulations assessed, only MIPs prepared with MAA in 1:1 and 1:2 ratios in  $\text{CHCl}_3$  exhibited moderate to impressive imprinting ( $I > 2$ ).

The novel synthesis of benzylpiperazine (4-vinylphenyl) carbamate was required for the preparation of the semi-covalent MIPs. This was obtained through the multi-step synthesis of 4-vinylphenol with thiophosgene, the product of which was reacted with BZP, neat. Two polymers were prepared in  $\text{CHCl}_3$  using EGDMA and TRIM as cross-linker.

The semi-covalent MIPs exhibited higher imprinting effect than the non-covalent MIPs. The highest imprinting factor obtained for the non-covalent polymers was 7.7 for the BZP:MAA 1:2 TRIM polymer bound in  $\text{CHCl}_3$  while the semi-covalent polymer prepared with TRIM gave an imprinting factor of 28. For both non- and semi-covalent systems, BZP binding equilibrium was established with two hours or less. Rapid BZP up-take was observed for all polymers, with more than 80% of the equilibrium up-take occurring prior to 10 minutes. Quantitative analysis of the binding isotherm, Scatchard and Langmuir plots, showed the semi-covalent polymers to exhibit a stronger affinity to BZP and more homogeneous binding sites than the non-covalent polymers.

Cross-reactivity and selectivity experiments were carried out in non-competitive and binary competitive environments with morphine (MO), cocaine (CO), ephedrine (EHP) and phenylpiperazine (PHP). Low affinity was observed for MO and CO analytes, with high selectivity for BZP in these systems. For PHP an equivalent affinity was observed, while the polymers had a greater affinity for EPH. No selectivity was observed for EPH in the competitive system. Both non-covalent and semi-covalent MIPs exhibited high selectivity towards BZP in the presence of MO and CO analytes but equivalent affinity towards PHP and EPH.

# 1

## Introduction

Illicit compounds are defined as substances that are illegal to use, sell or have in one's possession. Each country has its own set of regulations for restricting substances, which has led to compounds having different legality status around the world. However, there are a number of substances that are illegal throughout the world. Included in this are heroin, cocaine, 3,4-methylenedioxy-N-methylamphetamine (MDMA), lysergic acid diethylamide (LSD) and amphetamine type substances (ATS).

In Australia, drug regulation lies within individual state governments. In an attempt to standardise drug legality status, the National Drugs and Poisons Scheduling Committee (NDPSC) was formed. The NDPSC has produced a document called the Standard for the Uniform Scheduling of Drugs and Poisons (SUSDP), with the aim at standardising the scheduling, packaging and labelling of all substances. However, the SUSDP is only a recommendation so there are still discrepancies in drug scheduling across the Australian states and territories.

There are nine schedules in the SUSDP, however it is only Schedule 8 and 9 that are of import to us, as these schedules contain the controlled substances. Schedule 8 consists of controlled drugs, which are available for medicinal use, with restrictions on manufacturing, trade, distribution, possession and use, to prevent abuse, addiction and dependence. Schedule 9 includes substances that are drugs of abuse. The manufacture, possession, sale or use of Schedule 9 drugs are prohibited by law - except for amounts which may be necessary for analytical purposes, or for medical or scientific research conducted with the approval of

Commonwealth and/or State or Territory Health Authorities.

Illicit compounds are trafficked across nations and sold on the black market producing large revenues of money and funding organised crime. The quality of the substances can vary significantly from sample to sample, which can lead to overdoses and fatalities. In addition to the immediate impacts of drugs of abuse on the user and their extended family, stresses are also placed on the community as a whole through government agencies such as health and law enforcement. It is for this reason that detection and identification are required for all substances that enter the country.

It is the job of forensic scientists, customs and law enforcement agencies to detect and identify illicit compounds at and within Australian borders. Currently, this is achieved through the use of non-definitive, broad spectrum colour tests that are expensive and unreliable. Further analysis is then required, which utilises expensive instrumentation and laborious immunoassays. Replacing these tests with a method that is definitive, quick, reliable, mobile and inexpensive will remove the backlog of samples that require testing in forensics laboratories.

The aim of this project was to develop a method of detection for benzylpiperazine (BZP) that is rapid, accurate and inexpensive, with the prospect of being incorporated into an in-field sensor and detector. Molecularly Imprinted Polymers (MIPs) were investigated as the method of detection, as they have already shown potential in detecting illicit compounds. Compounds already investigated include diacetylmorphine and morphine<sup>1;2</sup>, cocaine<sup>2;3</sup>, ephedrine and amphetamines<sup>4-7</sup>, resulting in drug-specific synthetic receptors capable of binding a specific target from a solution matrix. As no MIP has yet been reported specifically for BZP, it was the aim of this project to prepare and evaluate the efficiency of covalent and non-covalent MIPs selective for BZP.

## 1.1 Benzylpiperazine

Benzylpiperazine (BZP), Figure 1.1 (1), is one of the dominant bioactive compounds in a relatively new class of piperazine-based designer drugs in circulation. Other members of this family of compounds include 1-(3,4-methylenedioxyphenyl)piperazine (MDBP) (2), 1-(3-trifluoromethylphenyl)piperazine (mTFMPP)

## 1.1 Benzylpiperazine

(**3**), 1-(3-chlorophenyl)piperazine (mCPP) (**4**) and 1-(4-methoxyphenyl)piperazine (pMeOPP) (**5**). In its free base form, BZP is a pale yellow liquid that is air and light sensitive. The compound is most frequently distributed as a hydrochloride salt, which exhibits greater stability. The BZP hydrochloride salt is a white powder that is usually sold as tablets or capsules. It acts as a stimulant, increasing blood pressure, auditory vigilance and heart rate<sup>8</sup>.

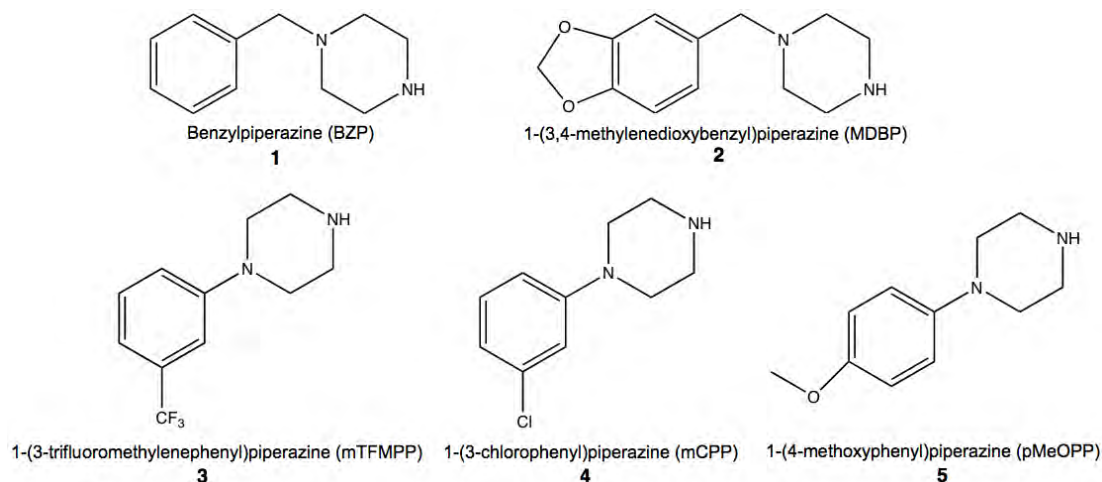


**Figure 1.1:** Structure of benzylpiperazine (**1**) and its related analogues 1-(3,4-methylenedioxyphenyl)piperazine (MDBP) (**2**), 1-(3-trifluoromethylphenyl)piperazine (mTFMPP) (**3**), 1-(3-chlorophenyl)piperazine (mCPP) (**4**) and 1-(4-methoxyphenyl)piperazine (pMeOPP) (**5**).

BZP was first synthesised in 1944 as a potential anti-parasitic agent but was later discarded as it was found to be less effective than the parent compound, piperazine<sup>9</sup>. It was also used as a chemical intermediate in pharmaceutical products<sup>10</sup>. However it was found to produce hyperactivity and stereotypical behaviour with subject responses in human performance tests similar to amphetamine<sup>8;9</sup>. The potency of BZP was found to be 10:1 (BZP:amphetamine). It has since been determined that BZP has a central serotonin mimetic action that involves 5-HT uptake-inhibition and 5-HT<sub>1</sub> receptor agonistic effects<sup>10-15</sup>. When BZP is used in conjunction with mTFMPP, psychoactive effects, including hallucinations, similar to 3,4-methylenedioxymethamphetamine (MDMA) have been reported<sup>16-18</sup>.

In 1973, Campbell *et al.*<sup>9</sup> suggested that the piperazine drugs should be sched-

uled alongside amphetamines, as they predicted possible abuse. It was not until 2004 that the US classified BZP as a Schedule 1 drug (DEA) after fatal intoxications were reported<sup>19</sup>. Following this decision, Denmark, Greece, Sweden and Australia<sup>20</sup> banned and scheduled it appropriately (Schedule 9 in Australia). However, BZP-based pills and tablets are still legal in a number of foreign countries including the United Kingdom and New Zealand (to people over 18 year of age)<sup>21</sup>.

Due to its relatively new status as an illegal substance, there are no rapid and specific in-field tests for BZP as there are for a number of other drugs of abuse such as heroin, cocaine and ATS's. The number of reported cases of BZP abuse is on the increase<sup>22</sup> and as such it is of the greatest import that a quick, simple and reliable method of detection is available to prevent further addiction or more critical fatalities.

## 1.2 Molecular Imprinting

### 1.2.1 Introduction to Molecular Imprinting

Johannes Diderik van der Waals' work in the 19th century was the beginning of the modern concept of molecular interaction. Emil Fischer then extended van der Waals' work, producing the "lock and key" analogy to depict interactions between enzymes and substrates. It was from these initial ideas that the concept molecular imprinting developed.

Non-covalent intermolecular interactions exist in all living systems and are dominated by events like hydrogen bonding and van der Waals forces. Individually, these bonds are weak, but their cumulative strength can result in very stable associations between molecular species. The process of molecular imprinting is a synthetic means of replicating the action of biological complexes such that it results in a chemically and physically stable synthetic enzyme.

Molecular imprinting has become an enterprising way of producing receptors, as they are cheap to produce (even on a kilogram scale), uncomplicated to synthesise and can be produced for large molecular-weighted templates. It is also possible to tailor-make a MIP for potentially any target using different combi-

nations of functional and cross-linking monomers. Extensive investigations have been applied to developing pre-synthetic techniques in an attempt to identify better performing MIPs. This has reduced the amount of time spent on synthesising and testing MIPs.

### 1.2.2 History of Molecular Imprinting

The technique of molecular imprinting was first utilised by Dickey<sup>23</sup> in the 1940s, using a silica matrix to separate dyestuffs. Dickey's work was performed to demonstrate the mechanism proposed by Pauling, involving the formation of antibodies using an antigen molecule as a template. The experiments used methyl orange and some of its analogs (ethyl orange, *n*-propyl orange and *n*-butyl orange) as the templates. These were imprinted into an aqueous sodium silicate that was subsequently dried, ground, sieved and the dye extracted out using methanol. Rebinding with the various templates showed that the silicas were able to rebind the dyes with a slightly greater preference for the original imprint template used.

In 1972, the first synthetic organic polymers were prepared independently, by the two groups Klotz *et al.*<sup>24</sup> and Wulff *et al.*<sup>25</sup>. Klotz *et al.*<sup>24</sup> extended the work of Dickey on the imprinting of methyl orange. The group thiolated methyl orange with thiobutyrolacetone before polymerising with a cross-linker. Also prepared was a polymer that had been cross-linked in the absence of methyl orange. After removal of the template, Klotz reintroduced the template to the polymer. It was found that the imprinted polymer prepared in the presence of methyl orange rebound the template more favourably than the polymer that was prepared in the absence of methyl orange.

Wulff *et al.*<sup>25</sup> used the template D-glyceric acid, modified to contain functional monomers in the form of divinyl benzene, using a reversible boronate ester group and an irreversible amide group. This approach covalently bound the functional monomer to the template. After polymerisation, the template was cleaved, forming a cavity. Rebinding of both L and D-glyceric acid showed the polymer to associate more favourably with the D-form. This technique, still employed to produce the polymers, is now commonly referred to as covalent imprinting.

Approximately ten years later, Mosbach and Norrlof<sup>26</sup> introduced non-covalent

imprinting. In this initial experiment, they prepared a monomer mixture containing a substrate, monomers possessing functional groups capable of forming complementary non-covalent associations with functional groups on the template molecule (so-called functional monomers), and a large proportion of cross-linker. Prior to polymerisation, the functional monomer (FM) and template were allowed to interact in solution to form a pre-association complex. At the completion of polymerisation, the template was removed by simple washing and then loaded into a chromatography column for testing. Rebinding studies performed showed that the polymers were preferential to the substrate they were prepared with. Due to the ease of preparation and template extraction, non-covalent imprinting dominates molecular imprinting.

Since the initial discovery of molecular imprinting, the continued input by significant groups such as Wulff, Mosbach and Shea has resulted in advances in molecular imprinting, with new and novel methods of polymerisation being developed, resulting in the production of a variety of new polymer formats including gels<sup>27-30</sup>, core-shells<sup>31;32</sup>, micro-spheres and beads<sup>33-36</sup> and thin films<sup>37-39</sup>.

### 1.2.3 The Imprinting Process

The general procedure for imprinting consists of three steps. Step one involves the pre-association of one or more functional monomers with the template molecule. The second step of the process is the polymerisation of the monomer-template adduct. This is achieved through addition of a cross-linking agent, forming a polymer backbone that holds the functional monomers in place. Polymerisation is performed in a porogen that all constituents are soluble in and is initiated by a thermal or photochemical radical initiator. The final step in MIP preparation involves the removal of the template from the polymer by grinding (in the case of monolith production) followed by washing with solvent, or by combined chemical treatment and washing. This yields a porous material that has cavities complementary in shape and functionality to the template. A diagram of the imprinting process is presented in Figure 1.2.

Two approaches (covalent and non-covalent imprinting) can be employed to achieve template recognition during MIP formation. Each approach has a number

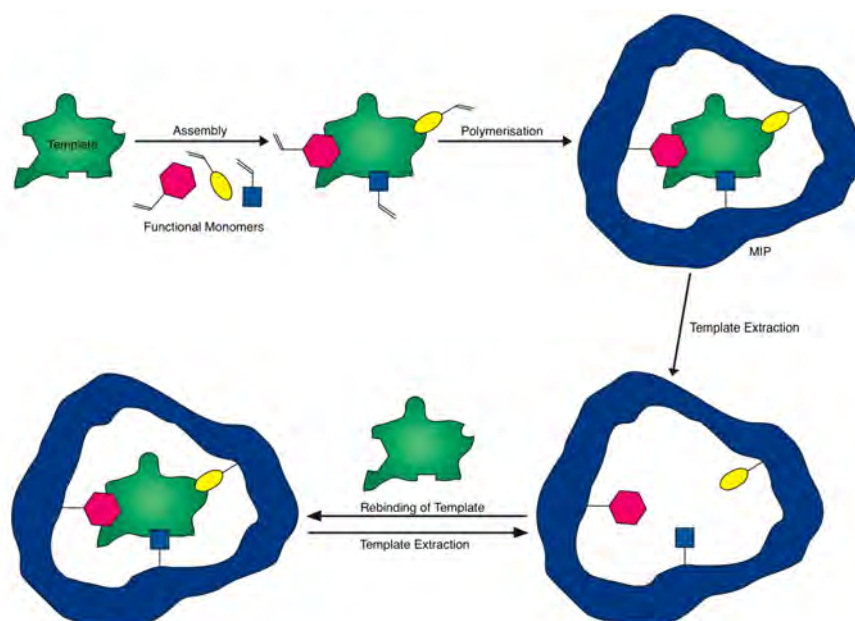


**Figure 1.2:** Schematic of the imprinting process showing the interaction of one template unit with monomer units.

of advantages and disadvantages with the choice of approach governed by the nature of the template and the final application of the MIP.

### 1.2.3.1 Covalent Molecular Imprinting

Covalent imprinting, where the template and functional monomer are covalently linked during the polymerisation, is used when well-defined recognition sites are required. The approach exclusively yields highly selective, stoichiometric polymer binding cavities<sup>40</sup>. A wide variety of polymerisation conditions can be used including high temperatures, polar solvents or extreme pH conditions<sup>41</sup>. However, the technique is restricted by the template structure, as the synthesis of a suitable template-monomer adduct is limited by the nature of the template functional groups. Extraction of the template can also be problematic, as it requires chemical cleavage from the polymer post-polymerisation. Due to the template being covalently bound to the polymer, chemical reactions are required for template removal and in the rebinding process.

Originally, covalent imprinting methods utilised readily reversible condensa-

tion reactions to produce template-monomer adducts. Commonly used reactions included the boronate ester used for imprinting 1,2 and 1,3 diols, the ketal-acetal reactions useful for imprinting diols, aldehydes and ketones and finally Schiff's base formation for imprinting amines<sup>40</sup>. The use of these reactions restricted the template that could be used in covalent imprinting.

Imprinting with the boronate ester was first performed by Wulff *et al.* to imprint glyceric acid, Figure 1.3 (1)<sup>25</sup>. Examples of other templates that have been imprinted using this method include derivatives of mannose<sup>42</sup>, Figure 1.3 (2), galactose and fructose<sup>43</sup>, castasterone<sup>44</sup>, and L-DOPA<sup>40</sup>.

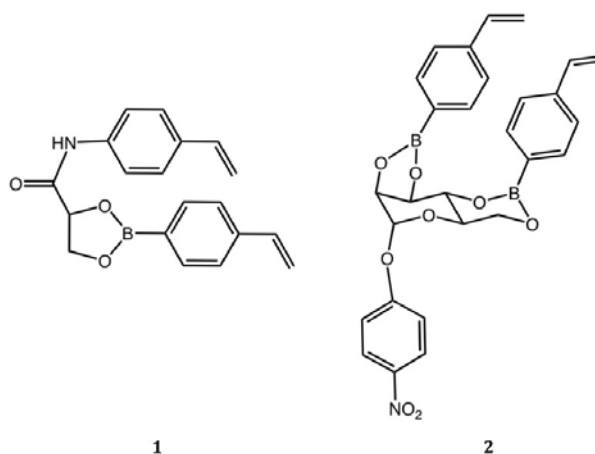


**Figure 1.3:** Reversible covalent imprinting using the boronate ester to prepare the template-monomer structures of 2,3-*O*-*p*-vinylphenylboronic ester derived from *D*-glyceric acid *p*-vinulanilide (1)<sup>25</sup> and *p*-nitrophenyl- $\alpha$ -*D*-mannopyranoside-2,3:4,6-di-*O*-(4-vinylphenylboronate) from *p*-nitrophenyl- $\alpha$ -*D*-mannopyranoside (2)<sup>42</sup>.

Covalent imprinting with ketals and acetals was extensively studied by Shea *et al.*<sup>45-47</sup> for the imprinting of mono and di-ketone templates. The reaction method used polymerisable diols as the functional monomer that were covalently attached to the carbonyl groups of the template. Using this technique a bis-ketal was prepared from 2-(*p*-vinylphenyl)-1,3-propanediol (Figure 1.4).

Schiff's base is used for imprinting templates with amine or aldehyde groups via a condensation reaction. Wulff *et al.* was able to imprint amino acid derivatives, including phenylalanine anilide, given in Figure 1.5<sup>48</sup>, using this technique.

Semi-covalent molecular imprinting offers a compromise between covalent and

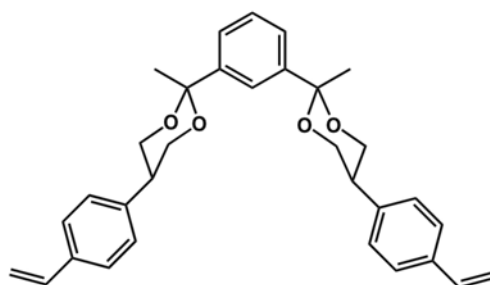


**Figure 1.4:** Covalent imprinting with ketals producing the template monomer structure of Bis-ketal prepared from 2-(*p*-vinylphenyl)-1,3-propanediol. Reproduced from Shea *et al.*<sup>45</sup>.

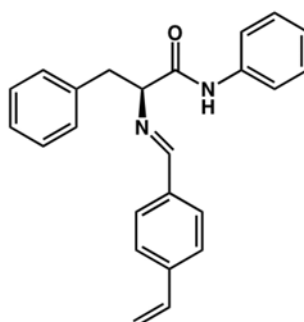


**Figure 1.5:** Covalent imprinting with Schiff's base producing the template monomer structure of phenylalanine anilide with 4-vinylbenzaldehyde. Reproduced from Wulff *et al.*<sup>48</sup>.

non-covalent imprinting. Polymer preparation follows the stoichiometric approach of covalent imprinting, with the template and functional monomer formally linked through a sacrificial hydrolysable functional group such as a carbamate or lactam. Severing of this linkage yields a hydrogen bond donor / acceptor site which interacts favourably with a complementary site on the template during subsequent rebinding. The approach offers the selectivity of covalent imprinting with the rapid rebinding kinetics of non-covalent imprinting.

The carbonyl group is the most commonly used spacer group and was first used in imprinting the template cholesterol<sup>49</sup> (Figure 1.6). Examples of urea<sup>50</sup>, carbamate<sup>27;51–53</sup> and carbonate esters<sup>54;55</sup> have also appeared in the imprinting literature (Figure 1.7). A number of other more unusual spacer groups including salicylate<sup>50;56</sup>, silyl ethers<sup>57</sup> and silyl esters<sup>58</sup> have also been utilised.

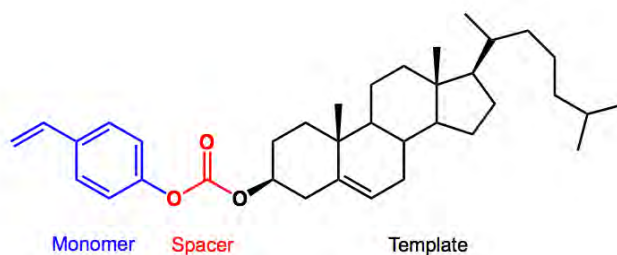


**Figure 1.6:** Template monomer of cholesteryl(4-vinyl)phenyl carbonate for imprinting via the semi-covalent method using a sacrificial spacer.

### 1.2.3.2 Non-Covalent Molecular Imprinting

The method of non-covalent imprinting has become increasingly more popular as the diversity of templates being imprinted expands due to the absence of a formal covalent association between the template and functional monomer, which dramatically increases the potential synthesis permutations in MIP design.

In non-covalent imprinting, the complementary arrangement of the functional monomer around the template occurs via non-covalent self-association. Weak interactions are formed between the template and functional monomer through hydrogen bonding, ion pairs, dipole-dipole interactions or van der Waals forces producing a template:functional monomer (T:FM) cluster. This process is simple

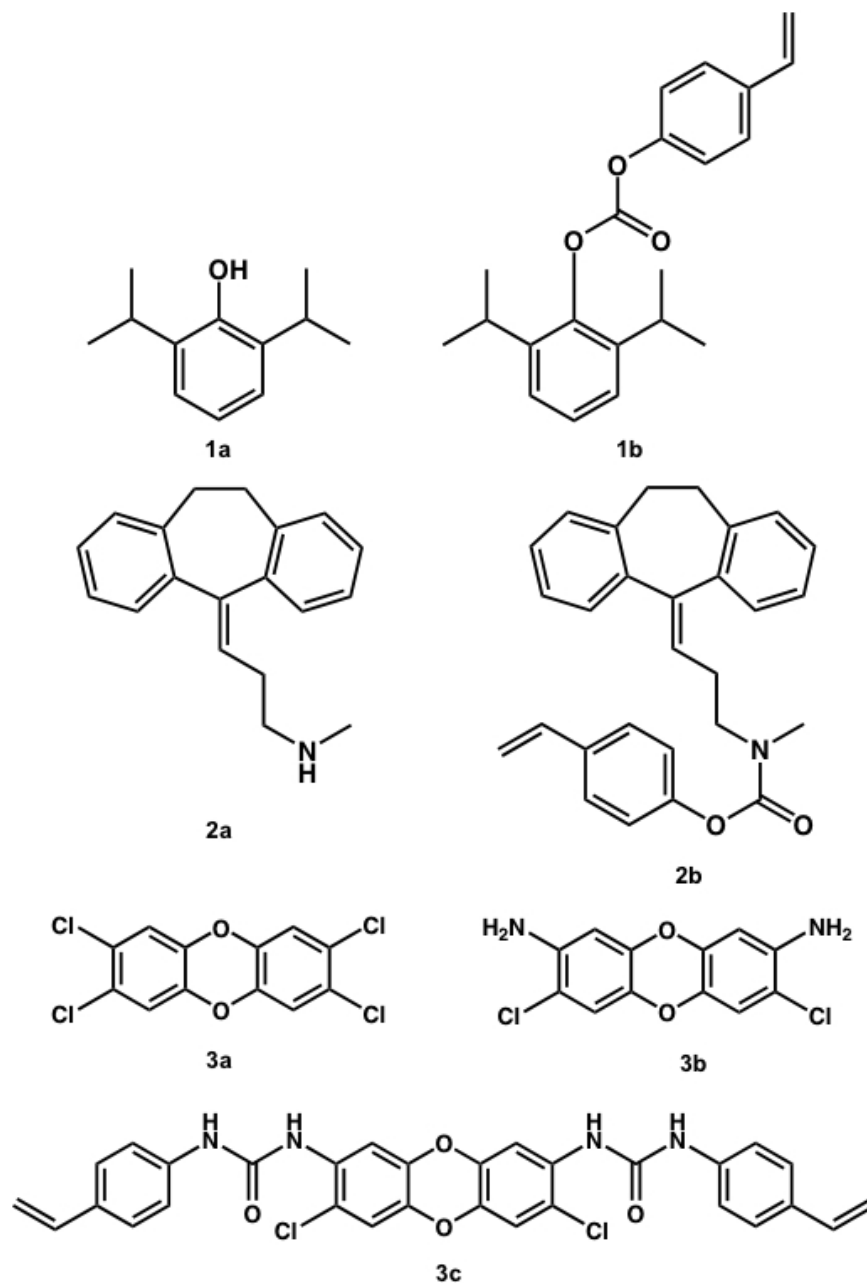


**Figure 1.7:** Templates and template monomers using the carbonyl sacrificial spacer technique: propofol (2,6-diisopropylphenol) (**1a**) and its template monomer propofol (4-vinylphenyl) carbonate (**1b**), incorporating a carbamate linkage<sup>54</sup>; nortriptyline (**2a**) and the template monomer (**2b**), incorporating a carbamate linkage<sup>51</sup>; 2,8-diamino-3,7-dichlorodibenzodioxin (**3b**) prepared from 2,3,7,8-tetrachlorodibenzodioxin (**3a**) to produce the template monomer (**3c**), incorporating a urea linkage<sup>50</sup>

to implement and can increase the potential number of contact points between template and functional monomer, resulting in a more defined cavity.

Figure 1.8 shows a proposed mechanism of how two methacrylic acid units could interact with morphine through hydrogen bonding<sup>40</sup>. The cluster is dynamic, allowing for continued reordering of the functional monomers around the template prior to and during polymerisation. Functional monomer self-association may also occur in solution. Extraction of the template is then achieved through washing with a solvent.

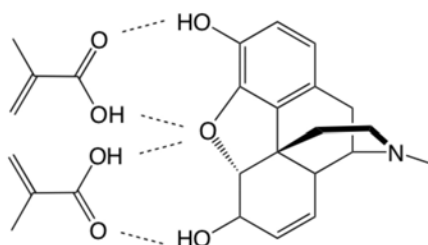


**Figure 1.8:** Proposed mechanism of template-functional monomer interaction of morphine with two methacrylic acid units. Reproduced from Mayes<sup>40</sup>.

Non-covalent imprinting is more favourable when time and cost is important, as the approach is quick and simple as no chemical synthesis is required and template removal and reintroduction is uncomplicated. However, there are a number of disadvantages associated with this technique, including decreased selectivity as a result of difficulties in controlling the cavities formed. This is the result of weaker interactions between the template and monomer prior to polymerisation. The polymerisation conditions are restricted and need to be maximised, as does the stoichiometry of the template-monomer system, as excess functional monomer can result in non-specific binding sites<sup>59</sup>.

### 1.2.4 Optimisation of Molecularly Imprinted Polymers

The performance of a MIP is dependent on how well it can recognise the template material used in the synthesis. This translates to how specific the cavities are to the template and how well the template can rebind to the polymer. Therefore, the affinity of the imprinted polymer towards the template is largely

influenced by the composition of the polymer and thus, must be optimised to obtain the most favourable polymer system.

For non-covalent MIPs, there are a substantial number of commercially available functional and cross-linking monomers that can be used in varying ratios and combinations for imprinting. This makes it extremely difficult to predict monomers that will interact most favourably with the template. The ratio of template to functional monomer and to cross-linker is critical. If there is insufficient functional monomer in the polymer then the binding capacity will be diminished. However if there is an excess of functional monomer in the formulation increased levels of non-specific binding will be observed<sup>59</sup>. In addition, if there is insufficient cross-linker in the polymer formulation, the polymer will not be structurally strong enough to hold its shape and form resulting in loss of template affinity. Last but not least, the polymerisation temperature and the type and amount of porogen used in polymerisation contributes to the overall morphology of the polymer. Therefore, determination of an optimum MIP system requires significant synthetic work.

In covalent imprinting, the stoichiometry and imprinting conditions of the polymer are pre-defined by the nature of the method. Thus, only the cross-linker, porogen and temperature can be modified to improve the imprinting factor. Optimisation of these variables is similar for both the covalent and non-covalent methods.

### 1.2.4.1 Optimisation of Template-Functional Monomer Interactions

The presence of functional groups on the template allows for complementary interactions with the functional groups on the functional monomer. This is the most critical interaction in non-covalent imprinting as this is what holds the template into the polymer cavity. Therefore, when optimising the MIP system, the ideal situation is to have maximum interactions between the template and functional monomer and minimal interaction between the template and the cross-linker and template and porogen. This is achieved through comparative analysis of all of these factors.

Initially, guess work and experience played a major role with choosing func-

tional monomers for imprinting and it was common to use systems that had shown success with other templates<sup>40</sup>. This approach however, was still based on selection of trial and error and resulted in the synthesis of a large number of polymers. In addition, newer functional monomers were overlooked. This was labour intensive, wasting time and resources. In response to this, substantial effort went into developing various approaches that would minimise the amount of time and synthesis required for optimising the MIPs. The aim of these methods was to introduce a systematic and wide ranging evaluation of functional monomers against a specific template. Examples of such approaches include combinatorial synthesis, molecular modelling and spectroscopic evaluation.

The combinatorial approach was independently developed by both Takeuchi and co-workers<sup>60</sup> and Sellergren and co-workers<sup>61</sup>. Takeuchi's approach was a rapid method of preparation and screening for a variety of MIPs. The methodology utilised automated liquid handling equipment that would dispense the reagents into the vial, polymerise using long-wave ultra violet light and wash by repeated dispensing and removal of porogen.

Triazine herbicides, ametryn and atrazine, were used as the templates as extensive investigations had already been performed and published on these compounds, allowing for comparison and verification between the newly developed method and those currently in use. Libraries of polymers were produced then assessed by batch analysis, measuring the desorption and adsorption of the template. Their results were in agreement with previous work that had implemented the conventional imprinting approach and thus, supported the use of high throughput combinatorial screening for optimisation.

Sellegren's group utilised a similar procedure for the preparation and screening of the polymers. However, they also implemented a full-scale analysis of the MIPs as a stationary phase in HPLC to validate the methodology for the template terbutylazine, another triazine herbicide compound<sup>61</sup>. In their investigations they measured the amount of template that was released back into the porogen during template extraction followed by evaluation of template uptake by the MIP and non-imprinted polymer (NIP). The results obtained for the small scale analysis concurred with previous work. As a result, normal-scale synthesis of the methacrylic (MAA) system was prepared for assessment as a stationary phase

in an high-pressure liquid chromatography (HPLC) system. It was observed that similarities in imprinting factors between small-scale and normal-scale existed<sup>61</sup>.

Further investigation by the Sellegren group<sup>62</sup> into optimisation of the semi-automated combinatorial procedure for synthesis of MIPs highlighted the advantages and disadvantages of the protocol. Small-scale polymerisation was used to find functional monomers, however, when the polymers were prepared at normal-scale, reproducible results were not obtained. It was suggested that selectivity at equilibrium will not produce similar selectivity in a non-equilibrium environment like HPLC<sup>62</sup>.

A number of techniques, including nuclear magnetic resonance (NMR), fourier transform infrared (FT-IR) and ultra violet - visible spectroscopy (UV-Vis), can be used to investigate non-covalent interactions between the template and monomer. All techniques enable the complexation to be studied in various conditions and from this it is possible to calculate the stoichiometry and in some cases the dissociation constants of the complex.

The use of NMR enables the presence of interactions between the template and functional monomer to be confirmed, by monitoring the shifts of each peak as monomer is added. It also enables the exact composition and stoichiometry of the complex to be determined. Sellegren *et al.*<sup>63</sup> was the first group to utilise NMR to show that non-covalent monomer-template interactions existed through calculating the total binding term ( $\Delta G_{bind}$ ). A similar approach was also adopted by Whitcombe *et al.* who calculated the dissociation constants from the NMR shifts<sup>64</sup>. NMR spectroscopic analysis has now been used to study the interactions occurring between a wide range of templates and functional monomers<sup>3;5;65-70</sup>.

FT-IR can be used to determine if bonds have formed between the template and monomer. When a bond forms, usually via hydrogen bonding, the stretching frequency of the hydroxyl or amine groups and carbonyl groups are displaced, resulting in a shift of the peak<sup>40</sup>. However, this technique is not frequently used, as there are a number of interferences such as solvent, which prevents interactions from being detected.

FT-IR has been used by Brune *et al.* to investigate interactions between phenolic compounds and ethyl propionate in hexane, by monitoring the OH stretching frequency of the template<sup>71</sup>. They observed a change in the sharp OH stretching

frequency for the uncomplexed hydroxyl group of the template to a broad band at a lower frequency as monomer was added. It is also possible to use FT-IR to determine the relative strength of the interaction. A smaller change in shift indicates a weaker interaction and vice versa.

UV spectroscopic titrations have also been used to study complexation within a system and to calculate dissociation constants<sup>72</sup>. Further to this, studies have been performed, using UV, to screen functional monomer and to determine the nature of interactions between the template and the cross-linker EGDMA<sup>73</sup>. Finally, UV has been used to choose the most favourable ligand for copper capable of providing effective functional monomers for carbohydrate imprinted polymers<sup>74</sup>.

The development of faster more powerful computers has seen polymer design shift from combinatorial and spectroscopic techniques to computer simulation. Piletsky *et al.* were the first to utilise computational simulation in 2001 to determine functional monomers that would best form complexes with creatine, ephedrine and microcystin-LR<sup>4;75;76</sup>. To achieve this they developed a computer that would be able to perform the required calculations.

Until only recently, it was not possible to model a complete molecular imprinted polymer, including all possible structures and all interactions between the template, monomers, cross-linker and solvent as this is too complex requiring extremely large computation workloads. By simplifying the system Piletsky *et al.*, were able to overcome this. By modelling the system prior to polymerisation, they were able to look at the interactions between the individual components involved. The rationale behind this was that the complexes formed prior to polymerisation will be preserved throughout the process<sup>65;77</sup>. However, with the rapid growth in computer power, it has been shown that it is almost possible to model the whole MIP system<sup>78</sup>.

With this development, it is now possible to model interactions between the template and new or existing monomers. Once a virtual library has been created, screening can be performed with the help of computer software like Spartan and SYBYL. Within these programs, different levels of theory can be used, which affects time, accuracy of calculations and computer workload required. At lower levels of theory, quick calculations can be performed as they use less computer memory however, the accuracy of the calculations are poorer. Higher levels of

theory take longer to perform resulting in greater accuracy in the calculations but they utilise significant amounts of computer memory and thus, more powerful computers need to be used.

In the simplest system, only the interactions between the template and monomer are analysed. To determine the most favourable monomers and stoichiometries, the total enthalpy of formation ( $\Delta E$ ) for the system needs to be calculated. This is achieved by taking the heat of formation ( $\Delta H_f$ ) values, produced by the modelling software, for the template, monomer cluster and the template-monomer cluster and entering them in to equation 1.1. The more favourable the system the more negative the  $\Delta E$  value is. Thus, systems with the greatest negative  $\Delta E$  are analysed further. This type of analysis is limited and has a number of drawbacks. It does not take into account cross-linker and solvent interactions in the system. In addition, monomers are selected based on the highest affinity towards the template. This is expected to produce MIPs with a strong affinity for the template however, it is possible that in the process it will produce MIPs and NIPs with no selectivity<sup>40</sup>. This can arise as the NIPs will also contain the FM that could produce non-specific binding.

No single method has been shown to predict the optimum configuration for an imprinted polymer. However, by using a combination of approaches it is possible to obtain a greater understanding of the system under investigation. From this, it should then be possible to reduce the number of combinations from thousands to just a select few, which is more practical to prepare and analyse.

$$\Delta E_{Interaction} = \Delta H_{fTemplate-Monomercluster} - [\Delta H_{fMonomercluster} + \Delta H_{fTemplate}] \quad (1.1)$$

### 1.2.4.2 Optimisation of the Cross-linking Agent

The cross-linker is the backbone of the polymer and can be present in concentrations anywhere between 70-95 mol%<sup>40</sup>. Such an excess of concentration

can result in non-specific interactions occurring with the template during re-binding. To limit these unwanted interactions particular care needs to be taken when selecting a cross-linker. A number of investigations into the effects of the cross-linker structure on template recognition have been reported including those presented by Wulff *et al.*<sup>79</sup> and Spivak<sup>80</sup>. One approach utilised to reduce non-specific template rebinding in a myoglobin imprinted thin-film polymer was performed by Lin *et al.*<sup>81</sup>. They evaluated template rebinding against a number of cross-linker only non-imprinted polymers. Their investigations found that the cross-linker tetraethylene glycol dimethacrylate (TEGDMA) had the least affinity with the template and thus, was an appropriate cross-linker of choice for their myoglobin MIPs.

There are a number of commercial cross-linkers available for polymerisation, with the most commonly used being ethylene glycol dimethacrylate (EGDMA). This monomer offers a degree of rigidity to the polymer as it has two prochiral methacrylate ester groups separated by a short spacer<sup>40</sup>. Divinylbenzene (DVB) is another linear cross-linker and is used when the template contains aromatic functional groups, or when chemical resistance is required. Tri- and tetra-functional cross-linkers are also available, which include trimethylolpropane trimethacrylate (TRIM)<sup>82</sup>, pentaerythritol triacrylate (PETA)<sup>5;83</sup> and pentaerythritol tetraacrylate<sup>83</sup>. Novel functional monomers have also been prepared, including *N,O*-bis-methacryloyl ethanolamine (NOBE). This showed superior performance when utilised in the dual role of cross-linker and functional monomer<sup>80;84</sup>. This cross-linker was later used to prepare a MIP labelled an OMNiMIP (one monomer molecularly imprinted polymer)<sup>80</sup>.

In covalent imprinting, the FM is already at its optimum ratio, however cross-linker is still required in the system to stabilise and produce rigidity to the polymer. Wulff *et al.* investigated the effects of cross-linker concentration on the selectivity of boronate ester template-bound functional monomer<sup>85</sup>. They were able to show that enantioselectivity of the MIPs increased as the cross-linker was maximised. Thus, for covalent polymers, the optimum amount of cross-linker to achieve optimum template binding is as great as possible.

In non-covalent systems, the cross-linker is empirically derived due to the incorporation of the functional monomer. Sellergren *et al.* investigated the

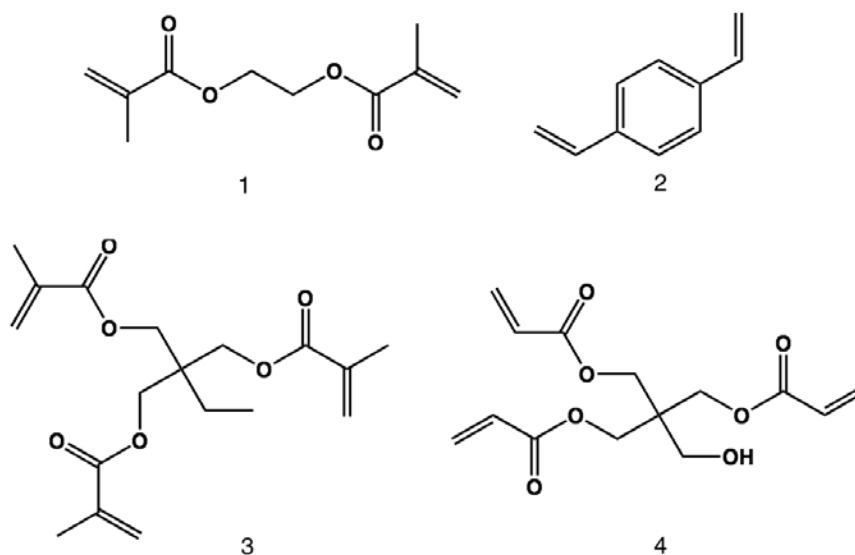


**Figure 1.9:** Chemical structure of common cross-linkers used in polymer preparation including ethylene glycol dimethacrylate (EGDMA) (**1**), divinylbenzene (DVB) (**2**), trimethylolpropane trimethacrylate (TRIM) (**3**), pentaerythritol triacrylate (PETA) (**4**).

cross-linker to functional monomer optimisation and found that selectivity was at its greatest when 20-30% functional monomer was used. However, when more than 30% functional monomer was used, polymer selectivity declined<sup>86</sup>. It was postulated that the excess MAA was producing non-specific binding and that there was not sufficient amounts of cross-linker to produce a rigid polymer, resulting in the polymer cavity collapsing. It is now accepted practice to use a cross-linker percentage in the range of 50 - 80 mol%<sup>59</sup>

#### 1.2.4.3 Porogen Selection for Polymerisation

Porogen selection is important to the polymerisation process as it influences the morphological properties of porosity and surface area<sup>59</sup>. When polymerisation occurs, the polymer phase separates from the porogen. Spivak proposed that the pore size of the polymer is determined through the phase separation of the porogen and the polymer during polymerisation. When the porogen has a low solubility, phase separation occurs early, resulting in large pores and low surface area. Alternatively, porogens with high solubility phase separate later, resulting

in smaller pore sizes and a higher surface area<sup>59</sup>.

The polarity of the porogen and the capability to accept or donate hydrogen atoms also influences the complexation between the template and functional monomer throughout the polymerisation process<sup>87;88</sup>. Sellegren and Shea<sup>87</sup> demonstrated that the enantioselectivity of 1-phe-an imprinted polymers increased as the porogen decreased in polarity. Subsequently, it was proposed by Spivak<sup>59</sup> that low polarity solvents enhance the polar, non-covalent interactions, such as hydrogen bonding, through Le Chateliers principle whereas, polar solvents interrupt these interactions.

Finally, it was determined that the rebinding capability is at its greatest when rebinding is performed in the same solvent used for polymerisation<sup>89;90</sup>. It was proposed that the solvation of the polymer has produced differences within the cavities. It is believed that the solvent is capable of producing different shapes and distance parameters within the polymer cavity which in turn affects template rebinding.

### 1.2.4.4 Temperature Effects

Polymerisation at various temperatures has shown that polymer structure and selectivity is affected. A number of studies, including those performed by Mosbach *et al.*, have shown that polymers prepared at lower temperatures produce polymers with greater selectivity to the template than when prepared at higher temperature<sup>89;91</sup>. Le Chateliers principal again has been proposed as the reason for the observed differences in selectivity<sup>59</sup>, suggesting that lower temperatures lower system energies, resulting in greater template-monomer complexation, leading to more imprinting sites forming in the resulting polymer.

### 1.2.5 Evaluation of Binding Capabilities

An essential step in developing MIPs is the evaluation of the rebinding efficiency of the polymer to (i) the template and (ii) other compounds of a similar nature. After the rebinding capacity has been established it is then possible to optimise the polymer's recognition of the template to produce a MIP with even greater rebinding efficiency. A number of methods exist for determining the binding

and selectivity of a MIP. The first method utilised was a batch method similar to that used to evaluate dialysis measurements in biomolecules<sup>59</sup>. Evaluation then progressed to chromatographic techniques, utilising the polymers as the separation media.

### 1.2.5.1 Evaluation by Batch methods

In batch rebinding experiments, efficiency of the polymer is determined by comparing the rebinding ability of the imprinted polymer against an identically formulated (save for the inclusion of the template molecule) non-imprinted polymer. To evaluate this, an aliquot of solution, of pre-determined analyte concentration ( $C_t$ ) is added to a designated amount of polymer. After a specified time, the polymer is removed and the analyte concentration remaining in solution is determined as per equation 1.2 where the amount bound ( $S_B$ ) is determined by subtracting the amount of free analyte,  $C_f$ , from the total initial analyte concentration added ( $C_t$ ).

$$S_B = C_t - C_f \tag{1.2}$$

Dividing  $S_B$  by the amount of polymer used produces  $S_B$  per gram of polymer. Filtration is commonly used to separate the free substrate from the polymer however, depending on the solvent used, it is also possible to carefully remove the supernatant by pipette.

The selectivity of a polymer is quantified by the ratio of the amount bound of the MIP ( $S_{B_{MIP}}$ ) and the amount bound of the NIP ( $S_{B_{NIP}}$ ). This is referred to as the imprinting factor (I), equation 1.3.

$$I = \frac{S_{B_{MIP}}}{S_{B_{NIP}}} \quad (1.3)$$

The role of the NIP in rebinding experiments is to enable the levels of non-specific surface binding to be quantified. As the I value takes into account non-specific binding, it is possible to state that this value represents binding linked solely to the imprint effect. It also indicates how much better the imprinting is to the non-specific binding, i.e. the greater the I value, the more selective the polymer is. A value less than unity indicates that non-specific binding dominates the sorption and that template uptake is therefore not occurring preferentially in the MIP. An imprinting factor can only be applied to a system that has been prepared and evaluated under the identical conditions as the term is relative.

Specificity of the polymer can be investigated in two ways. The first is through cross-reactivity studies and the other involves selectivity studies. In cross-reactive studies, template rebinding to the MIP is evaluated non-competitively against a range of structural analogues to determine cavity specificity. From this data, the specific selectivity factor can be calculated by taking the ratio of the imprinting factors for two different substrates, substrate 1 ( $I_1$ ) and substrate 2 ( $I_2$ ), equation 1.4.

$$S = \frac{I_1}{I_2} \quad (1.4)$$

In selectivity experiments, rebinding is conducted in a matrix of substrates, resulting in a competitive binding environment. By calculating the amount bound ( $S_B$ ) for each substrate, equation 1.2, the polymer preference for the template over other substrates in the solution can be determined, by again using equation 1.4.

In addition to calculating the imprinting factor and the specificity value, the binding kinetics, binding constant ( $K_d$ ) and number of binding sites ( $n$ ), can

be determined for each polymer. This is accomplished by producing a binding isotherm for the system. A binding isotherm is obtained by adjusting the analyte concentration while keeping the polymer mass constant. A typical binding isotherm is presented in Figure 1.10.

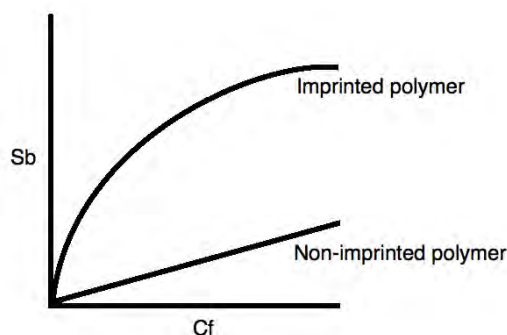


**Figure 1.10:** Appearance of MIP binding isotherm for an imprinted and non-imprinted polymer. Reproduced from Spivak<sup>59</sup>.

A curved line in a binding isotherm suggests that a number of different binding sites are present within the polymer, while a straight line is indicative of a single type of binding site, which in the NIP represents non-specific binding. If the plot is curved, it is difficult to extract specific information regarding the  $K_d$  value or  $n$  without applying non-linear computation methods. However, programs are now available that are readily capable of performing non-linear regression. The use of these programs give more accurate results as log functions and linear regression methods smooth out data imperfections.

If a non-linear method is not available the isotherm can be linearly transformed in order to establish the  $K_d$  and  $n$  values. Two plots that are commonly utilised are the Scatchard and Langmuir plots. The equations associated with these plots are given in equations 1.5 and 1.6, respectively.

$$\frac{S_B}{C_f} = KN - S_B \quad (1.5)$$

$$\frac{C_f}{S_B} = \frac{C_f}{N} + \frac{1}{KN} \quad (1.6)$$

The Scatchard plot is obtained by plotting  $S_B/C_f$  versus  $C_f$  and will produce a straight line if a single type of binding site (homogeneous) exists that binds independently. A line of best fit is then applied to the transformed data points and the  $K_d$  value is determined from the slope of the line, while the number of binding sites is then determined from the y-intercept.

In a system that has two or more types of binding sites present (heterogeneous), a non-linear Scatchard plot is obtained. In MIPs, this is interpreted as low affinity and high affinity binding sites present within the polymer. A common approach to determining the  $K_d$  and  $n$  values in a Scatchard plot of this nature is to fit two straight lines through the data, known as the limiting slopes method. A  $K_d$  and  $n$  value is then calculated independently for each line. However, this method has been shown to be inaccurate. It is also biased toward fitting data in the high concentration range<sup>92;93</sup>. An example of a binding isotherm and the corresponding Scatchard plot for heterogeneous binding is presented in Figure 1.11, obtained by Lin *et al.* in their investigations into optimising the formulation for a molecularly imprinted thin-film for myoglobin<sup>81</sup>.

The Langmuir regression is an alternative method used to determining the  $K_d$  and  $n$  values. By plotting the  $C_f/S_B$  versus  $C_f$ , a plot is obtained that yields a slope of  $1/N$  and a y-intercept of  $1/KN$ . A straight line will be produced in a system that has homogeneous sites, while non-linearity signifies heterogeneous binding. The Langmuir regression has some bias toward data in the mid to high concentration range. An example of a Langmuir plot can be observed in

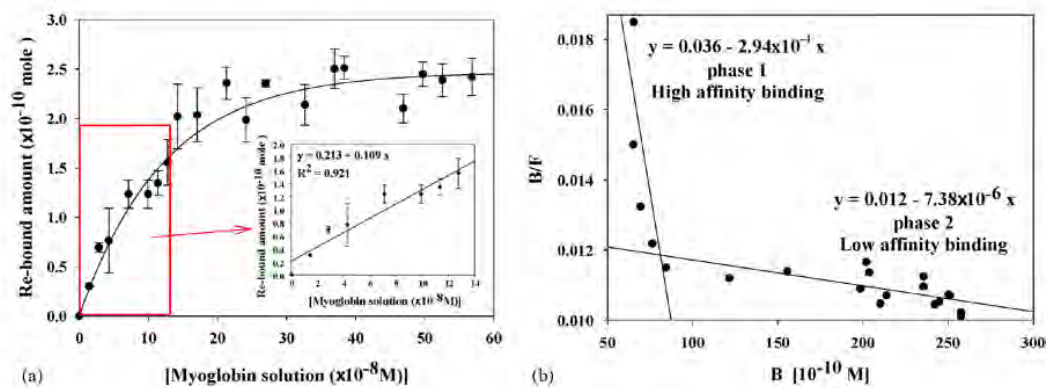


**Figure 1.11:** Binding isotherm (A) and corresponding Scatchard plot (B) for a myoglobin molecularly imprinted film. Reproduced from Lin *et al.*<sup>81</sup>.

Figure 1.12. The plot was used to determine the binding parameters of Neu5AC imprinted polymers<sup>94</sup>.

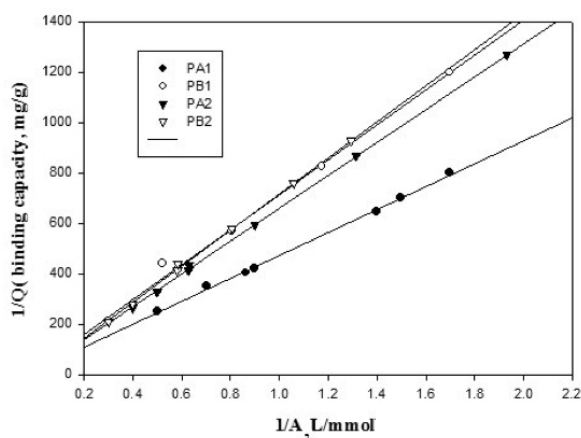


**Figure 1.12:** Langmuir plot for a Neu5AC-MIPs. Reproduced from Pan *et al.*<sup>94</sup>.

### 1.2.5.2 Evaluation by Chromatography

MIPs are capable of being used directly as a stationary phase in chromatography. After the polymer has been ground to a specific particle size it is packed into a stainless steel HPLC column, enabling a quick and easy method of analysis. Polymerisation of the MIP within the HPLC column has also been reported, making analysis even easier and quicker, as the grinding has been eliminated<sup>29;95–98</sup>.

However, once this has been performed the column becomes specific and cannot be reused for other polymers.

The equations used to determine the binding by chromatographic analysis are proportional to batch binding. However, this only holds true if both methods are at equilibrium<sup>59</sup>.

Molecularly imprinted solid phase extraction (MISPE) is another chromatographic method that can be used for assessing binding. It has been successfully used to clean-up or concentrate the analytes to levels greater than methods currently available<sup>99</sup>. This has resulted in higher accuracy and lower detection limits (LOD). Analysis is performed by loading the polymer into a MISPE tube and substrate is pushed or pulled through by a syringe or vacuum. The solution is then analysed. The amount bound ( $S_B$ ), the imprinting factor ( $I_f$ ) and specific selectivity factor ( $S$ ) can all be calculated by the same equations used for batch methods, equations 1.2, 1.3 and 1.4. It should be noted, that the results obtained by MISPE analysis cannot be directly compared to batch methods, as MISPE is not at equilibrium.

### 1.2.6 Characterisation of Polymers

The concept of molecular imprinting involves binding cavities being created within the polymer that are specific towards a selected template. The template is removed and then rebound and thus, for good template uptake, the template needs to be able to access the binding sites within the polymer as well as those on the surface. Morphological characterisation enables the determination of the physical characteristics of the polymer, which in turn, can lead to a greater understanding of template rebinding and ultimately imprinting effects. As MIPs are solid, amorphous macropolymers, physical characterisation techniques available are limited<sup>59</sup>. These include porosity and surface area as well as swelling, microscopy and spectroscopic techniques, such as IR and solid state NMR.

#### 1.2.6.1 Surface Area and Porosity

For template up-take to occur the template needs to gain access to the cavities that were originally created during polymerisation. Therefore, the polymer needs

to be porous to allow the template to penetrate. By measuring the porosity of the polymer, it is possible to gain some insight into how readily template up-take will occur.

The surface area and porosity are measured using a nitrogen adsorption porosimeter using a BET (Brunauer Emmett and Teller) analysis routine for surface area and a BJH (Barret, Joyner and Halenda) routine for porosity. There are three types of pores that form within a polymer. Macropores, which are of the size greater than 50 nm in diameter, mesopores, which are between 2 - 50 nm and micropores that are less than 2 nm. The pore size and resulting surface area are affected by the amount and type of porogen, the concentration of cross-linker and the temperature.

Studies have been performed by Sellergren and Shea, comparing the effects of different porogens on MIPs prepared for L-phe-an<sup>87</sup>. They found that different porogens produced polymers with different dry state morphologies including non-porous gels and macropores. However, after swelling, it was found that the morphology was more homogeneous. Most importantly, they found that polymer porosity was not a requirement for template up-take. Polymers with low porosity and surface area that were able to swell had similar binding characteristic to porous non-swelling polymers. The key point here is the swellability of the polymer and thus swelling measurements are crucial to characterisation and ultimately explaining rebinding capabilities.

### 1.2.6.2 Swelling Measurements

The ability of the polymer to swell was shown to be a crucial factor in template uptake, especially in polymers with low porosity, as this enhances mass transfer of the template to internal cavities. The solvent plays a major role in how much the polymer swells. This has been shown in a number of cases including that of nicotine, which showed that recovery of the template was reduced as the porogen (acetonitrile) was replaced by water<sup>100</sup>.

There are two methods available for measuring the swelling of polymer. The first method uses volumetric methods, in which percentage swelling is determined by subtracting the recorded volume of the dry polymer ( $V_{dry}$ ) for a particular mass

(m) from the wet polymer ( $V_{wet}$ ) after a set time, equation 1.7. This method however, is less accurate and has a number of difficulties including polymer buoyancy in chlorinated solvents.

$$\%swelling = \frac{V_{wet} - V_{dry}(mL)}{m(g)} \quad (1.7)$$

A more accurate technique for determining the swelling of a polymer is to measure the swelling of a single polymer bead by microscopy<sup>101</sup>. By measuring the diameter of a photo taken of the polymer bead, dry and wet, the percent swelling can be calculated by taking the ratio. In this experiment the same bead must be used, due to the irregularity of the individual particles.

### 1.2.6.3 Further Characterisation

Addition physical characterisation that can be performed on the polymers include determination of the thermal decomposition point, by thermal gravitational analysis (TGA). This value signifies how thermally stable the polymer is. The thermal decomposition point is required for other analyses, including porosity and DSC, and thus, it is a standard characterisation performed.

Microscopy such as SEM and AFM have been used to investigate the surface structure of MIPs. Through SEM it is possible to observe and photograph the polymer surface, resulting in a greater understanding of the macroscopic structure of the polymer. The images produced can show whether the polymer is composed of beads ranging in the size of micrometers to nanometers, whether it is of a fibrous structure or if it has a smooth surface. This information is used in conjunction with the swelling measurements and the porosity to give an overall physical analysis of the MIP.

## 1.3 Project Outline

The following work presents the development of benzylpiperazine molecularly imprinted polymers using both non-covalent and covalent imprinting techniques. Currently, there is no literature for either the preparation of a semi-covalent or non-covalent BZP molecular imprinted polymer. This work is thus the first on this compound.

In the development of non-covalent imprinted polymers, selection of functional monomers was facilitated by theoretical (molecular modelling) and spectroscopic investigations (NMR spectroscopy). After this had been established, non-covalent MIPs were developed. A series of MIP formulations were prepared to evaluate, optimise and characterise, with respect to their capacity to bind BZP, optimum binding time, and type and number of binding sites. The performance of the MIPs was also correlated to their morphology, surface area, porosity and their swelling behaviour. The formulations investigated included three FMs (AA, MAA and IA), shown to have favourable interactions with BZP, in three ratios (1:1, 1:2 and 1:4), and in two porogens (AN and  $\text{CHCl}_3$ ). The interactions of BZP with three cross-linkers was also investigated to (i) find cross-linkers that had minimal interaction with BZP and (ii) determine if the amount of cross-linking within a polymer would affect template up-take. In addition, rebinding studies were also performed in both AN and  $\text{CHCl}_3$  to determine the effects that different solvents have on rebinding.

An important part of this project was the synthesis of benzylpiperazine (4-vinylphenyl) carbamate, the template-monomer (TM) adduct used for the preparation of semi-covalent BZP MIPs. This was achieved by a three step synthesis in which acetoxystyrene was de-protected to 4-vinylphenol which was then reacted with thiophosgene to produce the pure product 4-vinylphenyl chlorothioformate. This was then incorporated with BZP through a neat reaction, producing the TM adduct, benzylpiperazine (4-vinylphenyl) carbamate. Once the TM adduct had been produced, the preparation and evaluation of BZP semi-covalent imprinted polymers were performed. To the best of my knowledge, this is the first reported synthesis of a BZP-based monomer and semi-covalent BZP MIPs and thus was novel. As with the non-covalent MIPs, the capacity to bind BZP, optimum bind-

ing time, and type and number of binding sites was determined in conjunction with the morphology, surface area, porosity and swelling behaviour. This enabled a comparison of the two imprinting methods (self assembly and semi-covalent) utilised for BZP MIPs.

In a final evaluation, the specificity and selectivity of the polymers was investigated through the use of cross-reactive and selectivity studies with various analytes in a non-competitive and binary competitive environment. The analytes included in this analysis were morphine, cocaine, ephedrine and a BZP analogue, phenylpiperazine. These compounds were selected as they are common drugs of abuse in Australia.

In summary, this project aimed to produce non-covalent and semi-covalent BZP MIPs. In-depth analyses was performed on both MIPs, that included establishing the binding capacity, affinity, binding kinetics and binding dynamics. Attempts to optimise the system were also carried out, to achieve the greatest possible imprinting effect. Finally, the polymers were screened with a number of other illicit compounds to determine the specificity towards BZP.

## 2

# Materials and Methods

## 2.1 Reagents

Benzylpiperazine (purum 97%) was obtained from Fluka, (1*R*,2*S*)-(-)-Ephedrine (EPH) was obtained from Sigma Aldrich, (98%), and used as received. Cocaine base and morphine was provided by the Australian Federal Police services and was used as received. 1-Phenylpiperazine (99%) and ethyl-1-piperazine carboxylate (99%) were obtained from Aldrich and used as received.

Itaconic acid (IA), methacrylic acid (MAA), acrylic acid (AA), divinylbenzene (DVB), ethylene glycol dimethacrylate (EGDMA) and trimethylolpropane trimethacrylate (TRIM) were obtained from Aldrich. MAA, AA, DVB and EGDMA were distilled under reduced pressure prior to use. TRIM was purified by washing with 0.1M sodium hydroxide solution (50 mL x 2), water (50mL), followed by a saturated brine solution (50mL) and then dried with magnesium sulfate. Azobisisobutyronitrile (AIBN, 99.95%) was obtained from DuPont and was recrystallised in acetone prior to use. Monomers 7-hydroxy-4-methylcoumarin acrylate (HMCA) and NOBE, and benzylpiperazine (4-vinylphenyl) carbamate (TM adduct) were synthesised following the procedure described in the succeeding section.

Acetoxystyrene (96%), thiophosgene (97%), ethanolamine (99%), sodium hydroxide (NaOH), glacial acetic acid, hydrochloric acid (HCl, 37%), triethylamine (TEA, 99.5%), potassium hydroxide (KOH) and potassium chloride (KCl, >99%)

were obtained from Sigma Aldrich, phosphoric acid ( $\text{H}_3\text{PO}_4$ , 85%) was obtained from BASF, methacryloyl chloride, potassium dihydrogen phosphate ( $\text{KH}_2\text{PO}_4$ , 99.5%) and potassium hydrogen phosphate ( $\text{K}_2\text{HPO}_4$ , 99.5%) were obtained from Fluka and acryloyl chloride (96%) was obtained from Lancaster. All compounds were used as received.

Deuterated chloroform (99.8%), dimethylsulfoxide (99.8%), for NMR analysis, were obtained from Cambridge Isotope Laboratories Incorporated. HPLC grade acetonitrile and chloroform were obtained from Merck and were used for HPLC analysis. All other solvents were distilled prior to use, unless otherwise stated.

## 2.2 Monomer Synthesis

### 2.2.1 Preparation of *N,O*-bismethacryloyl Ethanolamine (NOBE)

NOBE was prepared as per the method utilised by Spivak<sup>80</sup>. Ethanolamine (0.976 g, 16 mmol) was mixed with 15 mL of  $\text{CH}_2\text{Cl}_2$ . TEA (3.74 g, 5.15 mL, 37 mmol) was added in small portions to the initial mixture with stirring and the reaction mixture was cooled to  $0^\circ\text{C}$ . Methacryloyl chloride (3.867 g, 3.6 mL, 37 mmol) was added dropwise with vigorous stirring while keeping the temperature at  $0^\circ\text{C}$ . After complete addition of methacryloyl chloride, the temperature was increased to  $40^\circ\text{C}$  and allowed to react for 23 hrs at this temperature. The reaction mixture was filtered and the precipitate ( $\text{Et}_3\text{NHCl}$ ) discarded. The filtrate was extracted with 0.5 M  $\text{NaHCO}_3$  (3 x 15 mL) and 0.5 M sodium citrate (3 x 15 mL). The solvent was evaporated under vacuum, and the compound was isolated by column chromatography (EtOAc/hexanes 50:50, EtOAc 100%). NOBE was isolated as a pale yellow oil in a 59% yield. NMR data was consistent with the literature<sup>80</sup>.  $^1\text{H}$  NMR ( $\text{CDCl}_3$ , 300 MHz):  $\delta/\text{ppm}$  = 6.80, 5.99, 5.71, 5.60, 5.38, 4.25, 3.58, 1.97, 1.89.  $^{13}\text{C}$  NMR ( $\text{CDCl}_3$ , 75.5 MHz):  $\delta/\text{ppm}$  = 168.5, 167.4, 139.8, 135.9, 126.0, 119.4, 63.2, 39.0, 18.4, 18.1.

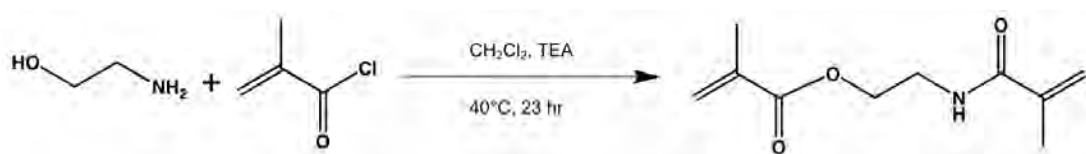


**Figure 2.1:** Synthesis of *N,O*-bismethacryloyl ethanolamine (NOBE).

### 2.2.2 Preparation of 7-Hydroxy-4-methylcoumarin Acrylate (HMCA)

7-Hydroxy-4-methylcoumarin acrylate (HMCA) was prepared by the literature method<sup>102</sup>. TEA (12.1 g, 120 mmol) and 7-hydroxy-4-methylcoumarin (8.809 g, 50 mmol) was dissolved in chloroform (150 mL) and cooled to 0°C. Acryloyl chloride (10.9 g, 120 mmol) was added drop-wise with vigorous stirring. The reaction mixture was then returned to room temperature and stirred for a further 12 hrs. The solvent was evaporated under vacuum and the product purified by dissolving the precipitate in methanol (200 mL). The methanol solution was then poured into water (1 L) and the precipitate collected by filtration. HMCA was isolated as a white flake. NMR data was consistent with the literature<sup>102</sup>. <sup>1</sup>H NMR (CDCl<sub>3</sub>, 300 MHz):  $\delta$ /ppm = 7.86, 7.39, 7.28, 6.67, 6.62, 6.52, 6.48, 6.24, 3.41. <sup>13</sup>C NMR (CDCl<sub>3</sub>, 75.5 MHz):  $\delta$ /ppm = 163.8, 159.7, 153.6, 153.0, 152.6, 134.4, 127.3, 126.5, 118.4, 117.7, 113.9, 110.2, 18.2.



**Figure 2.2:** Synthesis of 7-hydroxy-4-methylcoumarin acrylate (HMCA).

### 2.2.3 Preparation of Benzylpiperazine(4-Vinylphenyl) Carbamate (TM adduct)

#### 2.2.3.1 Step 1: Preparation of 4-Vinylphenol

4-Vinyl phenol was prepared as per the literature method of Corson *et al*<sup>103</sup>. 4-Acetoxy styrene (2.0 g, 13.22 mmol) was added to potassium hydroxide (2.0 g, 35.65 mmol) in water (25 mL) and stirred at 0-5°C until homogeneous (5 hrs). Gaseous carbon dioxide was passed into the stirred cold solution to pH 8 to produce *p*-vinylphenol (61% yield). <sup>1</sup>H and <sup>13</sup>C NMR (Bruker 300 MHz) data were found to agree well with the literature values<sup>103</sup>. <sup>1</sup>H NMR (CDCl<sub>3</sub>, 300 MHz):  $\delta$ /ppm = 7.30, 6.79, 6.63, 5.54, 5.04. <sup>13</sup>C NMR (CDCl<sub>3</sub>, 75.5 MHz):  $\delta$ /ppm = 158.4, 137.6, 130.3, 128.4, 116.0, 110.9.

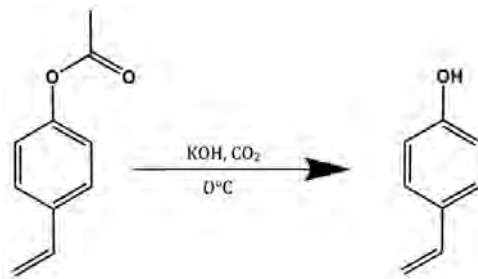


**Figure 2.3:** Synthesis of 4-vinylphenol from 4-acetoxy styrene.

#### 2.2.3.2 Step 2: Preparation of 4-Vinylphenyl Chlorothioformate

4-Vinylphenyl chlorothioformate was prepared by the literature method of Oh *et al*<sup>104</sup>. A solution of thiophosgene (0.45 g, 4.2 mmol) in chloroform (3 mL) was cooled to 0°C and then a solution of 4-vinylphenol (0.5 g, 4.2 mmol) in 5% NaOH (5 mL) was added dropwise with stirring. The reaction was stirred for 1 hrs at 0-5°C and the chloroform layer washed with dilute HCl and water. Solvent was removed under reduced pressure and product was separated by column chromatography (silica gel, 10% EtOAc:hexane) (yield >85%). <sup>13</sup>C NMR (Bruker 75.5 MHz CDCl<sub>3</sub>) data were found to agree well with the literature values<sup>104</sup>. <sup>1</sup>H NMR (CDCl<sub>3</sub>, 300 MHz):  $\delta$ /ppm = 7.46, 7.08, 6.67, 5.70, 5.26. <sup>13</sup>C NMR

## 2.2 Monomer Synthesis

(CDCl<sub>3</sub>, 75.5 MHz):  $\delta$ /ppm = 185.7, 154.0, 136.8, 135.4, 127.6, 121.2, 120.9, 115.2.

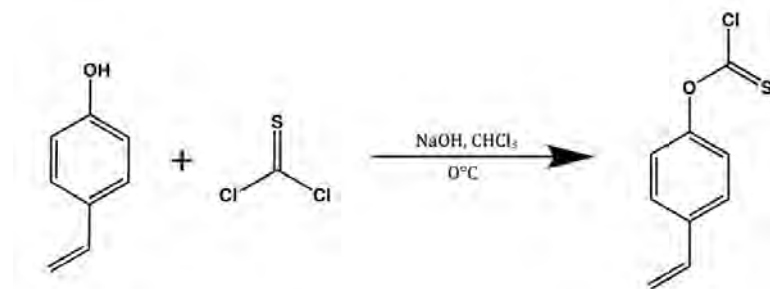


**Figure 2.4:** Synthesis of 4-vinylphenyl chlorothioformate.

### 2.2.3.3 Step 3: Preparation of Benzylpiperazine(4-Vinylphenyl) Carbamate

4-Vinylphenyl chlorothioformate (0.7 g, 3.54 mmol) was added dropwise to BZP (1.25g, 7.09 mmol) with stirring. The reaction was stirred for 1 hr and then the product was separated by column chromatography (silica gel, 5% EtOAc:hexane, 10% EtOAc:hexane). <sup>1</sup>H NMR (CDCl<sub>3</sub>, 300 MHz):  $\delta$ /ppm = 7.30 (d), 7.21 (m), 6.89 (d), 6.58 (q), 5.60 (d), 5.13 (d), 4.09 (m), 3.88 (m), 3.50 (s), 2.51 (d). <sup>13</sup>C NMR (CDCl<sub>3</sub>, 75.5 MHz):  $\delta$ /ppm = 186.9, 153.4, 136.1, 135.7, 129.5, 128.7, 127.8, 127.1, 123.0, 114.3, 62.8, 52.6, 52.4, 50.2, 46.3.

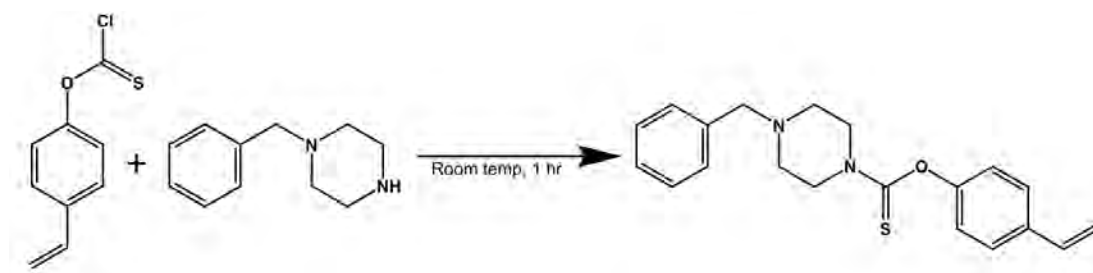


**Figure 2.5:** Synthesis of Benzylpiperazine(4-vinylphenyl)carbamate.

## 2.3 Molecular Modelling

Computer modelling (interaction studies) was performed using the molecular simulation software, Spartan '04 (Wavefunction, Inc. USA). Monomer molecules were then coupled to the template, in varying ratios of 1:1 through to 1:16, with no spatial conformational restrictions. Geometry optimisation calculations were performed on all T-M clusters using AM1 force field at the semi-empirical level. No preset limitations were imposed on the structures.

## 2.4 NMR Spectroscopic Analysis

$^1\text{H}$  and  $^{13}\text{C}$  Nuclear Magnetic Resonance (NMR) spectra were recorded at 300.13 and 75.47 MHz, respectively, using a Bruker Advance 300 MHz Spectrometer in conjunction with Bruker Topspin v1.3 software. Experiments involving MAA, AA and NOBE were performed in deuterated chloroform while IA experiments were performed in deuterated DMSO at a temperature of 301 K.

For the NMR titration, molar aliquots of monomer were sequentially added to the template BZP (0.1 mmol) up to a maximum of 16 equivalents. After each aliquot addition, the sample was mixed and allowed to spin for five minutes before spectrum acquisition. The experiment was repeated in the absence of BZP.

For the Job's experiment, 11 samples were prepared with varying BZP and monomer molar ratios, ranging from 0 to 1, using 0.2 mM solutions. The total volume was kept constant at 0.5 mL.

## 2.5 Polymer Synthesis

### 2.5.1 Non-covalent MIPs

Non-covalent MIPs were prepared following the procedure of Holdsworth<sup>3</sup>. The required amount of functional monomer (0.34 mmol, 0.68 mmol or 1.36 mmol) and crosslinker (6.64 mmol, equivalent to 20 x T) were added to a solution of BZP (60 mg, 0.34 mmol) in 7 mL porogenic solvent. Based on pre-synthesis interaction studies, MAA, AA and IA were selected as functional monomers and

EGDMA and TRIM as crosslinkers. MIPs were prepared using 1:1, 1:2 and 1:4 T:M ratios in chloroform and acetonitrile. The reaction mixture was degassed with N<sub>2</sub> before AIBN (50 mg) was added. The mixture was heated to 60°C in an oven (Thermoline). NIPs were prepared using the same method but without the addition of BZP.

Polymers were ground wet in methanol and sieved with the fraction between 32 and 65  $\mu\text{m}$  collected. Template removal was by soxhlet extraction for 48 hrs using a 1% acetic acid - methanol mix, followed by 100% methanol for 12 hrs. Finally, the polymers were dried at 40°C for 24 hrs.

### 2.5.2 Covalent MIPs

Covalent MIPs were prepared following the procedure of Whitcombe *et al*<sup>49</sup>. 115 mg of benzylpiperazine(4-vinylphenyl)carbamate (0.34 mmol) was mixed with 6.46 mmol of crosslinker (EGDMA or TRIM) and AIBN (1% mol ratio) in 2 mL/g of chloroform. The reaction mixture was degassed with N<sub>2</sub> and then heated to 60°C in an oven (Thermoline). NIPs were prepared using the same method but without the addition of BZP.

Polymers were ground wet in methanol and sieved with the fraction between 32 and 65  $\mu\text{m}$  collected. The template was removed by heating at reflux of the polymer over 1M NaOH for 12 hrs and then neutralised with dilute HCl. The polymers were then washed with methanol for 12 hrs using a Soxhlet extractor. Finally, the polymers were dried at 40°C for 24 hrs.

## 2.6 Batch Binding Experiments

Batch rebinding experiments were carried out using a known molarity of BZP stock solution in either acetonitrile or chloroform. The required mass of polymer was left in contact with the BZP solution for the required time. The amount of BZP bound was calculated from equation 1.2.

BZP quantification was achieved by HPLC using a Shimadzu High Performance Liquid Chromatograph (HPLC) (LC-20AD) fitted with an Econosphere<sup>TM</sup> C18, 5 $\mu\text{m}$  column (Grace<sup>®</sup>).

## 2.7 Selectivity and Cross-reactivity Studies

---

For BZP binding in acetonitrile, the mobile phase consisted of 50% acetonitrile and 50% buffer solution (25 mM  $K_2HPO_4$ ; 30 mM KCl; 7 mM TEA; adjusted to pH3 with  $H_3PO_4$ ). A 10  $\mu$ L injection volume was used with a run time of 10 minutes, flow rate of 2 mL/min and detection wavelength of 254 nm. For binding in  $CHCl_3$ , the mobile phase consisted of 70% acetonitrile and 30% buffer solution (25 mM  $K_2HPO_4$ ; 30 mM KCl; 7 mM TEA; adjusted to pH3 with  $H_3PO_4$ ). A 10  $\mu$ L injection volume was used with a run time of 15 minutes, flow rate of 0.95 mL/min and detection wavelength of 254 nm. A calibration curve was generated using six solutions in the range of 0.1 to 0.8 mM. Results were analysed using Shimadzu LC Solution software.

## 2.7 Selectivity and Cross-reactivity Studies

Twenty (20) mg of polymer with 1 mL of 0.8 mM BZP in  $CHCl_3$  was used. The stock solution was left in contact with the polymer for 1 hr after which the supernatant was removed, filtered and analysed by the required method.

Cocaine was analysed using a Shimadzu 2010 gas chromatograph coupled to a Shimadzu QP2010 mass spectrometer using a Shimadzu AOC-20s auto sampler. The column was a ZB-5MS capillary column (30 m x 0.25 mm), coated with 0.25  $\mu$ m of stationary phase. High purity helium was used as the carrier gas at 71 kPa with a column flow rate of 1 ml/min, a total flow rate of 9ml/min and a split ratio of 15. 1  $\mu$ L samples were injected and run using the following program: initial column temperature was 100°C which was held for 1 min before increasing to 300°C at a rate of 10°C/min.

L-Ephedrine was analysed using HPLC. The mobile phase consisted of 75% aqueous buffer solution (50 mM  $K_2HPO_4$  adjusted to pH3.5 with  $H_3PO_4$ ) and 25% 3:7 water:acetonitrile (with 10 mM TEA). A 10  $\mu$ L injection volume was used with a run time of 10 minutes, flow rate of 0.8 mL/min and detection wavelength of 190 nm. A calibration curve was generated using solutions in the range of 0.1 to 1 mM. Results were analysed using Shimadzu LC Solution software.

## 2.8 Characterisation

### 2.8.1 Swelling Measurements

The swelling capacity of each polymer was measured by packing 10 mg polymer in a graduated syringe. The dry volume was recorded prior to the addition of solvent ( $\text{CHCl}_3$  or AN). After one hour, the excess solvent was removed and the volume of the swollen polymer measured. Percentage swelling was calculated using equation 1.7.

### 2.8.2 Scanning Electron Microscopy (SEM)

Scanning Electron Microscopy (SEM) images were generated using a Philips XL30 SEM and Oxford ISIS EDS (1997) software. Surface photographs were taken at 20000x magnification.

### 2.8.3 Porosity and Surface Area

Porosity and surface area measurement were performed using Barret-Joyner-Halenda (BJH) and Brunauer-Emmet-Teller (BET) analysis, respectively. Measurements were conducted on a Micromimetics ASAP 3030 surface area and porosity analyser using a 5-point surface area analysis. Approximately 100 mg of polymer samples were analysed using  $\text{N}_2$  as the adsorption gas.

# 3

## Pre-synthesis: Template-Monomer Interaction Studies

### 3.1 Introduction

An important step in the synthesis of MIPs is the pre-association phase, where a complex is formed between the template (T) and one or more functional monomers (FM). It was proposed by Karim *et al.*<sup>77</sup> that more stable T-FM complexes result in highly selective MIPs. Therefore, the choice of functional monomer is critical to the performance of the MIP. Selection of the most appropriate functional monomer through trial using a synthesis - evaluation approach is a potentially laborious and time consuming process because of the the extensive range of commercially available functional monomers that may potentially interact with the template. MIP preparation is further complicated by additional requirements placed on other formulation components; a cross-linker (XL) that does not interact with the template and a porogen that dissolves all MIP reagents (T, FM and XL) and holds all species in solution to maximise resultant polymer porosity<sup>59</sup>.

Optimisation of the performance of an imprinted polymer is a challenge and generally only possible after extensively investigating different combinations of

monomers, cross-linkers and solvents. From these results, it is then possible to determine the combinations that yield a highly selective MIP. It is unrealistic however, to attempt to prepare and evaluate a wide range of MIP formulations, as conventional polymer synthesis is laborious and time consuming. Template availability may also be limited, thereby restricting the ability to adopt this approach. This has resulted in a tendency to utilise only those monomers that have previously worked or that have been previously reported by other researchers. Subsequently, this has led to the development of a range of approaches to optimise MIP formulations in the cheapest and least labour intensive way. Such approaches include virtual imprinting<sup>75;105;106</sup>, semi-empirical calculations<sup>3</sup>, thermodynamic studies that determine the energy of template-monomer complexation<sup>107;108</sup>, spectroscopic analysis including nuclear magnetic resonance (NMR)<sup>63;64</sup>, UV-Vis<sup>72;73</sup> and FTIR<sup>37</sup>, chemometric methods<sup>40</sup> and combinatorial screening<sup>60-62;105</sup>.

In an attempt to develop a more rational approach to the design of a MIP for benzylpiperazine (BZP) (Figure 3.1), our group have sought the use of a commercially available modelling package, Spartan '04, coupled with NMR spectroscopic analysis to identify favourable T-FM interactions. The modelling package enables the interactions of functional monomers with BZP to be quantitatively compared at different ratios to identify potentially favourable cluster stoichiometries. NMR analysis can then be used to confirm the existence and strength of the T-FM interactions to further assist in T:FM ratios.

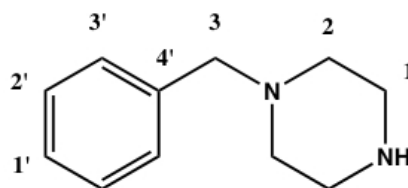


**Figure 3.1:** Chemical structure of BZP depicting the numbering system used in NMR investigations.

The behaviour of a number of commercially available monomers with the BZP template were examined by molecular modelling to identify favourable T:M clusters prior to synthesis. The selected functional monomers were then subjected to a secondary pre-synthetic screening involving NMR experiments to determine

the nature of T-FM interactions (NMR titration) and the stoichiometry of the predominant T-FM cluster (Job's plot).

## 3.2 Results and Discussion

### 3.2.1 Computer Generated Molecular Modelling Data

#### 3.2.1.1 Selection of Monomers

Our initial experiment utilised molecular modelling to identify monomers that favourably interacted with BZP. To achieve this, a virtual library of monomers with residue groups capable of non-covalent interactions with the template was created. Ten monomers were selected and screened with BZP in template:monomer (T:M) ratios of 1:1 through to 1:6 allowing us to determine the most favourable monomers (determined by calculating the system interaction energy) and the predicted optimum T:M ratio. The monomers modelled included acrylic acid (AA), methacrylic acid (MAA), acrylamide (AAm), methacrylamide (MAAm), 4-vinylpyridine (4VP), styrene (Sty), itaconic acid (IA), 2-hydroxyethyl methacrylate (HEM), N,O-bismethacryloyl ethanolamine (NOBE)<sup>80;84</sup> and 7-hydroxy-4-methylcoumarin acrylate (HMCA). These structures are presented in Figure 3.2. Calculations were performed using Spartan '04 software with semi-empirical AM1 theory.

The data obtained from individual modelling experiments included the heat of formation ( $\Delta H_f$ ) values.  $\Delta H_f$  values for the template, the corresponding monomer clusters (one through six units) and each template-monomer cluster stoichiometries were individually calculated. These  $\Delta H_f$  values were then entered into equation 1.1 producing an enthalpy of formation value designated a system interaction energy ( $\Delta E$ ) for each template-monomer cluster. Calculated  $\Delta E$  values showing favourable T:M clusters (cluster energy < reactant energy) are indicated by negative values; thus the more negative the  $\Delta E$  value the more favourable the cluster formation<sup>109;110</sup>. The  $\Delta E$  values for each T:M ratio can be observed in Table 3.1. Analysis of these values then allowed us to identify the most favourable T:M clusters.

NOBE obtained the most favourable interaction with a negative  $\Delta E$  of -30.2 kcal/mol at a ratio of 1:6. From examination of the modelling image obtained for the 1:6 ratio, it was possible to see that in addition to T-FM interactions, a number of monomer-monomer (M-M) interactions were occurring. This monomer

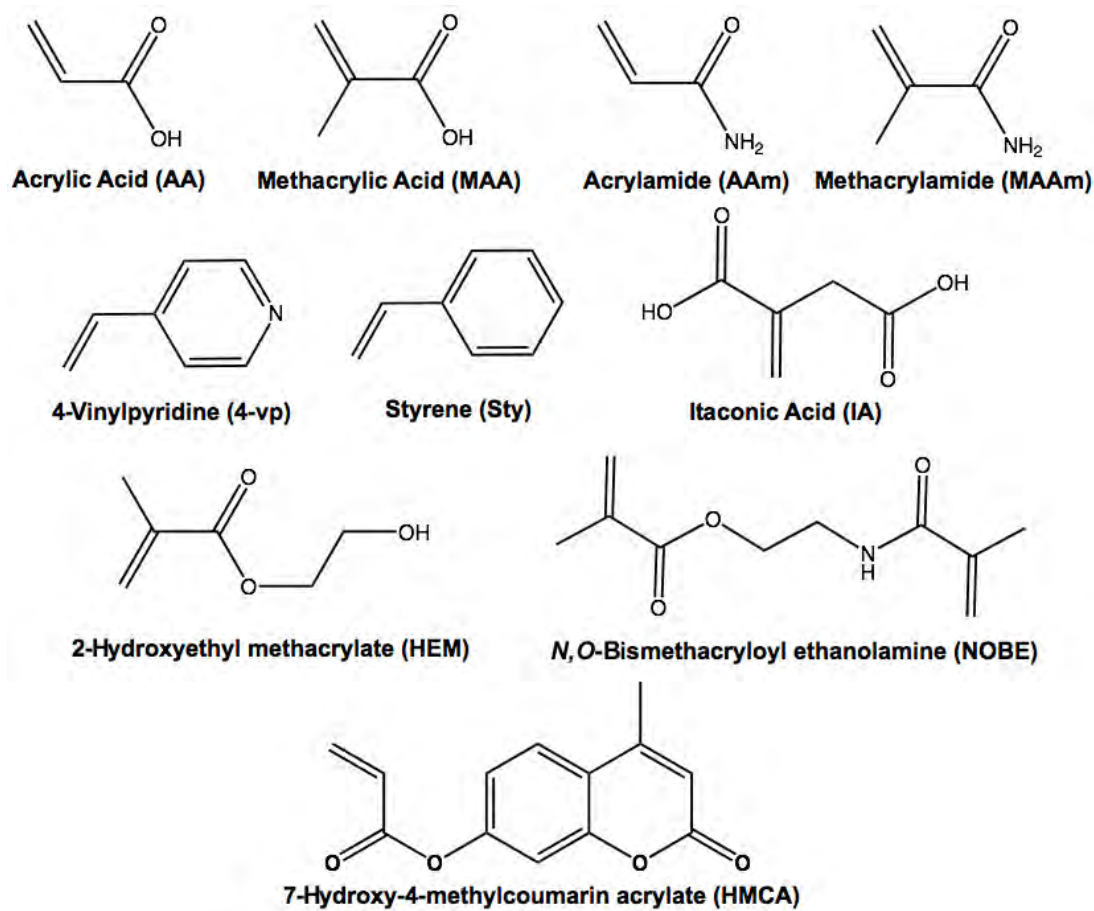


**Figure 3.2:** A library of potential functional monomers for the preparation of a MIP for BZP template.

## 3.2 Results and Discussion

**Table 3.1:** Calculated  $\Delta E$  values for the template-monomer clusters from molecular modelling studies. All calculations were performed in triplicate.

Monomer Units	$\Delta E$ values for the T:FM clusters (kcal/mol)									
	AA	MAA	AAm	MAAm	4VP	Sty	IA	HEM	NOBE	HMCA
1	-4.5	-6.1	-2.6	-2.5	-1.7	-1.0	-4.0	-5.0	-4.5	-1.9
2	-3.5	-4.2	-2.6	-2.7	-2.4	-2.6	-1.7	-1.2	-1.0	-2.5
3	-0.6	-6.6	-1.8	1.9	-2.8	-3.1	-1.8	-1.0	-0.4	-3.2
4	2.8	-5.7	-2.1	1.1	-3.3	-3.3	-1.1	-0.8	1.2	-1.2
5	0.5	-7.5	1.2	1.7	-3.9	-3.6	-1.4	-1.0	-1.4	-1.8
6	1.0	-7.0	-2.9	2.3	-3.9	-7.3	-3.0	1.6	-30.2	0.1

$$\Delta E_{Interaction} = \Delta H_{fTemplate-Monomercluster} - [\Delta H_{fMonomercluster} + \Delta H_{fTemplate}]$$

is a special type of monomer, capable of acting as the functional monomer as well as the cross-linker and thus, would be present in the polymer in a ratio of 1:20. As it is not possible to calculate the  $\Delta E$  value at this ratio, further BZP:NOBE interaction studies were conducted using spectroscopic, i.e. NMR, techniques.

Methacrylic acid (MAA) showed to be one of the most favourable monomers in the library as it gave the largest negative  $\Delta E$  values at all T:FM ratios examined. The 1:3 T:FM ratio was the most favourable ratio with a  $\Delta E$  value of -6.6 kcal/mol. Analysis of the modelling images for both the 1:1, 1:2 and 1:3 clusters given in Figure 3.3 showed that one monomer unit is capable of forming moderately strong hydrogen bonds (2.208 Å and 2.562 Å) with BZP in two positions, between the acidic hydrogen and carbonyl group of MAA and the -NH (Figure 3.3 (A)). When 2 monomer units are present, monomer-monomer interactions begin to occur, however, the hydrogen bonds between the monomers and BZP have strengthened (2.277 Å and 2.109 Å) (Figure 3.3 (B)). With the addition of a third monomer unit additional monomer-monomer interactions became evident (Figure 3.3 (C)). The increase in the magnitude of  $\Delta E$  values diminishes with the addition of each successive monomer unit suggesting that while the additional monomer units act through monomer-monomer interactions to stabilise the complex the value of this effect is greatly reduced beyond  $n = 2$  or 3 units.

Monomer AA behaved differently compared to MAA. The most favourable

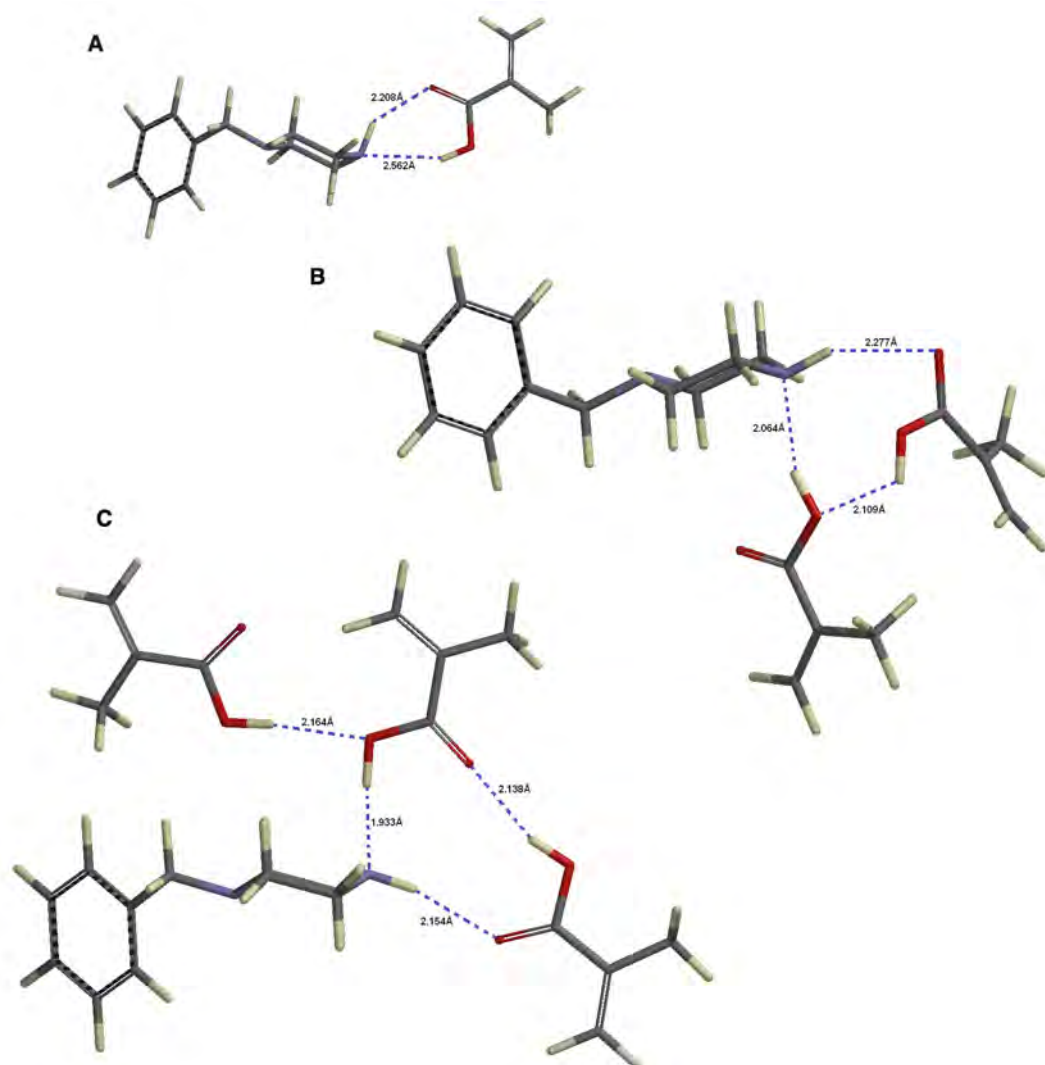


**Figure 3.3:** Computer generated molecular modelling images of BZP:MAA 1:1 (A), 1:2 (B) and 1:3 (C) for the geometry optimised BZP:FM clusters.

interaction observed was at a 1:1 T:FM ratio with -4.5 kcal/mol. In contrast to MAA, the addition of subsequent monomer units resulted in unfavourable positive  $\Delta E$  values. These results were unexpected as there is no significant difference in structure between AA and MAA. Examination of the modelling images showed that in T:FM ratios greater than 1:2, monomer-monomer interactions were present. The modelling images of 1:1, 1:2 and 1:3 BZP:AA ratios are presented in Figure 3.4. It is suggested that the presence of the methyl group in MAA, sterically hinders the monomer unit, thereby limiting self-association, leading instead to association with the BZP amine units and consequently forming stronger H-bonds. By contrast, AA, appears to preferentially self-associate in favour of interactions with BZP. This was supported further, as it was observed that interactions between AA and the tertiary amine of BZP were evident. These interactions were not present in MAA, suggesting significant steric hindrance.

The modelling results also showed less favourable results for AAm and MAAm with -2.9 kcal/mol (1:6 T:FM ratio) and -2.7 kcal/mol (1:2 T:FM ratio) as the most negative  $\Delta E$  values for BZP:AAm and BZP:MAAm, respectively. For all other BZP:MAAm clusters tested, positive  $\Delta E$  values were obtained, while  $\Delta E$  values for other BZP:AAm clusters remained around the low negatives as with the 1:6 T:FM value.

For the functional monomer HEM, a  $\Delta E$  value of -5.0 kcal/mol was obtained at a T:FM ratio of 1:1, however with the addition of a second monomer unit, the  $\Delta E$  value was significantly reduced to -1.2 kcal/mol, with subsequent monomer additions producing similar results. The drop in interaction energy was attributed to the bulkiness of the HEM system. One monomer unit is able to form a two point acceptor / donor interaction with the BZP secondary amine unit through the HEM carbonyl (2.206 Å) but the presence of additional HEM units breaks the C=O association and leads to an increase in the N-HO bond interaction (2.701 Å) and prevents BZP:HEM interactions from occurring. Figure 3.5 shows the bond changes between the BZP:HEM 1:1 and 1:4 T:FM clusters.

For the diprotic acid itaconic acid (IA)  $\Delta E$  values obtained were all just over -1 kcal/mol except for the 1:1 and 1:6 T:FM ratio, which had -4.0 kcal/mol and -3.0 kcal/mol, respectively. The modelling image for the BZP:IA 1:1 cluster (Figure 3.6) show a two point interaction with the BZP secondary amine, however,

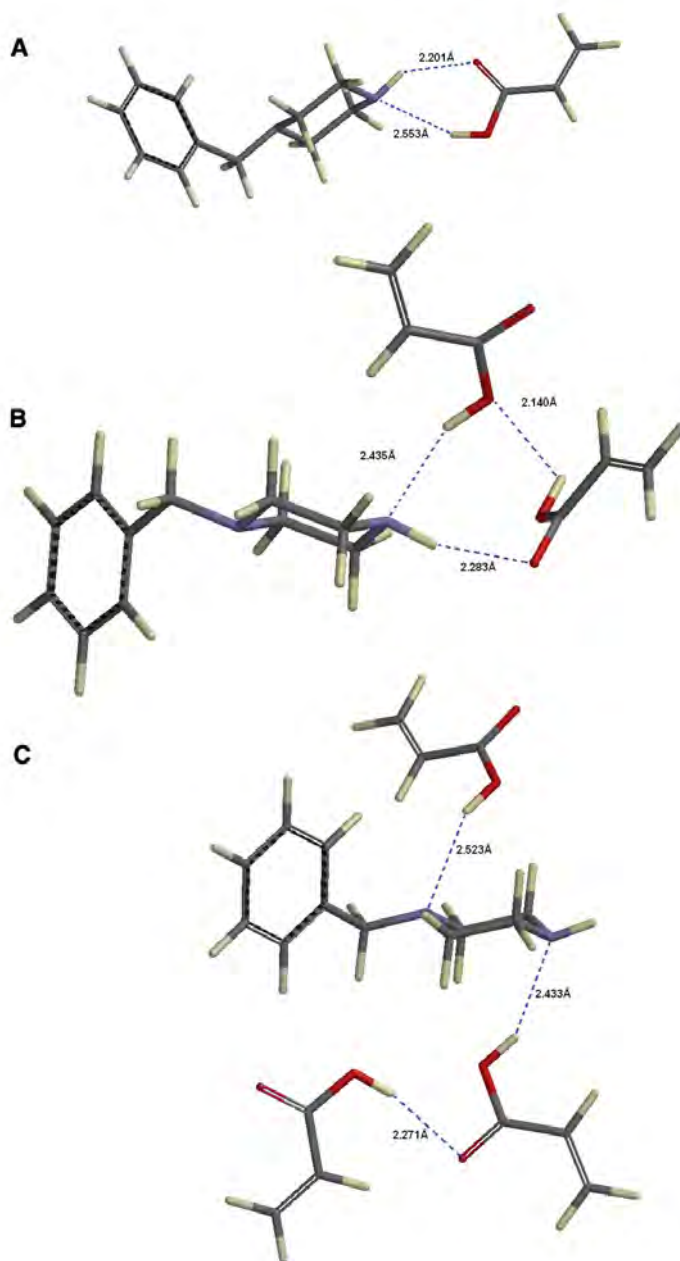


**Figure 3.4:** Computer generated molecular modelling images of BZP:AA 1:1 (A), 1:2 (B) and 1:3 (C) for the geometry optimised BZP:FM clusters.

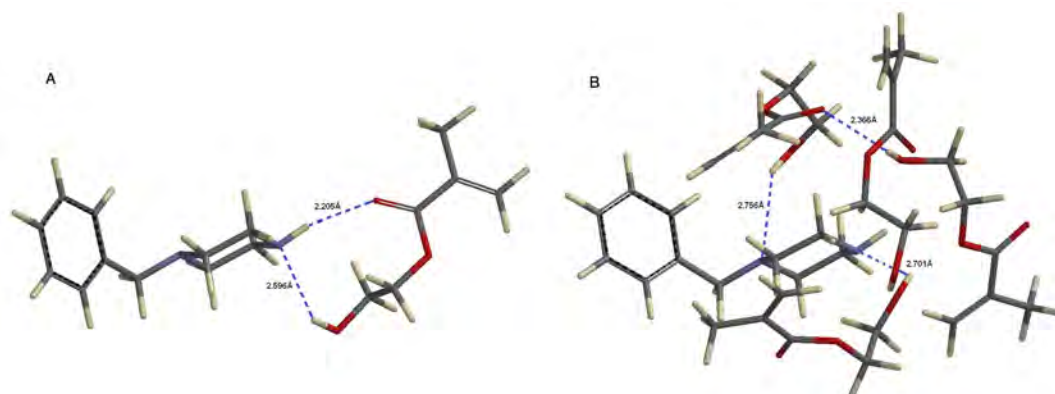


**Figure 3.5:** Computer generated molecular modelling images of BZP:HEM 1:1 (A) and 1:4 (B) for the geometry optimised BZP:FM clusters.

only one IA carboxyl units participates in the interaction. With the addition of subsequent monomer units, the hydrogen bond lengths increased from 2.221Å and 2.539Å for BZP:IA 1:1 cluster to 2.222Å and 2.585Å for the BZP:IA1:2 cluster, suggesting the presence of steric hindrance between the IA units.

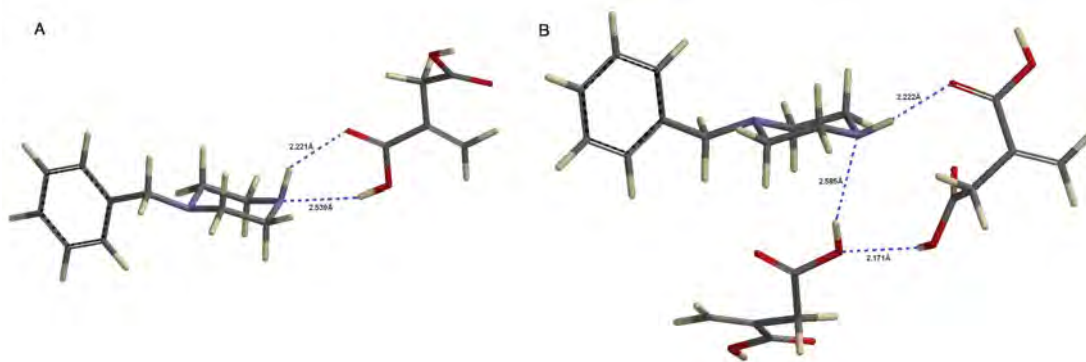


**Figure 3.6:** Computer generated molecular modelling image of BZP:IA 1:1 (A) and 1:2 (B) for the geometry optimised BZP:FM cluster.

There was a trend of increasing negative  $\Delta E$  values observed for the aromatic FMs, styrene and 4-vinylpyridine, as the number of FM units increased. This behaviour is believed to be due to monomer-monomer interactions stabilising and “caging”. There is no functional group present in this system to produce hydrogen bond association. However, it is evident that weak non-covalent interactions, such as pi-pi interaction, are occurring as the  $\Delta E$  values are negative. The AM1 level

of theory is not capable of showing pi-pi interactions and thus, their presence could not be confirmed. The preferred position of the functional monomers was around the piperazine ring forming a cage like structure. This can be seen in the modelling images for 4VP and Sty at a 1:3 T:FM ratio given in Figure 3.7.

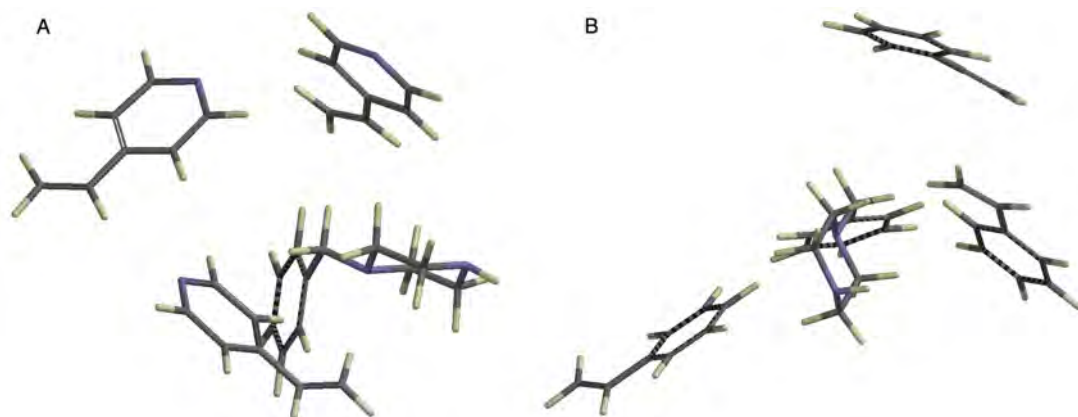


**Figure 3.7:** Computer generated molecular modelling images of BZP with 4-vinyl pyridine (4-VP) (**A**) and styrene (STY) (**B**) for the geometry optimised 1:3 BZP:FM clusters.

Finally, molecular modelling was conducted to determine whether 7-hydroxy-4-methylcoumarin acrylate (HMCA) would favourably interact with BZP and thus could be utilised as a functional monomer for the preparation of a fluorescent MIP for BZP. From the results, it can be seen that the most favourable BZP:HMCA ratio was 1:3 with a  $\Delta E$  of -3.2 kcal/mol. The molecular modelling image of the 1:3 BZP:HMCA complex given in Figure 3.8 shows one point of interaction occurring between the secondary amine and one HMCA unit, with a bond distance of 2.249Å. A second interaction was observed between the hydrogen on the bridging carbon between the two rings and a carboxylate group of a subsequent HMCA unit. Finally, there were a number of monomer-monomer interactions occurring. It is proposed that it is the combination of all interactions identified within the BZP:HMCA 1:3 cluster that is stabilising the complex.

From the modelling data it is evident that the most favourable point of interaction was at the secondary amine forming a N-HO or H-O hydrogen bond with the FM. With the acidic monomers and HEM, both these bonds were forming between BZP and one FM unit producing a cluster with a large negative enthalpy

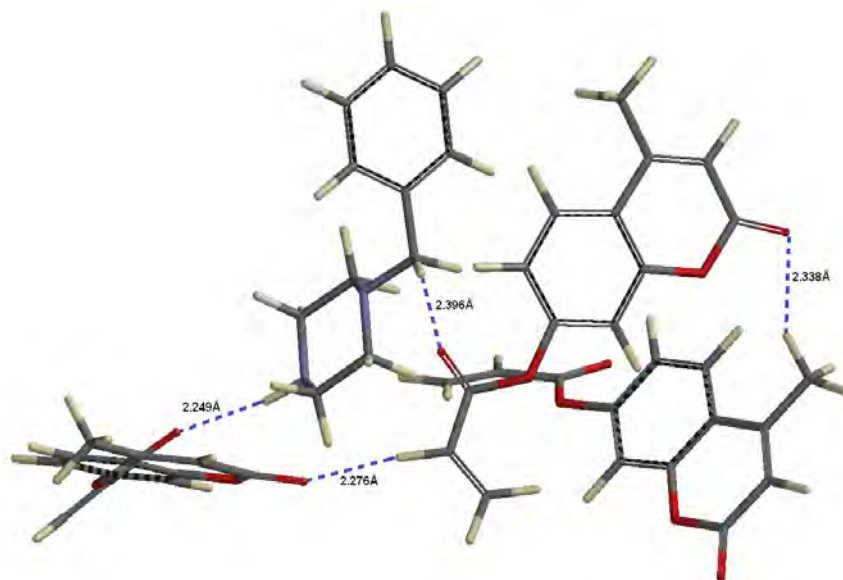


**Figure 3.8:** Molecular modelling images of BZP:HMCA for the computer generated images of the geometry optimised 1:3 BZP:HMCA cluster.

of formation. As a result, the most favourable T:FM ratio for AA, MAA, IA and HEM was 1:1. Some interactions were observed at the tertiary amine however, this was only at an excess of monomer units. With smaller FMs, additional units present in the polymerisation process can facilitate in defining the cavity, through additional H-bonding. The result of this, would be a more specific polymer toward the template.

## 3.2.2 NMR Analysis

### 3.2.2.1 Template-Functional Monomer Investigations

Results of the molecular modelling showed NOBE, AA, MAA, IA, HEM and HMCA interacting favourably with BZP. Accordingly, interactions of these monomers with BZP were further verified by NMR analysis, specifically  $^{13}\text{C}$  NMR titrations and Jobs plots (mole-ratio method).

Figure 3.9 show the results of the NMR studies conducted for the BZP/MAA system. The  $^{13}\text{C}$  NMR titration revealed that MAA interacted with BZP at its secondary amine site as indicated by the movement of the resonance of the car-

bons in the piperazine ring adjacent to the amines (Figure 3.9(A)). This point of interaction was also observed in the modelling (Figure 3.3(A)) of this system. With the addition of the first MAA molar equivalent, significant peak movement was experienced by the two carbons C1 and C2, with the largest shift exhibited by carbon 2, shifting 5.79 ppm up-field. However, with the addition of subsequent molar equivalents there was only a small shift experienced. As evident in Figure 3.9 (B), the BZP:MAA ratio showing the most favourable interaction is 1:1 reaching an optimum at 1:4.

A Job's plot was performed to formally establish the stoichiometry of the most predominant BZP:MAA complex. The results obtained in this experiment were manipulated as per the Job's method and plotted<sup>111</sup>. Figure 3.9(C) shows that the most predominant stoichiometry of the BZP:MAA complex is 1:1. The Job's plot supported the NMR titration, which showed minimal peak shifting after the addition of the first MAA molar equivalent. It would seem that both NMR experiments were able to detect the interaction between the NH of BZP and the acidic H of MAA. Molecular modelling, however, presented previously (Figure 3.3) suggested that other interactions, for example between the tertiary amine and the acidic H of MAA, may also contribute to the over-all T:M interactions such that higher T:FM ratios, i.e. 1:3 to 1:5, are shown to be more favourable stoichiometries than 1:1.

The <sup>13</sup>C NMR titration for BZP with IA also showed that IA interacted with BZP. The interactions were again located at the piperazine ring of BZP and were observed by the shifting of the carbon peaks adjacent to the amine groups (C1, C2 and C3 on BZP) (Figure 3.10(A)). The maximum shift observed was on carbon 2, which shifted 4.93 ppm up-field (Figure 3.10(B)). This shift was slightly smaller than that observed in the BZP:MAA titration for the same carbon. The modelling image, previously presented in Figure 3.6 (A), showed the hydrogen bond distance between the IA carbonyl oxygen atom and the -NH of BZP to be 2.221Å, which is slightly longer, 2.208Å, than the identical point of interaction between BZP and MAA (Figure 3.3(A)). This slightly smaller shift is consistent with the results obtained in the modelling, which showed the MAA complex to be stronger in nature. An alternate theory is that the solvent could be influencing the interaction<sup>88</sup>, as MAA was analysed in CHCl<sub>3</sub> while IA in DMSO. It has been

### 3.2 Results and Discussion

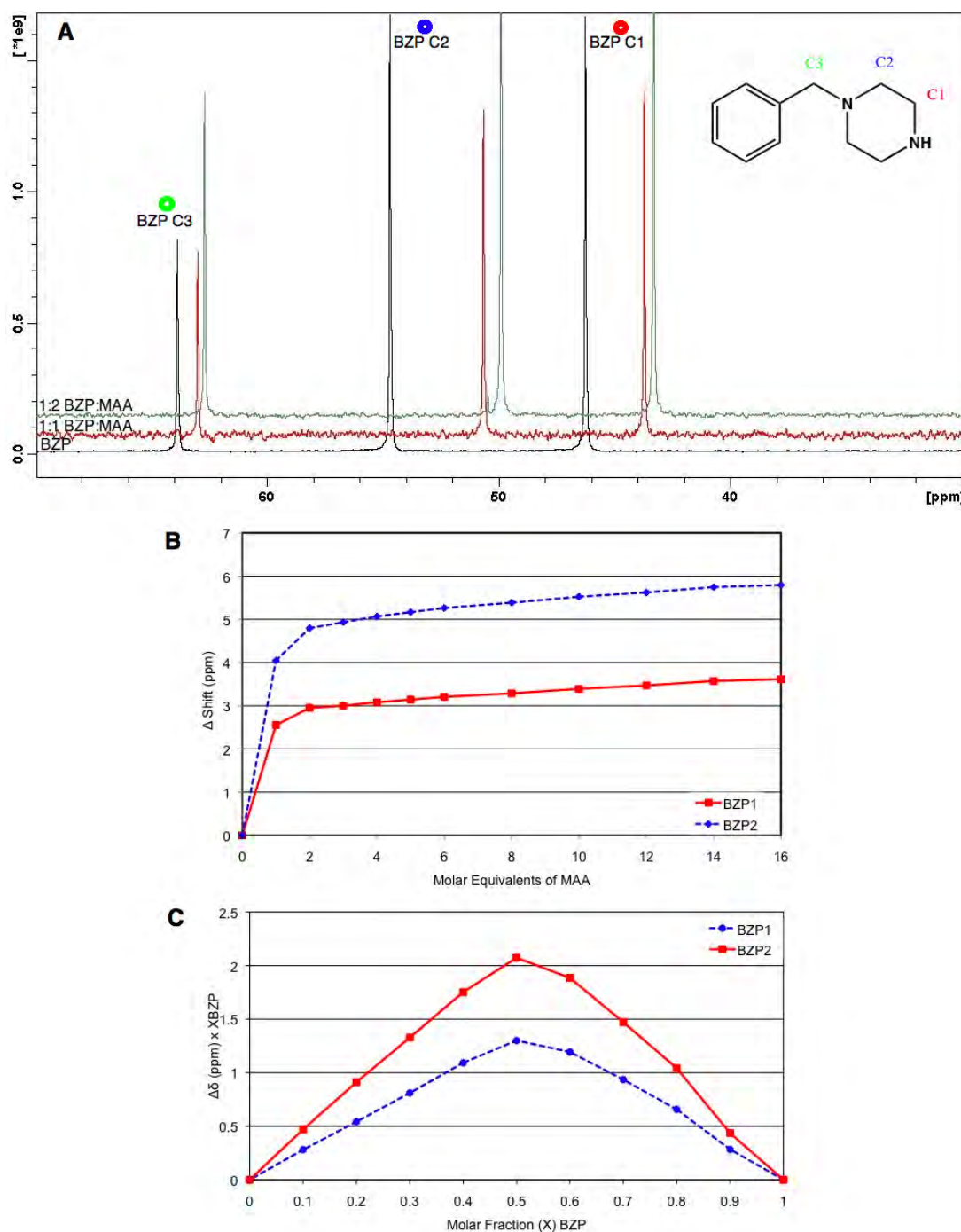


**Figure 3.9:** NMR analysis of BZP with MAA showing (A) the  $^{13}\text{C}$  NMR spectra for the NMR titration of BZP with MAA at a T:FM ratio of 1:0, 1:1 and 1:2 BZP:MAA, (B) the changes in chemical shift of carbons 1 and 2 on BZP as a function of increasing MAA concentration, and (C) Job's plot of two selected BZP carbon s (C1 and C2) in the presence of MAA showing the predominant cluster stoichiometry as 1:1.  $^{13}\text{C}$  NMR spectra obtained at  $28^\circ\text{C}$  in deuterated chloroform.

previously shown by Dong *et al.* using  $^1\text{H}$  NMR that the H-bond, the major force in molecular recognition, is affected by the solvent.

The stoichiometry of the BZP:IA complex was determined via Job's method using  $^{13}\text{C}$  NMR. From the plot obtained presented in Figure 3.10 (C), it can be seen that the favoured complex is in a 1:1 T:FM ratio a result consistent with both the modelling and the NMR titration outcomes.

$^{13}\text{C}$  NMR titration and Job's plot were also performed with BZP and AA. The NMR titration showed that, once again, the interactions occurred between the amine group of BZP and the carboxyl group of AA. This can be observed in Figure 3.11 (A). The maximum shift observed was on carbon 2 of BZP, with a shift of 5.17 ppm, seen in Figure 3.11 (B). This suggests that AA is interacting with BZP in a similar way as MAA and IA. The Job's plot, Figure 3.11 (C), showed that the most favourable stoichiometry of the BZP:AA complex is 1:1. Both NMR experiments gave evidence to interactions occurring between the NH of BZP and the acid group of AA. The molecular modelling also suggested a similar point of interaction, previously seen in Figure 3.4. The modelling also indicated that the BZP:AA 1:2 ratio would be favourable, however interactions between monomers are contributing to the over-all stability of the complex.

The NMR results suggest that monomers MAA, IA and AA interact with BZP within a common site, that is the secondary (and more basic) NH. This is expected, as all three monomers are acids and thus would be creating an acid-base complex with the basic BZP.

The NMR titration for BZP with HMCA showed that the two compounds are capable of interacting with each other. However, the degree of interaction was considerably less than those observed between BZP and MAA, IA or AA. It can be seen in Figure 3.12 (A) that the maximum shift observed was 2.119 ppm after the addition of six HMCA molar equivalents, although the greatest shift observed was after the first molar addition of HMCA, shifting 1.784 ppm. When the results obtained for HMCA are compared to those of MAA (maximum observed shift of 5.79 ppm) it is possible to see there is less interaction occurring between HMCA and BZP and thus, less favourable as a FM. This weaker interaction could result in a polymer with less selectivity towards BZP.

The Job's plot, Figure 3.12 (B), in this instance, failed to detect the predom-

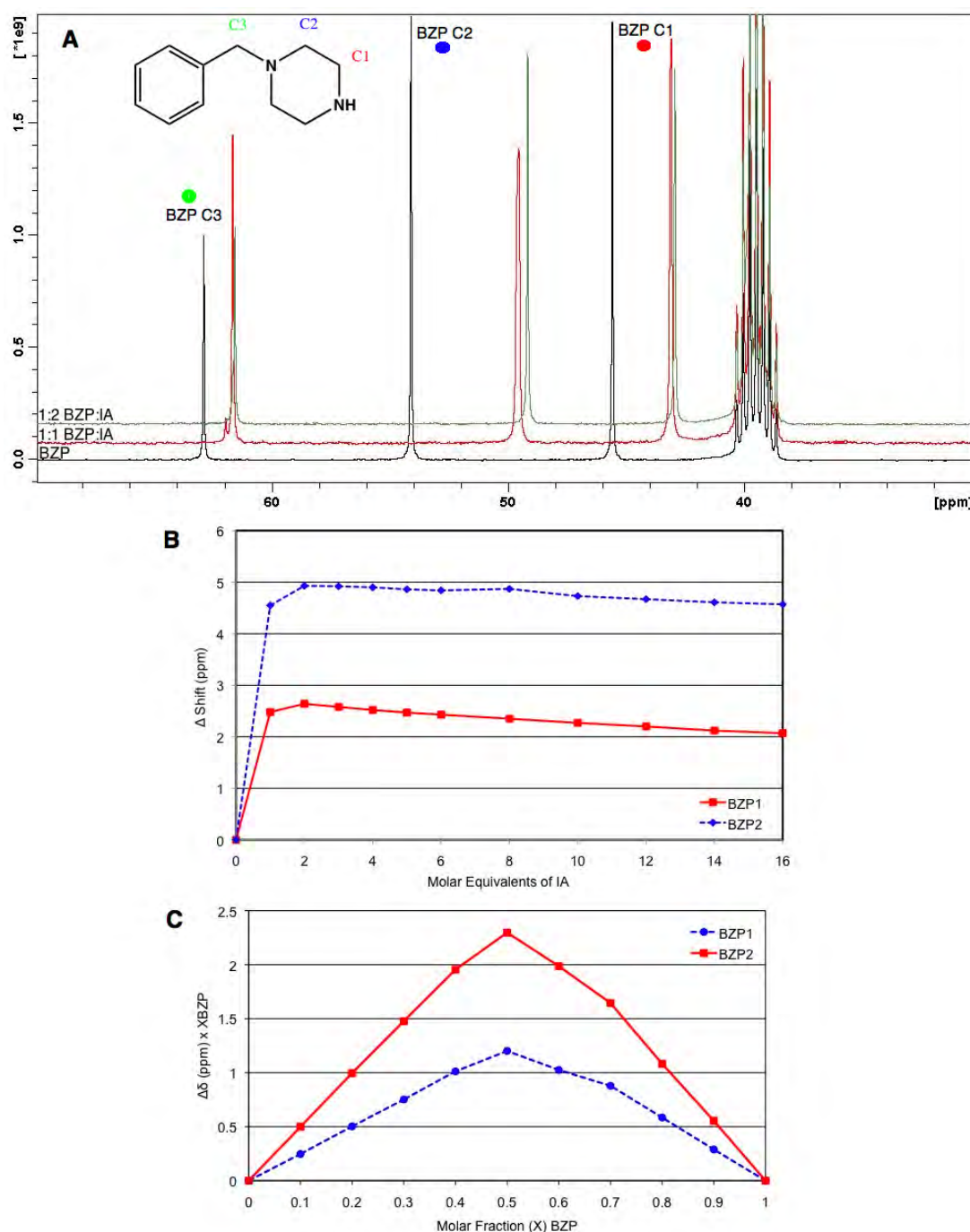


**Figure 3.10:** NMR analysis of BZP with IA showing (A) the  $^{13}\text{C}$  NMR spectra for the NMR titration of BZP with IA at a T:FM ratio of 1:0, 1:1 and 1:2 BZP:IA, (B) the changes in chemical shift of carbons 1 and 2 on BZP as a function of increasing IA concentration, and (C) Job's plot of two selected BZP carbon resonances (C1 and C2) in the presence of IA. Cluster stoichiometry is 1:1.  $^{13}\text{C}$  NMR spectra obtained at 28°C in deuterated DMSO.

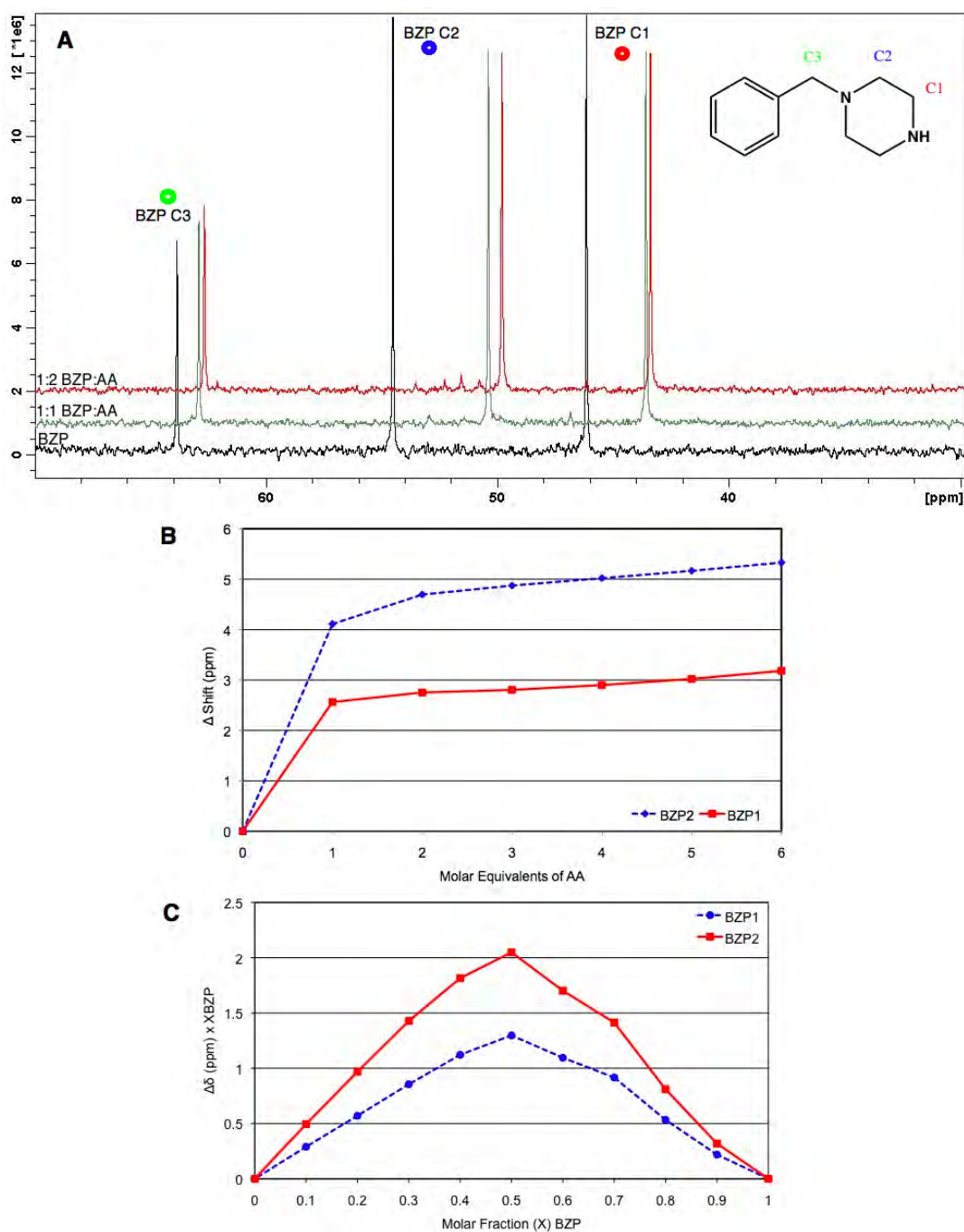


**Figure 3.11:** NMR analysis of BZP with AA showing (A) the  $^{13}\text{C}$  NMR spectra for the NMR titration of BZP with AA at a T:FM ratio of 1:0, 1:1 and 1:2 BZP:AA, (B) the changes in chemical shift of carbons 1 and 2 on BZP as a function of increasing AA concentration, and (C) Job's plot of two selected BZP carbon resonances (C1 and C2) in the presence of AA. Cluster stoichiometry is 1:1.  $^{13}\text{C}$  NMR spectra obtained at 28°C in deuterated chloroform.

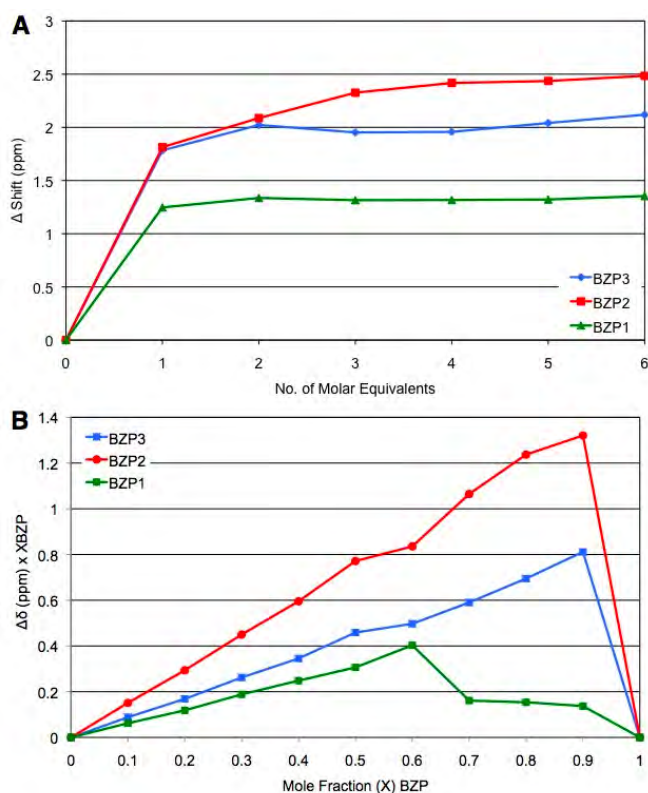


**Figure 3.12:** NMR analysis of BZP with HMCA showing (A) the changes in chemical shift of carbons 1 and 2 on BZP as a function of increasing HMCA concentration, and (B) Job's plot of two selected BZP carbon resonances (C1 and C2) in the presence of HMCA. Cluster stoichiometry was 9:1 BZP:HMCA.  $^{13}\text{C}$  NMR spectra obtained at 28°C in deuterated chloroform.

inant T:FM (BZP:HMCA) stoichiometry necessary for HMCA to act as FM as it showed that the pair tends to favour the formation of 9:1 BZP:HMCA complex. However, the results suggest that in order for HMCA to act as a FM, it has to be present in amounts larger than BZP during MIP preparation to induce the formation of BZP:HMCA complexes of ratios  $> 1:1$ . It is noteworthy that molecular modelling results point to favourable formation of BZP:HMCA complexes of  $< 1:6$  ratios.

The NMR titration performed with BZP and NOBE showed that there was minimal interaction occurring between BZP and NOBE. The maximum shift observed was experienced by BZP carbon 1, shifting 0.38 ppm. This data along with that obtained for BZP carbon 2 is presented in Figure 3.13. When these values were compared to the maximum shifts obtained for MAA (5.79 ppm) and EGDMA (0.806 ppm) it could clearly be seen that NOBE would be more suited as a cross-linking agent and not a functional monomer, Figure 3.14. The cross-linker is the predominant component within a MIP. If the cross-linker was to interact with the template a significant amount of non-specific binding would occur. Therefore, it is optimal to have minimal to no interaction between the template and cross-linker. This is what was observed for NOBE and EGDMA.

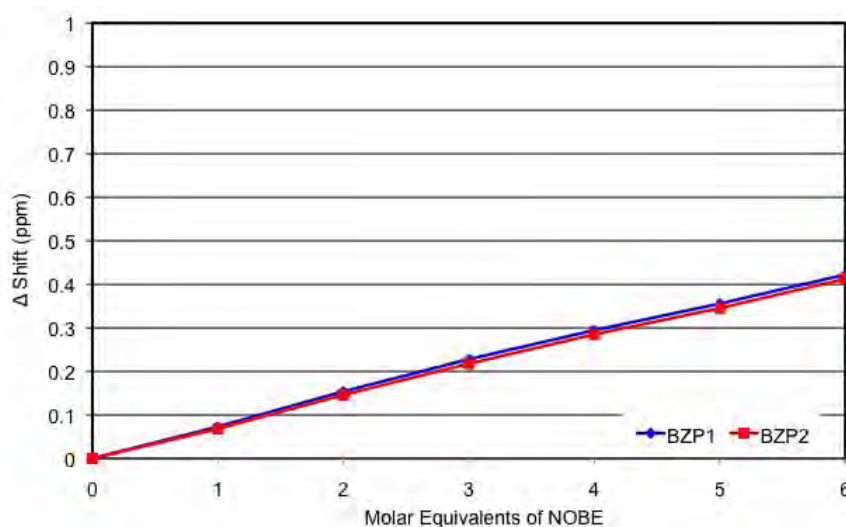


**Figure 3.13:** NMR titration of BZP with NOBE showing the changes in chemical shift of carbons 1 and 2 on BZP as a function of increasing NOBE concentration.

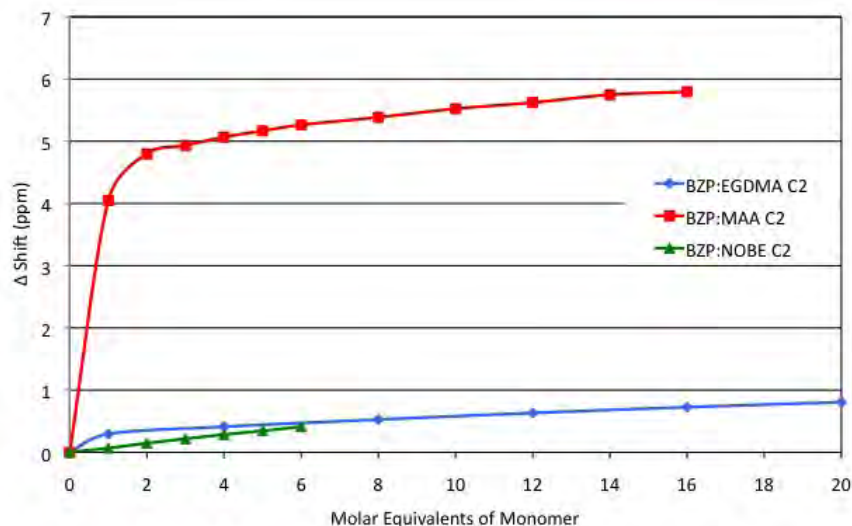


**Figure 3.14:** NMR titration of BZP with NOBE, MAA and EGDMA showing the changes in chemical shift of carbon 1 on BZP as a function of increasing monomer concentration.

### 3.2.2.2 Optimisation of the Cross-linker

The cross-linker makes up approximately 80% of the MIP. Consequently, this can be a large source of non-specific binding. Due to this, it is crucial that there are minimal interactions between the template and the cross-linker. To establish the extent of interaction between BZP and three common cross-linkers, EGDMA, TRIM and DVB (Figure 1.9), NMR titrations were performed.

The  $^{13}\text{C}$  NMR titrations for BZP with EGDMA showed minimal interactions were occurring between the two compounds (Figure 3.15). On the addition of the first molar aliquot of EGDMA there was an initial shift up-field of 0.294 ppm experienced by BZP C2. This was the most significant shift observed and suggests that EGDMA weakly interacts with the NH of BZP via H-bonding. This interaction was also observed in the molecular modelling of BZP with EGDMA presented in Figure 3.16. All subsequent aliquot additions produced an up-field shift of approximately 0.1 ppm or less with the maximum shift of 0.806 ppm observed at a BZP:EGDMA ratio of 1:20.

In the case of TRIM, BZP carbon 2 experienced the largest peak movement albeit minimal, with only a maximum of 0.625 ppm up-field shift observed at a

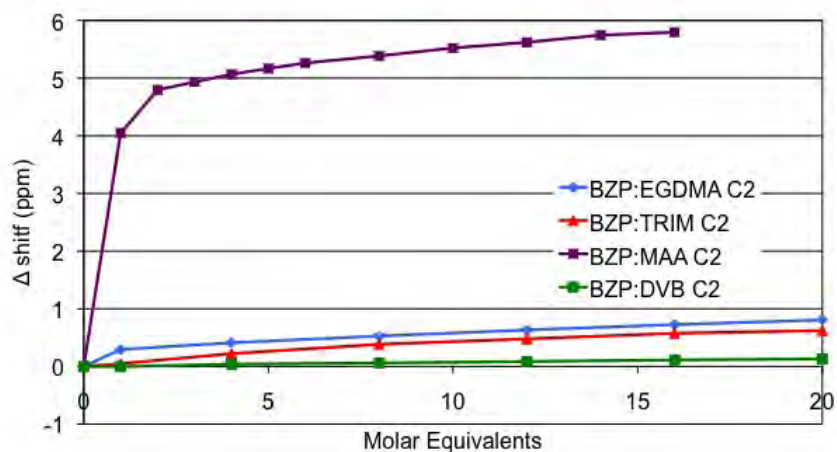


**Figure 3.15:** NMR titration of BZP with EGDMA, TRIM, DVB and MAA showing the most significant change in chemical shift experienced as a function of increasing EGDMA, TRIM, DVB and MAA concentration, respectively. MAA has been included for comparison



**Figure 3.16:** Computer generated molecular modelling image for BZP:EGDMA for the geometry optimised 1:1 cluster.

BZP:TRIM ratio of 1:20 (Figure 3.15). This result suggests that TRIM is also weakly interacting with the NH of BZP via H-bonding. The molecular modelling image produced for BZP:TRIM (Figure 3.17) showed this interaction. However, the bond distance between one carbonyl group of TRIM and the -NH of BZP was 2.437Å, which was slightly longer than the H-bond between BZP and EGDMA (2.389Å).

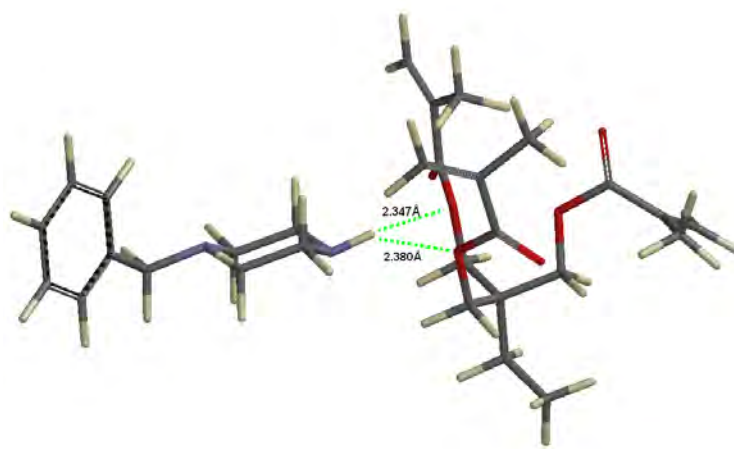


**Figure 3.17:** Computer generated molecular modelling image for BZP:TRIM for the geometry optimised 1:1 cluster.

Finally, Figure 3.15 also showed minimal interaction between BZP and DVB based on BZP C2 with a maximum shift of 0.132 ppm observed at a BZP:DVB ratio of 1:20. This result was expected, as DVB should have pi-pi interactions with the aromatic region of BZP. However, it was not possible to detect these interactions in the  $^{13}\text{C}$  spectra due to the complexity of assigning peaks in this region. Molecular modelling was performed to determine where points of interaction, if any, would occur. It can be seen in Figure 3.18 that there are no points of interaction between DVB and BZP. In conjunction to this, the aromatic rings are not aligned, suggesting that pi-pi stacking is not occurring in the modelling.

When these results were compared with the results obtained for the FM MAA, (Figure 3.15), it could clearly be seen that there was almost no interaction occurring for all three cross-linkers. From these results it was decided that all three cross-linkers were appropriate agents for polymer preparation. Subsequently they

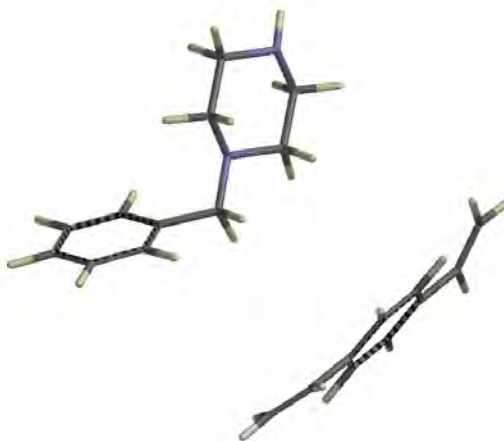


**Figure 3.18:** Computer generated molecular modelling image for BZP:DVB for the geometry optimised 1:1 cluster.

were investigated further for the preparation of MIP's.

## 3.3 Conclusions

Semi-empirical molecular modelling data suggested that the acrylic acid monomers MAA, AA and IA along with NOBE, HEM and HMCA would have favourable interactions with BZP. Estimated energies of interaction suggested optimum BZP:FM ratios of 1:1 for AA, IA and HEM, 1:3 for MAA and 1:6 for NOBE and <1:6 for HMCA.

NMR analysis of the above FMs confirmed favourable interaction of MAA, AA and IA with BZP showing optimum stoichiometry of 1:1, which can be attributed to the formation of an acid (FM)- base (BZP) complex. NMR titration showed the interaction of the fluorescent monomer HMCA with BZP to be less favourable than with MAA or AA. Job's experiment suggests favourable formation of BZP:HMCA >1:1 complexes, hence, BZP:HMCA ratios to be used for MIP preparation must be 1: >1. NMR results obtained for NOBE showed minimal interactions occurring between NOBE and BZP. The data suggested that this monomer would be better suited as a cross-linking agent and not a FM.

NMR analysis showed minimal interactions between BZP and cross-linking agents EGDMA, TRIM and DVB, hence any of these crosslinkers are suitable to be used for the preparation of BZP MIPs.

# 4

## Preparation of Benzylpiperazine MIPs: The Self-assembly (non-covalent) Approach

### 4.1 Introduction

The non-covalent or self-assembly approach to imprinting requires four key components for fabricating MIPs: the template, functional monomer (FM), cross-linker (XL), and the porogen. The approach utilises weak interactions including hydrogen bonding, ion pairs, dipole-dipole interactions or van der Waals forces to hold the template in place. Therefore it is essential that the FM has strong interactions with the template. It is also essential that interaction between the template and the cross-linker is minimised, which can contribute to non-specific binding in the bulk polymer.

Non-covalent polymers are prepared by three steps: pre-association of the functional monomer with the template via non-covalent self-association, polymerisation of the template-monomer adduct and finally, removal of the template from the polymer (Section 1.2.3.2).

The approach is more favourable when time and cost is important, as the approach is quick and simple, requiring no chemical synthesis to prepare the template-monomer adduct or rebind the template back into the polymer. In

addition, the absence of a formal covalent association between the template and functional monomer has made the approach more popular, resulting in a greater diversity of templates being imprinted.

There are disadvantages associated with this technique, which is the result of the simplistic and rapid nature of the method. Decreased selectivity is often observed resulting from difficulties in controlling the cavities formed, the polymerisation conditions are restricted and need to be optimised, as does the stoichiometry of the template-monomer system.

This chapter deals with the development, optimisation and characterisation of non-covalent BZP imprinted polymers. The MIP formulation and performance were optimised by selecting the appropriate cross-linkers and FMs. Three FMs: methacrylic acid (MAA), itaconic acid (IA) and acrylic acid (AA), chosen on the basis of their favourable interaction with BZP (Chapter 2) were investigated at various ratios (1:1, 1:2 and 1:4) in two different porogens ( $\text{CH}_3\text{CN}$  and  $\text{CHCl}_3$ ) with respect to their capacity to bind BZP, optimum binding time, and type and number of binding sites. The performance of the MIPs was also correlated to their morphology, surface area, porosity and their swelling behaviour.

All MIPs were prepared using AN and  $\text{CHCl}_3$  as porogens and were chosen as all components were soluble. Their selection was crucial as the solvent utilised for polymerisation is known to influence the complexation of the template with the functional monomer as well as affect the polymer's morphological properties, such as porosity and surface area<sup>59;87</sup>. Hence, the ultimate requirement of porogen selection was that all components must be soluble so that the polymer composition can be guaranteed.

## 4.2 Results and Discussion

### 4.2.1 Selection of Cross-linker

The cross-linking agent makes up approximately 80% of the MIP on a per mole basis, and thus potentially has the greatest influence on non-specific binding. To achieve the best performance, non-specific binding interactions between the MIP and template must be controlled by choosing a cross-linker that has minimal interaction with the template.

Experiments to determine the affinity of BZP with three common cross-linkers, EGDMA, TRIM and DVB (Figure 1.9) were conducted. These cross-linkers were polymerised in AN and  $\text{CHCl}_3$  in the absence of the template and functional monomer. The resulting polymers were ground, with the fraction between 32 and 63  $\mu\text{m}$  collected and extracted in methanol to remove any non-polymerised cross-linker. The polymers were then used to bind BZP from 1.0 mL of a 0.8 mM solution in both AN and  $\text{CHCl}_3$  for 30 minutes. By varying the amount of polymer used in the binding assays, it was possible to determine the polymer concentration at which the minimum and maximum amount of BZP binding occurred.

As shown in Figure 4.1 (A), the EGDMA polymers bound in AN produced negative BZP up-takes. Negative binding could be the result of either solvent evaporation or solvent up-take by the polymer (swelling), resulting in effectively concentrating the BZP in the remaining non-occluded solvent. As these results were observed in AN (b.p.  $82^\circ\text{C}$ ) and the bound solutions were analysed immediately after binding, solvent evaporation could not have been the major cause for the observed results. In addition, these EGDMA-prepared polymers were observed to swell in AN (3% swelling after 1 hour) as a result of AN uptake.

The same EGDMA polymers gave minimal BZP binding in  $\text{CHCl}_3$  (Figure 4.1 (B)). The maximum amount of BZP up-take obtained was 6%, observed in the  $\text{CHCl}_3$  prepared and bound polymer when 5 mg of polymer was used. As the polymer mass increased, the amount of BZP bound dropped off, resulting in negligible binding for 30 mg polymer. Similarly, the AN prepared EGDMA polymer gave BZP binding of  $< 3\%$ , when bound in  $\text{CHCl}_3$ .

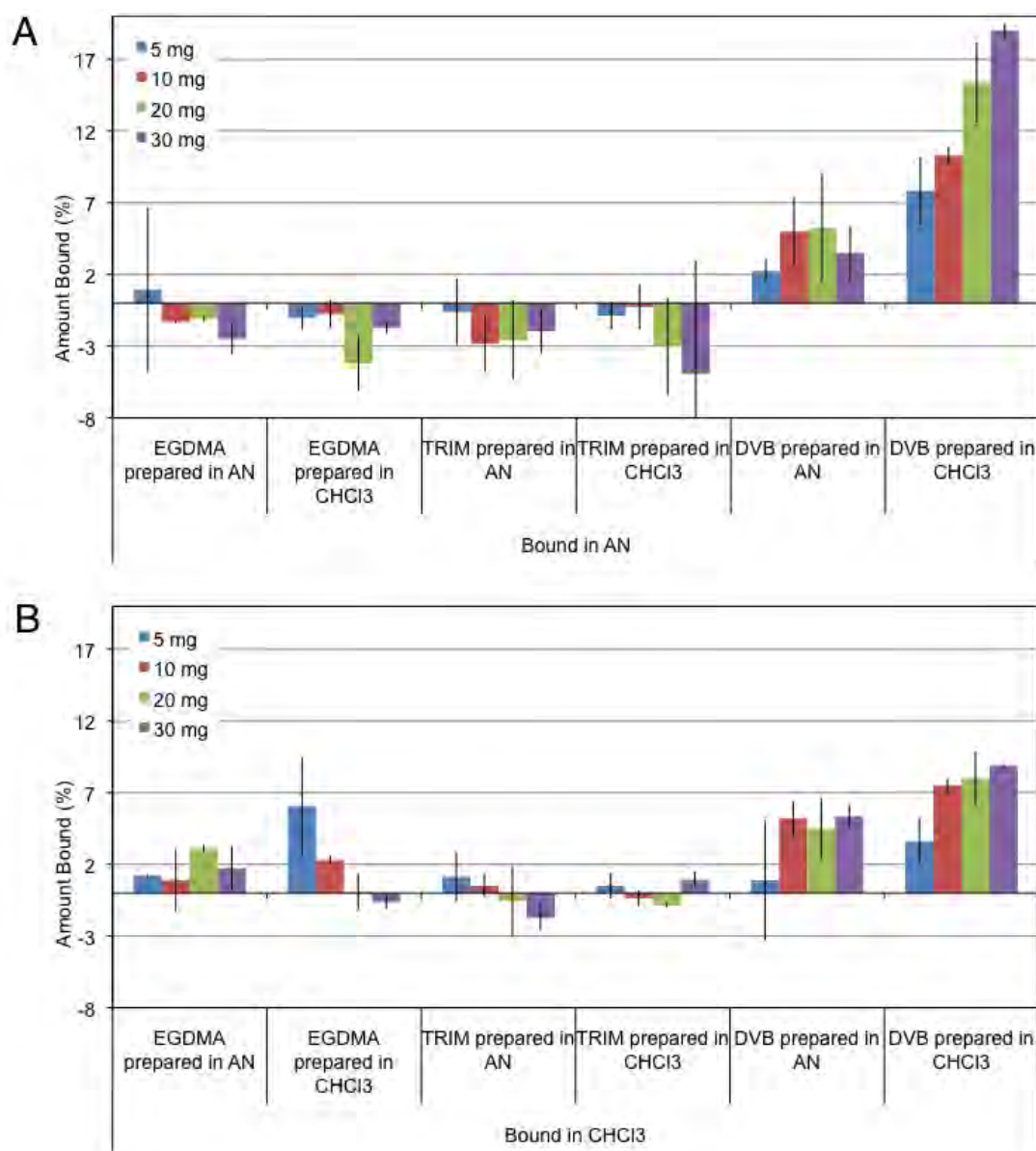


**Figure 4.1:** BZP binding results for EGDMA, TRIM and DVB polymers bound in (A) AN and (B) CHCl<sub>3</sub> using 1 mL of 0.8 mM solution after 30 minutes with all experiments performed in triplicate. Amount bound =  $\left(\frac{[Total] - [Free]}{[Total]}\right) \times 100$ .

As shown in Figure 4.1 (**A** and **B**), a trend similar to that observed for EGDMA polymers was observed for the TRIM polymers. Negative binding was observed for the polymers bound in AN, with the 30 mg of the  $\text{CHCl}_3$  prepared polymers exhibiting the most negative binding result of -4.9%. TRIM polymers were also observed to swell in AN, with up to 5% swelling observed after 1 hour. Minimal BZP binding was observed in  $\text{CHCl}_3$ , with 5 mg of the AN-prepared polymer exhibiting the highest BZP up-take of 1.1%.

The results obtained for the batch binding analysis for BZP with DVB polymers are presented in Figure 4.1 (**A** and **B**). From the results obtained for the DVB prepared polymers it can clearly be seen that significantly larger amounts of template was bound. For the AN-prepared polymer, a maximum of approximately 5% BZP up-take was observed when binding was performed in both AN and  $\text{CHCl}_3$ . This was observed for all masses tested greater than 5 mg. With 5 mg, reduced amounts of template up-take was obtained; binding in AN produced 2% template up-take, while binding in  $\text{CHCl}_3$  produced 0.9% template up-take. The polymer prepared in  $\text{CHCl}_3$  exhibited the largest BZP up-take, increasing linearly with polymer mass. Maximum up-take of 19% and 9% were obtained for 30 mg polymer when bound in AN and  $\text{CHCl}_3$ , respectively.

In this investigation, the cross-linker DVB was deemed unacceptable due to the large amount of binding observed. However, the results obtained for EGDMA and TRIM suggest that both polymers would be acceptable cross-linking agents. Solvent up-take was observed for both polymers, which would have reduced the amount of observed BZP binding in the MIPs. This would have produced errors in regards to the absolute amounts of BZP bound however, the imprinting factor is a relative term, based on the amount of binding of both MIP and NIP. As both polymers would have been exposed to the same effect, the amount of solvent up-take is negated. A limited amount of interaction was observed between BZP and EGDMA and BZP and TRIM, based on BZP up-take (this experiment) and the NMR spectroscopic study (Chapter 3). These results suggest that the amount of non-specific binding in the MIPs would most likely be minimal, a desirable requirement for a cross-linking agent. TRIM is a tri-functional cross-linker and thus, a highly cross-linked polymer is expected when used in polymer synthesis. This additional amount of cross-linking could promote or inhibit template

transfer to the binding cavities within the polymer, which could affect template binding. Conversely, EGDMA is a linear cross-linker, and expected to introduce less cross-linking to the polymer than TRIM. Consequently, two sets of BZP MIPs utilising EGDMA and TRIM were prepared. The polymer masses examined here ranged between 5 and 30 mg, the same range of polymer masses will be used for subsequent experiments.

### 4.2.2 Preparation of BZP Imprinted Polymers: Physical Characterisation

Having selected the appropriate cross-linkers, EGDMA and TRIM, BZP-imprinted polymers (MIPs) and control polymers (non-imprinted polymers known as NIPs) were prepared. The FMs investigated were IA, MAA and AA in three T:FM formulations: 1:1, 1:2 and 1:4. These FMs in the 1:1 and 1:2 ratios were selected due to their favourable affinity with BZP as observed in the molecular modelling and NMR analyses (Chapter 3). The 1:4 ratio was investigated as this is the ratio most frequently used in literature. The basis of using a 1:4 ratio is that the system is in a dynamic state during polymerisation. Consequently, complexes are not finite. It is also hypothesised that additional FM promotes complex formation, through Le Chatalier's principle. Again, the two porogens, acetonitrile (AN) and chloroform ( $\text{CHCl}_3$ ) were used to determine if the polarity of the solvent would affect the binding capabilities of the polymers. Finally, two different cross-linkers (EGDMA and TRIM) were incorporated to determine if the amount of cross-linking within the polymer would affect template up-take. All these permutations created a polymer library consisting of 30 different polymer combinations.

Due to the vast number of polymers prepared, a coding system was created to enable easy identification and referencing. The first part of the label is NC, referring to non-covalent polymer. This is followed by the FM, i.e. MAA, AA or IA, then the cross-linker that was used (EGDMA or TRIM), the ratio of BZP:FM (1, 2 or 4) and finally the porogen (A or C). For example, the polymer BZP:MAA 1:2 AN EGDMA has been labelled NC-MAA-EGDMA-2A.

The polymers were prepared in 7 mL of the porogen, with 40 mg of initiator

(AIBN) and polymerised at 60°C for 12 hours. The resulting MIPs were ground, with the fraction between 32 and 63  $\mu\text{m}$  collected, and extracted in acidified methanol (acetic acid) by Soxhlet extractor.

Scanning electron microscope (SEM) images, obtained for all polymers prepared, revealed macroporous surfaces. Based on these SEM images, no significant difference in surface morphology was observed between MIPs and NIPs. This is evident in the sample SEM images given in Figure 4.2, those of NC-MAA-EGDMA-2A MIP (**A**) and its corresponding NIP (**B**). The surface morphology of the MIPs were also observed not to be affected by the variation in FM and T:FM ratio (Figures 4.3 and 4.4).

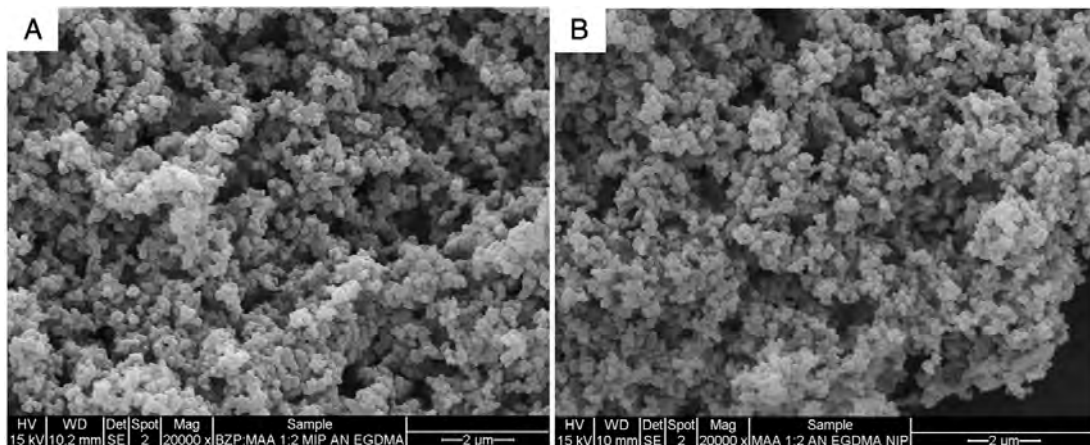


**Figure 4.2:** SEM images for NC-MAA-EGDMA-2A MIP (**A**) and NIP (**B**).

Differences, however, were observed between the EGDMA and TRIM prepared polymers. TRIM cross-linked polymer surface appears to be more compact, denser and less porous than the EGDMA cross-linked polymer. This is consistent with other reported results which showed that the nature of the cross-linker can affect the surface morphology of polymers<sup>59</sup>. Examples of an EGDMA (**A**) and TRIM (**B**) cross-linked polymer (NC-MAA-2A) are given in Figure 4.5.

The porogen was also observed to produce a significant difference in the surface morphology of the polymers. More porous macrostructure was obtained for polymers prepared in AN, in contrast, the surfaces of  $\text{CHCl}_3$  prepared polymers showed a smoother very dense surface with less pores and spaces. An example of an SEM image for an AN prepared polymer (**A**) and a  $\text{CHCl}_3$  prepared polymer

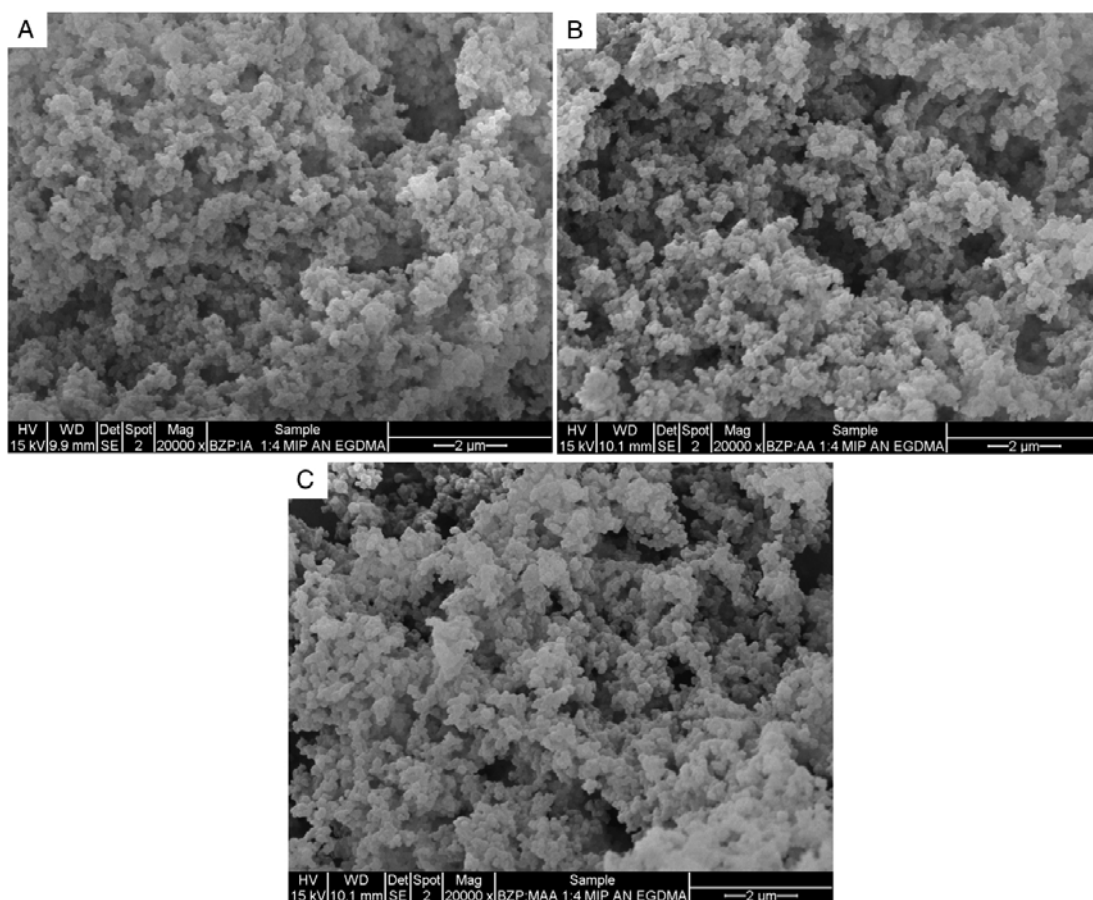


**Figure 4.3:** SEM images for the polymers prepared for the three functional monomers IA (A) and AA (B) and MAA (C).

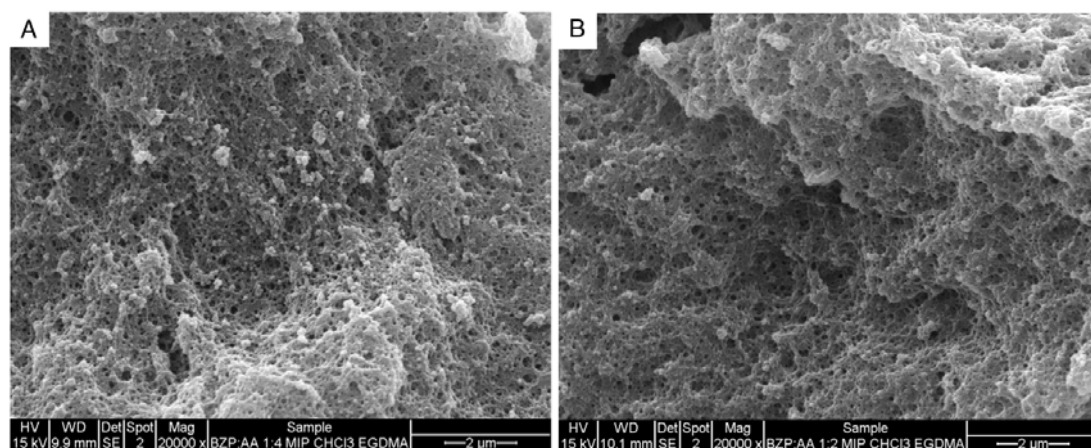


**Figure 4.4:** SEM images for two different ratios NC-AA-EGDMA-4C (A) and NC-AA-EGDMA-2C (B).

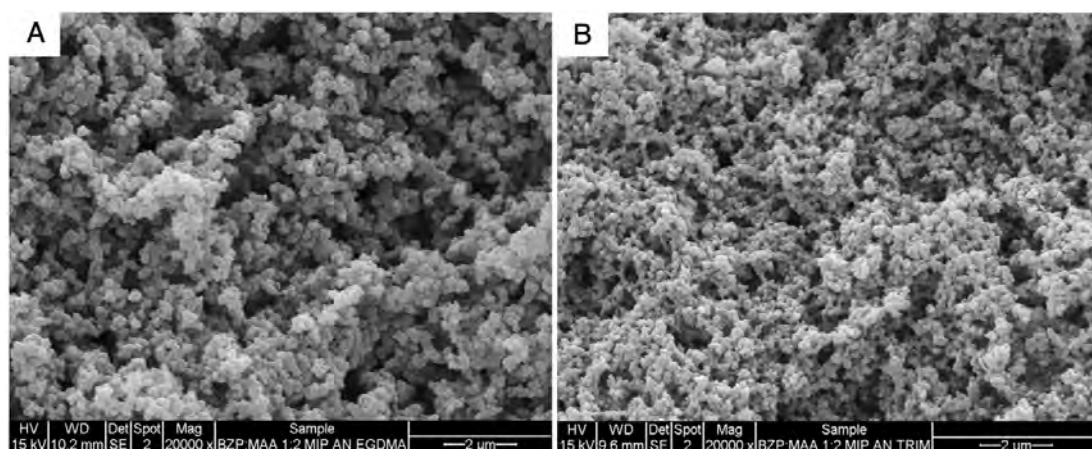


**Figure 4.5:** SEM images for NC-MAA-2A MIPs prepared with EGDMA (A) and TRIM (B).

(B) is presented in Figure 4.6. It has been hypothesised that the more spherical structure indicates that the non-polar polymer adopts this shape in response to the more polar solvent conditions<sup>112</sup>. This suggests that the polymer is remaining in the  $\text{CHCl}_3$  solution longer than is observed in AN, where the polymer phase separates earlier.

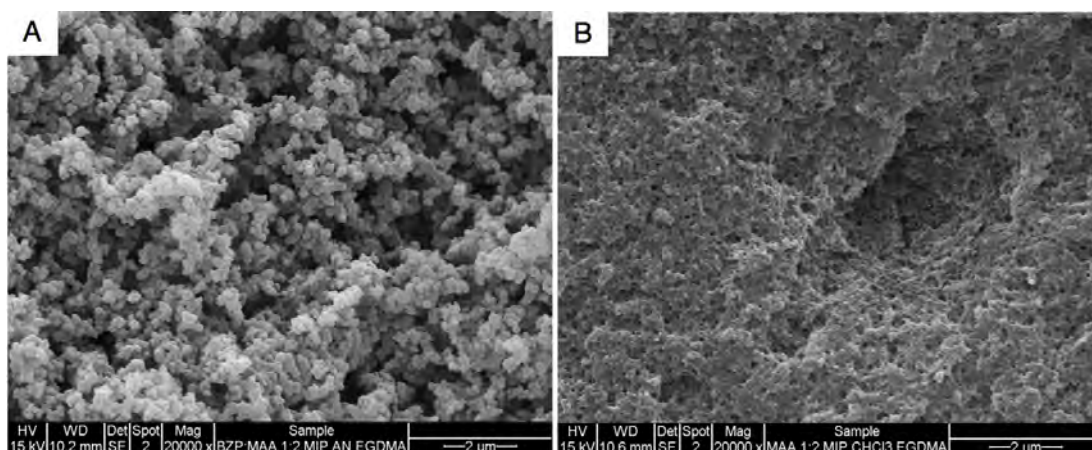


**Figure 4.6:** SEM images for NC-MAA-EGDMA-2 MIPs prepared in acetonitrile (A) and chloroform (B).

Swelling was measured on all polymers in different solvents (AN and  $\text{CHCl}_3$ ) from the dry state. The volume of 10 mg of dry polymer was measured prior to the addition of solvent. After an hour the solvent was removed and the new

volume recorded.

For all polymers prepared, a certain degree of swelling was observed in both AN and CHCl<sub>3</sub>. However, no distinct trends were observed. It was noted though that polymers that were prepared in CHCl<sub>3</sub> exhibited a greater amount of swelling in both AN and CHCl<sub>3</sub>. This is a behaviour consistent with the surface morphology observed for these polymers (Figure 4.6). The CHCl<sub>3</sub> prepared polymers would be expected to exhibit greater volume change upon solvent uptake being denser compared to AN-porogenated polymers which has more void volume. The results obtained for the swelling experiments are presented in Figure 4.7.

### 4.2.3 Polymer Absorption of BZP: Evaluation of Imprinting Effect

BZP rebinding was evaluated by using batch absorption experiments. The imprinting efficiency was determined by comparing the ability of the MIP to bind BZP against the non-imprinted reference polymer, NIP, expressed as a ratio, referred as the imprinting factor (I), Equation 1.3. A high I value indicates a strong affinity of the template towards the MIP.

The initial experiments performed were binding analyses to determine the maximum amount of template up-take from a 0.8 mM BZP solution after 30 minutes of polymer-template contact time. This experiment identifies polymers that have little or no affinity for the template and/or do not show any imprinting effect. As a means of screening, only MIPs that exhibit an I of 2 or greater were considered for further tests. A secondary benefit of this experiment is that it identifies the maximum amount of polymer, between the 5 and 30 mg range, required to obtain an acceptable level of template absorption (40 - 60%), to reduce inaccuracies and error. The results obtained from these analyses are presented in Figures 4.8, 4.9, 4.10, 4.11 and 4.12.

Template up-take was observed in all the 30 MIPs prepared from various formulations ranging from 1% to 100% with respect to the binding solution. For all polymers investigated, the mass of polymer used in the experiments influenced the amount of BZP bound, with the amount of BZP up-take increasing then plateauing between 20 and 30 mg. As all maxima were observed at 30 mg, the

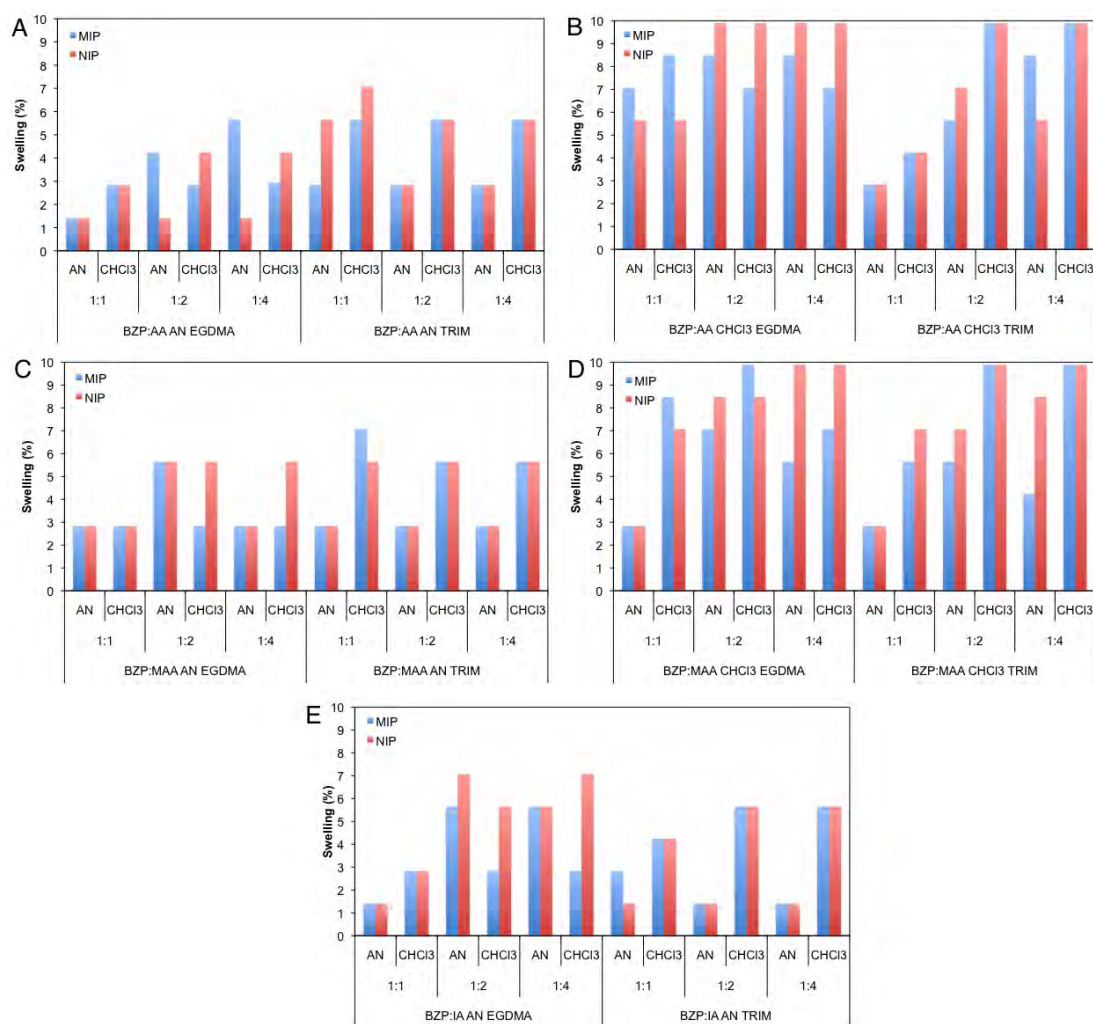


**Figure 4.7:** Swelling results for all NC-AA-A (A), NC-AA-C (B), NC-MAA-A (C), NC-MAA-C (D and NC-IA-A (E). Measurements were performed on 10 mg of polymer in AN and CHCl<sub>3</sub> in the dry state and after 1 hr had elapsed.

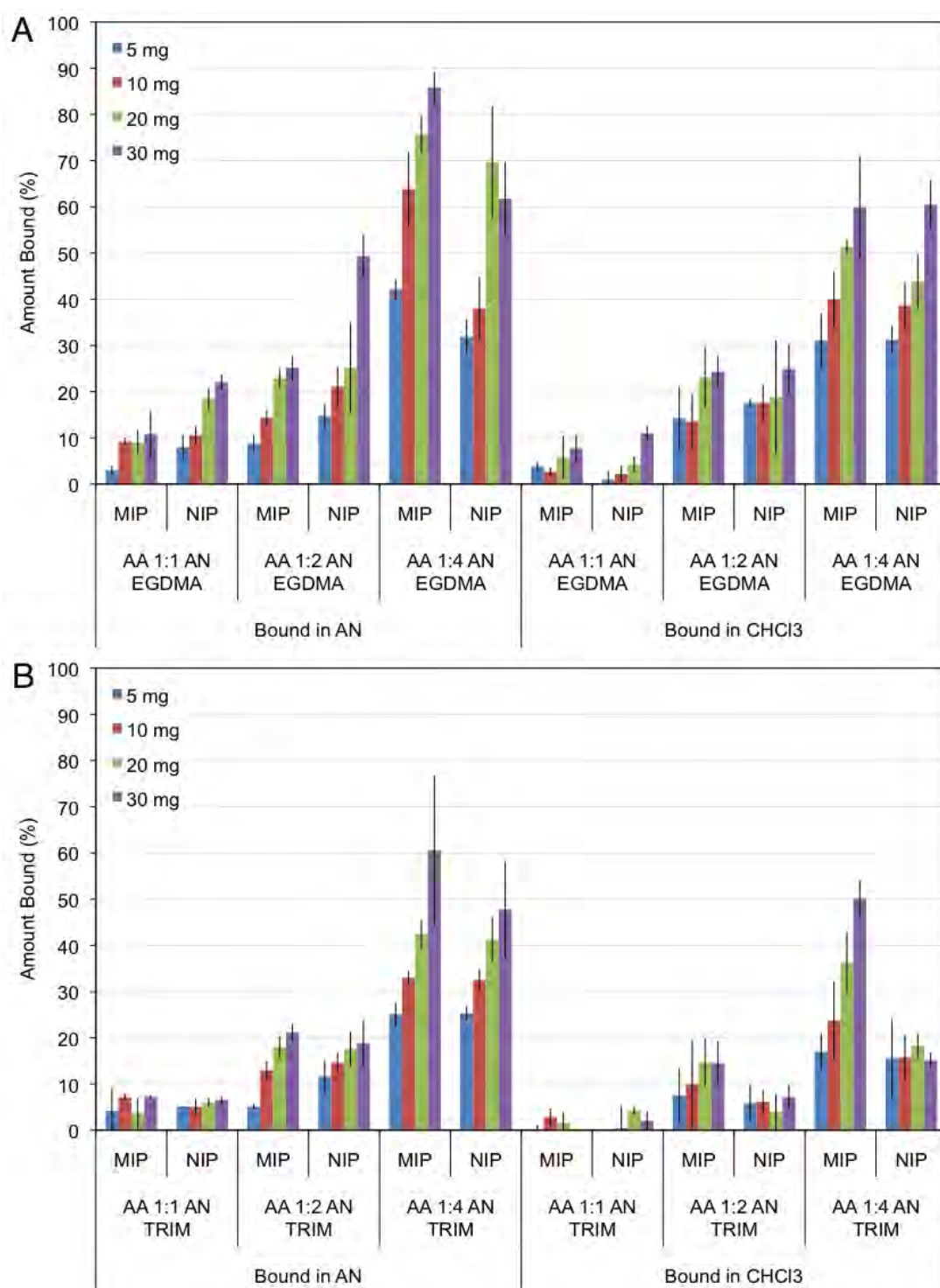


**Figure 4.8:** BZP binding results for BZP:AA polymer formulations prepared in AN with EGDMA, bound in AN and CHCl<sub>3</sub> (**A**) and TRIM, bound in AN and CHCl<sub>3</sub> (**B**), using 1 mL of 0.8 mM solution measured after 30 minutes with all experiments performed in triplicate. Amount bound =  $\left(\frac{[Total] - [Free]}{[Total]}\right) \times 100$ .

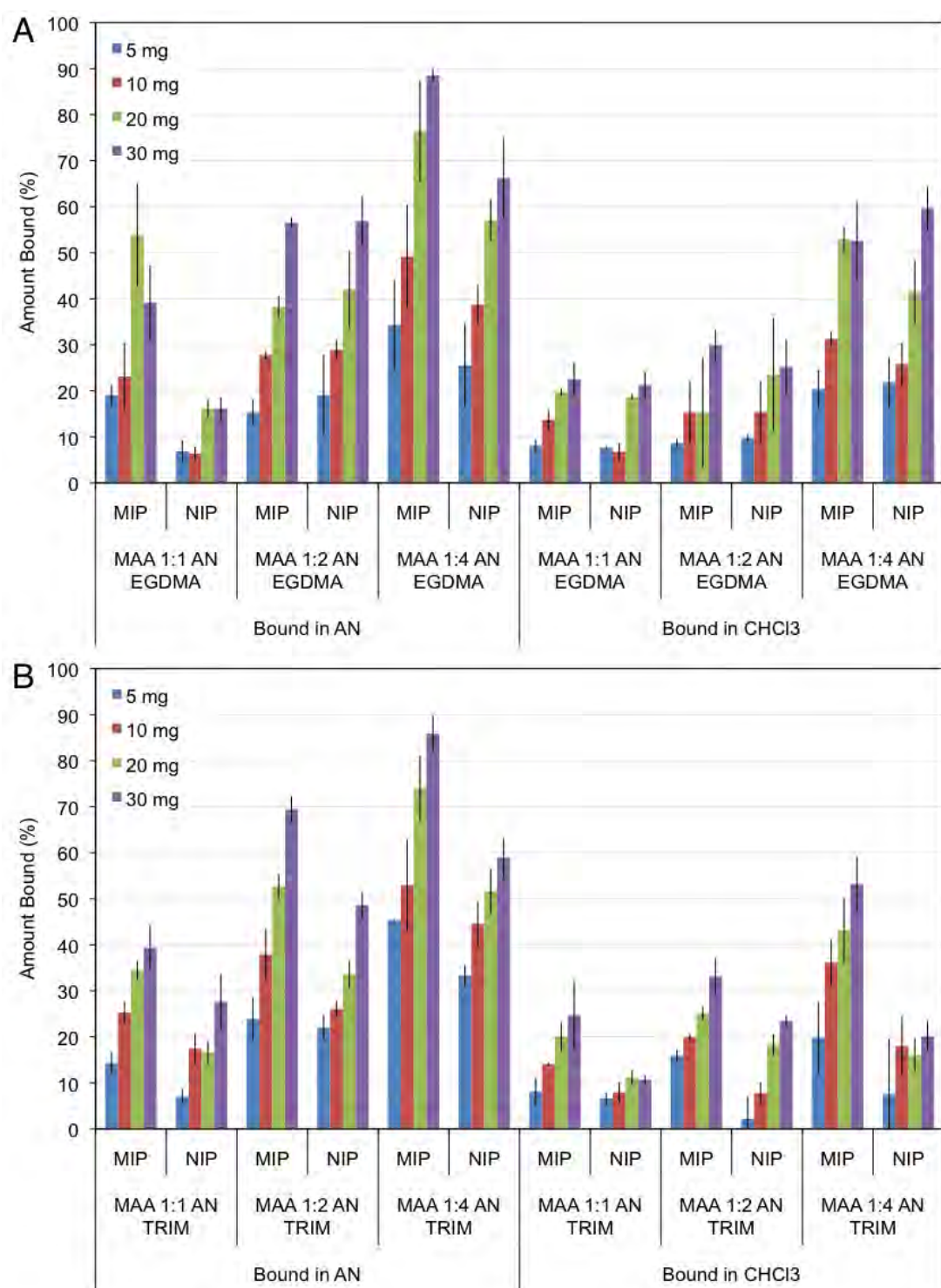


**Figure 4.9:** BZP binding results for BZP:MAA polymer formulations prepared in AN with EGDMA, bound in AN and CHCl<sub>3</sub> (A) and TRIM, bound in AN and CHCl<sub>3</sub> (B), using 1 mL of 0.8 mM solution measured after 30 minutes with all experiments performed in triplicate. Amount bound =  $\left(\frac{[Total] - [Free]}{[Total]}\right) \times 100$ .

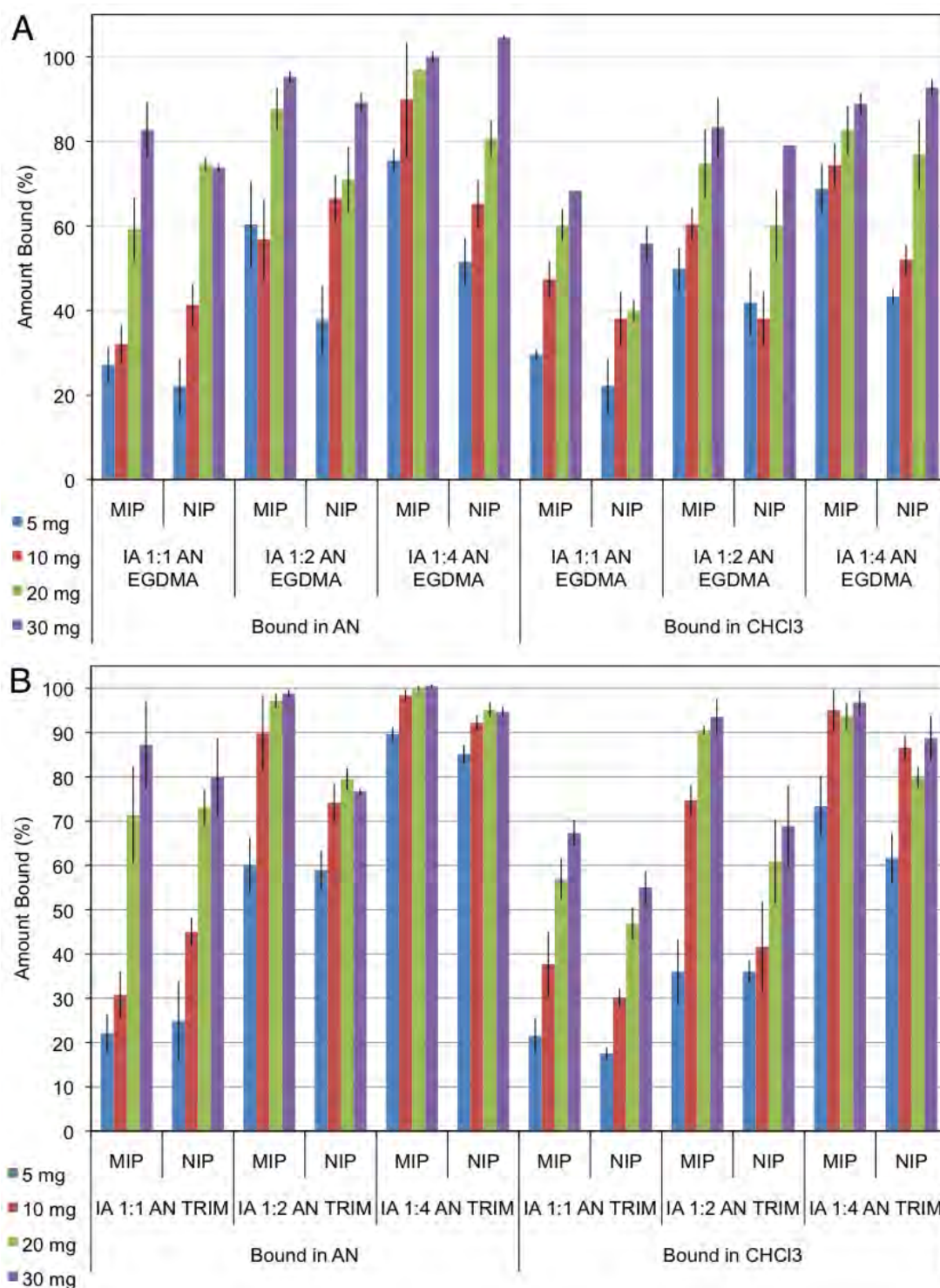


**Figure 4.10:** BZP binding results for BZP:IA polymer formulations prepared in AN with EGDMA, bound in AN and CHCl<sub>3</sub> (**A**) and TRIM, bound in AN and CHCl<sub>3</sub> (**B**), using 1 mL of 0.8 mM solution measured after 30 minutes with all experiments performed in triplicate. Amount bound =  $\frac{([Total] - [Free])}{[Total]} \times 100$ .

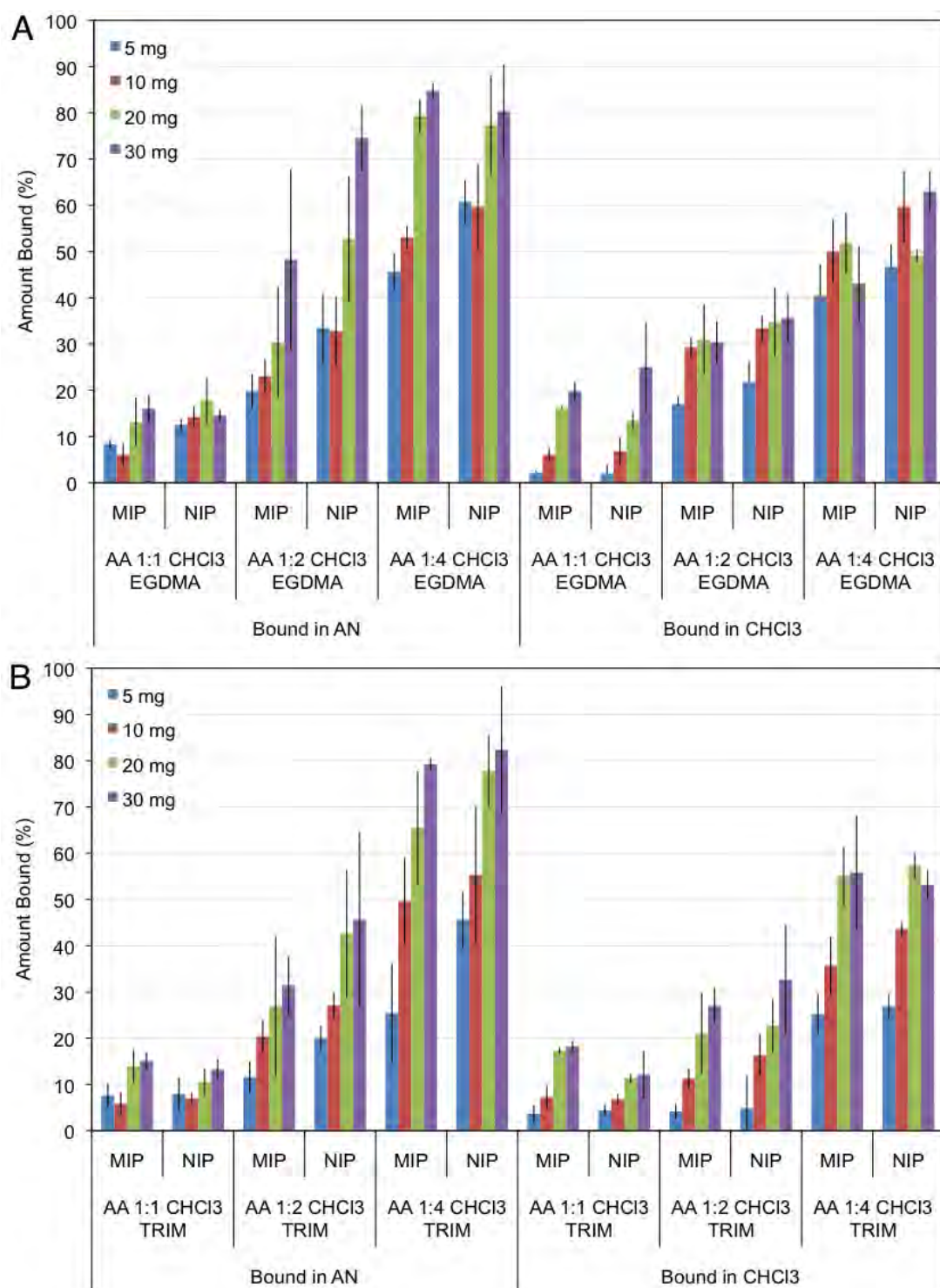


**Figure 4.11:** BZP binding results for BZP:AA polymer formulations prepared in CHCl<sub>3</sub> with EGDMA, bound in AN and CHCl<sub>3</sub> (**A**) and TRIM, bound in AN and CHCl<sub>3</sub> (**B**), using 1 mL of 0.8 mM solution measured after 30 minutes with all experiments performed in triplicate. Amount bound =  $\left(\frac{[Total] - [Free]}{[Total]}\right) \times 100$ .

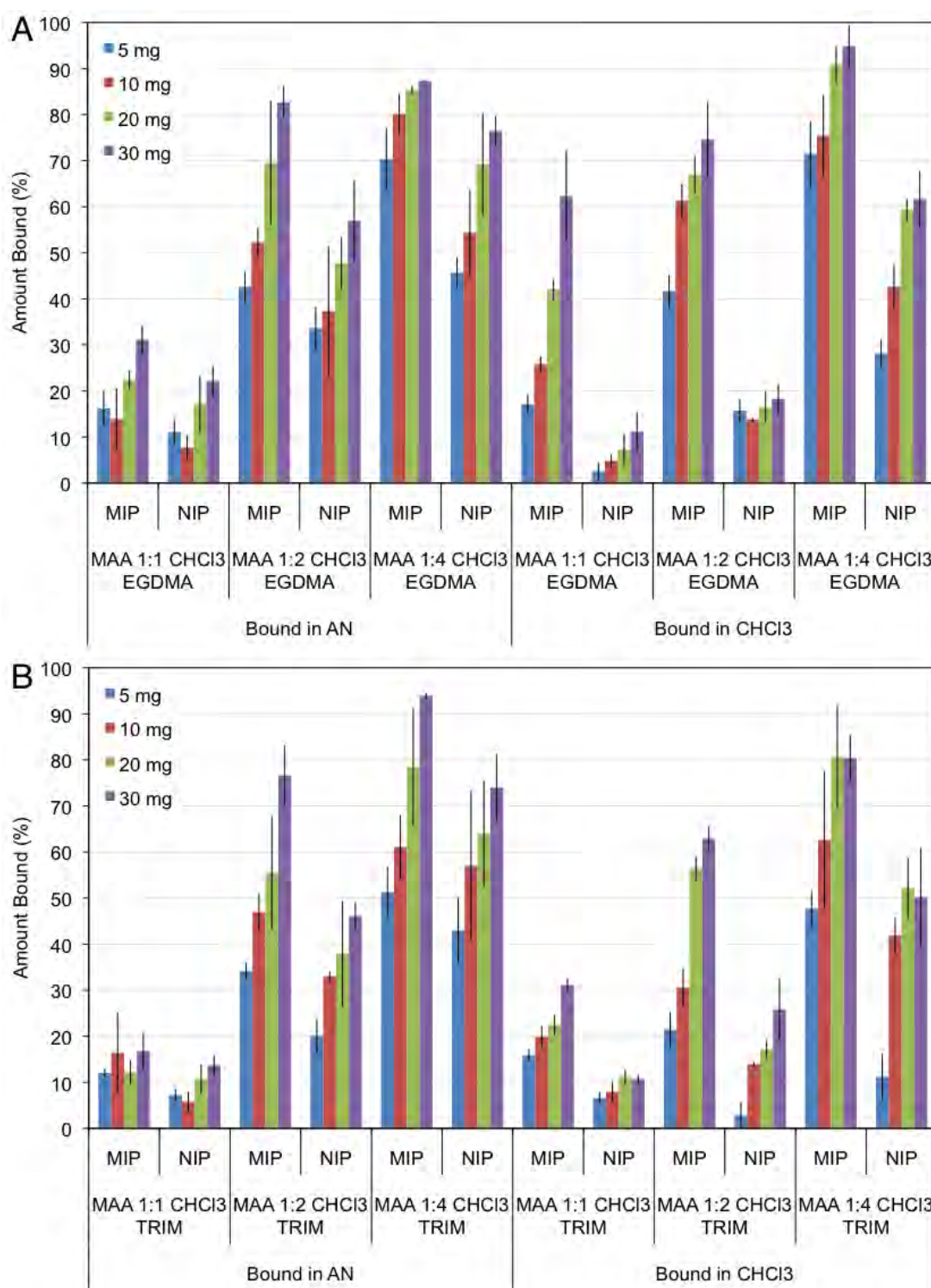


**Figure 4.12:** BZP binding results for BZP:MAA polymer formulations prepared in CHCl<sub>3</sub> with EGDMA, bound in AN and CHCl<sub>3</sub> (**A**) and TRIM, bound in AN and CHCl<sub>3</sub> (**B**), using 1 mL of 0.8 mM solution measured after 30 minutes with all experiments performed in triplicate. Amount bound =  $\frac{([Total] - [Free])}{[Total]} \times 100$ .

results discussed from this point on will be for this polymer mass unless otherwise stated. A second trend that was observed for the total polymer collection was the effect of functional monomer concentration, i.e. BZP:FM ratio, on BZP absorption. The trend observed was symbiotic, with the amount of BZP bound increasing with the ratio.

Of the three functional monomers investigated (MAA, AA and IA), it was observed that MIPs prepared with IA exhibited the greatest affinity for BZP. The amount of BZP absorbed ranged between 82 and 100% for binding in AN and 67 to 92% for the  $\text{CHCl}_3$  solutions. The FM MAA had the second most favourable BZP affinity, with BZP up-take in the range of 16 to 94%. Finally, AA exhibited the least template affinity with bindings in the range of 1 to 85%, with the minimum up-take observed for the 1:1 ratio and the maximum by the 1:4 ratio.

BZP up-take was also observed in the NIPs, with the lowest up-take by the 1:1 ratios. As with the MIPs, the largest up-take was observed for the polymers prepared with IA, binding 55 to 100%. This was followed by AA with sorption in the range of 2 to 82% and finally, MAA, which exhibited the lowest up-takes of 10 to 76%. For the AA and MAA polymers, up-take was greatest in the polymers that were prepared in  $\text{CHCl}_3$ .

BZP up-take did not seem to be affected by the nature of the cross-linkers used. This result further supports previous results in this study, which have shown that EGDMA and TRIM have minimal interaction with BZP.

The porogen used for preparation and rebinding exhibited significant effects on the amount of template absorbed. Template up-take was higher in all polymers when binding was performed in AN. However, the difference in BZP binding between MIP and NIP and, subsequently, the I values, were more enhanced in  $\text{CHCl}_3$ .

The imprinting factor (I) gives an indication of the extent of the binding efficiency of the MIP through direct comparison with an identically formulated but non-imprinted (i.e. no template present) reference polymer (NIP). The presence of the template in the MIP formulation creates template cavities leading (in theory) to a greater binding capacity. As a consequence, the MIP would be expected to exhibit a greater binding capacity towards the target than the NIP. The NIP,

however, would still be expected to superficially bind the template. An ideal MIP would have a high I value, i.e. high selective template binding via the MIP and minimal non-specific NIP binding.

The results of the BZP up-take of the 30 MIPs presented in Figures 4.8, 4.9, 4.10, 4.11 and 4.12 expressed as I values (Figures 4.13, 4.14 and 4.15) showed that an imprinting effect of  $I \geq 2$ , for all polymer masses tested, was only obtained with the MAA polymers, prepared using MAA polymer formulations of 1:1 and 1:2, with EGDMA and TRIM in  $\text{CHCl}_3$ . In addition, NC-MAA-EGDMA-1A, when bound in AN also gave consistent I values greater than 2 (2.4 to 3.6). For each of these polymers, minor change in the I value was observed as polymer mass increased (5 mg - 30 mg).

A number of other significant I values were also obtained for a single mass (usually 5 mg) of a particular polymer. Included in this were NC-AA-TRIM-2A, NC-AA-TRIM-4A, NC-AA-EGDMA-1A, NC-AA-TRIM-1A, NC-MAA-EGDMA-1A and NC-MAA-TRIM-4A. This was only observed when  $\text{CHCl}_3$  was used as the binding solvent. It is suspected that due to the small volumes, error has been generated. As a result, these values were considered to be outliers and not investigated further.

Although the MIPs prepared with IA gave the greatest binding capacity, their corresponding NIPs also gave high binding suggesting that the imprinting of BZP was inefficient. The amount of BZP bound in the NIPs (55-100%) was comparable to the amount of BZP bound by the MIP (67-100%), resulting in I values ranging between 0.69 (for 5 mg) and 1.79 (30 mg). These results suggest that specific binding cavities were not created in polymerisation, with binding being the result of non-specific interactions. Previous work using molecular modelling and NMR, (Chapter 3) suggested that the optimum stoichiometry of a BZP:IA polymer is 1:1. IA is a di-protic acid and thus there are two locations in which binding can occur, hence if BZP is binding to one of these sites, then the second acid group is free, which can then form non-specific interactions

Lastly, polymer formulations with AA as the FM generally gave higher NIP binding than the MIP. The polymers that were prepared in  $\text{CHCl}_3$  had  $I \leq 1$  ( $I = 0.36 - 1.5$ ). For the AN prepared polymers, a greater range of values was obtained ( $I = 0.1 - 3.5$ ) however, in total 56 out of 96 values were less than 1. The

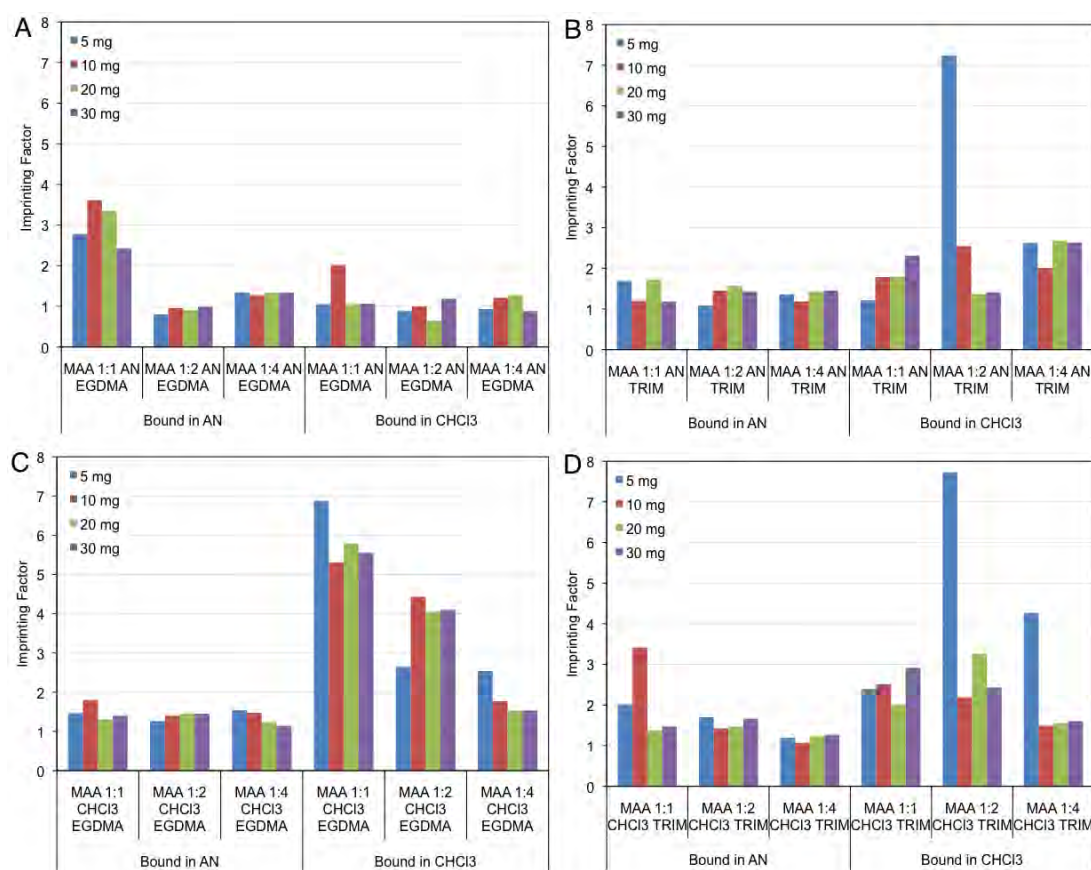


**Figure 4.13:** Imprinting factors calculated from the rebinding studies for MAA prepared polymers: NC-MAA-EGDMA-A (A), NC-MAA-TRIM-A (B), NC-MAA-EGDMA-C (C) and NC-MAA-TRIM-C (D) polymers, prepared and bound in AN and CHCl<sub>3</sub> using 1 mL of 0.8 mM solution measured after 30 minutes with all experiments performed in triplicate.  $I = \text{MIP} / \text{NIP}$

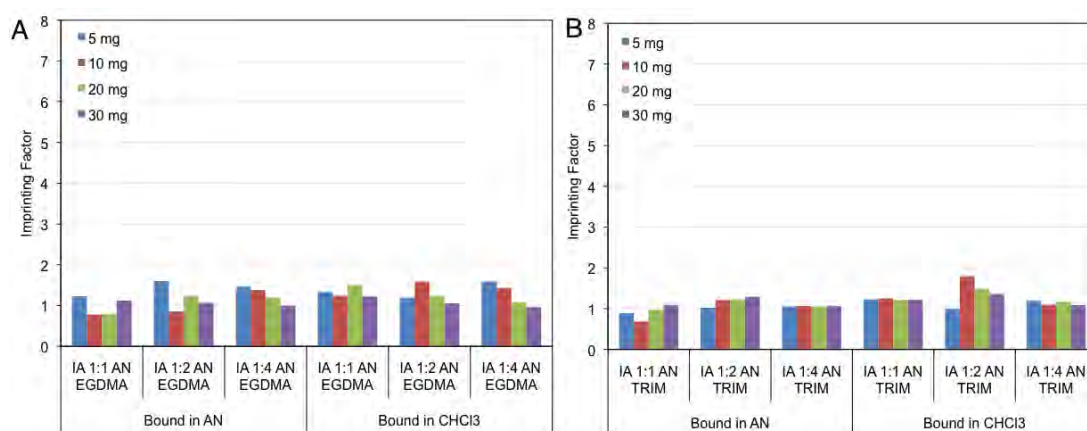


**Figure 4.14:** Imprinting factors calculated from the rebinding studies for IA prepared polymers: NC-IA-EGDMA-A (**A**), and NC-IA-TRIM-A (**B**) polymers prepared in AN and bound in AN and CHCl<sub>3</sub> polymers, prepared and bound in AN and CHCl<sub>3</sub> using 1 mL of 0.8 mM solution measured after 30 minutes with all experiments performed in triplicate.  $I = \text{MIP} / \text{NIP}$

polymers NC-AA-TRIM-2A and NC-AA-TRIM-4A were the only polymers that had  $I \geq 1$ , however there was a large variance across the masses ( $I = 1.1 - 3.5$ ). The binding capacity of these polymers was poor for both MIP and NIP and a large amount of non-specific binding was observed, resulting in low imprinting factors. This could be the result of poor transport, or the loss of recognition in the binding cavity. It has also been suggested that the methyl group on MAA is enhancing binding through non-polar interactions with the phenyl ring, which is absent in both AA and IA.

In general, the porogen was observed to influence the imprinting efficiency. CHCl<sub>3</sub> was observed to reduce the amount of non-specific binding. This was most evident in the formulations where CHCl<sub>3</sub> had been used for both the polymerisation solvent as well as the rebinding solvent ( $I = 1.54 - 7.72$ ). When a solvent other than the polymerisation porogen was used, the  $I$  values were reduced with  $I$  values of 0.88 to 2.68 for AN prepared polymers bound in CHCl<sub>3</sub> and 1.07 to 2.01 for CHCl<sub>3</sub> prepared MIPs bound in AN. When AN was used for both polymerisation and rebinding, the greatest variance was observed ( $I = 0.65 - 3.6$ ).

BZP binding in MIPs and NIPs did not seem to be influenced by swelling

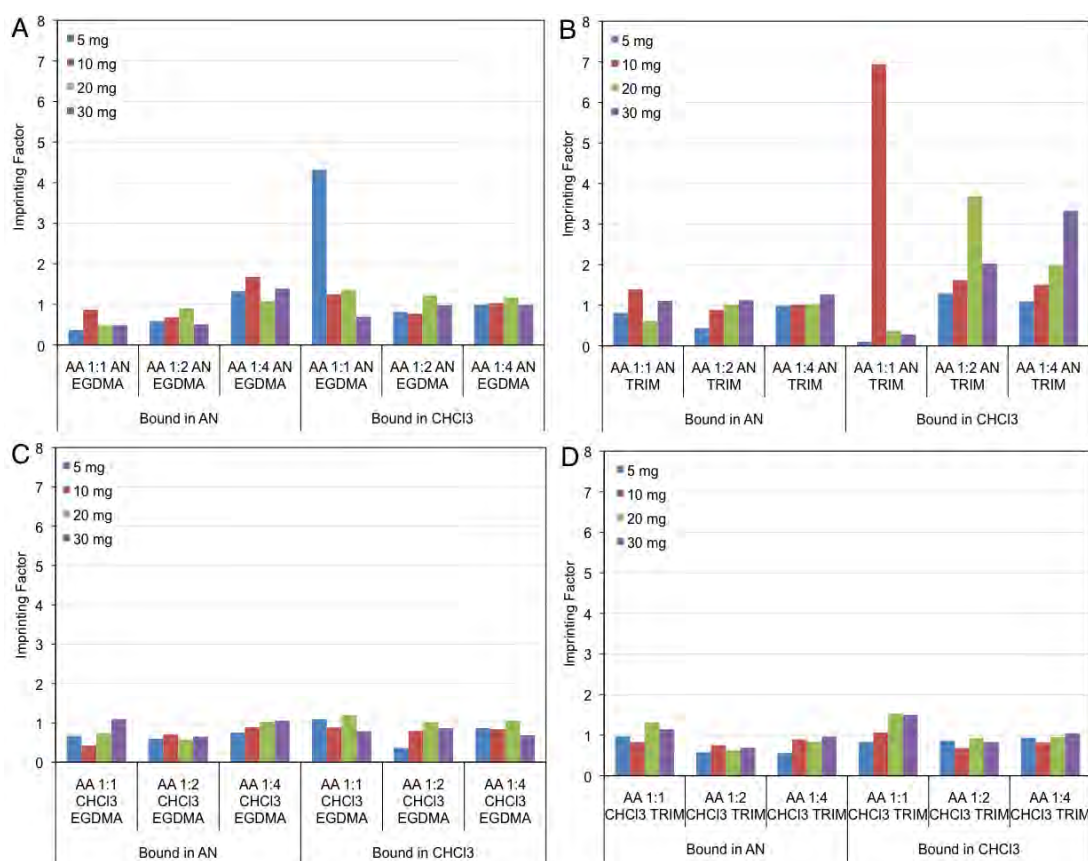


**Figure 4.15:** Imprinting factors calculated from the rebinding studies for the AA prepared polymers: NC-AA-EGDMA-A (**A**), NC-AA-TRIM-A (**B**), NC-AA-EGDMA-C (**C**) and NC-AA-TRIM-C (**D**) polymers, prepared and bound in AN and CHCl<sub>3</sub> using 1 mL of 0.8 mM solution measured after 30 minutes with all experiments performed in triplicate.  $I = \text{MIP} / \text{NIP}$

(Figure 3.9). In general, comparable degree of swelling was observed between the MIP and NIP and between formulations prepared in the same solvent. A higher degree of swelling was observed for the polymers prepared in  $\text{CHCl}_3$  and moderate swelling observed of the polymers prepared in AN.

Of all the formulations investigated, only the 1:1 and 1:2 NC-MAA-EGDMA-C and NC-MAA-TRIM-C polymer formulations bound in  $\text{CHCl}_3$  and the NC-MAA-EGDMA-1A polymer when bound in AN exhibited  $I \geq 2$  for all masses tested. From these results, it can be seen that the NC-MAA-EGDMA-C MIPs showed the greatest imprinting effect with the 1:1 ratio performing the best ( $I = 5.3 - 6.9$ ). The TRIM prepared polymers and NC-MAA-EGDMA-1A had similar values in the range of  $I = 2.0$  to  $3.6$ . An unexpectedly high  $I$  value of  $7.7$  was obtained for the  $5 \text{ mg}$  for NC-MAA-TRIM-2C but was not assessed further.

As NC-MAA-EGDMA-1A bound in AN was the only polymer in its set of formulations to exhibit imprinting, further analysis was not performed for this polymer and any of the MIPs prepared using AN as porogen. For the other four polymers, NC-MAA-EGDMA-1C, NC-MAA-EGDMA-2C, NC-MAA-TRIM-1C and NC-MAA-TRIM-2C, further studies were performed to establish the binding kinetics and dynamics of the systems. A polymer mass of  $20 \text{ mg}$  was selected for use in all subsequent experiments, as at this mass polymer saturation was generally established (Figure 4.16).

### 4.2.4 Determination of Optimal Time of Contact

For MIPs to be utilised as detection devices, their binding response needs to be rapid. Hence, it is important to assess the template binding kinetics and dynamics. Only the BZP:MAA 1:1 and 1:2 EGDMA and TRIM polymers prepared in  $\text{CHCl}_3$  were investigated, based on the polymer absorption results, which showed these polymers exhibiting imprinting factors greater than 2. The rebinding parameters for this experiment used  $20 \text{ mg}$  of polymer (template-polymer saturation point) with  $1 \text{ mL}$  of  $0.8 \text{ mM}$  BZP solution. The time range investigated was between 10 minutes and 24 hours. As Figures 4.17 and 4.18 demonstrate, rapid up-take of BZP was observed for each of the four polymers investigated. This then dropped off before equilibrium was established. As equilibrium was estab-

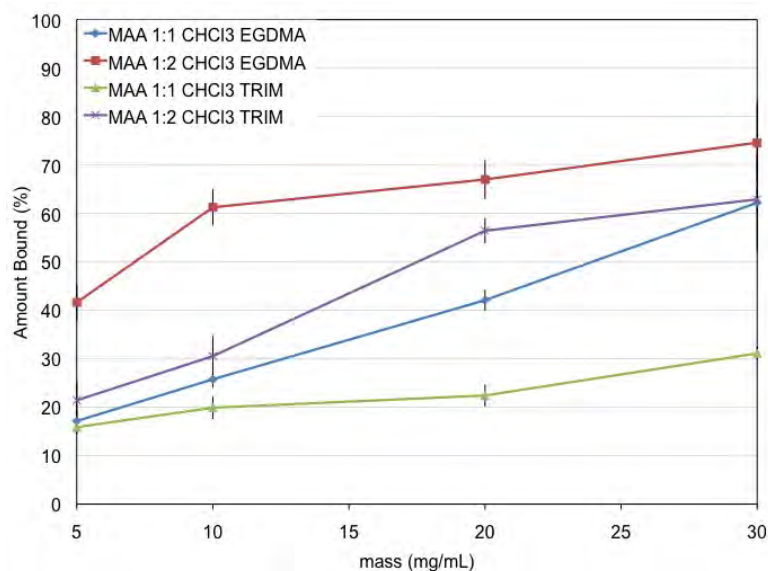


**Figure 4.16:** Rebinding results for BZP:MAA formulations showing polymer saturation between 20 - 30 mg of polymer for 1 mL of 0.8 mM solution after 30 min binding time. All experiments were performed in triplicate. Amount bound =  $(([\text{Total}] - [\text{Free}]) / [\text{Total}]) \times 100$ .

lished prior to 8 hours, only the time range of 0 to 8 hours has been plotted. The binding observed after this point was similar to what was observed at eight hours.

With the NC-MAA-EGDMA-1C polymer (Figure 4.17(A)), equilibrium was not established until after 8 hours, with 71% of the template being bound after this time. However, the highest imprinting factor ( $I = 6$ ) was achieved at 2 hours dropping back to  $I = 3$  after 2 hours, due to increasing amount of non-specific binding of the NIP. The amount bound after 10 minutes was 55% (80% of the maximum amount bound ( $B_{\text{max}}$ )), indicating that template up-take was rapid. The NC-MAA-EGDMA-2C (Figure 4.17(B)) had lower imprinting values, with the maximum of  $I = 2.1$  obtained after 1 hour. It was also after this time that equilibrium had been achieved and maximum template up-take of 86%, had occurred. The amount of template bound before 10 minutes was 82% (95% of the  $B_{\text{max}}$ ). It was observed in this study, that the 1:1 ratio has a lower MIP up-take but a much lower NIP up-take compared to the 1:2 ratio. This suggests that a ratio between these two maybe more optimal. The 1:2 produces more non-specific

## 4.2 Results and Discussion

binding but this is achieved relatively quickly, with equilibrium established within 1 to 2 hours. The 1:1 polymer takes longer, however up-take is still acceptable in this time range.

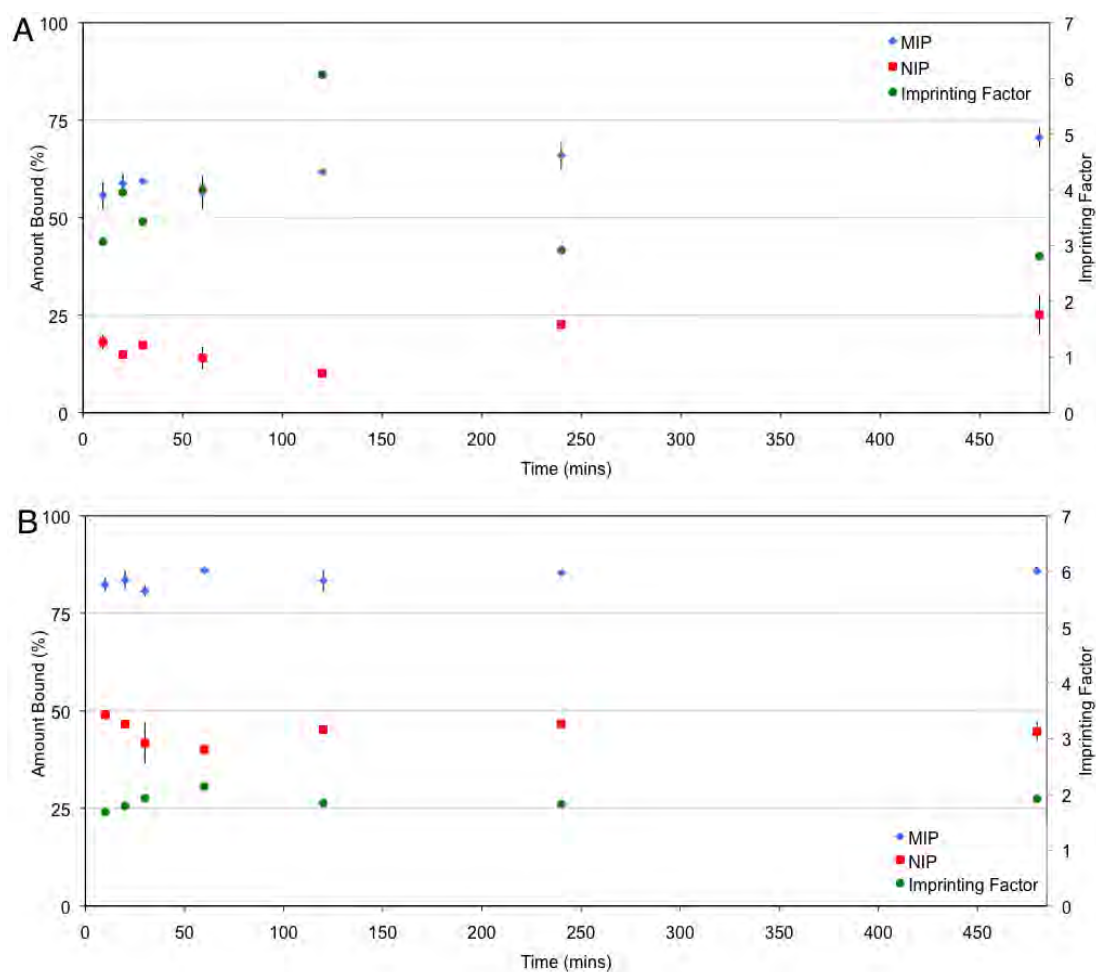


**Figure 4.17:** Time rebinding results for BZP:MAA 1:1 (**A**) and 1:2 (**B**)  $\text{CHCl}_3$  EGDMA using 20 mg of polymer with 1 mL of 0.8 mM BZP solution. All experiments were performed in triplicate. Amount bound =  $\left(\frac{[\text{Total}] - [\text{Free}]}{[\text{Total}]}\right) \times 100$

For the TRIM prepared polymers the 1:1 BZP:MAA ratio (Figure 4.18(**A**)) had a maximum template up-take of 46% after 2 hours. This was the smallest amount of BZP up-take observed for all polymers. The imprinting value at this time was  $I = 3.2$  however, this was not the maximum imprinting value. The maximum imprinting value obtained was  $I = 4.4$  observed after 8 hours. The

## 4.2 Results and Discussion

amount of template bound before 10 minutes was 93% of the equilibrium up-take, indicating that near equilibrium conditions exist at this time. The NC-MAA-TRIM-2C polymer (Figure 4.18(B)) had an equilibrium established after one hour with a maximum template binding of 74%. The maximum imprinting value was 2.9 obtained after 1 hour. The amount of template bound before 10 minutes was also 93% of the equilibrium up-take.

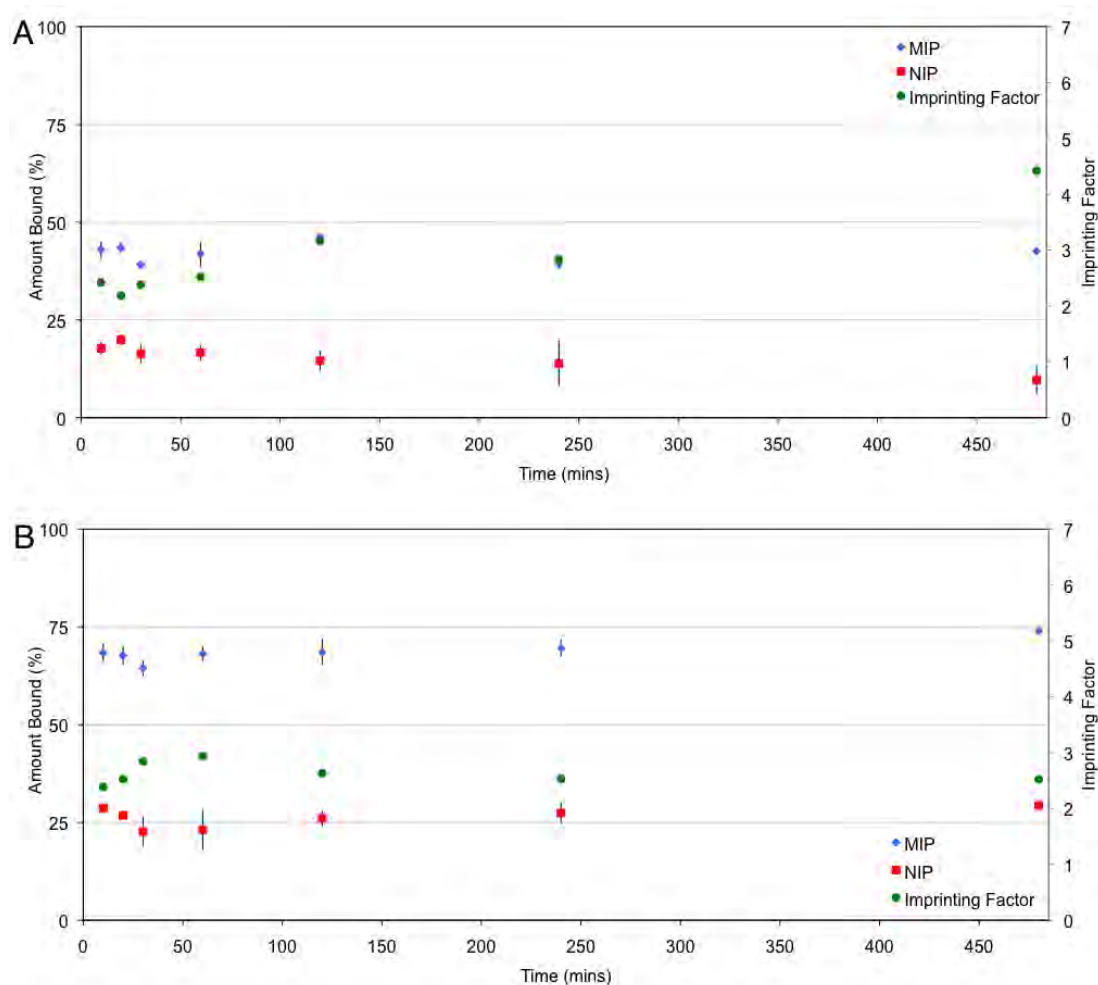


**Figure 4.18:** Time rebinding results for BZP:MAA 1:1 (A) and 1:2 (B)  $\text{CHCl}_3$  TRIM using 20 mg of polymer with 1 mL of 0.8 mM BZP solution. All experiments were performed in triplicate. Amount bound =  $\frac{([Total] - [Free])}{[Total]} \times 100$

In all time experiments performed, rapid template up-take was observed, which was then followed by a decrease in binding before equilibrium was es-

established. This was more prominent in the 1:2 BZP:MAA formulations. The rate at which de-sorption occurred was also prolonged in the NIPs. The cause of this behaviour is unknown at this stage and thus requires further investigation.

To enable a comparison between polymers in further analyses, a common binding time was required. The time that was selected was 60 minutes, as equilibrium, based on the imprinting factor, had been achieved for three of the four polymers.

The four polymers investigated bound greater than 80% of the equilibrium template up-take within 10 minutes. This result is ideal for the use as an in-field sensor as a quick response is needed especially when time is either critical or limited.

### 4.2.5 Saturation Curve and Analysis

The binding isotherm, also known, as a saturation curve, was generated for the BZP:MAA 1:1 and 1:2 EGDMA and TRIM polymers by varying the BZP concentration while holding the polymer mass and time constant. Studies were conducted, in triplicate, under saturation conditions, using 20 mg polymer in 1 mL binding solution with 1 hour contact time. The concentration range investigated was between 0.5 and 10 mM.

The binding isotherm for each polymer produced from this experiment is presented in Figure 4.19. The binding isotherms for the four MIPs clearly show the binding capacity of the 1:2 BZP:MAA formulation to be twice that of the 1:1 ratio. The non-specific binding exhibited for all NIPs was approximately equivalent, therefore the difference observed between MIPs is most likely the result of cavity-based binding of BZP and not superficial non-specific binding.

From the binding isotherms, it is possible to determine the  $K_d$  and  $n$  values of the MIPs by employing the following methods: a direct calculation from the binding isotherm using computer based, non-linear regression analysis (Prism 5, Graphpad Software, 2009,), or linear transformation techniques such as Scatchard regression using limiting slopes analyses and the Langmuir linear regression. The use of the three methods will enable a comparison to be made as inaccuracies exist within each method used. The  $K_d$  and  $n$  values determined from these three

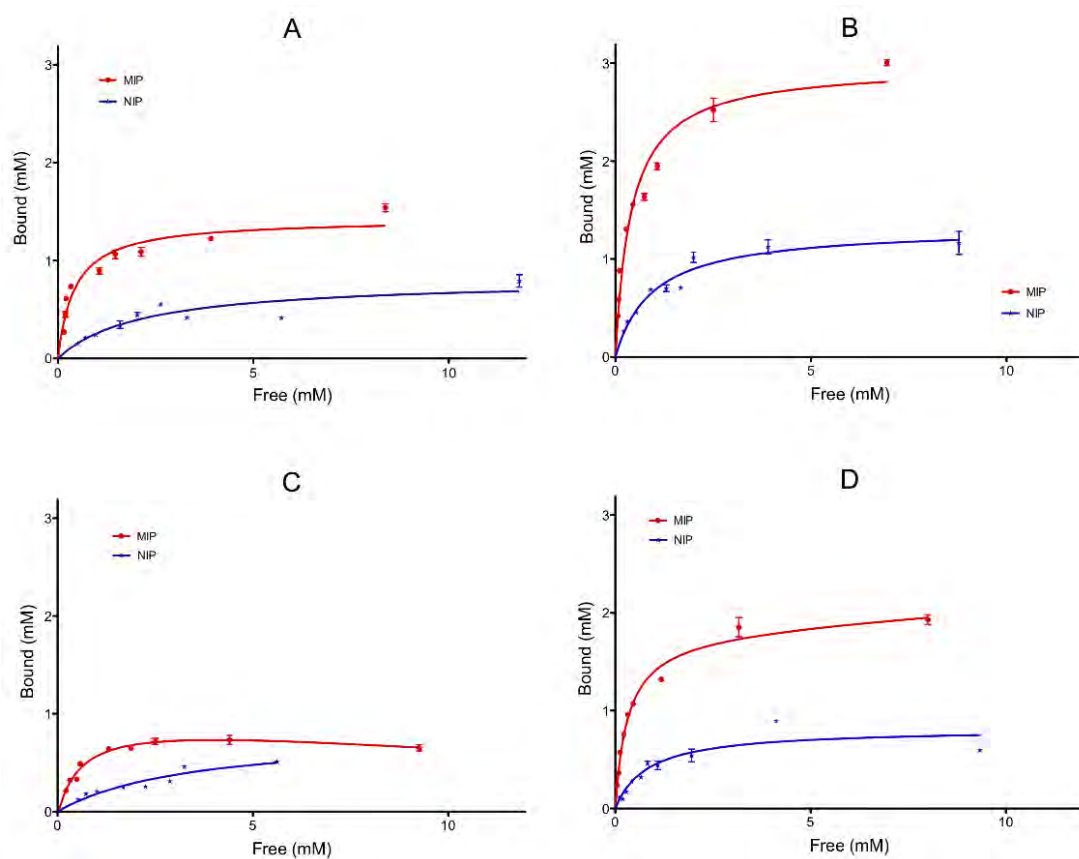


**Figure 4.19:** Binding isotherm data produced for NC-MAA-EGDMA-1C (**A**), NC-MAA-EGDMA-2C (**B**), NC-MAA-TRIM-1C (**C**) and NC-MAA-TRIM-2C (**D**) using 20 mg of polymer with varying BZP solution concentrations for a contact time of 1 hr. All analyses were performed in triplicate and the average plotted.

## 4.2 Results and Discussion

methods are presented in Table 4.1. The  $K_d$  value is the equilibrium dissociation constant and is the concentration of analyte which occupies half of the binding cavities at equilibrium. A small  $K_d$  means that the polymer has a high affinity for the analyte. A large  $K_d$  means that the polymer has a low affinity for the analyte. The  $n$  value is the number of binding sites in the polymer.

**Table 4.1:** Binding constants ( $K_d$  and number of binding sites ( $n$ ) extracted from the binding isotherm, Scatchard plot and Langmuir plot for the BZP:MAA 1:1 and 1:2, EGDMA and TRIM polymers prepared in  $\text{CHCl}_3$ .

	$K_d$ Value $\times 10^{-3}$ (M)							
	MAA 1:1 EGDMA		MAA 1:2 EGDMA		MAA 1:1 TRIM		MAA 1:2 TRIM	
	MIP	NIP	MIP	NIP	MIP	NIP	MIP	NIP
Binding Isotherm	0.4292	2.149	0.4096	0.9507	0.6074	3.502	0.3259	0.8308
Scatchard	$K_{d1}=0.255$ $K_{d2}=1.726$	2.788	$K_{d1}=0.1919$ $K_{d2}=0.7602$	0.9326	0.6748	2.975	0.3041 $K_{d2}=0.7811$	1.170
Langmuir	0.6792	2.626	0.4737	0.8915	0.2305	2.907	0.2600	0.5511
	$n \times 10^{-3}$ (M)							
	MAA 1:1 EGDMA		MAA 1:2 EGDMA		MAA 1:1 TRIM		MAA 1:2 TRIM	
	MIP	NIP	MIP	NIP	MIP	NIP	MIP	NIP
Binding Isotherm	1.424	0.8116	2.975	1.325	1.603	0.812	1.802	0.8174
Scatchard	$n_1=1.230$ $n_2=1.756$	0.9465	$n_1=2.185$ $n_2=3.3189$	1.334	0.9171	0.7668	1.783 $n_2=2.209$	0.9610
Langmuir	1.601	0.8665	3.164	1.296	0.6920	0.7346	1.631	0.6756
	$r^2$							
	MAA 1:1 EGDMA		MAA 1:2 EGDMA		MAA 1:1 TRIM		MAA 1:2 TRIM	
	MIP	NIP	MIP	NIP	MIP	NIP	MIP	NIP
Binding Isotherm	0.9023	0.7466	0.9551	0.8949	0.9326	0.9349	0.9840	0.8272
Scatchard	$r_1^2=0.8346$ $r_2^2=0.7397$	0.5970	$r_1^2=0.8608$ $r_2^2=0.9989$	0.8671	0.8402	0.5642	0.9037 $r_2^2=0.9208$	0.5533
Langmuir	0.9871	0.8529	0.9953	0.9910	0.9906	0.5394	0.9933	0.9562
	$K_d \text{ NIP} / K_d \text{ MIP}$							
	MAA 1:1 EGDMA		MAA 1:2 EGDMA		MAA 1:1 TRIM		MAA 1:2 TRIM	
	Binding Isotherm	5.007		2.321		5.766		2.549
Langmuir	3.866		2.321		12.612		2.119	
	$n \text{ MIP} - n \text{ NIP}$							
	MAA 1:1 EGDMA		MAA 1:2 EGDMA		MAA 1:1 TRIM		MAA 1:2 TRIM	
	Binding Isotherm	0.6124		1.6500		0.791		0.9846
Langmuir	0.7345		1.868		-0.043		0.9554	

Scatchard equation:  $S_B/C_f = Kn - S_B$

Langmuir equation:  $C_f/S_B = C_f/n + 1/Kn$

The  $K_d$  values of the MIPs ( $K_d$  MIP) calculated from curve fitting of the binding isotherm, were consistently lower ( $3.3 - 6.1 \times 10^{-4}$  M) than the NIPs ( $K_d$  NIP =  $8.3 \times 10^{-4} - 3.5 \times 10^{-3}$ ), which indicate stronger affinity of the template towards the MIP than the NIP. The effect of cross-linker on the  $K_d$  values was not evident, the  $K_d$  values of the EGDMA polymers were between the two values

for the TRIM polymers. The  $K_d$  MIP and  $K_d$  NIP were observed to be greater in the 1:1 formulations than the 1:2 formulations but the ratio of the  $K_d$  NIP to  $K_d$  MIP (Table 4.1) was observed to be higher for the 1:1 ratios (5.0 and 5.8 for the EGDMA and TRIM prepared polymer, respectively) than for the 1:2 ratios where values of 2.3 and 2.5 were obtained for EGDMA and TRIM, respectively. These results suggest that while the 1:2 T:FM ratio exhibit stronger affinity to BZP than the 1:1 ratio, the difference in the degree of BZP affinity between the MIP and the NIP is greater in the 1:1 ratio than in the 1:2 ratio. This is consistent with the binding results (Figure 4.12) showing the NIP binding for the 1:1 ratios to be lower than that for the 1:2 ratios.

The  $n$  values for the MIPs, calculated for the four polymers were higher  $n$  value ( $1.42 \times 10^{-3}$  -  $2.98 \times 10^{-3}$ ) than the NIPs ( $8.11 \times 10^{-4}$  -  $1.23 \times 10^{-3}$ ), which was not surprising considering that the MIPs contain both selective and non-selective binding sites. The 1:2 formulations also gave higher  $n$  values with a greater difference between MIP and NIP, than the 1:1 ratios. This implies the existence of a mixture of BZP:MAA associations (1:1 and 1:2 in the case of the 1:2 formulation) when the T:FM ratio is  $> 1:1$ . These interactions have been shown to be favourable by molecular modelling and NMR studies (Chapter 3).

The binding isotherms were transformed into Scatchard plots by plotting the amount bound/free template concentration verses bound. A line of best fit was then applied to the data and the  $K_d$  and  $n$  values calculated from the slope and the y-intercept. The Scatchard plots for the four polymers are displayed in Figure 4.20. The Scatchard plots for three of the polymers were curved in nature. Consequently, the limiting slopes analysis method was applied, producing two lines, resulting in two  $K_d$  and two  $n$  values (Table 4.1). This result suggests that low and high affinity (heterogeneous) binding sites are present in these polymers. For NC-MAA-TRIM-1C MIP, a single straight line was fitted to the data. A comparison of this plot with the MIPs of the other three polymers shows that the amount bound is comparable to the high affinity binding sites of these MIPs. The low affinity binding sites have not been observed, which is why the plot was not curved. Similar trends were observed for the  $K_d$  and  $n$  values obtained from the Scatchard analyses to the binding isotherm with the  $K_d$  MIP values smaller than the  $K_d$  NIP values and the  $n$  values greater in the MIPs.

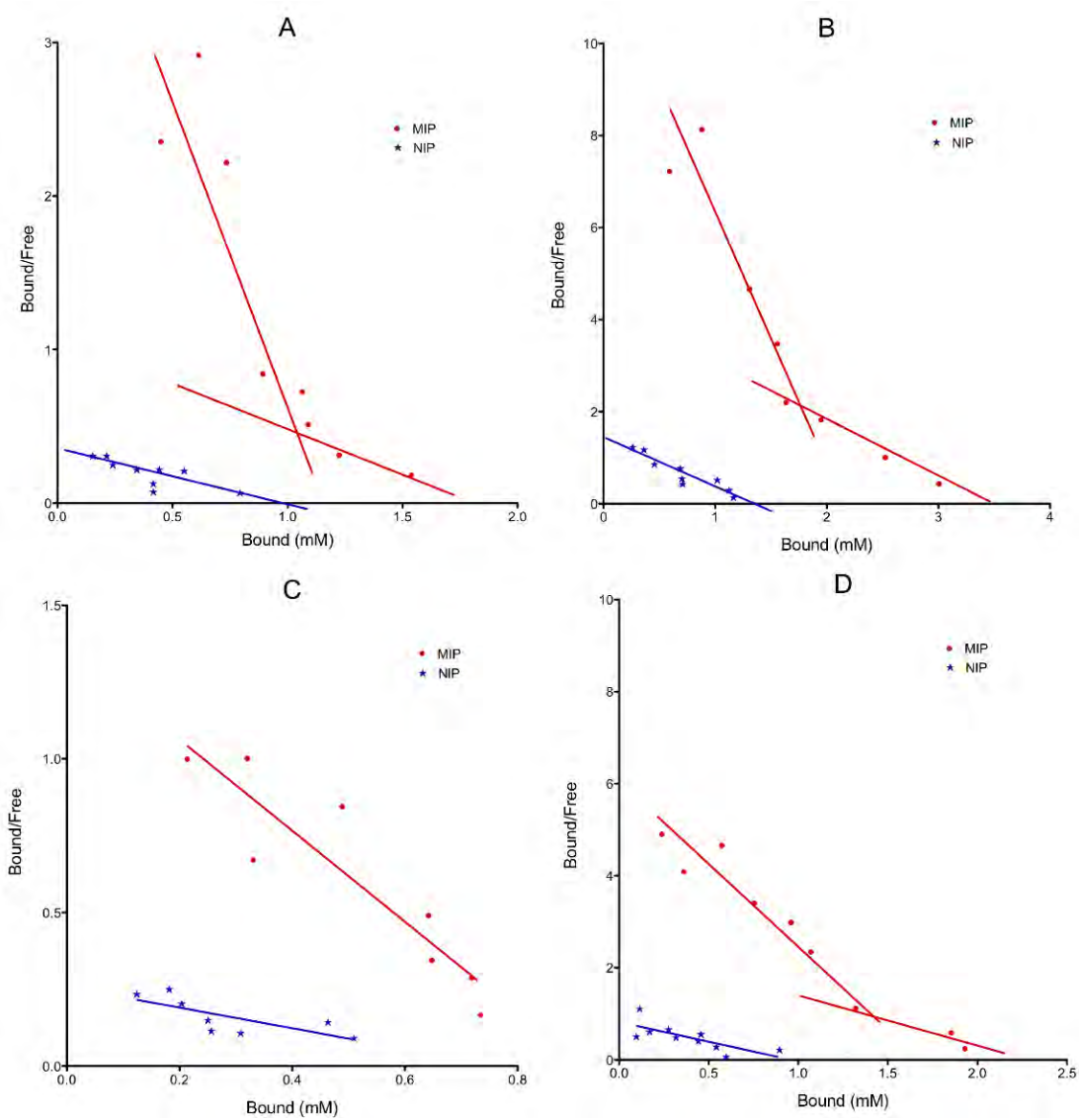


**Figure 4.20:** Scatchard plots produced for NC-MAA-EGDMA-1C (**A**), NC-MAA-EGDMA-2C (**B**), NC-MAA-TRIM-1C (**C**) and NC-MAA-TRIM-2C (**D**).

The Langmuir plot was obtained by plotting free/bound versus free. Again a line of best fit was applied to the data, from which the  $K_d$  and  $n$  values were calculated. The Langmuir plots generated for NC-MAA-EGDMA-1C (**A**), NC-MAA-EGDMA-2C (**B**), NC-MAA-TRIM-1C (**C**) and NC-MAA-TRIM-2C (**D**) are displayed in Figure 4.21. In the Langmuir plot, homogeneity is present when all points are linear and lie on a line of best fit. When heterogeneous binding sites are present, points are scattered or a curve is produced. These plots are known to be biased when high analyte concentrations are used, causing the data into a forced linearity. As a result, attention needs to be paid to the lower concentrations, as heterogeneity can exist in this region<sup>113</sup>

The Langmuir plots obtained for the MIPs exhibited greater homogeneity than expected as the plots were generally linear in nature. However, on closer examination, it could be observed that at low concentrations the data were clustered, not linear. This suggests that the MIPs are in fact heterogeneous with low and high affinity sites. The  $K_d$  and  $n$  values calculated using the Langmuir regression also followed the same trend as the previous two methods with the  $K_d$  MIP values smaller than the  $K_d$  NIP values and greater  $n$  values for the MIPs compared to the NIPs. The Langmuir plots generated for the NIPs exhibited a more scattered array of points. This suggests that a variable distribution of non-selective binding sites is present within these polymers. The  $K_d$  and  $n$  values are in Table 4.1.

The calculated  $K_d$  values from all three methods showed that binding was stronger in the MIPs of all formulates than their corresponding NIPs. High congruency was observed for the calculated  $n$  values from all three methods.

In all cases, the number of binding sites was greater in the MIPs than the NIPs indicating that the imprinting process has formed additional and specific binding sites in the MIPs. The three methods utilised to determine the  $K_d$  and  $n$  values, direct calculation from the binding isotherm, Scatchard regression using limiting slopes analyses and the Langmuir linear regression, provided insightful information regarding the binding of the polymers investigated. Each method has advantages and disadvantages associated with it. The direct non-linear fitting method requires an understanding of the data and the equation needed to fit the data. With this established, the method does not differentiate between

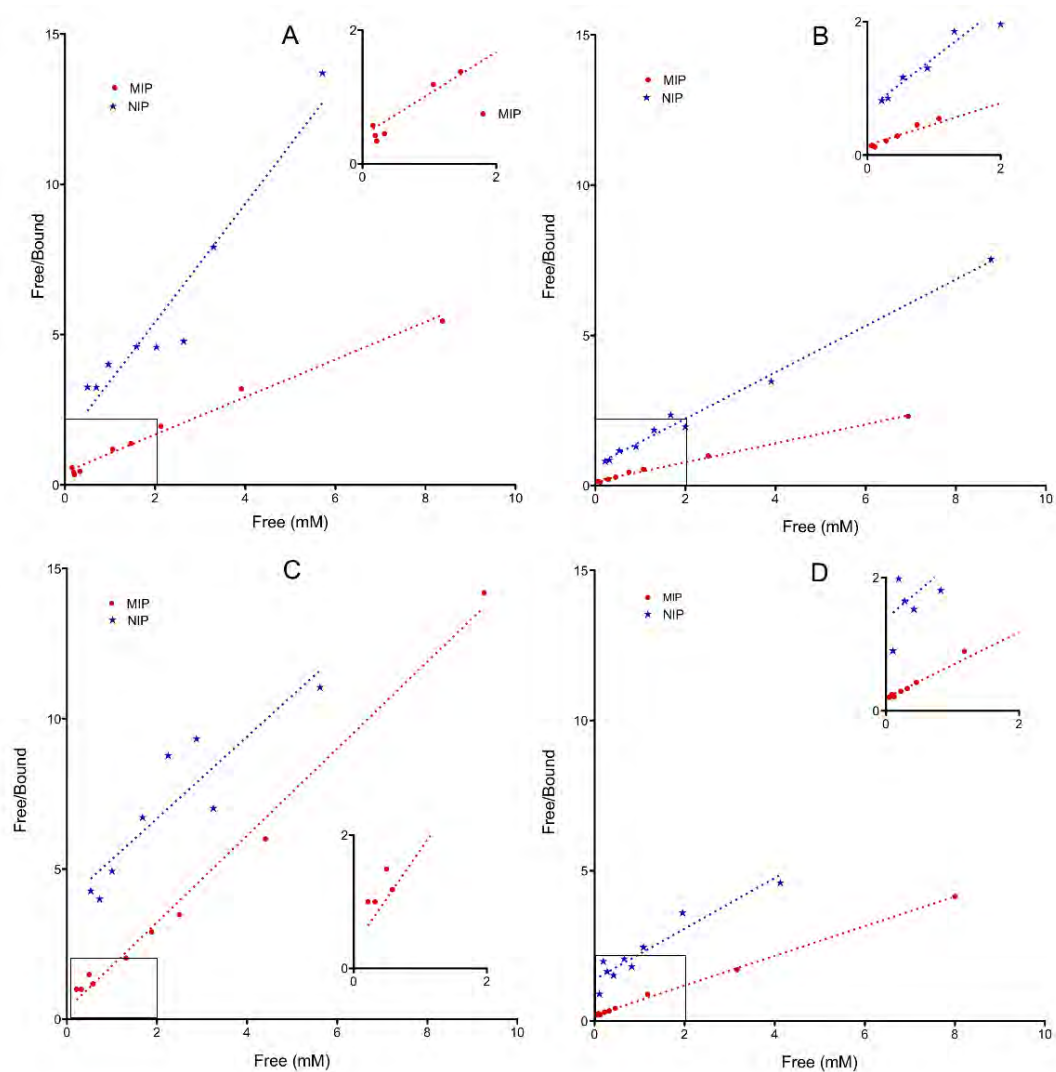


**Figure 4.21:** Langmuir linear plots produced for MAA 1:1 CHCl<sub>3</sub> EGDMA (A), MAA 1:2 CHCl<sub>3</sub> EGDMA (B), MAA 1:1 CHCl<sub>3</sub> TRIM (C) and MAA 1:2 CHCl<sub>3</sub> TRIM (D). Inserts are included for clarity.

homo- or heterogeneous bindings sites in MIPs. In contrast, the Scatchard plot is capable of separating binding sites (low and high affinity) present in the polymer through slope fitting. However this method has been shown to be inaccurate for calculating the  $K_d$  and  $n$  values<sup>92</sup>, as linear transformation distorts the experimental error. Scatchard transformation also alters the relationship between X and Y and violates the assumptions of linear regression. Finally, the Langmuir plot is also a good indicator of whether multiple binding sites are present. From this plot it is especially easy to see when homo- or heterogeneity is present, as the data is either linear or scattered. This plot is known to produce inaccuracies, as it can become biased when high concentrations of solutions are used.

If access to a curve fitting program is possible, the best method for calculating the  $K_d$  and  $n$  values would be through a combination of both the non-linear regression and Langmuir plots. The curve fitting program provides an accurate and easy method for the calculation of the  $K_d$  and  $n$  values, while the Langmuir plot, using both MIPs and NIP, then enables the type of binding sites to be determined.

## 4.3 Conclusion

Initial BZP binding assays were conducted on polymers prepared from 100% cross-linkers EGDMA, TRIM and DVB to determine the extent of their interaction with BZP. From this experiment, it was observed that both EGDMA and TRIM had minimal interaction with BZP, binding a maximum of 6% of the 0.8 mM solution when a low polymer concentration (5 mg) was used. The cross-linker DVB had more significant template up-take, binding up to 20% of BZP from solution (30 mg, 0.8 mM BZP solution). Results obtained from this investigation indicate that both EGDMA and TRIM are appropriate cross-linkers, i.e. do not promote non-selective binding, for the preparation of BZP imprinted polymers.

Based on T:FM interaction studies presented in Chapter 3, three functional monomers, namely, MAA, AA and IA were used for the MIP preparation. BZP MIPs were prepared at 1:1, 1:2 and 1:4 BZP:FM ratios using acetonitrile and chloroform as porogens and TRIM and EGDMA cross-linkers resulting in 30 different formulations.

Among all the polymers, only the MAA polymers from T:M ratios 1:1 and 1:2 prepared and bound in  $\text{CHCl}_3$  using both cross-linkers and the 1:1 MAA-EGDMA polymer prepared and bound in AN showed appreciable selectivity towards BZP (0.8 mM BZP solution, 30 minutes binding time) with imprinting factors greater than 2 obtained for all polymer concentrations (5 to 30 mg range) tested. A summary of the results is presented in Table 4.2.

The swelling behaviour was found to be affected by the porogen, greater swelling was observed in  $\text{CHCl}_3$  than in AN. The surface morphology of the polymers were also observed to be influenced by the porogens AN and  $\text{CHCl}_3$  and crosslinkers EGDMA and TRIM. Both swelling behaviour and surface morphology, however, did not show any apparent effect to the binding behaviour of the MIPs. In addition, the results suggest that  $\text{CHCl}_3$  is the more effective porogen for polymerisation as it creates the most open structure in the resulting polymer.

The polymers NC-MAA-EGDMA-1C, NC-MAA-EGDMA-2C, NC-MAA-TRIM-1C and NC-MAA-TRIM-2C were analysed further to optimise their binding behaviour. Optimal binding time was reached after 1 hour giving I values of 4.0, 2.1, 2.5 and 2.9 and maximum binding of 56, 86, 46 and 68% of the BZP from a

**Table 4.2:** Summary of absorption and time rebinding results for BZP:MAA non-covalent imprinted polymers

Polymer	Absorption (%)					Time (mins)	
	5 mg	10 mg	20 mg	30 mg	I	Equ. <sup>a</sup>	> I <sup>b</sup>
NC-MAA-EGDMA-1C MIP	17	26	42	62	6.7	480	120 (I=6.1)
NC-MAA-EGDMA-1C NIP	3	5	7	11			
NC-MAA-EGDMA-2C MIP	42	61	67	75	4.4	60 240	60 (I=2.1)
NC-MAA-EGDMA-2C NIP	16	14	17	18			
NC-MAA-TRIM-1C MIP	16	20	22	31	2.9	120 30	480 (I=4.4)
NC-MAA-TRIM-1C NIP	7	8	11	11			
NC-MAA-TRIM-2C MIP	21	31	56	63	7.7	60 120	60 (I=2.9)
NC-MAA-TRIM-2C NIP	3	14	17	26			

<sup>a</sup> Time at which equilibrium was established

<sup>b</sup> Time at which the greatest imprinting factor was observed

0.8 mM solution. For the four polymers investigated, it was observed that over 80% of the total BZP absorption occurred within a 10 minute timeframe. This result is ideal for the intended use of the MIPs as an in-field sensor when quick response is needed especially when time is either critical or limited.

Quantitative binding analysis of the four selected polymers (1:1 and 1:2 T:FM ratios, EGDMA and TRIM cross-linkers, chloroform porogen) based on the  $K_d$  and  $n$  values estimated using three different methods (direct non-linear regression of the binding isotherm, a Scatchard regression using limiting slopes analyses and the Langmuir linear regression) showed the MIPs to exhibit a stronger binding affinity toward BZP and greater number of binding sites than their corresponding NIPs. A stronger affinity was also observed for the 1:2 formulations than the 1:1 formulations however the ratio of the  $K_d$  NIP to  $K_d$  MIP was observed to be higher for the 1:1 ratios. This suggested that while the 1:2 T:FM ratio exhibit stronger affinity to BZP than the 1:1 ratio, the difference in the degree of BZP affinity between the MIP and the NIP is greater in the 1:1 ratio than in the 1:2 ratio.

# 5

## Preparation of Benzylpiperazine MIPs: The Semi-covalent Approach

### 5.1 Introduction

Covalent imprinting utilises readily reversible covalent bonds to attach the functional monomer to the template, forming a template-monomer (TM) adduct. This requires chemical synthesis that can be complex in nature. However, once the TM adduct has been obtained, it can then be incorporated into the polymer by polymerisation in the presence of a cross-linker and initiator in a porogen. The synthetic limitations imposed by covalent imprinting have made it a less favourable option in comparison to non-covalent imprinting. However, covalent imprinting produces well-defined recognition sites that makes highly selective MIPs that are stable and stoichiometric<sup>40</sup>.

When covalent imprinting is used, chemical methods are required to remove and rebind the template to the polymer. A modification to this technique is to implement semi-covalent imprinting. In semi-covalent imprinting, covalent methods are used to prepare the polymer and to remove the template however, non-covalent interactions are subsequently utilised to rebind the template. Using non-covalent interactions for template rebinding is accomplished by incorporat-

ing a sacrificial spacer between the template and the functional group during TM adduct preparation. The carbonyl group of the carbonate ester is the most commonly used spacer group, first used for imprinting cholesterol<sup>49</sup>, however it has also been employed in urea<sup>50</sup> and carbamate<sup>27;51-53</sup> linkages as well as other carbonate esters<sup>54;55</sup> as the sacrificial group.

This chapter deals with the synthesis, preparation and performance of BZP semi-covalent imprinted polymers. As with the self-assembly approach, MIPs were prepared using both EGDMA and TRIM as cross-linkers and AN and CHCl<sub>3</sub> as porogens.

## 5.2 Results and Discussion

### 5.2.1 Synthesis of Benzylpiperazine (4-vinylphenyl) carbamate and Semi-covalent MIPs

Benzylpiperazine (4-vinylphenyl) carbamate was used as the TM adduct for the synthesis of BZP MIPs by the semi-covalent approach. Figure 5.1 shows the proposed sacrificial spacer group and the functional monomer that will be attached to BZP. Post polymerisation, the template is removed via hydrolysis of the thiocarbamate spacer group, leaving behind an acidic phenol unit ( $pK_a = 9.98$ ) that is capable of hydrogen bonding with the template. It is for this reason that the group has been labelled sacrificial.

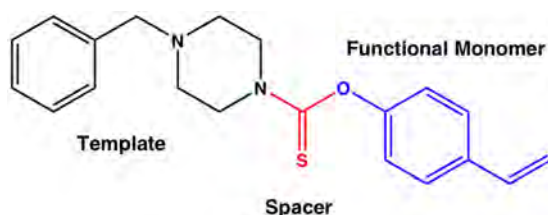


**Figure 5.1:** Chemical structure of BZP TM adduct with proposed sacrificial spacer and functional monomer.

The synthesis of benzylpiperazine (4-vinylphenyl) carbamate required a multi-step protocol in order to de-protect the starting material, attach the spacer to the functional monomer and finally attach BZP to the spacer-monomer adduct. The reaction scheme for this synthesis is illustrated in Figure 5.2.

The monomer 4-vinylphenol was chosen as the starting monomer as it contains a phenolic donor group that is capable of interacting with the amine on the piperazine. This monomer has also previously been successfully incorporated in covalent MIPs for a number of substrates including cholesterol<sup>49</sup>, N-heterocycles<sup>114</sup> and small substituted phenols<sup>54</sup>. 4-Vinylphenol was prepared by de-protecting the 4-acetoxystyrene by the method published by Corson and co-workers<sup>103</sup>. The product was purified by recrystallisation from hexane before further synthesis was performed.

The sacrificial spacer group was created using thiophosgene, as this was capable of readily reacting with both the alcohol group of 4-vinylphenol and the

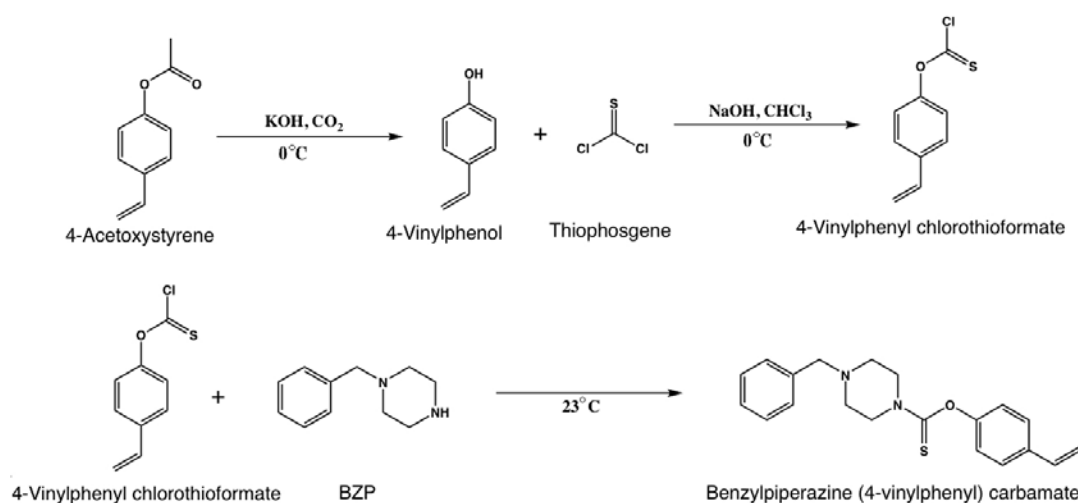


**Figure 5.2:** Synthetic scheme for the preparation of TM adduct benzylpiperazine (4-vinylphenyl) carbamate.

amine group of BZP. The thionyl group is not commonly used as a spacer, as it is less reactive than the carbonyl counterpart. It was successfully incorporated as a carbamate linkage by first reacting thiophosgene with the less reactive phenol, before attaching it to the secondary amine of BZP. Thiophosgene was attached to 4-vinylphenol via the procedure of Oh and co-workers<sup>104</sup>. The reaction was considerably fast and yielded a yellow liquid that was pure, determined by TLC and NMR analysis.

The final step in the synthesis was attaching the thiocarbamate to BZP. The reaction was done neat in an excess of BZP to act as a base to remove excess acid that was formed. The final product, purified by flash chromatography using 5% ethyl acetate/hexane followed by 10% ethyl acetate/hexane, was a pale yellow solid, identified to be pure through TLC and NMR analysis.

### 5.2.2 Preparation of Semi-covalent MIPs

Once the synthesis of the TM adduct had been accomplished, the polymers were prepared following the procedure of Whitcombe *et al*<sup>49</sup>. Two MIPs, that mimic the composition of the better performing non-covalent MIPs (1:1), were prepared using  $\text{CHCl}_3$  as porogen. MIPs were prepared in a 1:19 TM adduct to cross-

linker (TM:XL) ratio using EGDMA and TRIM, forming the polymers labelled SC-EGDMA-1 and SC-TRIM-1. These two cross-linkers were used as it was determined that they had minimal interaction with the template in the preparation of the non-covalent polymers (Chapter 3). Non-imprinted polymers (NIPs) were also prepared under identical conditions but in the absence of the TM adduct, 0:19 TM:XL ratio. The use of cross-linkers as the sole monomer making up the NIP for semi-covalent and covalent MIP systems is common in the literature<sup>49;54</sup>. Polymerisation was performed at 60°C for 12 hours. Following this, the MIPs were ground, with the fraction between 32 and 63  $\mu\text{m}$  collected.

The template was extracted by heating at reflux in 1 M methanolic NaOH for 12 hours. This was neutralised with HCl and washed with methanol for a further 12 hours. The polymers were dried at 40°C under vacuum prior to analysis.

The resulting functionality of the MIP cavity after the template and spacer group had been removed is illustrated in Figure 5.3 and provides the binding site for rebinding of the BZP analyte.

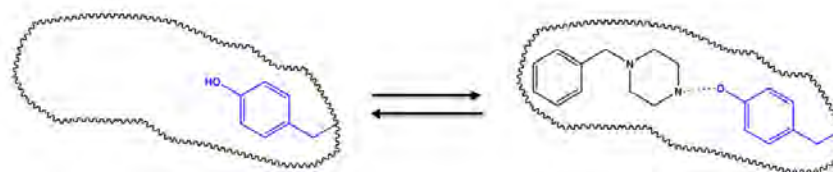


**Figure 5.3:** Proposed mechanism of BZP rebinding into the empty covalent polymer cavity using non-covalent bonds.

### 5.2.3 Physical Characterisation of the MIPs

Scanning electron microscope (SEM) images were produced for all polymers prepared. From these images it was possible to observe the surface morphology of each polymer.

The SEM micrographs of SC-EGDMA-1 MIP and NIP are presented in Figure 5.4 (A) and (B), respectively. Both polymers show macroporous surfaces although the MIP has larger pores and showed more uniform porosity than the NIP. In contrast, the SEM images produced for the SC-TRIM-1 prepared poly-

mers, given in Figure 5.5, showed a marked difference in surface macrostructure between the MIP and NIP. The surface of SC-TRIM-1 MIP is very smooth with very small pores while the NIP has larger pores which are uniformly distributed. The surface structures of SC-EGDMA-1 and SC-TRIM-1 are also very different with the former exhibiting visible surface porosity as with SC-TRIM-1 NIP and the latter showing a smoother surface structure. It has been hypothesised that the low polarity solvents ( $\text{CHCl}_3$ ) produce these characteristics suggesting that the polymer is remaining in solution longer than what is observed in more polar solvents like AN<sup>112</sup>.

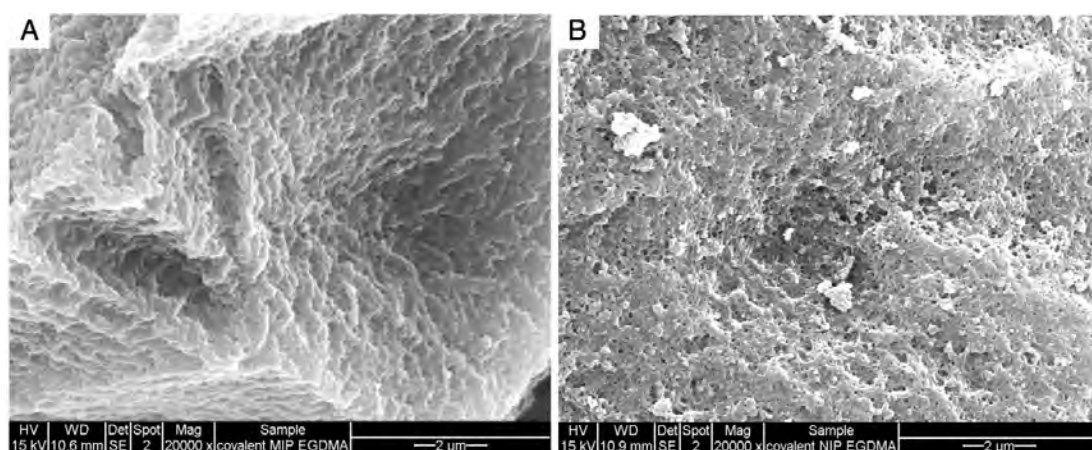


**Figure 5.4:** SEM images for the covalent EGDMA polymers prepared in  $\text{CHCl}_3$  showing the MIP (**A**) and NIP (**B**).

Swelling was measured for EGDMA1 and TRIM1 in  $\text{CHCl}_3$  from the dry state. The volume of 10 mg of dry polymer was measured prior to the addition of solvent. After an hour the solvent was removed and the new volume recorded. The results of this experiment can be observed in Figure 5.6. Both EGDMA1 and TRIM 1 showed minimal swelling in  $\text{CHCl}_3$  with the NIPs growing 4% of their original size while the MIPs increased to just 3% from their original volume.

#### 5.2.4 Polymer Absorption of BZP: Evaluation of Imprinting Effect

The semi-covalent MIPs were tested for their capacity to sorb BZP. This experiment establishes the efficiency of the MIPs to rebind the template and allows

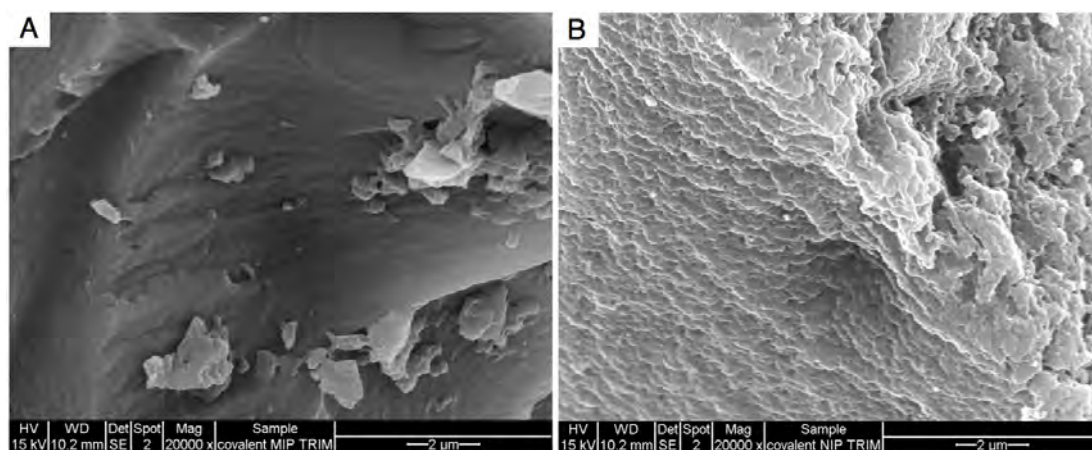


**Figure 5.5:** SEM images for the covalent TRIM polymers prepared in  $\text{CHCl}_3$  showing the MIP (A) and NIP (B).

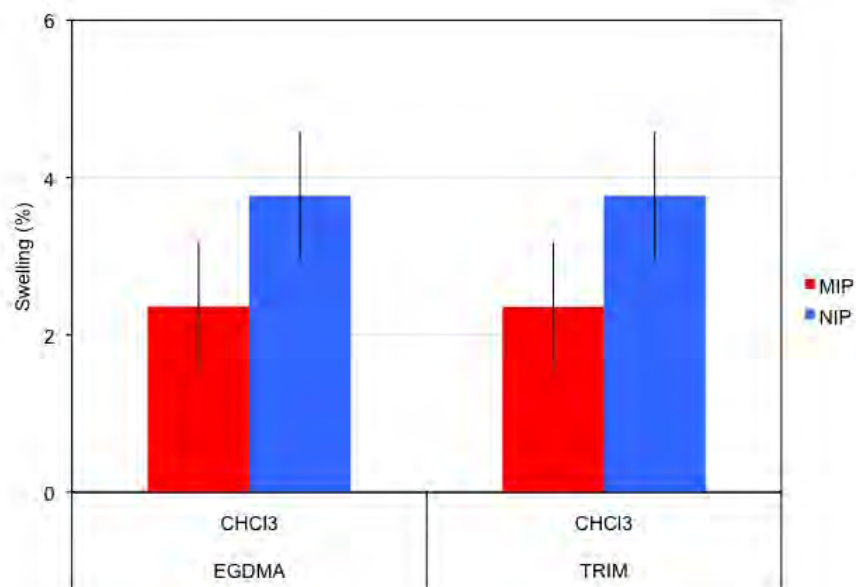


**Figure 5.6:** Swelling results for the EGDMA and TRIM covalent polymers prepared in chloroform. Measurements were performed on 10 mg of polymer in  $\text{CHCl}_3$  in the dry state and after 1 hr had elapsed.

screening of poor performing MIPs. It also enables the optimum polymer concentration for a set BZP solution to be determined. BZP rebinding was evaluated by using batch adsorption experiments with 1 mL of 0.8 mM BZP solution with a polymer-template contact time of 30 minutes, as per the polymer adsorption analyses performed on the non-covalent imprinted polymers.

In both SC-EGDMA-1 and SC-TRIM-1 polymers, a uniform increase in the amount of template bound was observed as the polymer concentration increased, suggesting homogeneity of the binding sites. This trend was in contrast to the cross-linker only NIPs, which had minimal binding across all masses examined (5 mg - 30 mg). The results from this experiment are presented in Figure 5.7. In covalent and semi-covalent imprinting, NIPs are prepared from cross-linker only as non-covalent NIPs cannot be used due to the incorporation of FM. The non covalent NIP is not a true representation of the non imprinted reference for covalent MIPs, as there is no randomization of the FM in the covalent MIP.

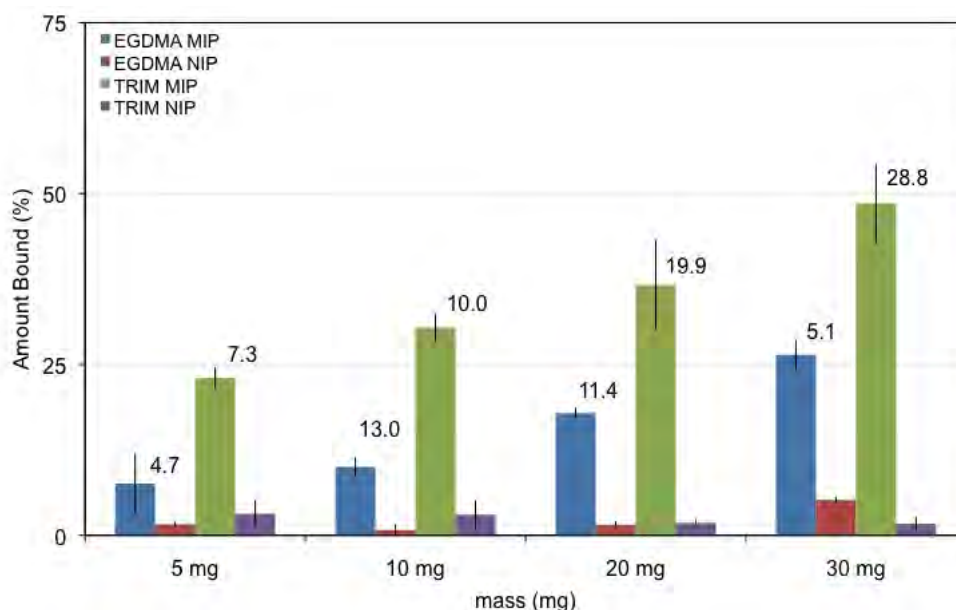


**Figure 5.7:** Rebinding results for semi-covalent BZP polymers prepared with EGDMA and TRIM in  $\text{CHCl}_3$ . 1 mL 0.8 mM solution with a binding time of 30 minutes was used. All experiments were performed in triplicate. Amount bound =  $\frac{([Total] - [Free])}{[Total]} \times 100$

SC-TRIM-1 showed a greater affinity for the template, binding twice the

amount sorbed by SC-EGDMA-1. The maximum amount of template bound by the SC-EGDMA-1 MIP was 26.4% while the SC-TRIM-1 polymer recorded 48.6% both at a 30 mg polymer concentration. The imprinting factors, however, did not increase consistently with increasing polymer mass due to small variations in NIP binding. Nevertheless, the  $I$  values ranged from 5 to an impressive 29, which indicates the presence of well-defined BZP cavities.

The method of semi-covalent imprinting has produced MIPs with a high affinity toward BZP. From the results obtained, it was possible to see that both polymers bound BZP and as a result, all subsequent experiments were performed for both polymers. Polymer saturation had still not been achieved with 30 mg of polymer in 1 mL of 0.8 mM BZP solution, however this mass (30 mg) was subsequently used as a polymer mass greater than this, prevented the removal of enough analyte solution to perform accurate analysis.

### 5.2.5 Determination of Optimal Time of Contact

Time binding studies were performed to establish the binding kinetics and point of equilibrium for each system. Again, a rapid quantification time is desirable for these polymers to be used as sensors for the detection of BZP. The time range investigated was between 10 minutes and 24 hours and used 30 mg of polymer and 1 mL 0.8 mM BZP solution in  $\text{CHCl}_3$ . The results of the time binding studies are given in Figure 5.8. Equilibrium was attained prior to 8 hours, consequently only the results obtained prior to this time are displayed.

Both SC-EGDMA-1 and SC-TRIM-1 polymers showed extremely rapid up-take of the template. For SC-EGDMA-1, a maximum of 35% of the template was bound after a 2 hour contact time. The amount of template bound after 10 minutes, the first point of time investigated, was 28%. This up-take constitutes 82% of equilibrium template binding and confirming rapid mass transfer kinetics of the polymer. The maximum imprinting value calculated was  $I = 376$ , obtained after a 1 hour binding time. This impressive value is the result of less than 1% template up-take by the NIP, which does not contain functional monomer and thus no point for non-specific binding to be generated.

For the TRIM prepared polymer, the maximum amount of template bound

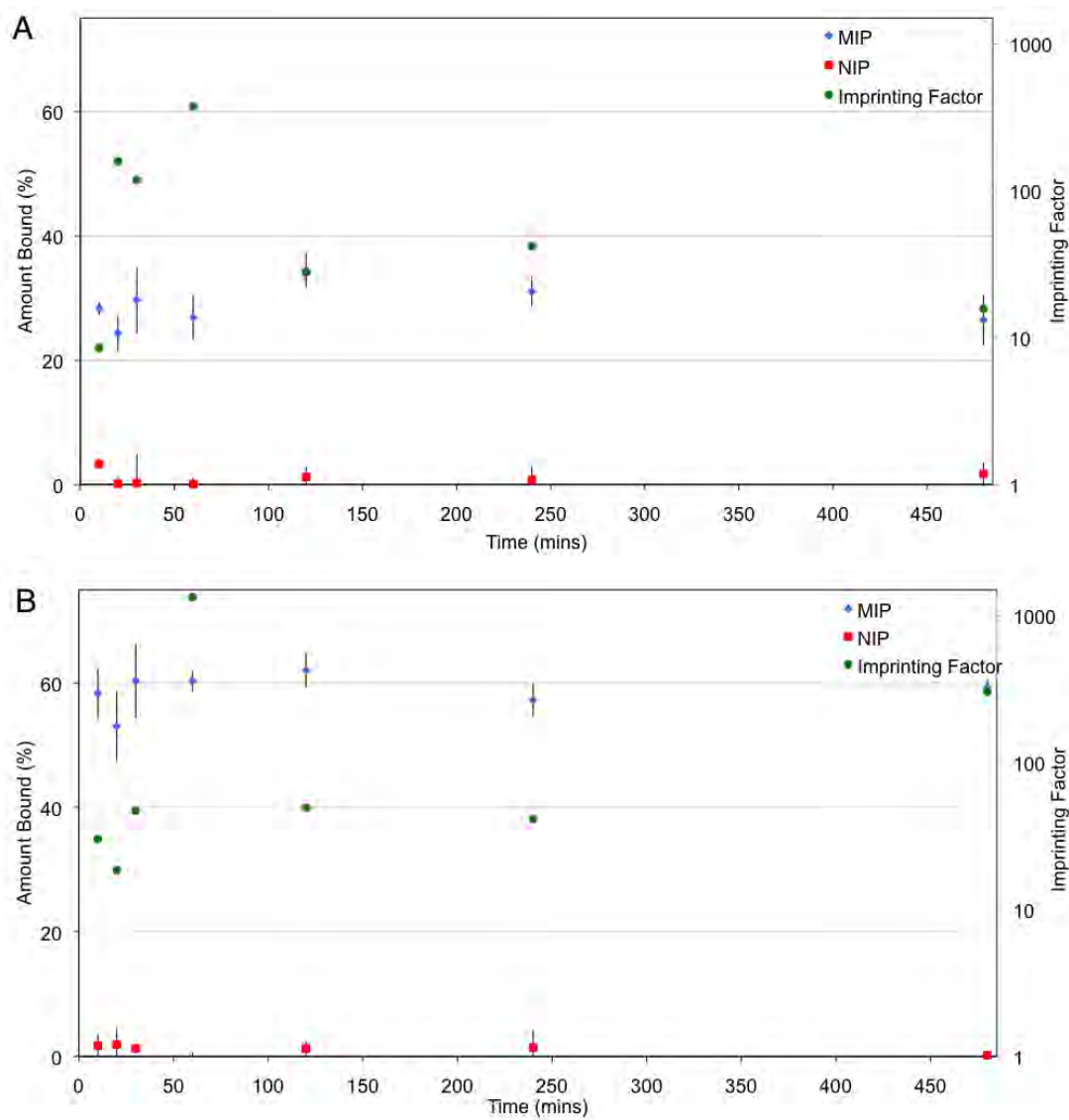


**Figure 5.8:** Time rebinding results for covalent BZP polymers prepared with EGDMA (**A**) and TRIM (**B**) in  $\text{CHCl}_3$ , using 30 mg of polymer with 1mL 0.8 mM BZP. All experiments were performed in triplicate. Amount bound =  $\frac{([Total] - [Free])}{[Total]} \times 100$

was 62%, also after 2 hours binding time. The greatest imprinting factor obtained was an I value of 1340. This was also obtained after a 60 minute contact time and like the SC-EGDMA-1 NIP, was the result of less than 1% BZP binding. For this polymer system, 94% of the maximum amount of template bound was rebound prior to 10 minutes. This value also makes the TRIM polymer acceptable as a rapid sensor, especially in conjunction with the selectivity of the system.

An additional time binding study was performed with the TRIM prepared polymer using water as the binding solvent. Rebinding was performed in water as it is more readily accessible in-field and is a greener alternative to volatile organic compounds (VOCs) like  $\text{CHCl}_3$ . It also means that the end user distribution can be widened as it does not require formal safety training with respect to hazardous solvents. The time range investigated was between 10 minutes and 8 hours using 30 mg of polymer and 1 mL 0.8 mM BZP solution in water. The pH of the solution was not controlled in this experiment.

Figure 5.9 shows that TRIM1 is capable of BZP up-take in an aqueous solution however, both the rebinding capacity (34% at 2 hours) and largest imprinting factor ( $I = 4.9$ ) were reduced from the  $\text{CHCl}_3$  system ( $B_{\text{max}} = 62\%$  and  $I = 1340$ ). This was due to template up-take by the NIP. Eventually, binding discrimination between the MIP and the NIP decreased to a minimum after 4 hours. It is hypothesised that the increased NIP up-take is due to the forced hydrophobic interactions in the polar solvent conditions. It can be seen that as time progressed the amount of template bound by the NIP increased. Equilibrium was established for the MIP at 2 hours (33%) and the NIP at 4 hours (22%). The imprinting factor for the system after this time was 1.4. Rapid up-take was also observed for this system, with 24% BZP up-take at 10 minutes. The imprinting factor at this time was 4.3 showing that good selectivity is achieved in the initial stages of imprinting, suggesting that selective occupation of the binding cavities is occurring first before non-specific binding.

These results show that this polymer has potential. If water is to be used as the rebinding solution, a short binding time of 30 minutes or less should be used. Studies in which the pH is controlled could enhance up-take and reduce non-specific binding. In addition, more polar aprotic porogens such as AN and THF can be investigated, or a mixed solvent study could also be undertaken with

the possible use of a surfactant as a means to improve rebinding behaviour.

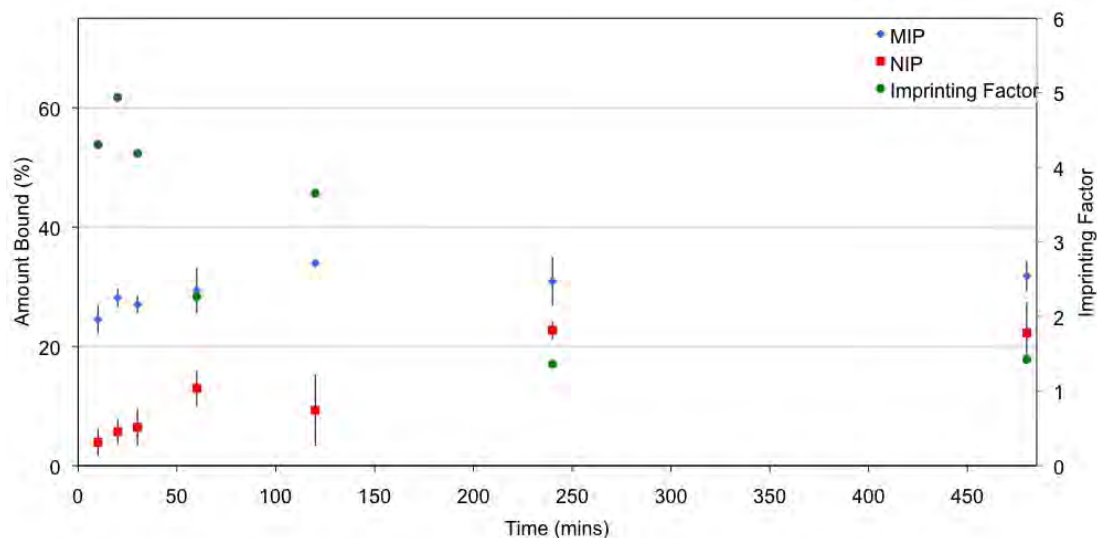


**Figure 5.9:** Rebinding results for covalent BZP polymer prepared with TRIM in water, using 30 mg of polymer with 1mL 0.8 mM BZP. All experiments were performed in triplicate. Amount bound =  $\frac{([Total] - [Free])}{[Total]} \times 100$

For the time studies performed in  $CHCl_3$ , the results have shown that both polymers have similar binding dynamics for the up-take of BZP. Equilibrium was established after 1 hour. It was also at this time that the greatest imprinting factor for each polymer was obtained. As a result, a 1 hour binding time was used for subsequent analysis. In addition, it should be noted that for SC-EGDMA-1, more than 80%, and for SC-TRIM-1, more than 90% of the maximum amount of template bound had been absorbed by the polymers prior to the 10 minute analysis.

### 5.2.6 Saturation Curve and Analysis

Binding isotherms were generated for the two semi-covalent MIPs, EGDMA1 and TRIM1. One mL of BZP solution ( $CHCl_3$ ) in the concentration range of 0.3 to 3 mM was used with 30 mg of polymer and bound for 1 hour. The saturation curves produced are presented in Figure 5.10. Only the MIPs were investigated, as the NIPs showed minimal binding. The binding isotherms produced for the

two polymers showed that in the range examined, saturation of the polymer was achieved and that TRIM1 has a higher binding capacity than EGDMA1.

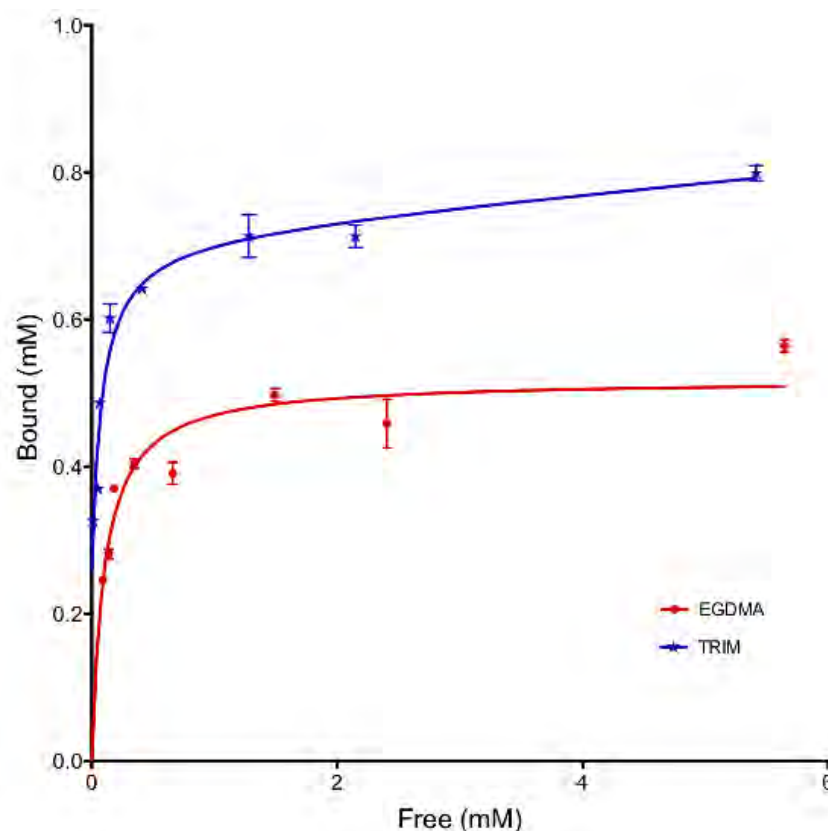


**Figure 5.10:** Binding isotherm data produced for the semi-covalent EGDMA MIP (A) and TRIM MIP (B) using 30 mg of polymer with 1mL of BZP solution concentrations (0.3 - 3 mM) and a contact time of 1 hr. All experiments were performed in triplicate.

The binding constants, ( $K_d$ ) and ( $n$ ), for the two MIPs were calculated by the following methods as with the non-covalent polymers: a directly from the binding isotherm, by Scatchard regression using limiting slopes analyses, and by the Langmuir linear regression.

The  $K_d$  and  $n$  values calculated directly from the binding isotherm was achieved using a curve fitting program (Prism 5, Graphpad Software, 2009) and are displayed in Table 5.1. The  $K_d$  values calculated for SC-EGDMA-1 ( $1.34 \times 10^{-4}$  M) is 1.26 x higher than SC-TRIM-1 ( $2.94 \times 10^{-5}$  M). This result shows that SC-TRIM-1 has a greater binding affinity for BZP than SC-EGDMA-1. The  $n$

## 5.2 Results and Discussion

values calculated for the two polymers,  $5.18 \times 10^{-2}$  M for SC-EGDMA-1 and  $7.28 \times 10^{-2}$  M for TRIM1 were comparable.

**Table 5.1:** Binding constants,  $K_d$  and number of binding sites ( $n$ ), extracted from the binding isotherm, Scatchard plot and Langmuir plot for the semi-covalent EGDMA and TRIM polymers prepared in  $\text{CHCl}_3$ .

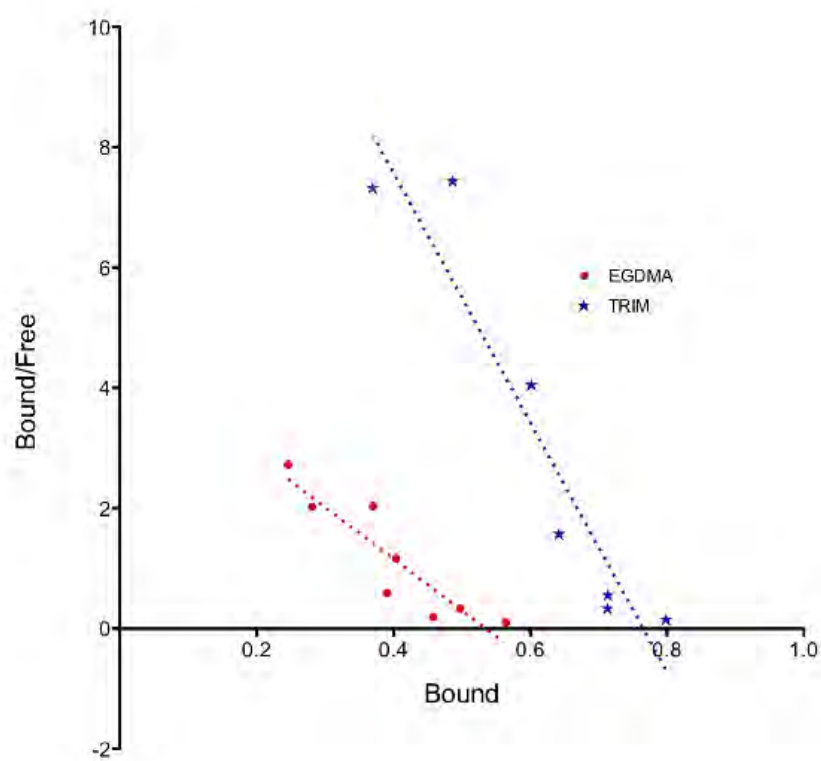
	$K_d$ Value $\times 10^{-4}$ (M)	
	SC-EGDMA-1	SC-TRIM-1
Binding Isotherm	1.025	0.814
Scatchard	1.164	0.4818
Langmuir	2.037	0.8415
	$n \times 10^{-2}$ (M)	
	SC-EGDMA-1	SC-TRIM-1
Binding Isotherm	5.180	7.279
Scatchard	5.349	7.652
Langmuir	5.684	7.985
	$r^2$	
	SC-EGDMA-1	SC-TRIM-1
Binding Isotherm	0.8412	0.9480
Scatchard	0.8254	0.8969
Langmuir	0.9922	0.9979

Scatchard equation:  $S_B/C_f = Kn - S_B$

Langmuir equation:  $C_f/S_B = C_f/n + 1/Kn$

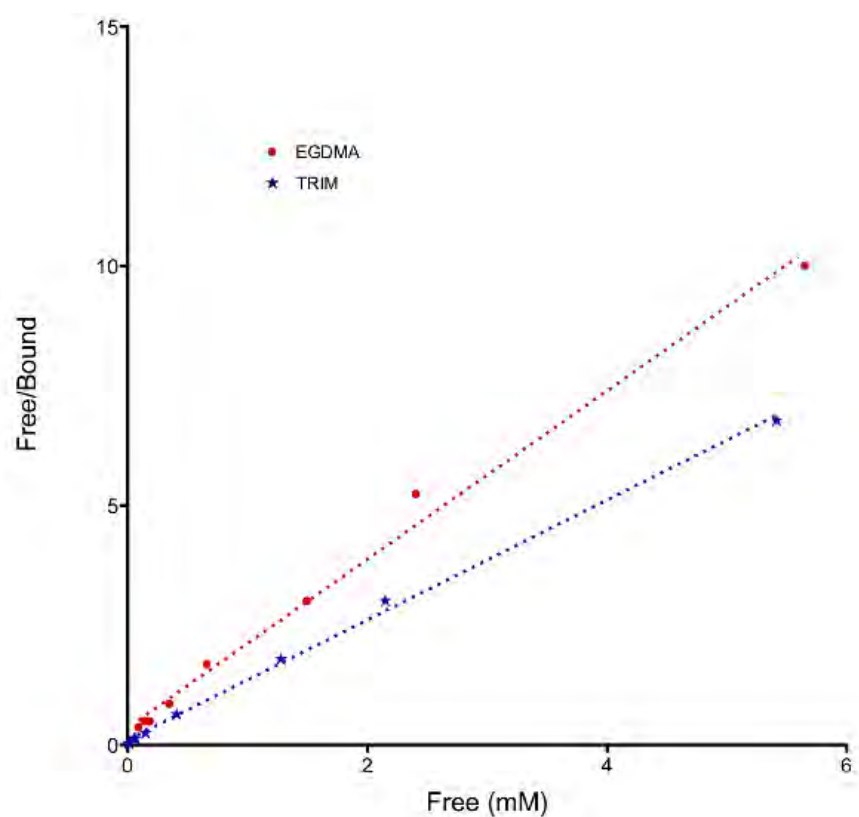
The Scatchard plots for the EGDMA and TRIM prepared semi-covalent polymers are displayed in Figure 5.11 and the calculated  $K_d$  and  $n$  values from the plots are in Table 5.1. The Scatchard plots produced for SC-EGDMA-1 and SC-TRIM-1 were linear in nature suggesting that only one type of binding site is predominant at the concentration range studied. The plots show that the concentration of bound BZP is at the lower range suggesting that the BZP occupied higher affinity binding sites. In addition, the  $K_d$  values calculated from the slopes of the curve for both polymers are within the range of values expected from high affinity sites of other MIPs. More importantly, these  $K_d$  values and their corresponding  $n$  values are comparable to those obtained directly from the binding isotherm for the same MIP systems.

Figure 5.12 shows the Langmuir plots generated for SC-EGDMA-1 and SC-TRIM-1 to be linear, with  $r^2$  values of 0.9868 and 0.9979 for the SC-EGDMA-



**Figure 5.11:** Scatchard plots produced for the semi-covalent polymers SC-EGDMA-1 MIP (**A**) and SC-TRIM-1 MIP (**B**).

1 and SC-TRIM-1 polymers, respectively. This also suggests homogeneity of the binding sites within the polymers, which is consistent with the theory of imprinting by the covalent method. As with both the other methods previously discussed, the  $K_d$  for SC-EGDMA-1 is 2.42 x higher than SC-TRIM-1 indicating a stronger affinity of BZP with SC-TRIM-1 than with SC-EGDMA-1. The  $n$  values for both polymers are also close in magnitude and comparable to the values estimated by the alternate methods.



**Figure 5.12:** Langmuir regression plots produced for the semi-covalent polymers SC-EGDMA-1 MIP (A) and SC-TRIM-1 MIP (B).

As with the non-covalent polymers, the three methods utilised to determine the  $K_d$  and  $n$  values provided an insight into the dynamics of EGDMA1 and TRIM1. Again, congruency was not observed across all three methods for the calculated  $K_d$  values however, it could still be established that TRIM1 had the stronger binding affinity for BZP. The number of binding sites calculated by the three methods showed TRIM had a larger number of binding cavities, which

explains the higher binding capacity observed for this polymer. As discussed in Chapter 4, the three methods have a number of advantages and disadvantages associated with their use. As a result, the use of a combination of methods would be advantageous, to provide a full understanding of the polymers under investigation.

## 5.3 Conclusion

The synthesis of the BZP-monomer adduct proved to be a relatively straightforward three step synthesis when thiophosgene was incorporated. Thiophosgene was reacted with 4-vinylphenol to produce the pure product 4-vinylphenyl chlorothioformate. This was then incorporated with BZP through a neat reaction, producing the TM adduct, benzylpiperazine (4-vinylphenyl) carbamate.

The semi-covalent MIPs, synthesised in a 1:19 TM:XL ratio with SC-EGDMA-1 and SC-TRIM-1, showed significant binding affinity toward BZP, in comparison to the NIPs. SC-TRIM-1 showed greater template up-take, absorbing up to 50% of a 0.8 mM BZP solution when 30 mg of polymer was used. This was twice the amount of template bound SC-EGDMA-1 (25%). The imprinting factors produced by the two polymers in these conditions, measured under variable polymer mass, ranged from a low of 4.6 and 7.3 to a high of 13.0 and 28.8 for SC-EGDMA-1 and SC-TRIM-1, respectively.

Physical characterisation of the polymers showed that swelling and surface morphology did not influence BZP absorption. Both EGDMA and TRIM MIPs and NIPs showed minimal swelling (3 - 4%) in  $\text{CHCl}_3$  after 1 hour. The SEM images for SC-EGDMA-1 showed the MIP to have larger pores and more uniform porosity than the NIP, however both were macroporous surfaces. In contrast, SC-TRIM-1 polymers showed a significant difference in surface macrostructure between the MIP and NIP. The surface of MIP was very smooth with very small pores while the NIP had larger pores that are uniformly distributed.

The time binding studies performed on the two polymers showed that template up-take was rapid, with 82% and 94% of the maximum amount of template bound being absorbed prior to 10 minutes for EGDMA and TRIM, respectively. For both polymers, equilibrium was not established until 2 hours, however the greatest imprinting factors ( $I = 376$  and  $I = 1340$ ) were obtained after 1 hour. These values were the result of low NIP up-take ( $< 1\%$ ). From these experiments, the high selectivity and rapid template up-take observed for both these polymers makes them both appealing for use as sensors.

A time binding trial of the SC-TRIM-1 polymer in a water solution was also investigated as a greener alternative to VOCs. This experiment showed that

BZP could be bound by TRIM1 in a water solution however, the capacity was reduced and greater non-specific binding was observed by the NIP. This reduced the imprinting factor for the system ( $I = 5$ ). This system could be optimised by modifying the pH of the solution or by utilising a solvent/water mixture.

Finally, the  $K_d$  and  $n$  values calculated for SC-EGDMA-1 and SC-TRIM-1 showed that SC-TRIM-1 had the stronger binding affinity for BZP while both polymers have comparable number of binding sites. In addition, the linear nature of the Scatchard and Langmuir plots produced from the binding isotherms indicated that homogenous binding sites were present within each polymer at the range of BZP concentration studied.

# 6

## Semi-Covalent versus Non-covalent BZP MIPs: A Comparative Assessment

### 6.1 Introduction

This work involved the preparation of BZP imprinted polymers employing two approaches. The first approach utilises self assembly or non-covalent interactions in which the complementary arrangement of the functional monomer around the template occurs via hydrogen bonding, ion pairs, dipole-dipole interactions or van der Waals forces. As a result of this association, this approach has been labelled the self-assembly or non-covalent imprinting method. The second approach, known as semi-covalent imprinting, requires chemical synthesis to attach the functional monomer to the template using covalent bonds and a sacrificial spacer group prior to polymerisation.

Each approach has a number of advantages and disadvantages with the choice of approach governed by the nature of the template and the final application of the MIP. The non-covalent approach is simple to implement and can be applied to a diverse number of templates however, polymers produced using this method are less selective due to the formation of a variety of cavities, i.e. heterogeneous binding sites. In covalent and semi-covalent imprinting, well-defined recognition

sites are produced yielding highly selective and stoichiometric binding cavities (homogeneous)<sup>41</sup>. However, this technique is restricted by the template structure, as the synthesis of a suitable template-monomer adduct is limited by the nature of the template functional groups. This synthesis can also be quite complex.

This chapter aims to provide a comparison of the results obtained from the polymers prepared by the self assembly approach (Chapter 4) with those of the semi-covalent approach (Chapter 5). From this, it is envisaged that a number of conclusions will be drawn detailing the more appropriate method of imprinting for the template BZP.

## 6.2 Polymer Synthesis

The process of preparing non-covalent and semi-covalent BZP MIPs vary significantly in the pre-synthetic preparation stage. The non-covalent (NC) approach required considerable time and effort for screening functional monomers due to the large number that are commercially available. Thus, a combination of molecular modelling and NMR spectroscopic studies was performed to identify favourable FMs (from a number of potential FMs) and their optimum ratios (Chapter 3). Nevertheless, laboratory screening was still necessary since the pre-synthetic evaluation did not take into account T:FM interactions in the presence of the cross-linker and porogenic solvent. Thus, considering all possible combinations arising from the choice of 3 FMs (IA, MAA and AA), 2 cross-linkers (EGDMA and TRIM), 2 porogens (AN and CHCl<sub>3</sub>) and 3 T:FM ratios (1:1, 1:2 and 1:4), 30 MIP formulations were screened. From these 30 MIPs, only four formulations exhibited moderate to high BZP binding ( $I$  greater than 2), for all masses (5 - 30 mg) tested, to warrant further analysis.

In contrast, the semi-covalent (SC) imprinting method did not involve extensive pre-synthetic design but a chemical synthesis, to produce the TM adduct as it is specific to the template and, hence, not commercially available. The synthesis of a TM adduct for SC MIP preparation could be labour intensive and, in most cases, would require experimental skills in organic synthesis. In this work, a number of synthetic methods were attempted based on various types of sacrificial spacers<sup>103;104;115</sup>. It is necessary to incorporate a spacer between the template and the polymerisable group. The spacer is subsequently lost during template extraction but the remaining functionality provides for the interaction necessary for template/target rebinding. Among the syntheses attempted, the preparation of benzylpiperazine (4-vinylphenyl) carbamate was the most successful, requiring a 3 step synthesis, and has been utilised for the preparation of SC BZP MIPs.

Extraction of the template from SC MIPs needs to be in harsher conditions, and more labour-intensive than required for the NC MIPs, as a covalent bond needs to be hydrolysed in order to remove the template. For this work, complete extraction of the BZP template was easily achieved by washing the NC polymers with methanol in a Soxhlet cycle for < 12 hours, whilst the SC polymers needed

to be subjected to reflux in 1M methanolic NaOH for > 12 hours, neutralised with HCl then washed with methanol in a Soxhlet extractor for a further 12 hours.

Finally, the composition of the non-imprinted polymer (NIP) differs for the two approaches. For the NC approach, the NIPs were prepared using the same FM and XL composition as the corresponding MIP, following convention. The NIPs for the SC MIPs, however, have been reported to be prepared, either with only the cross-linker<sup>49;54</sup> or with the addition of an FM analogue to the XL formulation<sup>36;85</sup>. For this work, the SC NIPs were prepared from 100% cross-linker. Thus, caution has been taken in the interpretation of the binding results of the SC MIPs, in particular, the use of I which is the ratio of MIP binding to NIP binding because of apparent difference in polymer composition and bulk structure between MIP and NIP.

### 6.3 Binding Affinity

For the purpose of this Chapter, only the NC 1:1 BZP:MAA formulations prepared with EGDMA (NC-MAA-EGDMA-1C) and TRIM (NC-MAA-TRIM-1C) in CHCl<sub>3</sub> will be assessed in comparison to the SC polymers prepared at a 1:19 TM:XL ratio with EGDMA (SC-EGDMA-1) and TRIM (SC-TRIM-1). As only the 1:1 ratios and the MAA NC polymers will be compared the labels assigned to these polymers will be shortened to NC EGDMA and NC TRIM for the non-covalent polymers and SC EGDMA and SC TRIM for the semi-covalent polymers.

The binding capacities, determined for both polymer sets (NC and SC, Sections 4.2.3 and 5.2.3, respectively) from 1 mL of a 0.8 mM BZP solution measured after 30 minutes binding time in CHCl<sub>3</sub> using 30 mg polymer mass, are presented in Figure 6.1.

Of the two EGDMA prepared MIPs, the NC polymer, NC EGDMA, had the higher binding capacity of 62% compared to the SC EGDMA MIP with only 26%. This was also the largest affinity observed of the four polymers. In contrast, for the TRIM MIPs, the SC MIP exhibited a higher binding capacity (49%) than the non-covalent (31%).

The NIPs of the NC polymers showed comparable up-take of 11% which is

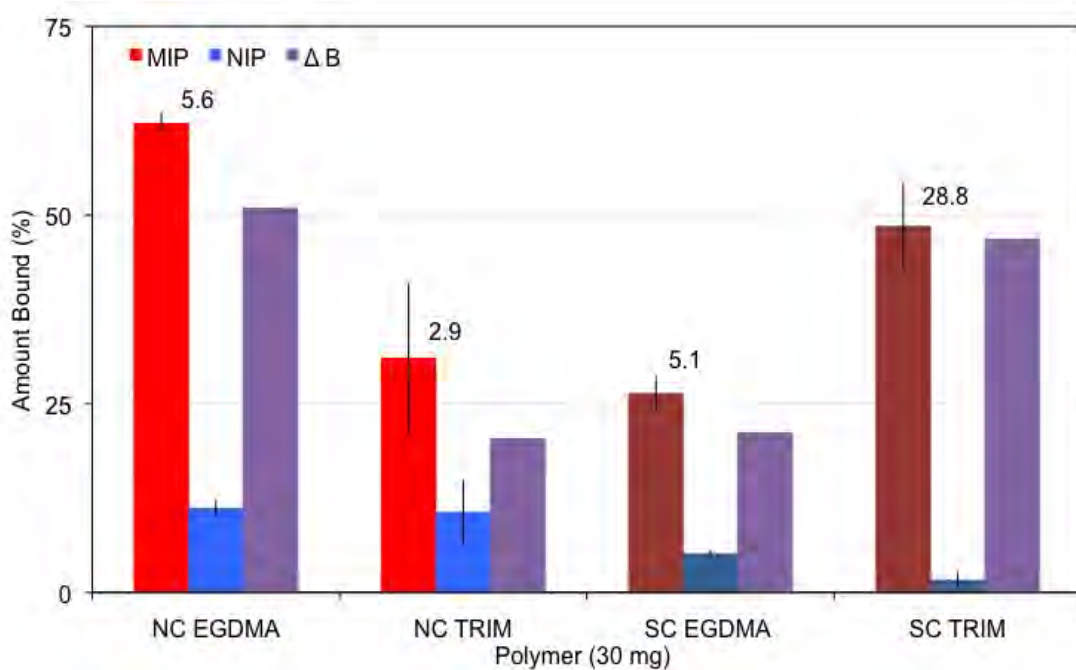


**Figure 6.1:** BZP binding capacities and imprinting factors for 30 mg of the 1:1 BZP:MAA NC MIPs and the SC MIPs in 1 mL of 0.8 mM solution ( $\text{CHCl}_3$ ) after 30 minutes. All experiments were performed in triplicate. Amount bound =  $(\frac{[\text{Total}] - [\text{Free}]}{[\text{Total}]} \times 100)$ ,  $\Delta B = B_{MIP} - B_{NIP}$ .

higher than those of the SC NIPs (5% and 2% for EGDMA and TRIM, respectively). It is to be noted that the NC and SC NIPs have different composition. The NC NIPs contain FM that would be capable of stronger interaction and binding with BZP, on the other hand, the SC NIPs only contain cross-linker, which has been shown to have minimal interaction with BZP (Chapter 3 and 4.2.1).

Cavity-based BZP binding can be estimated from the difference in binding ( $\Delta B$ ) obtained by subtracting the amount of non-specific binding (NIP) from the amount bound by the MIP and gives an idea about the recognition capability of the polymer imparted by the imprinting process. As shown in Figure 6.1,  $\Delta B$  for NC EGDMA MIP is double that of the TRIM MIP (51% vs. 20%) whilst in the case of SC MIPs, it is the TRIM polymer that exhibited a  $\Delta B$  2x higher than that of its EGDMA equivalent (21%). The selective binding capacity of NC EGDMA MIP is comparable to the SC TRIM MIP. These results suggest that the cross-linker has a marked influence on binding capacity<sup>116</sup>.

For the NC polymers, the selective binding ( $\Delta B$ ) of the EGDMA MIP is 2 x higher than that of the TRIM MIP. This result is contrary to some literature reports that show higher binding capacity for non-covalent TRIM MIPs and suggests that the cross-linker effect can be template-dependent<sup>117</sup>. It is hypothesised that with BZP, EGDMA, being a linear symmetrical cross-linker, seems to have the required flexibility, symmetry and complementarity to keep the BZP:MAA clusters in place during polymerisation better than the branched TRIM. This is essential for low T:FM ratios such as the NC MIPs, which were prepared in a 1:1 T:FM ratio. In contrast, with the SC MIPs, the selectivity of TRIM MIP is twice that of the EGDMA MIP. In semi-covalent and covalent systems, imprinting is not dependent on the formation of the T:FM clusters. Hence, the TM adduct, being able to move freely, can fit itself tightly between the TRIM branches and stay secured during polymerisation. The bulk arrangement is expected to be loose in the presence of the linear EGDMA chains.

The calculated imprinting factors also showed similar trend to  $\Delta B$ , with the I of NC EGDMA (5.6) > NC TRIM (2.9) and SC TRIM (29) > SC EGDMA (5.1).

## 6.4 Physical Characterisation

The SEM micrographs of NC EGDMA, NC TRIM, SC EGDMA and SC TRIM are presented in Figure 6.2. The surface macrostructure of the SC MIPs were very different to those of the NC MIPs. Both NC MIPs showed similar surface morphology and exhibited higher surface macroporosity than the SC MIPs. Differences between the two SC MIPs are also apparent with EGDMA showing a surface with moderate macroporosity and spaces while TRIM was very smooth with very small pores.

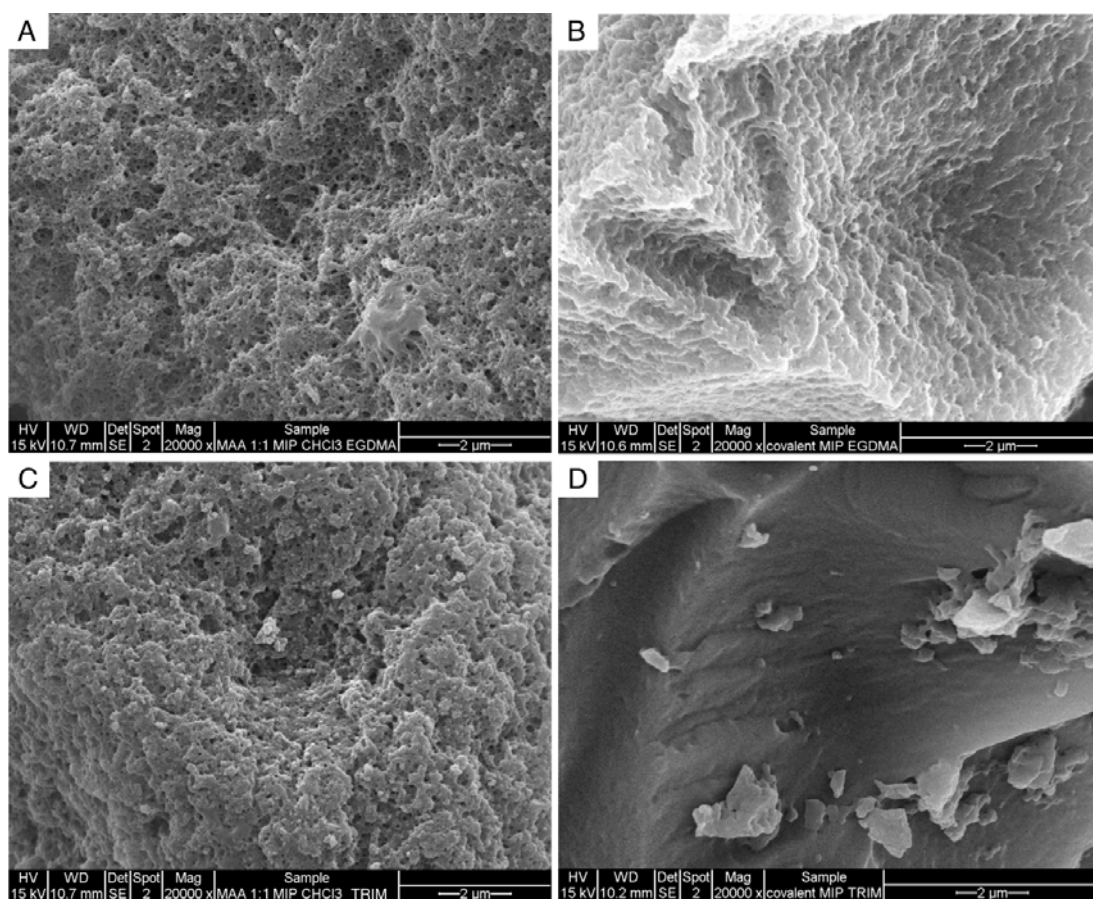


**Figure 6.2:** SEM images for NC EGDMA (A), NC TRIM (B), SC EGDMA (C) and SC TRIM (D).

It seems for both NC and SC MIPs, the cross-linker has a greater influence in their binding capacities than their porosity although simply based on their surface

macrostructure. Both EGDMA and TRIM NC polymers show comparable surface macroporosity yet the selective binding ( $\Delta B$ ) of EGDMA MIP is 2x that of the TRIM MIP. Similarly, SC TRIM exhibited a higher binding capacity than its EGDMA counterpart although the former showed less surface porosity than the latter.

It is presumed that the surface macrostructure of the polymers resembles their bulk structure. Porosity measurements were attempted by the BET method but due to operational and time constraints, valid results were not obtained as of this writing.

The swelling measurements obtained (Chapter 4 and 5), showed that for the four polymers, greater swelling was observed in the non-covalent polymers than the semi-covalent polymers. This can be observed in Figure 6.3. This is consistent with the observed surface macrostructure of the polymers. Both the NC polymers are more macroporous than the SC polymers and could be expected to be able to take in more solvent and exhibit higher volume change. The rebinding results indicate that swelling does not influence template binding. While SC TRIM exhibits a lower swelling in the rebinding solvent ( $\text{CHCl}_3$ ) than NC EGDMA, their binding capability towards BZP are comparable. Similar observation applies to SC EGDMA and NC TRIM.

## 6.5 Binding Dynamics

For both NC and SC polymers, rapid up-take of BZP was observed, with greater than 80% of the maximum binding absorbed prior to 10 minutes. This shows that rapid transfer of BZP in the polymers is occurring. For the non-covalent polymers, equilibrium was established at approximately 2 hours with the greatest selectivity observed after 1 hour. In contrast, the covalent polymers reached equilibrium in  $< 1$  hour, with rebinding for longer than 2 hours reducing the amount of template absorbed.

The binding dynamics of all polymers were analysed by three different methods (Chapters 4 and 5). The over-all  $K_d$  values, for the NC and SC MIPs compared in this chapter, estimated using the direct non-linear regression of the binding isotherms shown in Figure 6.4 are presented in Table 6.1. From the val-

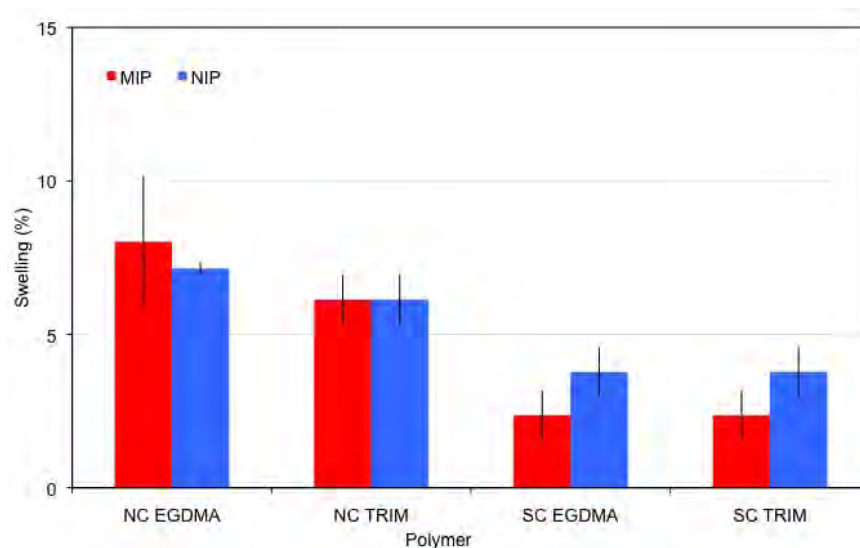


**Figure 6.3:** Swelling results for non-covalent and semi-covalent BZP imprinted polymers in chloroform. Measurements were performed in triplicate on 10 mg of polymer in AN and  $\text{CHCl}_3$  in the dry state and after 1 hr had elapsed.

ues obtained, it can be observed that the  $k_d$  and  $n$  values of the SC MIPs are lower than those of the NC MIPs. These results suggest that the affinity of BZP with the SC MIPs is stronger than with the NC polymers, although there is a greater number of binding sites in the NC polymers. The greater  $n$  arising from the NC MIPs indicate the presence of a mixture of binding sites (high and low affinity) as demonstrated by the Langmuir regression analysis shown in (Figures 6.5). This heterogeneity was not apparent in 3 out of 4 Scatchard plots (Figure 6.6) within the binding concentration range investigated.

A Langmuir regression (Figures 6.5) performed on the binding isotherms support the presence of heterogeneous binding sites in the NC MIPs. The plots of the non-covalent polymers were non-linear, indicating that low and high affinity binding sites were present. In contrast, the plots for the semi-covalent polymers showed a high degree of linearity, which indicates homogeneity and the presence of only one type of binding, most likely the high affinity sites.

Further, the shapes of the binding isotherms also highlight the difference in the nature of the binding sites between the NC and SC MIPs. The binding saturation of the NC MIPs occurred at a slowly increasing pace indicating the presence of

## 6.5 Binding Dynamics

---

more than one type of binding sites, while that of the SC MIPs was reached quickly (close to a linear increase) at lower BZP concentrations, suggesting the presence of only one type of binding site.

**Table 6.1:** Binding constants ( $K_d$  and number of binding sites ( $n$ )) extracted from the binding isotherm for NC EGDMA, NC TRIM, SC EGDMA and SC TRIM

Polymer	$K_d$ value (M) $\times 10^{-4}$	$K_d$ St. dev (M) $\times 10^{-4}$	$n$ (M) $\times 10^{-3}$	$n$ St. error (M) $\times 10^{-4}$	$r^2$
NC EGDMA	4.29	0.60	1.42	5.46	0.9023
NC TRIM	6.07	3.79	1.60	1.31	0.9326
SC EGDMA	1.03	0.14	0.52	0.15	0.8410
SC TRIM	0.81	0.02	0.73	0.23	0.9480

Scatchard equation:  $S_B/C_f = Kn - S_B$

Langmuir equation:  $C_f/S_B = C_f/n + 1/Kn$

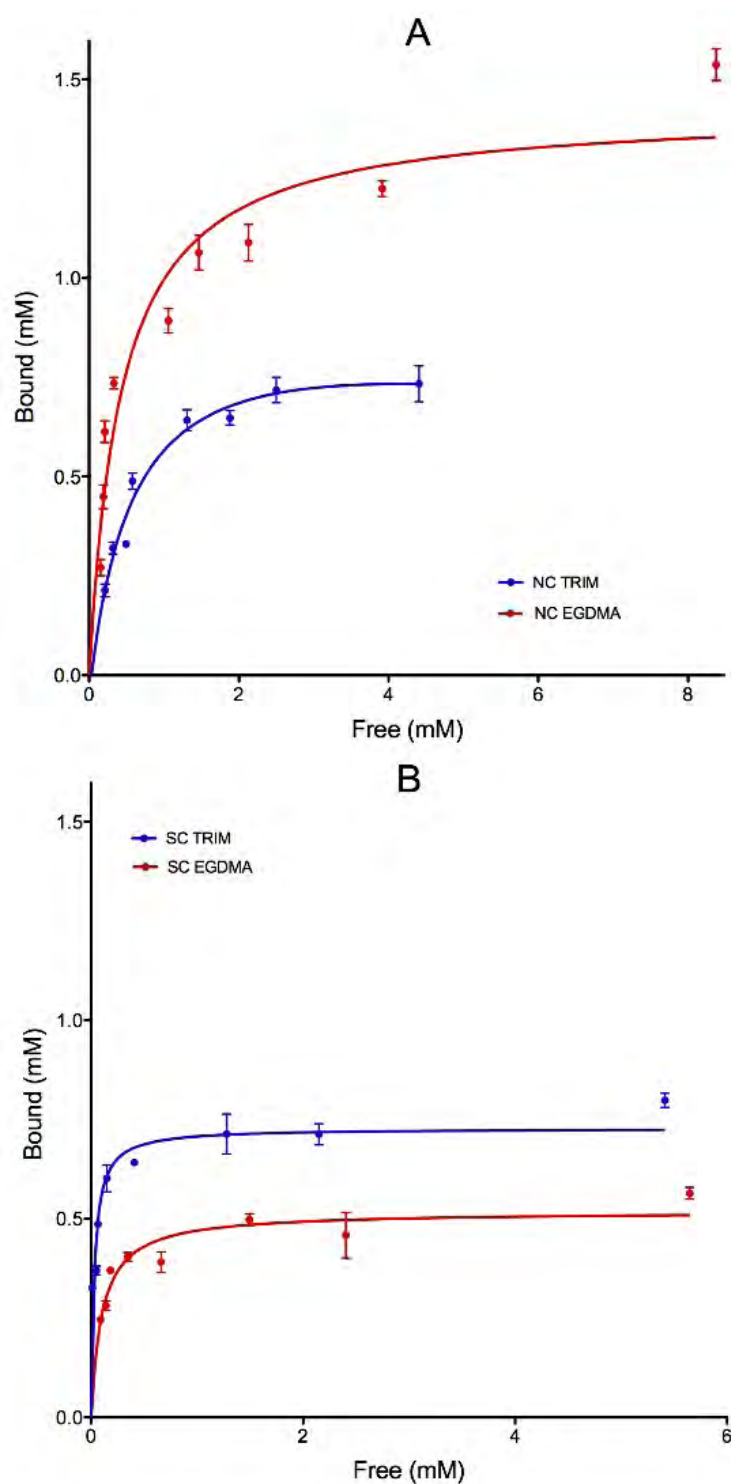


**Figure 6.4:** Binding isotherm for NC EGDMA and NC TRIM (**A**) and SC EGDMA and SC TRIM (**B**) All analyses were performed in triplicate with the average plotted.

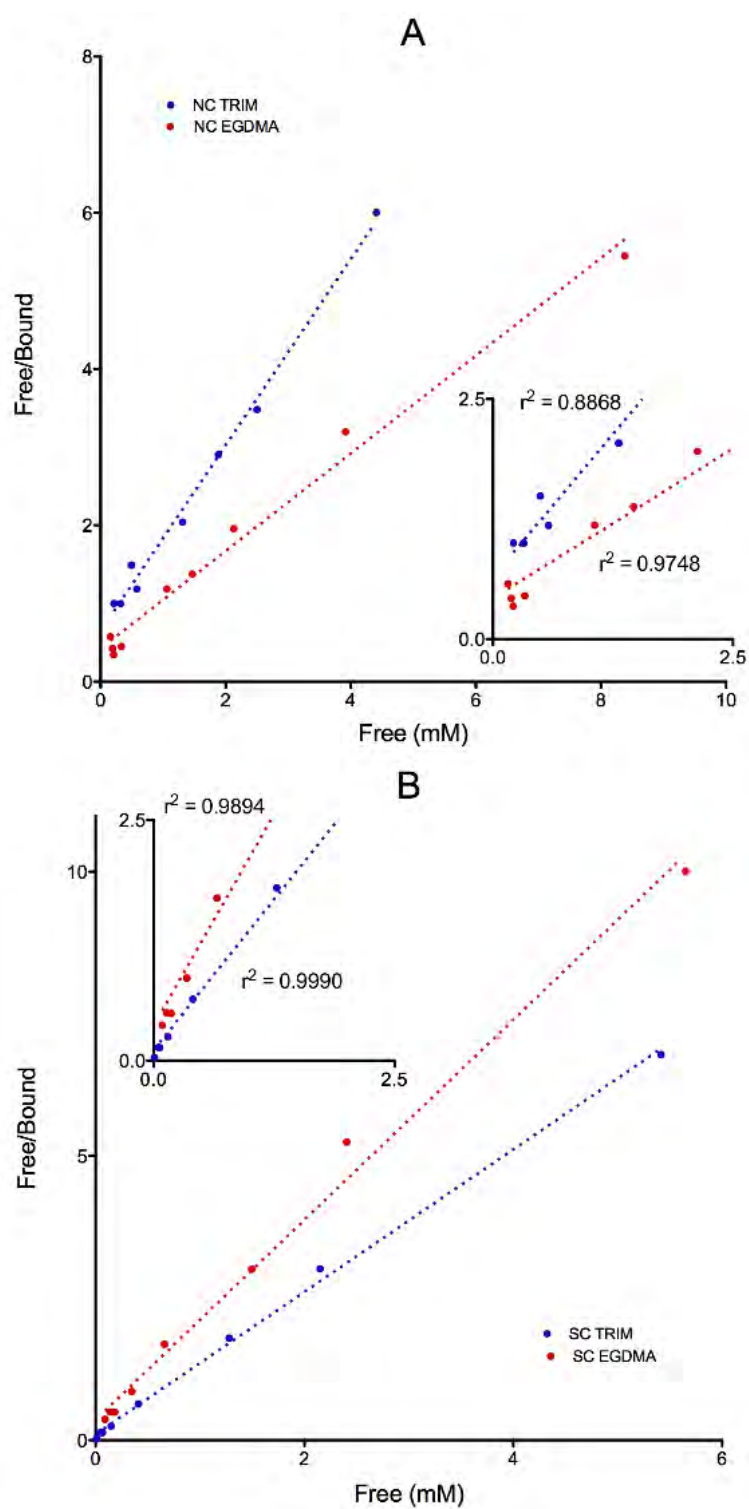


**Figure 6.5:** Langmuir regression plot for NC EGDMA and NC TRIM (A) and SC EGDMA and SC TRIM (B)

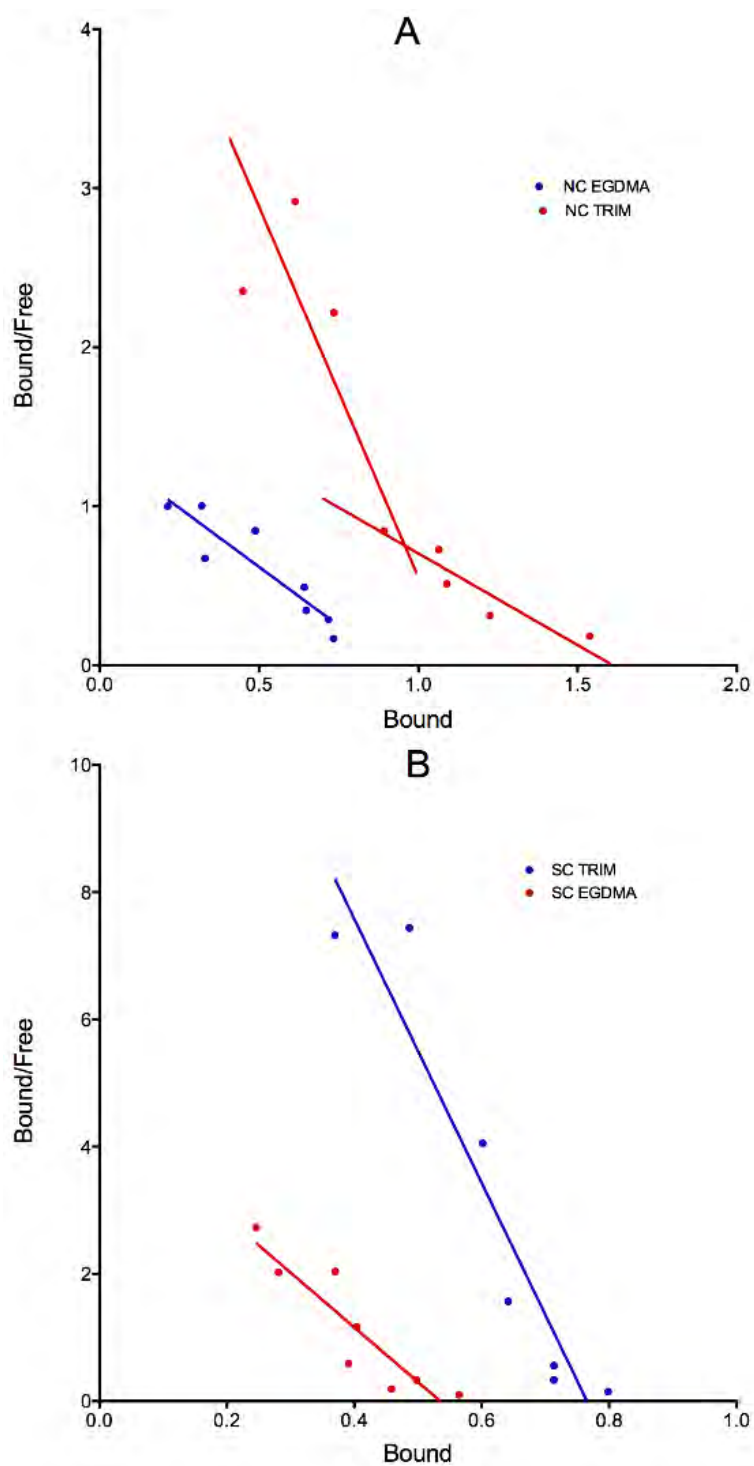


**Figure 6.6:** Scatchard regression plot for NC EGDMA and NC TRIM (A) and SC EGDMA and SC TRIM (B)

## 6.6 Conclusion

The data obtained in this study has provided substantial insight to the different binding characteristics of two sets of polymers prepared using the two imprinting approaches, semi-covalent imprinting and non-covalent (self-assembly) imprinting.

The preparation of the two types of polymers is both laborious, with the semi-covalent method being laboratory intensive while the non-covalent method computationally intensive.

Analysis of the binding isotherms showed the semi-covalent polymers to have stronger affinity for BZP, as demonstrated by lower  $K_d$  values, than the NC MIPs. The presence of only one type of binding sites, more likely the strong affinity site, in the SC MIPs is supported by the high linearity of the Langmuir plots, rapid binding saturation and lower number of binding sites. In contrast, the NC MIPs exhibited a heterogeneous binding profile as demonstrated by higher number of binding sites, slow binding saturation and non-linear Langmuir plots.

In terms of binding capacity, the NC EDGMA and SC TRIM MIPs afforded comparable BZP up-take and exhibited higher selectivity, between the MIP and NIP, than NC TRIM and SC EGDMA, respectively. The cross-linker has been shown to impart a greater influence on the binding capacities of both NC and SC MIPs. Swelling behaviour did not show any influence on the binding behaviour of the polymers.

Both methods can be used to produce MIPs that can imprint and rebind BZP. The findings here suggest that EGDMA produces higher capacity non-covalent MIPs than TRIM, while TRIM produces a MIP that is higher binding than EGDMA by the semi-covalent method. There are a number of advantages and disadvantages associated with the two imprinting approaches. In order to choose the most appropriate method to utilise, these should be considered carefully along with the final application of the polymer.

# 7

## Cross-Reactivity and Selectivity Studies

### 7.1 Introduction

The desired attributes of an in-field sensor are that it is rapid, accurate and specific. The current methods utilised for drug detection suffer from poor selectivity and frequently produce false positives. They are also only drug class specific, not capable of distinguishing between drugs of a similar nature. MIPs have been shown to respond rapidly to template up-take and highly template specific. In addition, they are also cheap, robust and easy to prepare. It is for this reason that MIPs have been investigated as a possible new in-field sensor for the detection of drugs of abuse.

In order to assess the specificity and selectivity of the BZP imprinted polymers towards BZP, cross-reactivity and competitive binding assays were conducted. A cross-reactivity analysis involves binding the polymers with a number of different analytes, usually analogues or competitors of the template in a non-competitive environment. The second experiment extends this investigation by producing a competitive environment by rebinding the polymers with a number of analytes, template included, simultaneously.

In this work, three drugs of abuse that are commonly detected within Australian borders, morphine (MO), cocaine (CO) and ephedrine (EPH), a pre-

cursor to amphetamine type substances (ATS), as well as an analogue of BZP, phenylpiperazine (PHP) have been selected for cross-reactivity and competitive studies. The chemical structures of these compounds are given in Figure 7.1.

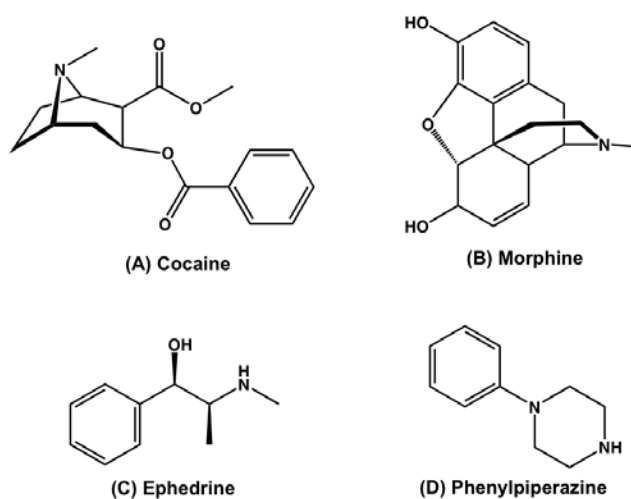


**Figure 7.1:** Chemical structures of three common drugs of abuse, cocaine (A), morphine (B) and ephedrine (C) and a BZP analogue, phenylpiperazine (D).

The affinity of these compounds with the BZP imprinted polymers were determined in a non-competitive environment to establish the specificity of the polymers to BZP. Binding was also performed in a binary competitive environment in order to determine the selectivity of the MIP to BZP over one other competing compound.

## 7.2 Results and Discussion

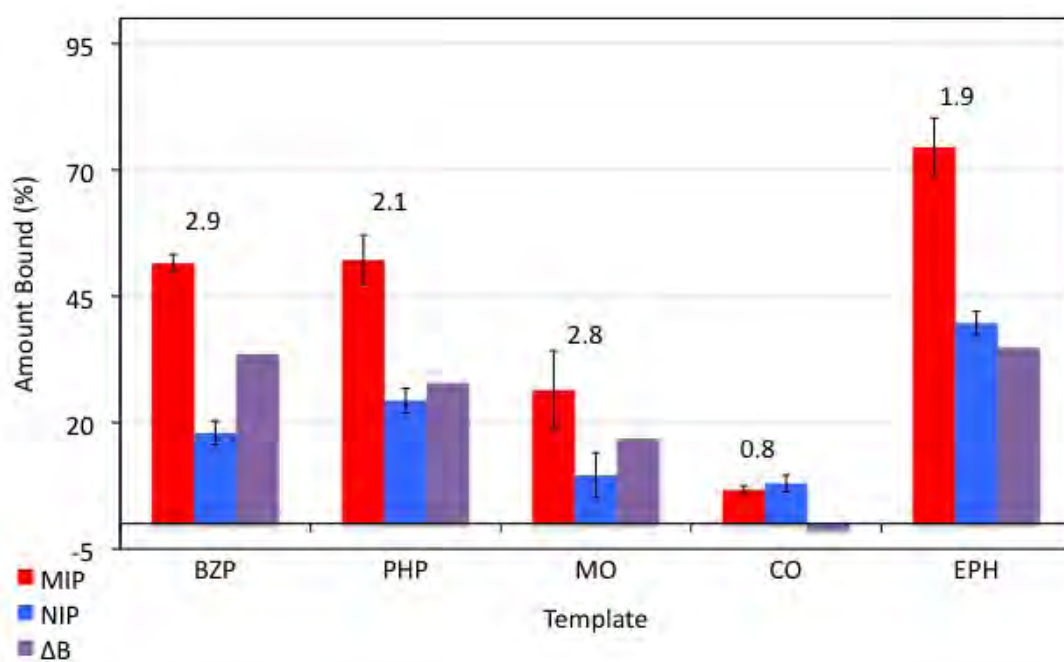
### 7.2.1 Cross-reactivity Studies

Four non-covalent polymers, NC EGDMA-1, NC EGDMA-2, NC TRIM-1 and NC TRIM-2, and two covalent polymers, SC EGDMA-1 and SC TRIM-1, were investigated. A binding time of one hour was used for all polymers with 0.8 mM of analyte dissolved in  $\text{CHCl}_3$ . For the non-covalent polymers, 20 mg of polymer was used, while 30 mg of covalent polymer was used for analysis. These conditions were previously determined from absorption and time binding experiments (Chapter 3 and 4) as this was when the highest imprinting factor and polymer saturation were observed.

#### 7.2.1.1 Non-Covalent Imprinted Polymers

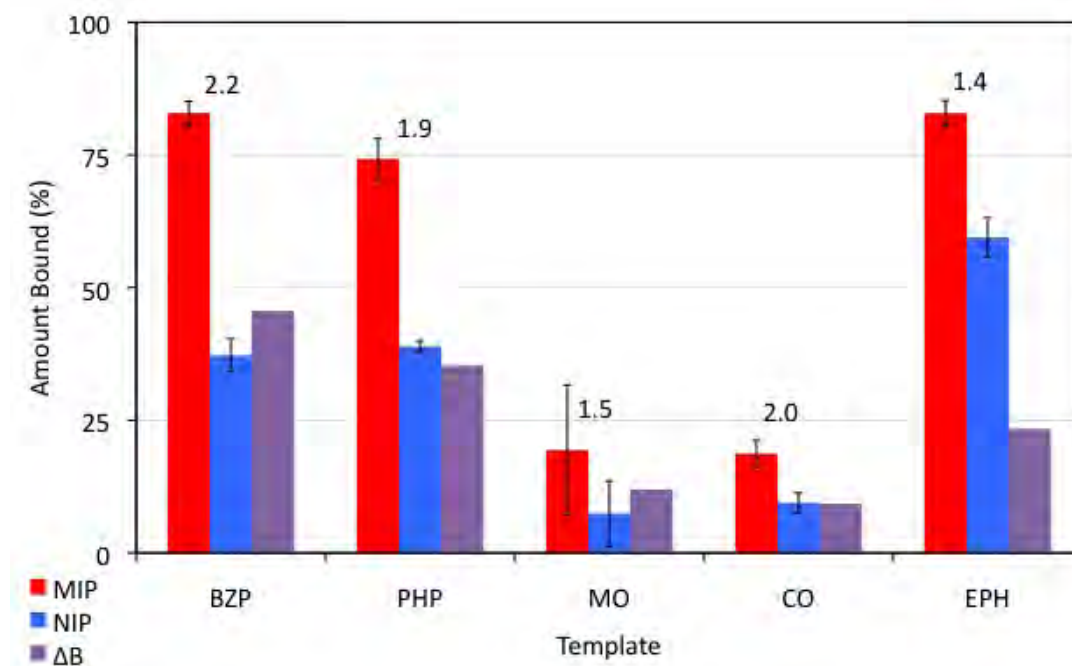
From the cross-reactivity studies performed on NC EGDMA-1 presented in Figure 7.2, it was observed that the MIP displayed similar binding capacities for both PHP (52%) and BZP while the NIP bound slightly more PHP (24%) than BZP. This increase in non-specific binding reduced the imprinting factor to 2.1. The amount of MO bound was approximately half (MIP = 26% and NIP = 9%) that observed for the MIP and NIP when bound with BZP. As the amount bound was halved for both MIP and NIP, a similar imprinting value, of  $I = 2.8$ , was observed for MO. CO had the smallest amount of absorbance of the four analytes investigated. Similar up-take was observed for both MIP (7%) and NIP (8%), suggesting that non-specific binding was contributing to the amount bound. Lastly, the amount of EPH bound was greater in both MIP (75%) and NIP (18%) than what was observed for BZP.

Figure 7.3 shows the results obtained from the cross-reactivity study for polymer NC EGDMA-2. For this polymer set, the amount bound of PHP (74%) was less than that observed for BZP (83%) for the MIP and equal for the NIP (39%). The analytes, MO and CO, had similar up-take, of approximately 20% by the MIPs and 8% by the NIPs. The amount of EPH bound was equivalent to the binding capacity for BZP however, greater non-specific binding was observed by the NIP (60%). This produced the lowest  $I$  value ( $I = 1.4$ ) of the analytes



**Figure 7.2:** Cross-reactivity studies of NC EGDMA1 with benzylpiperazine (BZP), phenylpiperazine (PHP), morphine (MO), cocaine (CO) and ephedrine (EPH). 20 mg of polymer was used with 1 mL 0.8 mM analyte solution in  $\text{CHCl}_3$  for a binding contact time of 1 hr. All experiments were performed in triplicate. Amount bound =  $\left(\frac{[\text{Total}] - [\text{Free}]}{[\text{Total}]}\right) \times 100$ .

investigated. For the other three analytes, PHP, MO and CO, I values of 1.9, 1.5 and 2.0 were obtained, respectively.



**Figure 7.3:** Cross-reactivity studies of NC EGDMA2 with benzylpiperazine (BZP), phenylpiperazine (PHP), morphine (MO), cocaine (CO) and ephedrine (EPH). 20 mg of polymer was used with 1 mL 0.8 mM analyte solution in  $\text{CHCl}_3$  for a binding contact time of 1 hr. All experiments were performed in triplicate. Amount bound =  $\frac{([Total] - [Free])}{[Total]} \times 100$ .

The NC TRIM-1 polymer exhibited the lowest BZP capacity (Chapter 3), which resulted in lower analyte up-take, compared to the other three non-covalent polymers. The results of this experiment are presented in Figure 7.4. The amount of PHP bound was less in the MIP (36%) and greater in the NIP (18%), in comparison to BZP absorbed by the polymer (MIP = 43%, NIP = 12%). This reduced the imprinting factor from 3.6, for BZP, to 2.0, for PHP. Again for this polymer, approximately 18% of the MO analyte was absorbed from solution by the MIP and 9% was absorbed by the NIP. This amount of up-take was exhibited by three of the polymers (NC EGDMA-2, NC TRIM-1 and NC TRIM-2). This polymer had the least affinity for CO, binding only 3% from solution. Again, the amount bound is the result of non-specific binding as the MIP and NIP had

similar results. EPH up-take was slightly greater for this polymer with 52% bound by the MIP and 30% by the NIP.

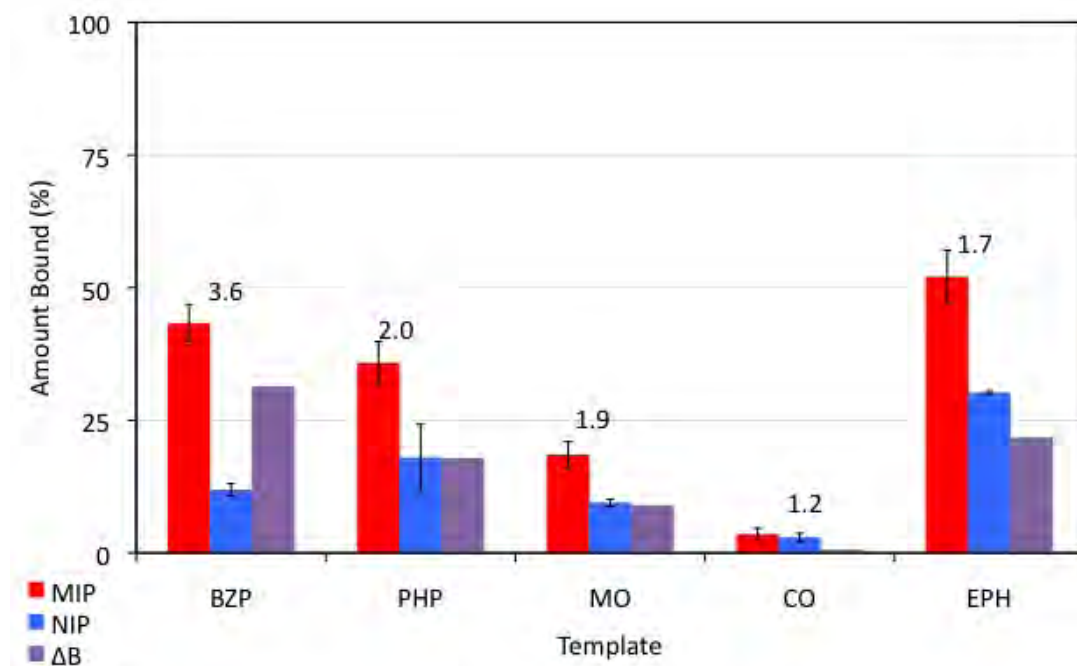


**Figure 7.4:** Cross-reactivity studies of NC TRIM1 with benzylpiperazine (BZP), phenylpiperazine (PHP), morphine (MO), cocaine (CO) and ephedrine (EPH). 20 mg of polymer was used with 1 mL 0.8 mM analyte solution in  $\text{CHCl}_3$  for a binding contact time of 1 hr. All experiments were performed in triplicate. Amount bound =  $\frac{([Total] - [Free])}{[Total]} \times 100$ .

Finally, NC TRIM-2 MIP (Figure 7.5) bound 62% of the PHP template and the NIP bound 27%. Again, this was reduced for the MIP and increased for the NIP, compared to the BZP affinity of the polymer (MIP = 76% and NIP = 24%). The amount of MO bound by the MIP was 18%, with the NIP binding 9%. This was a similar value to the previous two polymers discussed. The amount of CO bound was from non-specific binding as approximately 10% was bound by both MIP and NIP. Finally, NC TRIM-2 MIP had a similar binding capacity for EPH, binding 77%. More non-specific binding was observed by the NIP, which bound 50%, twice that observed when binding was performed with BZP.

In all analytes examined, a greater amount of template up-take was observed for both MIPs and NIPs in the 1:2 ratios than the 1:1 ratios. This is the result

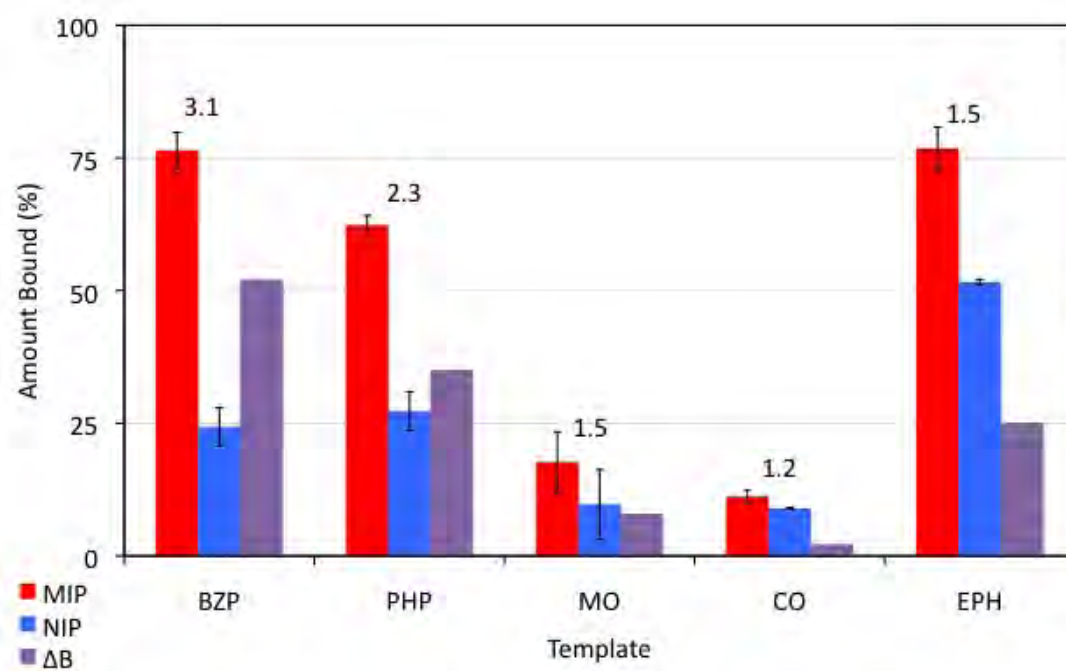


**Figure 7.5:** Cross-reactivity studies of NC TRIM2 with benzylpiperazine (BZP), phenylpiperazine (PHP), morphine (MO), cocaine (CO) and ephedrine (EPH). 20 mg of polymer was used with 1 mL 0.8 mM analyte solution in  $\text{CHCl}_3$  for a binding contact time of 1 hr. All experiments were performed in triplicate. Amount bound =  $\frac{([Total] - [Free])}{[Total]} \times 100$ .

of a greater amount of FM present in the 1:2 ratios, enabling a greater number of interactions to occur.

PHP is a structural analogue of BZP, differing only in the loss of the bridging carbon between the two rings. As a result, it was hypothesised that the MIPs would exhibit high affinity for PHP. This was observed in the results obtained, with all polymers having a large up-take of this analyte. The absorbance of PHP was approximately 10% less than that observed for BZP in all polymers investigated, excluding NC EGDMA1, which had an equivalent up-take. The large up-take of PHP could be attributed to the similarities in size and functionalities between BZP and PHP. The volume of PHP is  $186.00 \text{ \AA}^3$ ,  $18 \text{ \AA}$  smaller than BZP ( $204.55 \text{ \AA}^3$ ), enabling easier access to the BZP cavity. In addition, the removal of the methylene unit from BZP, has reduced the energy of the system and complexation of the PHP, without dramatically affecting the size or electronic characteristics. These similarities are highlighted in Figure 7.6 which shows the size and electron potential of the two analytes, BZP and PHP. Figure 7.7 also shows the H-bond distance between the secondary amine and the acid of MAA (N–OH) to be  $2.573 \text{ \AA}$ , quite similar to what was observed for BZP and MAA ( $2.562 \text{ \AA}$ , Chapter 3 Figure 3.3 (A)).

In the case of MO, the amount sorbed by all MIPs was less than 25%, with the NIP up-take approximately half of the MIP. This resulted in  $\Delta B$  values of approximately 10%. MO and BZP are substantially different in size, structure and functionality. This can be observed in Figure 7.8, which also shows the electron potential for the two molecules. The volume of MO is  $281.90 \text{ \AA}^3$  and the potential range is between  $-62.7$  and  $27.64$ , which is larger and more positive than BZP ( $204.55 \text{ \AA}^3$ ,  $-69.79$  to  $21.07$ ). MO also has different functional groups (phenol, tertiary amine, ether and a cyclic OH) that are orientated differently, although strong H-bonds ( $2.132 \text{ \AA}$  and  $2.147 \text{ \AA}$ ) are able to form between MO and MAA (Figure 7.9). It is hypothesised that the low affinity of the polymers towards MO is a result of the size of the molecule, which is restricting its access into the binding cavities produced by the smaller BZP molecule.

The analyte CO had the lowest affinity of the analytes examined. The amount of sorption between MIP and NIP was also equivalent, suggesting that up-take is attributed to non-specific surface binding. Again, the low binding capacity

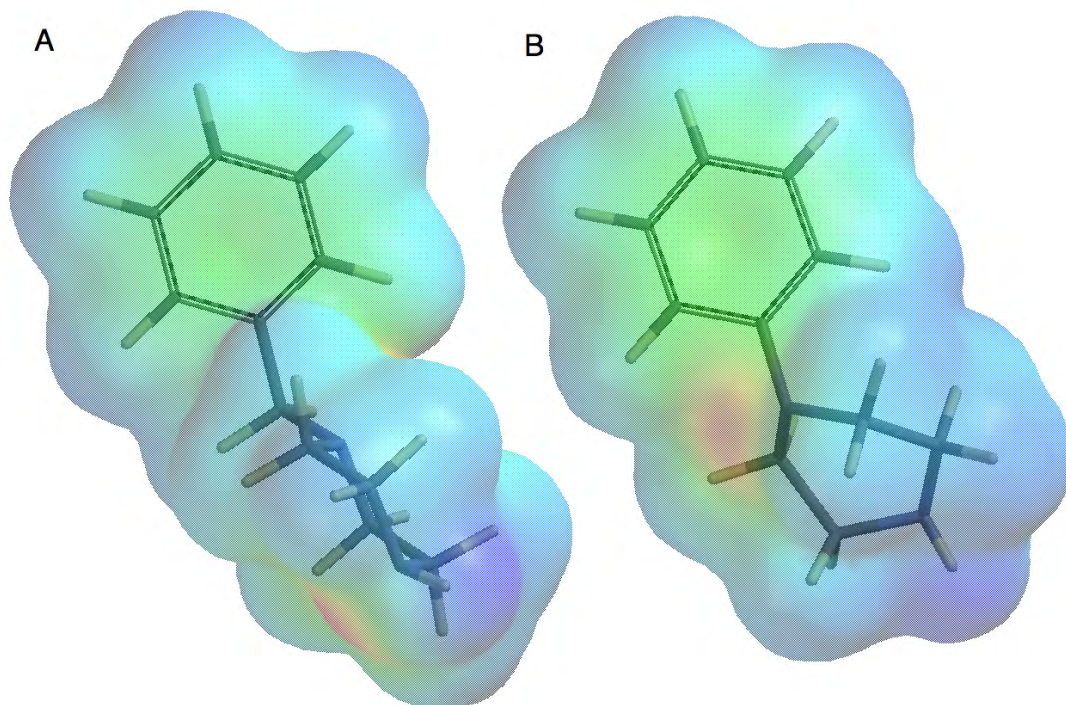


**Figure 7.6:** Molecular modelling images of BZP (A) and PHP (B) showing the similar surface potential and size. The red and blue areas on the images indicate the high and low electron density, respectively.

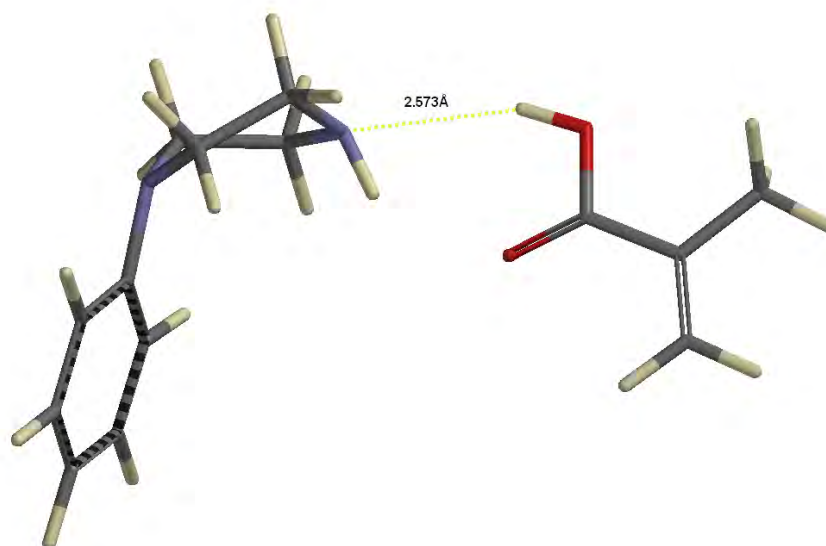


**Figure 7.7:** Molecular modelling image of PHP with 1 MAA unit.

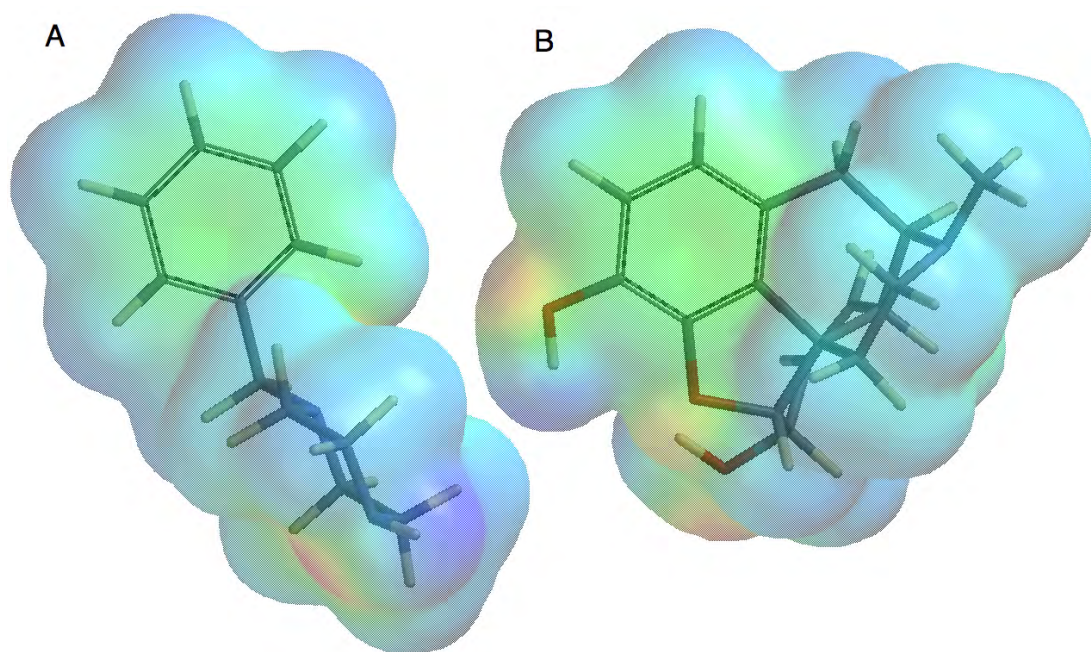


**Figure 7.8:** Molecular modelling images of BZP (A) and MO (B) showing the differences in surface potential and size.

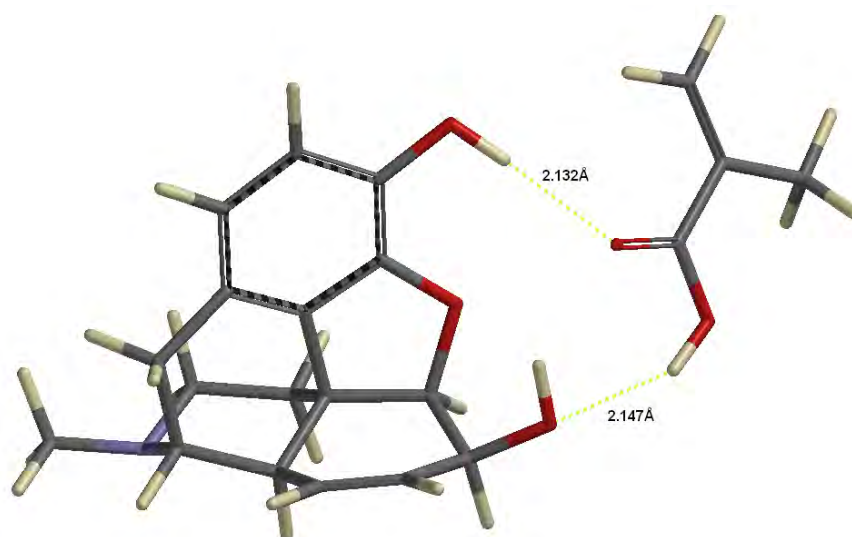


**Figure 7.9:** Molecular modelling image of MO with 1 MAA unit.

is hypothesised to be the result of size, shape and functionality, as this is the largest analyte investigated ( $313.53 \text{ \AA}^3$ ). Figure 7.10 shows the difference in size and orientation of functional groups between BZP and CO. It can be seen that the position of the hydrogen bond donating groups of CO do not align with BZP, suggesting that these bonds are not forming in the cavities between CO and the polymer. A strong H-bond ( $2.147 \text{ \AA}$ ) is also capable of forming between CO and MAA (Figure 7.11 (A)) however, the arrangement is quite different from BZP (Figure 7.11 (B)), supporting the theory that CO is not capable of interacting within the cavity.

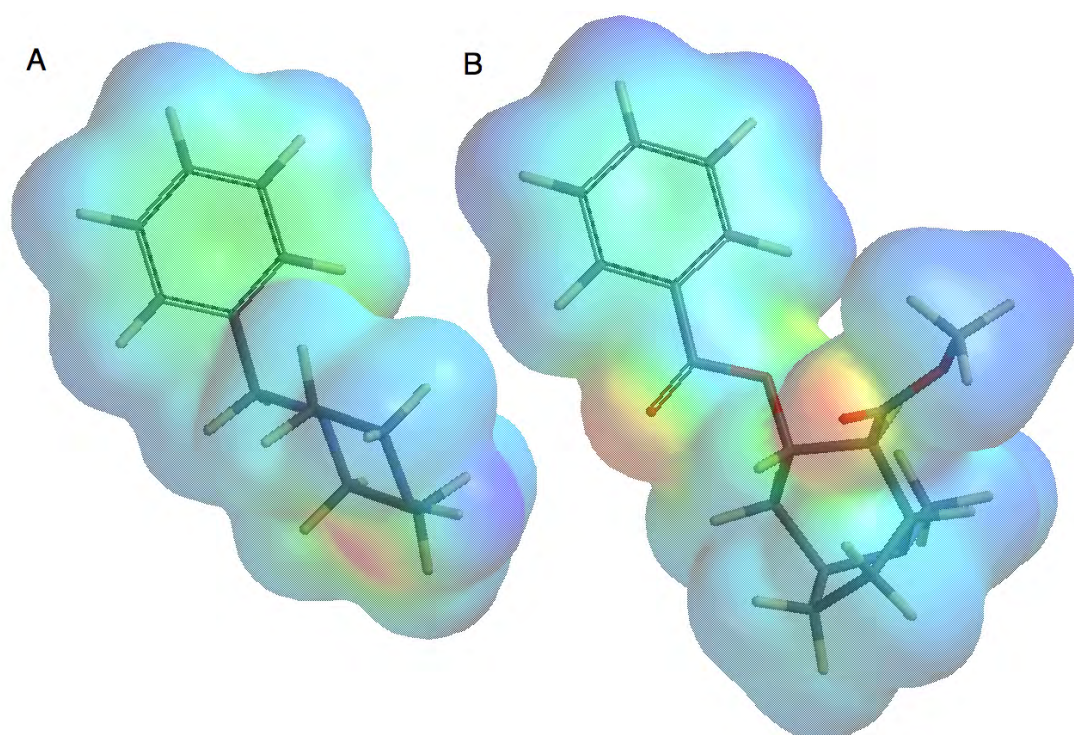


**Figure 7.10:** Molecular modelling images of BZP (A) and CO (B) showing the differences in surface potential and size.

The EPH molecule possesses functional groups similar to BZP (arene and amine) in conjunction with a hydroxyl group, making it highly capable of forming non-covalent interactions with the polymer. In addition, EPH is similar in size ( $191.13 \text{ \AA}^3$ ) and has a greater potential range ( $-72.79$  to  $27.95$ ), in comparison to BZP ( $204.55 \text{ \AA}^3$ ,  $-69.79$  to  $21.11$ ). This can be observed in Figure 7.12,

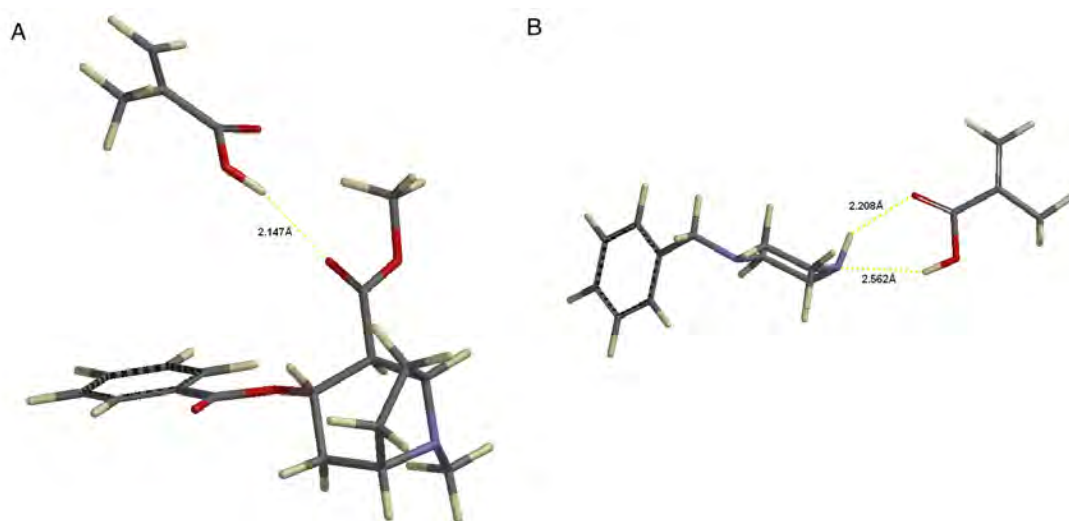


**Figure 7.11:** Molecular modelling image of CO with 1 MAA unit (A) and BZP with 1 MAA unit (B).

which shows the electron potential of both BZP and EPH and the orientation of functional groups of the two compounds. EPH also exhibited strong H-bonding (2.180 Å) with MAA (Figure 7.13). Consequently, it was hypothesised that the MIPs would exhibit a high affinity toward EPH. As expected, all polymers (MIPs and NIPs) had a high degree of up-take, which was attributed to the similarities in size and shape. The increase in binding of the NIPs showed that non-specific binding was also contributing to the amount of EPH absorbed.

### 7.2.1.2 Covalent Imprinted Polymers

The results for the cross-reactivity studies performed for SC-EGDMA-1, given in Figure 7.14, showed that for all analytes investigated, the affinity of the MIP was equivalent or less than that observed for BZP. In the presence of PHP, SC-EGDMA-1 MIP bound 19% of the analyte from solution. For the NIP, a total of 5% of the PHP was removed from the stock. MO had the lowest affinity, with only 11% binding in the MIP and 7% by the NIP. The amount of CO bound from solution was also less than BZP, with 17% and 8% up-take by the MIP and NIP, respectively. Binding with EPH produced a similar amount of analyte up-take in the MIP (26%) and an increased up-take by the NIP (14%).

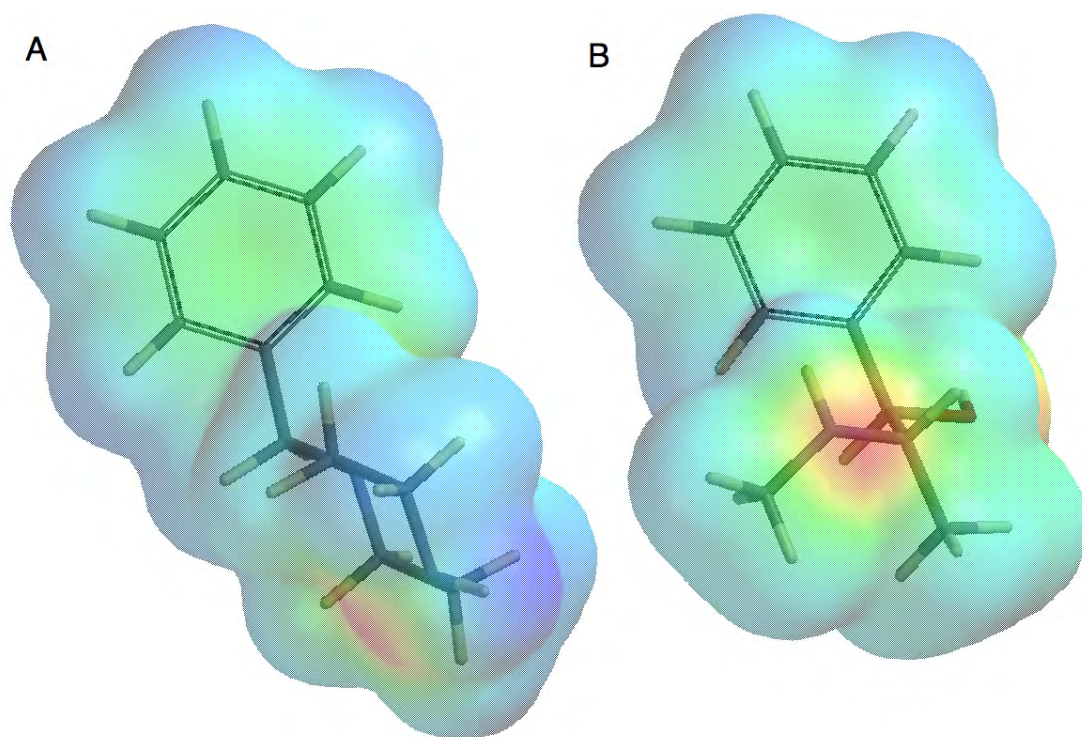


**Figure 7.12:** Molecular modelling images of BZP (A) and EPH (B) showing the similarities in surface potential and size.

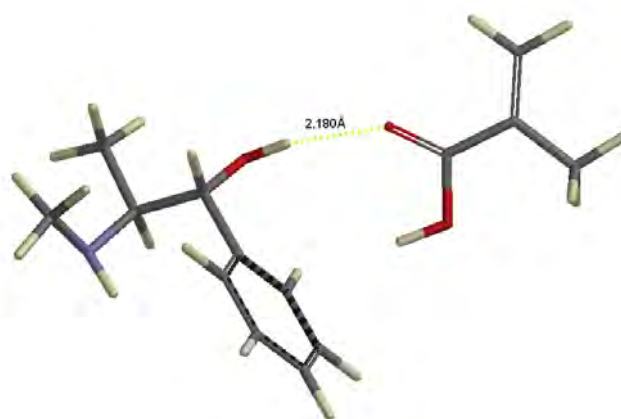


**Figure 7.13:** Molecular modelling image of EPH with 1 MAA unit

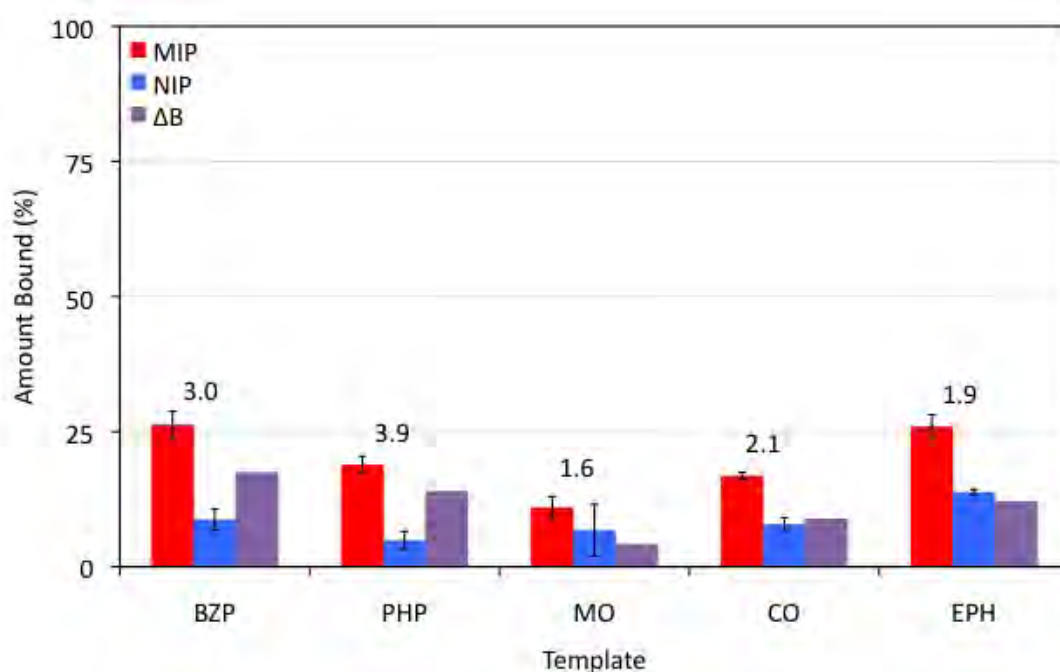


**Figure 7.14:** Cross-reactivity studies of the EGDMA prepared semi-covalent imprinted polymers with benzylpiperazine (BZP), phenylpiperazine (PHP), morphine (MO), cocaine (CO) and ephedrine (EPH). 30 mg of polymer was used with 1 mL 0.8 mM analyte in  $\text{CHCl}_3$  for a binding contact time of 1 hr. All experiments were performed in triplicate. Amount bound =  $\frac{([Total] - [Free])}{[Total]} \times 100$

## 7.2 Results and Discussion

Figure 7.15 depicts the results for the cross-reactivity studies performed with the polymer SC TRIM1. From the results obtained, it can be seen that the amount of each analyte bound by the MIP was less than the binding capacity for BZP. For PHP, 35% of the analyte was bound by the MIP, with 3% bound by the NIP. This produced a binding factor of 12.5, slightly greater than that observed for BZP ( $I = 11.8$ ). MO had the smallest amount with only 16% of the template being removed from solution by the MIP and 8% for the NIP. The analytes, CO and EPH, had similar binding with 45% and 40% by the MIPs, respectively. For these two analytes negative binding was observed for the NIPs, with -4% up-take for CO and -2% for EPH. This negative binding is believed to be the result of the polymer absorbing the solvent, resulting in a concentration effect of the template in solution.

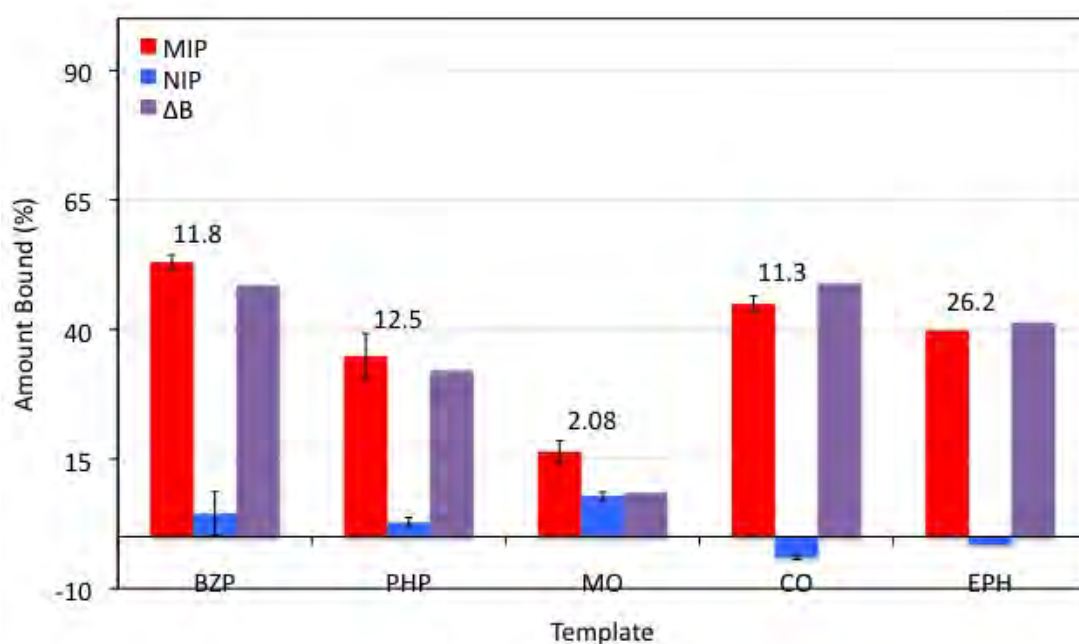


**Figure 7.15:** Non-competitive cross reactive study of TRIM prepared covalent imprinted polymers with benzylpiperazine (BZP), phenylpiperazine (PHP), morphine (MO), cocaine (CO) and ephedrine (EPH). 30 mg of polymer was used with 1 mL 0.8 mM analyte in  $\text{CHCl}_3$  for a binding contact time of 1 hr. All experiments were performed in triplicate. Amount bound =  $(([\text{Total}] - [\text{Free}]) / [\text{Total}]) \times 100$

Similar results were obtained for the semi-covalent polymers as the non-

covalent polymers, with comparable sorption of PHP and EPH to BZP, and reduced sorption of MO. It is hypothesised that similar mechanisms (size, shape and functional groups), proposed for the non-covalent polymers, are present in the semi-covalent polymers as Figures 7.16 and 7.17 shows that all analytes are capable of forming strong H-bonds with phenol, the functionality resulting from template hydrolysis from the TM adduct.

For the semi-covalent polymers, a significant amount of sorption was observed for CO, with SC EGDMA binding 16% by the MIP and 8% by the NIP, and SC TRIM 45% by the MIP and approximately 0% by the NIP. This up-take was unexpected, as this compound was shown to be bulky with differently orientated functional groups. The mechanism behind this anomaly is unclear and requires further analysis.

### 7.2.2 Selectivity Studies

Selectivity studies were performed in a binary competitive environment, to determine if the BZP imprinted polymers would selectively bind BZP in the presence of another analyte. The systems investigated were BZP/CO, BZP/EPH and BZP/MO in  $\text{CHCl}_3$ . PHP was not investigated in this experiment, as separation in HPLC was not possible.

#### 7.2.2.1 Non-Covalent Polymers

In the selectivity studies performed for NC EGDMA1, the presence of CO enhanced the binding capacity of the MIP for BZP. However, the amount of non-specific binding of BZP by the NIP also increased. This can be observed in Figure 7.18 and is speculated to be the result of colligative effects, where the presence of CO in solution is making it more attractive for BZP to adhere to the polymer surface. This was suggested as the increase in the amount of BZP bound by MIP and NIP is similar to the decrease in the amount of CO bound by MIP and NIP, in the competitive environment from the non-competitive environment. This reduced the imprinting factor of BZP from 2.9 to 1.6. The amount of CO absorbed by the polymer was negligible, with -3% and 4% up-take for the MIP and NIP, respectively. NC EGDMA1 was observed to be highly selective for BZP

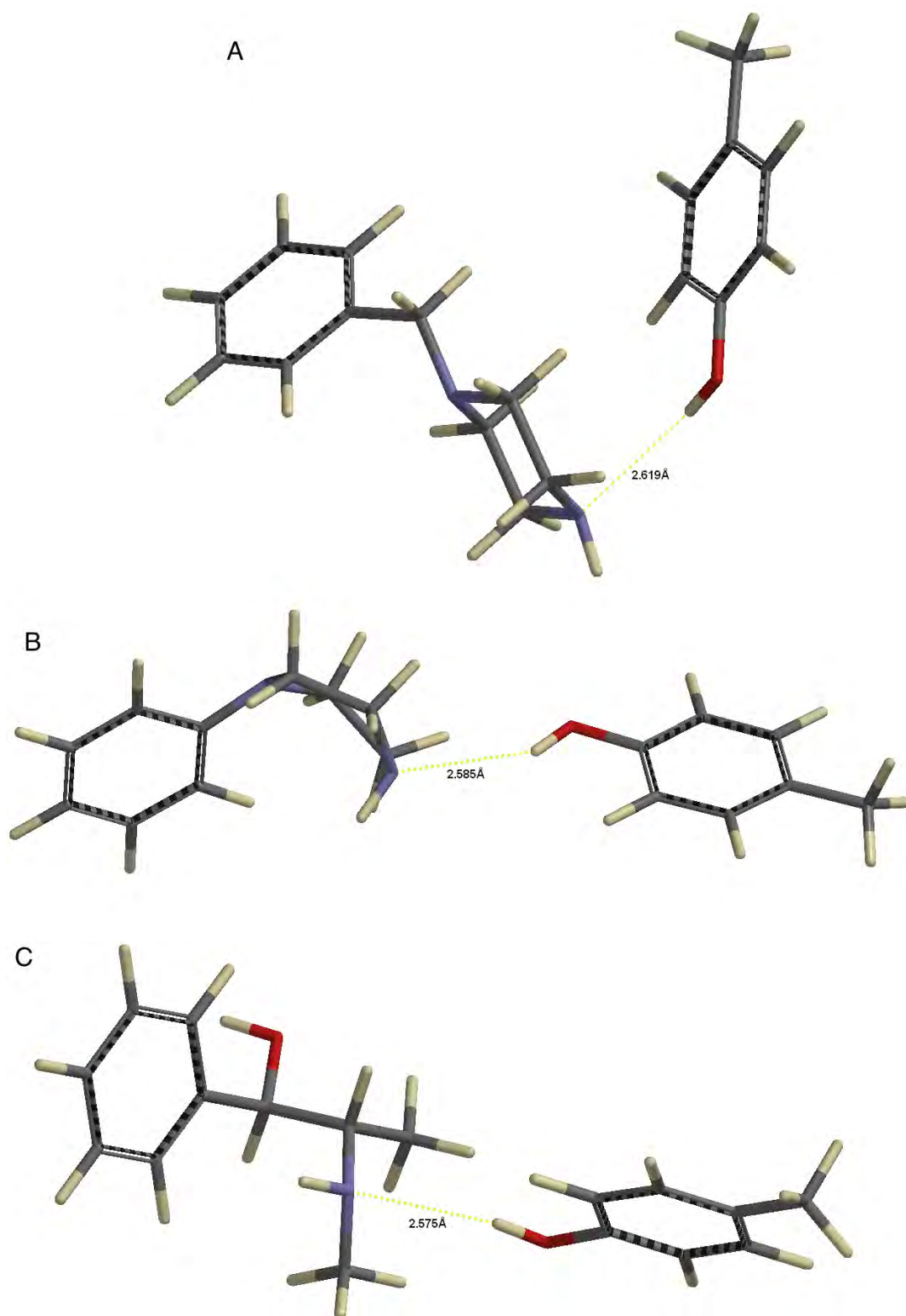


**Figure 7.16:** Molecular modelling image of 1 phenol unit with the analytes BZP (A), PHP (B), EPH (C).

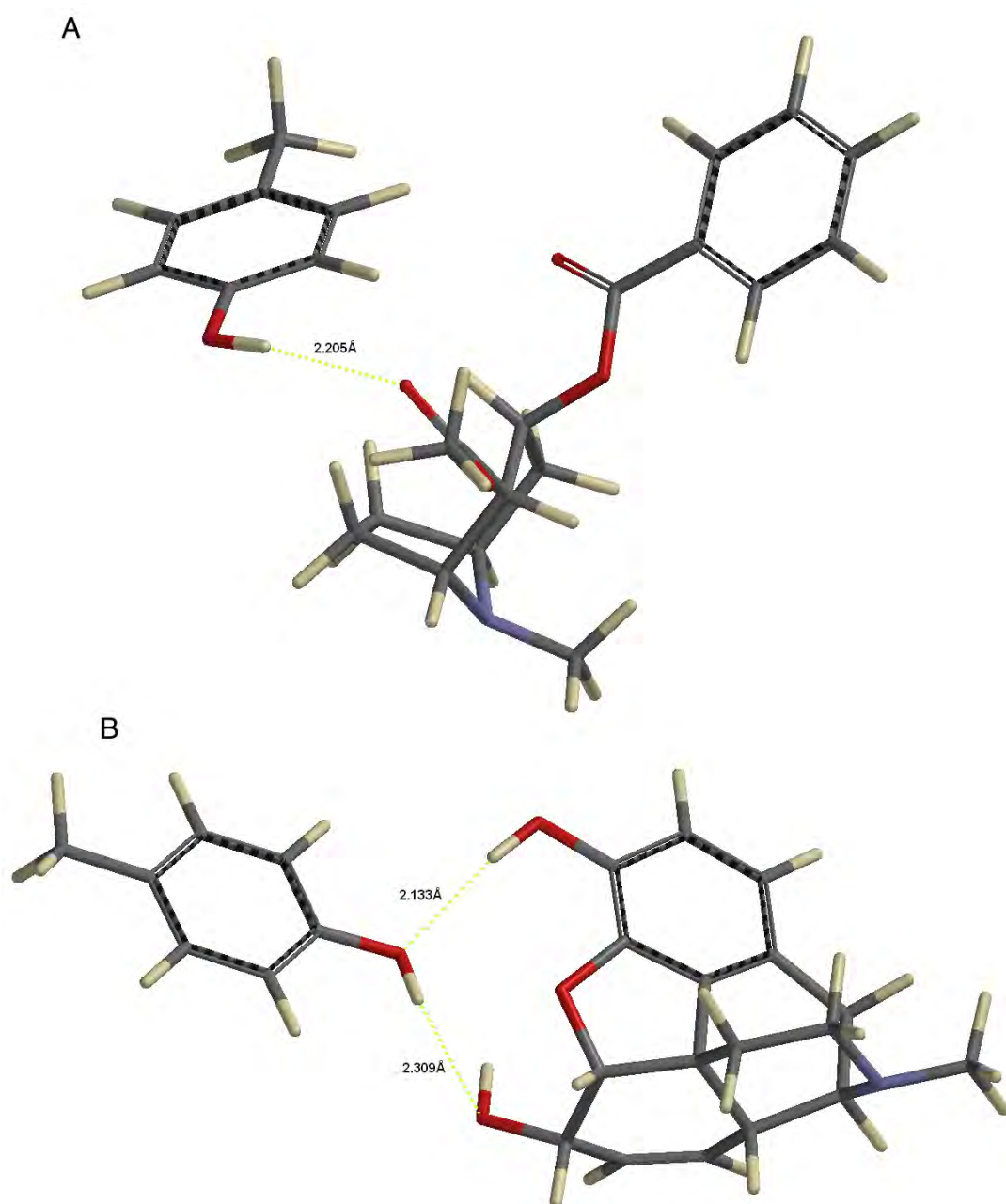


**Figure 7.17:** Molecular modelling image of 1 phenol unit with the analytes CO (A), MO (B).

when in the presence of the analyte CO.

In the BZP/MO selectivity study, BZP (MIP = 53%, NIP = 14%) was also favourably bound in preference to MO (MIP = 15%, NIP = -6%). For BZP, low non-specific binding was also observed by the NIP producing an imprinting factor for the system of 3.9. The amount of MO bound by the polymer in the BZP/MO competitive environment was less than when MO was bound in the non-competitive environment.

In the selectivity study performed with BZP and EPH, it was observed that the binding affinity of NC EGDMA1 was greater for EPH than BZP. The binding capacity observed for BZP, by this polymer, was similar in both the selectivity and cross-reactivity studies, which produced a similar imprinting value (4.1). However, a significant amount of EPH was bound by both the MIP (89%) and the NIP (45%), suggesting that the binding sites in the polymers are not BZP specific, which as discussed earlier, could be due to similarities in functionality, size and shape between BZP and EPH

A similar trend was observed for the NC EGDMA2 polymer (Figure 7.19), with CO enhancing the binding capacity of the MIP and NIP to BZP, with a BZP up-take of 100% and 66%, respectively. The imprinting factor for BZP in the presence of CO was 1.6, reduced from 2.2 when only BZP was present. The amount of CO bound by the polymer was minimal (< 12%), showing that the system has minimal affinity to CO.

For the BZP/MO binary system, the amount of BZP bound when MO was present was similar to the amount of BZP bound in the non-competitive environment. In contrast, the amount of MO bound was reduced to 13% and 1% in the competitive system for the MIP and NIP, respectively. This result shows that BZP has a higher affinity for the polymer.

The amount of EPH bound by the MIP and NIP in the BZP/EPH system was 88% and 70%. This was greater than the amount of BZP bound (MIP = 71%, NIP = 33%). The significant amount of non-specific binding observed by the NIP for ephedrine produced an imprinting factor of 1.2.

Figure 7.20 shows the results of the competitive studies performed of BZP/CO, BZP/MO and BZP/EPH with NC TRIM1. From the results, it can be seen that the amount of BZP bound in both the BZP/CO and BZP/MO systems was sim-

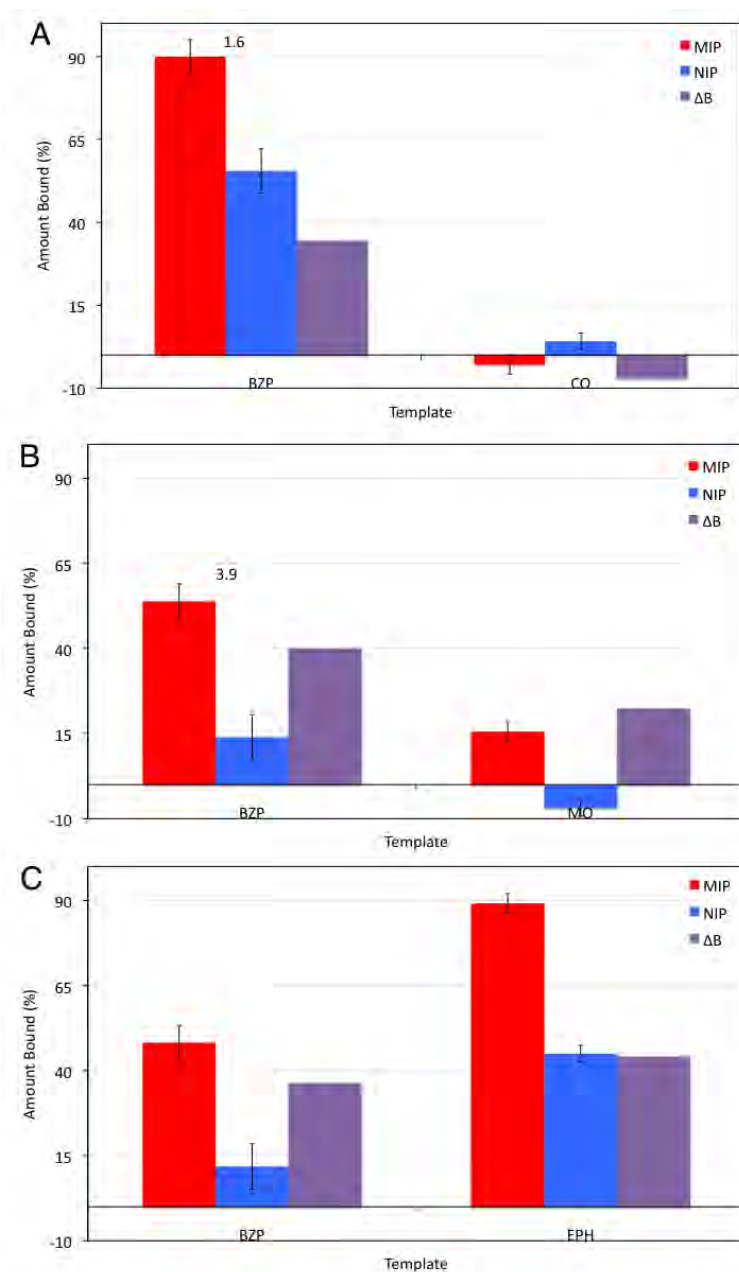


**Figure 7.18:** Selectivity studies of NC EGDMA1 with benzylpiperazine (BZP), and cocaine (CO) (A), BZP and morphine (MO) (B) and BZP and ephedrine (EPH) (C). 20 mg of polymer was used with 1 mL 0.8 mM analyte in  $\text{CHCl}_3$  solution for a binding contact time of 1 hr. All experiments were performed in triplicate. Amount bound =  $(([Total] - [Free]) / [Total]) \times 100$ .

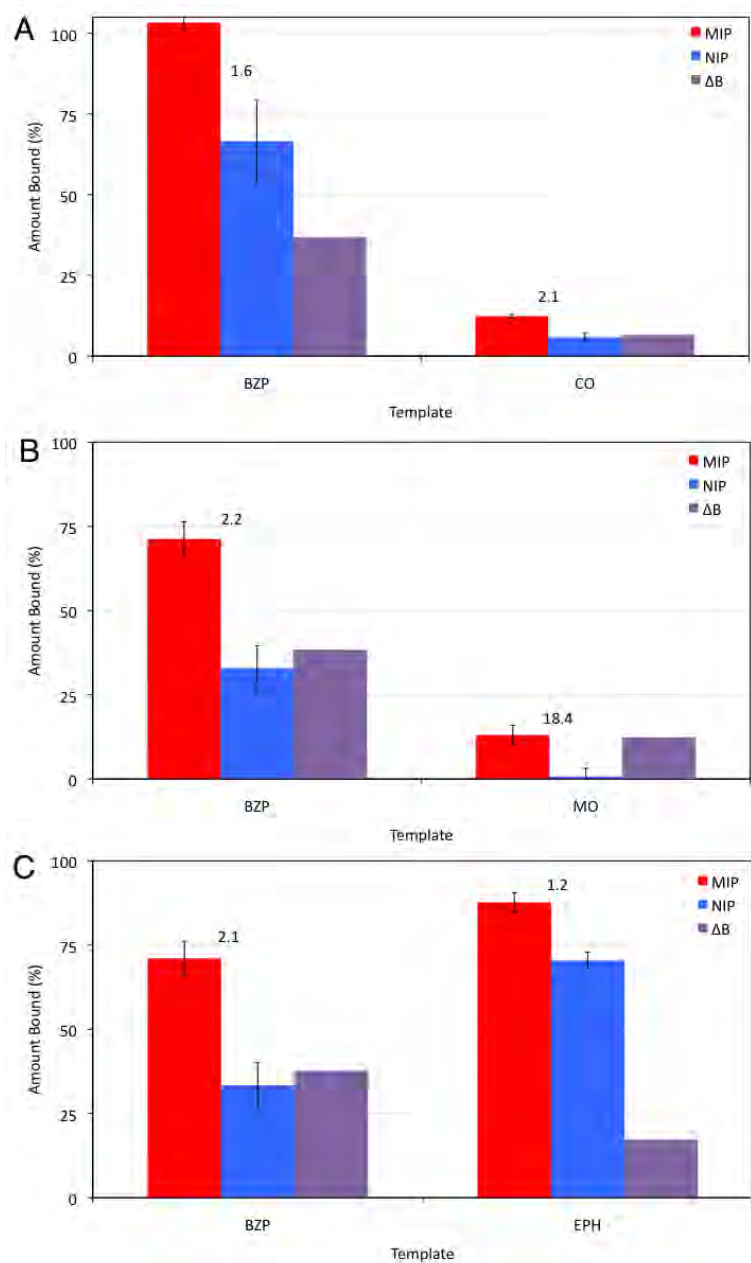


**Figure 7.19:** Selectivity studies of NC EGDMA2 with benzylpiperazine (BZP), and cocaine (CO) (A), BZP and morphine (MO) (B) and BZP and ephedrine (EPH) (C). 20 mg of polymer was used with 1 mL 0.8 mM analyte in  $\text{CHCl}_3$  solution for a binding contact time of 1 hr. All experiments were performed in triplicate. Amount bound =  $(\frac{[Total] - [Free]}{[Total]} \times 100)$ .

ilar for the MIP (48% and 53%) and slightly greater in the BZP/MO system for the NIP (23% and 38%). These values were also similar to the BZP affinity of the polymers when only BZP was present. The amount of up-take of CO and MO by both the MIP and NIP was < 8%. This suggests that only non-specific binding is occurring and that NC TRIM-T is not able to bind either analyte. Again, in the BZP/EPH system, a greater amount of binding was observed for EPH than BZP. In addition, the amount of BZP bound by the MIP in this system was reduced to 32%, suggesting a binding site preference for EPH over BZP.

Lastly, selectivity studies for NC TRIM2, given in Figure 7.21 showed that the binding capacity of the MIP for BZP in all three systems (BZP/CO, BZP/MO and BZP/EPH) was similar (60 - 68%). Non-specific binding of BZP, for the NIP, was similar when CO and EPH were present, with absorbances of 30 and 22%, however it was enhanced in the presence of MO (45%). As observed in the cross-reactivity studies, the amount of CO (6%) and MO (12%) absorbed was low, producing a selective system for either CO or MO. For the BZP/EPH system, this polymer was also not able to selectively bind BZP over EPH. The amount of EPH up-take in this system was greater than the BZP up-take, for both the MIP and NIP.

### 7.2.2.2 Covalent Polymers

For the covalent polymers examined, when rebinding was performed in the competitive binding system with MO, presented in Figure 7.22, the amount of BZP bound by the polymers was reduced. In a BZP pure system, the binding capacity of SC EGDMA and SC TRIM MIPs was approximately 25% and 50%, respectively, while the NIPs had negligible template up-take. When MO was incorporated, the amount of template bound by the MIPs decreased to 9% and 17%. The amount of template bound by the NIPs was not effected, staying negligible. The amount of MO bound in the competitive system by the MIPs was 4% and 10%. This was reduced from the amount of MO bound in the cross-reactivity studies with MO. The low amount of binding observed for MO was expected, as the polymers have shown to have a minimal binding capacity for this molecule. The reduced amount of binding observed by the MIPs for BZP

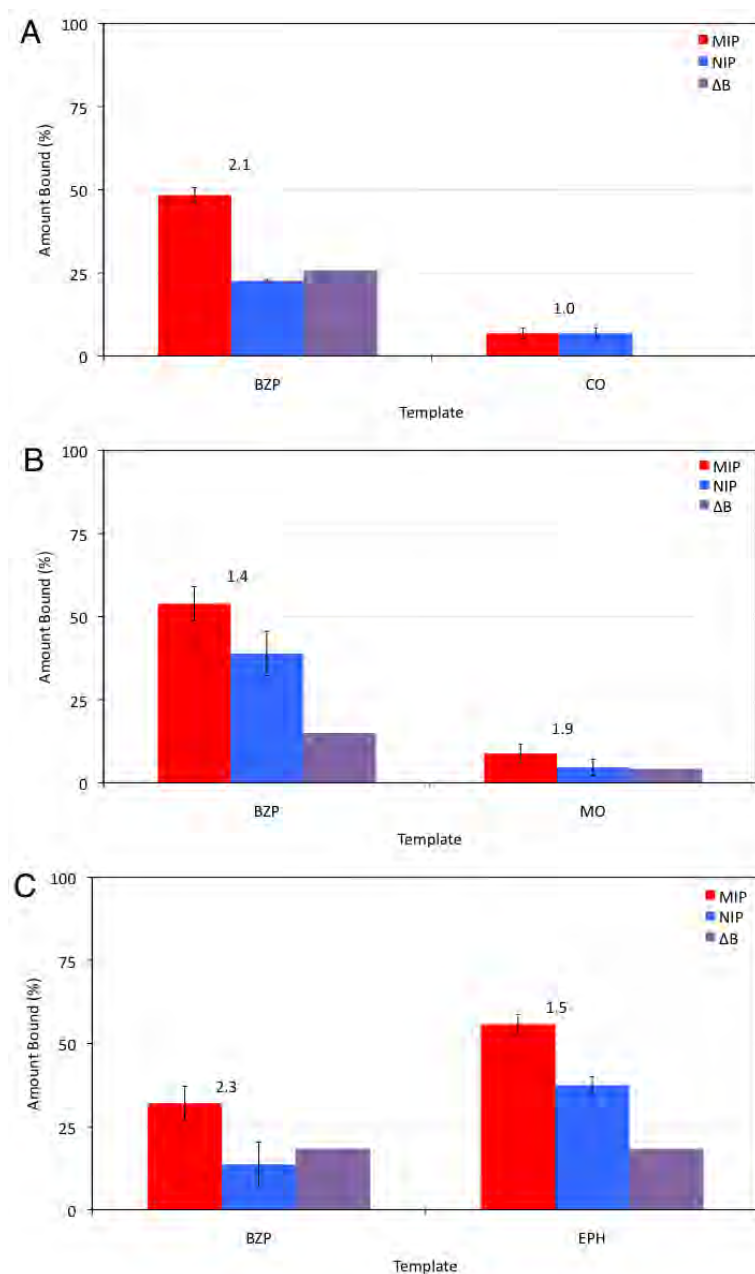


**Figure 7.20:** Selectivity studies of NC TRIM1 with benzylpiperazine (BZP), and cocaine (CO) (A), BZP and morphine (MO) (B) and BZP and ephedrine (EPH) (C). 20 mg of polymer was used with 1 mL 0.8 mM analyte in  $\text{CHCl}_3$  solution for a binding contact time of 1 hr. All experiments were performed in triplicate. Amount bound =  $\frac{([Total] - [Free])}{[Total]} \times 100$ .

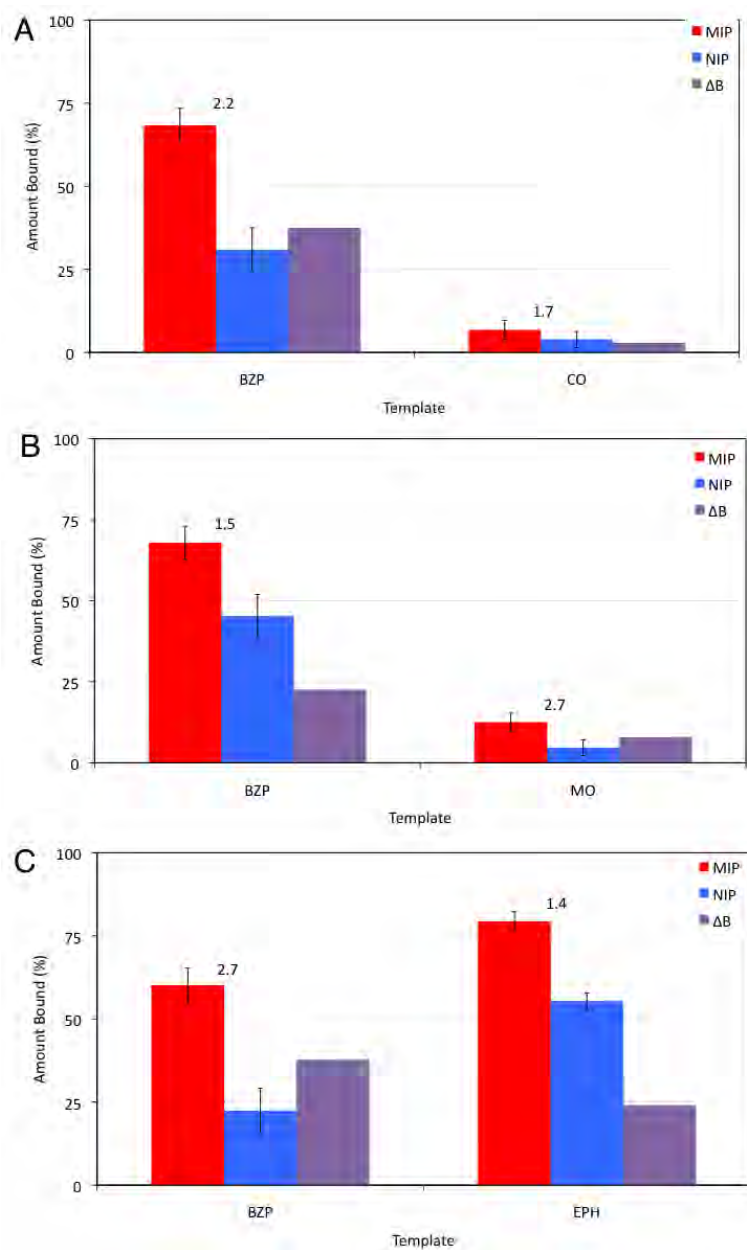


**Figure 7.21:** Selectivity studies of NC TRIM2 with benzyloperazine (BZP), and cocaine (CO) (A), BZP and morphine (MO) (B) and BZP and ephedrine (EPH) (C). 20 mg of polymer was used with 1 mL 0.8 mM analyte in  $\text{CHCl}_3$  solution for a binding contact time of 1 hr. All experiments were performed in triplicate. Amount bound =  $\left(\frac{[\text{Total}] - [\text{Free}]}{[\text{Total}]}\right) \times 100$ .

however, was unexpected. This observation could be the result of MO binding and blocking the binding cavities, inhibiting BZP sorption.

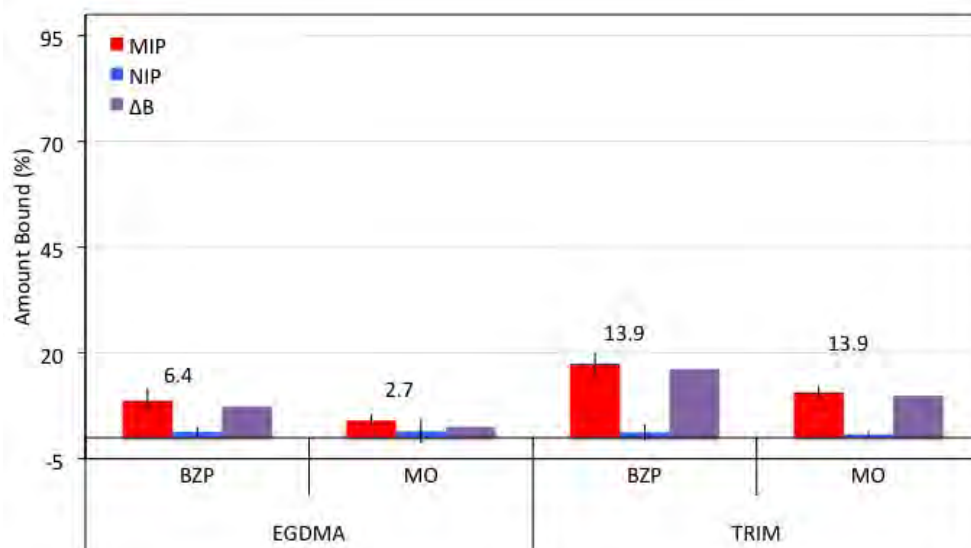


**Figure 7.22:** Competitive studies of BZP semi-covalent imprinted polymers with BZP and morphine. 30 mg of polymer was used with 1 mL 0.8 mM analyte ( $\text{CHCl}_3$ ) solution for a binding contact time of 1 hr. All experiments were performed in triplicate. Amount bound =  $(([\text{Total}] - [\text{Free}]) / [\text{Total}]) \times 100$ .

When competitive binding was performed with BZP and CO, good selectivity was observed by both polymers, favourably binding BZP in preference to CO. The results of this can be observed in Figure 7.23. For SC EGDMA, minimal analyte up-take was exhibited for CO, with bindings of approximately 1% for the MIP and NIP. For the BZP template, 27% and 16% template up-take was observed by the MIP and NIP, respectively. For this polymer, the presence of CO increased the amount of non-specific binding of the NIP. For SC-TRIM-1, the MIP absorbed approximately 37% of the BZP template and only 6% of CO. The NIP of this polymer had negligible up-take of both BZP and CO. This separation is ideal and shows that the covalent TRIM polymer is BZP specific in a BZP/CO system.

For the EPH/BZP competitive binding, the covalent polymers were unable to selectively bind BZP over EPH. This can be seen in Figure 7.24 as a greater amount of EPH absorption was observed in both SC EGDMA-1 and SC TRIM-1

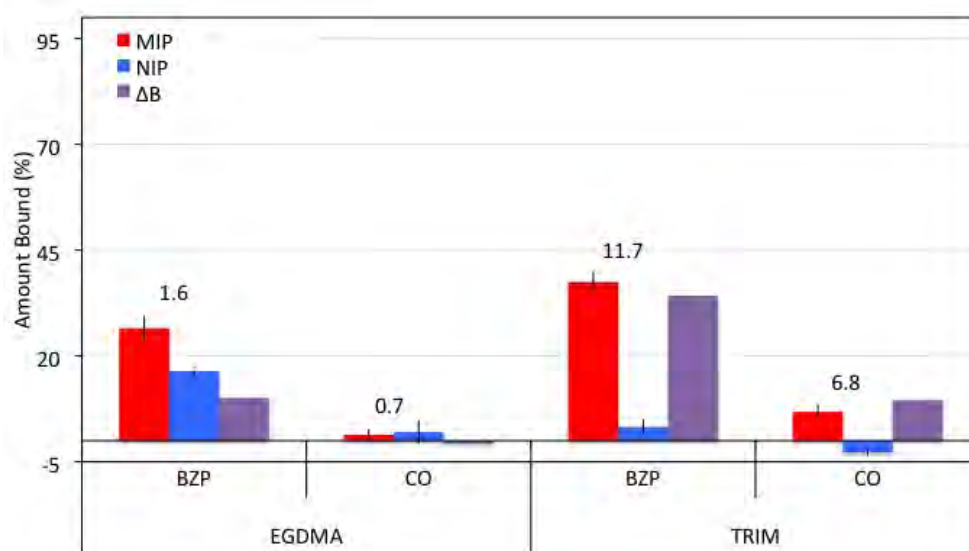


**Figure 7.23:** Competitive study of BZP semi-covalent imprinted polymers with BZP and cocaine. 30 mg of polymer was used with 1 mL 0.8 mM analyte ( $\text{CHCl}_3$ ) solution for a binding contact time of 1 hr. All experiments were performed in triplicate. Amount bound =  $(([\text{Total}] - [\text{Free}]) / [\text{Total}]) \times 100$ .

MIPs, compared to the amount of BZP bound. The binding capacity of the MIPs in the competitive binding environment for BZP less than what was observed for BZP alone. The NIPs of both polymers also exhibited an affinity for EPH, which was not observed for BZP, with approximately 13% and 4% analyte up-take for SC EGDMA-1 and SC TRIM-1 NIPs, respectively. For the BZP template, 1% or less was bound by the NIPs. The results from this experiment showed that the EPH template is capable of forming interactions with the two cross-linkers EGDMA and TRIM, resulting in non-specific binding in the polymers.

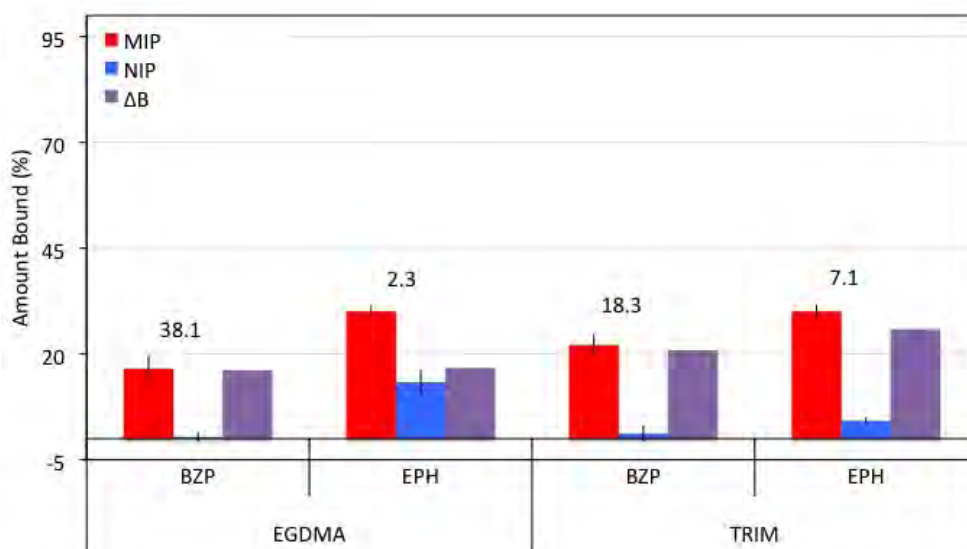


**Figure 7.24:** Competitive study of BZP semi-covalent imprinted polymers with BZP and ephedrine. 30 mg of polymer was used with 1 mL 0.8 mM analyte ( $\text{CHCl}_3$ ) solution for a binding contact time of 1 hr. All experiments were performed in triplicate. Amount bound =  $\frac{([Total] - [Free])}{[Total]} \times 100$

## 7.3 Conclusions

Cross-reactivity and binary competitive studies were conducted to ascertain the selectivity and specificity of the MIPs towards the BZP template in comparison to PHP, EPH, MO and CO.

In the cross-reactivity assay (non-competitive binding) performed with PHP, it was observed that the amount of template bound by both NC and SC MIPs was less than the BZP binding capacity. A greater PHP up-take was observed in the NC NIPs compared to that observed for BZP and for the SC NIPs a reduced amount of PHP up-take was observed. For CO, the amount of analyte bound by the NC polymers was < 10%, with MIP and NIP up-takes comparable. This suggests that sorption is the result of non-specific binding. The SC polymers had significant variance, with SC EGDMA MIP binding 17% and SC TRIM MIP binding 45%. The amount of MO sorbed by both NC and SC polymers was similar, with less than 20% up-take. Lastly, EPH had equivalent or greater up-take by all polymers, than what was observed for BZP.

Selectivity studies were performed in a binary competitive environment with

BZP and CO, BZP and MO and BZP and EPH. In the BZP/CO system, minimal CO up-take was observed for all polymers. In addition, the presence of CO increased the amount of BZP bound by the NC polymers. The amount of MO bound by both NC and SC polymers was reduced in the selectivity study, suggesting that selectivity toward BZP is occurring. However, the amount of BZP bound by the SC MIPs was reduced in the presence of MO, the result of which has been speculated to be the result of MO hindering BZP binding. Finally, no selectivity was observed between BZP and EPH, with EPH up-take greater than BZP.

In an effort to normalise and compare these results, the selective uptake of the competing analyte by the MIP with respect to BZP are expressed as selectivity factor (S) obtained from the ratio of the difference in analyte binding between the MIP and NIP ( $\Delta B_{Analyte}$ ) to the difference in BZP binding between the MIP and NIP ( $\Delta B_{BZP}$ ). The S values for cross-reactivity and competitive binding are presented in Table 7.1 and Table 7.2, respectively.

The non-competitive cross-reactivity assays for both the NC and SC polymers show lower reactivity towards CO and MO ( $S < 0.5$ ) but higher reactivity towards PHP and EPH ( $S > 0.5$ ) compared to the BZP template. The high S value (1.01) obtained for CO in SC TRIM 1 seems to be an anomaly and warrants further investigation.

The selectivity factors estimated for the competitive binding studies presented in Table 7.2 also show both NC and SC MIPs to be highly selective towards BZP in the presence of CO ( $S < 0.3$ ), moderately selective in the presence of MO ( $S \leq 0.6$ ) non-selective in the presence of EPH ( $S > 0.6$  to 1.0).

It is speculated that the results obtained in the two studies, cross-reactivity and selectivity, are the result of the size and functional group orientation of the analytes in respect to BZP. The analytes CO and MO are both large molecules that differ in potential and available functional groups that are capable of forming H-bonds in the BZP cavity. As a result, these two compounds had low affinity, resulting in low analyte up-take. In contrast, PHP and EPH are similar in size and nature to BZP and as a result, it was hypothesised that the MIPs would exhibit the high affinity toward these compounds. This was observed with PHP up-take slightly less than BZP while EPH had a greater sorption than BZP.

**Table 7.1:** Selectivity factors calculated from the  $\Delta B$  values for the cross-reactivity study with the NC and SC polymers

Polymer	Selectivity Factor (S)			
	PHP	MO	CO	EPH
NC EGDMA1	0.83	0.50	0	1.04
NC EGDMA2	0.77	0.26	0.20	0.51
NC TRIM1	0.57	0.29	0.02	0.69
NC TRIM2	0.67	0.15	0.04	0.48
SC EGDMA1	0.80	0.24	0.51	0.69
SC TRIM1	0.66	0.18	1.01	0.85

$$\text{Selectivity Factor} = \Delta B_{\text{analyte}} / \Delta B_{BZP}$$

$$S_{BZP} = 1.00$$

**Table 7.2:** Selectivity factors calculated from the  $\Delta B$  values for the selectivity study with the NC and SC polymers

Polymer	Selectivity Factor (S)		
	BZP/CO	BZP/MO	BZP/EPH
NC EGDMA1	$\sim 0$	0.56	1.21
NC EGDMA2	0.18	0.32	0.46
NC TRIM1	$\sim 0$	0.28	1.00
NC TRIM2	0.08	0.35	0.64
SC EGDMA1	$\sim 0$	0.35	1.04
SC TRIM1	0.28	0.61	1.24

$$\text{Selectivity Factor} = \Delta B_{\text{analyte}} / \Delta B_{BZP}$$

$$S_{BZP} = 1.00$$

### 7.3 Conclusions

---

From these experiments, it can be concluded that all polymers prepared were capable of selectively binding BZP in the presence of MO and CO. However, no selectivity was observed between BZP and EPH. Further investigation is required to optimise the system and obtain selectivity between these two compounds.

# 8

## Summary and Recommendations

### 8.1 Summary of Results

The work carried out in this study is the first for this class of designer drugs and has provided the ground work toward the development of a benzylpiperazine (BZP) specific Molecularly Imprinted Polymer (MIP) that is rapid, accurate and capable of BZP recognition in a complex matrix of drugs.

A combination of molecular modelling and NMR spectroscopy was applied at the start of the study and proved to be a useful tool in identifying functional monomers (FM) that could form non-covalent interactions with BZP. The molecular modelling allowed a library of ten different FMs to be screened with BZP, from which the three most favourable were selected for further analysis using NMR spectroscopy. Through the use of NMR experiments, the relative strength of the interaction between the template and functional monomer cluster (T:FM) was observed. It also enabled the optimum stoichiometry of each cluster to be determined.

With the completion of the theoretical and spectroscopic investigation, polymer synthesis was initiated. Three cross-linkers (EGDMA, TRIM and DVB) were screened with BZP to reduce the non-specific binding in the system. In this investigation, it was found that DVB had a certain amount of affinity for BZP whereas EGDMA and TRIM had little to no affinity. As a result, these two cross-linkers were used. Once this was established, MIPs were prepared with an

investigation into both the semi-covalent and non-covalent imprinting methods.

Examination of the non-covalent imprinted polymers showed that of the three FMs investigated (AA, MAA and IA) only the MAA prepared polymers, at 1:1 and 1:2 BZP:MAA ratios prepared in chloroform ( $\text{CHCl}_3$ ) with EGDMA or TRIM, exhibited considerable imprinting effect ( $I \geq 2$ ) for BZP. The highest imprinting factor (I) of 6.8 was observed when EGDMA was used as the cross-linker, for the BZP:MAA ratio of 1:1. For the TRIM prepared polymers, the largest I value was 3.3 using the 1:2 BZP:MAA ratio. The FM AA had minimal BZP sorption in all polymer combinations examined. In addition to this, the NIPs had a greater binding capacity for BZP than the MIPs resulting in I values of less than one in more than half the systems investigated. The polymers prepared with IA had a significant BZP up-take, absorbing more than 80% of the BZP solution. However, these polymers showed no selectivity, with the MIP and NIP binding equal amounts. This produced I values of approximately one. The selectivity of the polymers was found to be influenced by a number of factors including the solvent and the polymer mass. Two solvents were investigated as the rebinding solution, AN and  $\text{CHCl}_3$ . It was determined that polymer performance was enhanced when  $\text{CHCl}_3$  was used as the rebinding solvent.

The synthesis of the template-monomer adduct for the preparation of semi-covalent MIPs was a relatively straight-forward three step synthesis involving the reaction of thiophosgene with 4-vinylphenol after de-protection from acetoxystyrene. Once the chlorothioformate had been obtained, it was then reacted with BZP neat, to form the product, benzylpiperazine (4-vinylphenyl) carbamate. Two covalent polymers were prepared with this compound, utilising EGDMA or TRIM as the cross-linker. The use of the semi-covalent imprinting method improved template selectivity, with imprinting factors as high as 29, observed for the TRIM prepared polymer. For the EGDMA counterpart, an I value of 13 was observed.

Investigations into the optimum rebinding time showed that for all polymers, rapid BZP up-take occurred, with more than 80% of the amount bound at equilibrium sorbed prior to 10 minutes. This result showed that the binding kinetics of the polymers was rapid. For the non-covalent polymers, equilibrium was established at approximately 2 hours with the greatest selectivity observed after 1

hour. In contrast, the covalent polymers reached equilibrium at  $< 1$  hour, with rebinding for longer than 2 hours reducing the amount of template absorbed. Again, the greatest selectivity was observed after 1 hour, with imprinting values enhanced to 375 for the EGDMA prepared MIP and 1340 for the TRIM MIP.

Water was investigated as an alternative rebinding solvent to the organic solvents commonly used. A time binding study was performed using the covalent TRIM prepared polymer. This investigation demonstrated that template uptake could occur, however the binding capacity of the MIP was diminished. The selectivity of the system was also reduced ( $I = 5$ ) from that previously obtained when  $\text{CHCl}_3$  was utilised ( $I = 1340$ ).

Quantitative analysis of the binding isotherm, Scatchard and Langmuir plots showed the semi-covalent polymers to exhibit a stronger affinity to BZP and more homogeneous binding sites than the non-covalent polymers. For the non-covalent polymers MIPs to exhibit a stronger binding affinity toward BZP and had a greater number of binding sites than their corresponding NIPs. A stronger affinity was also observed for the 1:2 formulations than the 1:1 formulations however the ratio of the  $K_d$  NIP to  $K_d$  MIP was observed to be higher for the 1:1 ratios. For the semi-covalent polymers, SC TRIM exhibited stronger binding affinity for BZP while both polymers had comparable number of binding sites.

BZP selectivity was shown to occur for both the non-covalent and semi-covalent polymers. In cross-reactivity studies, a higher affinity was observed for BZP than CO and MO. In the competitive studies, only non-specific binding was observed for the CO and MO templates, while a high affinity was observed for BZP. In both the cross-reactivity and selectivity studies, selectivity between BZP and EPH was not observed in any of the polymers prepared.

The work performed here has provided the ground work for a BZP specific MIP. The choice of functional monomer, solvent and other rebinding conditions has shown to influence polymer sensitivity and selectivity toward BZP. The number of functional monomers, cross-linkers and porogens that are available provides an almost limitless number of permutations that could be investigated. Added to this, investigations into variations into the rebinding conditions, provides a whole new area for MIP optimisation. Through further investigations, the preparation of a BZP specific polymer that is rapid and accurate should be possible.

## 8.2 The Next Step

All the polymers prepared in this study were of the monolithic format, polymerised at 60°C. This type of polymer format requires grinding prior to use, the process of which destroys the binding cavities. For both the semi-covalent and non-covalent polymers, a number of different areas can be investigated to try and improve the imprinting effect and selectivity of the polymer. The temperature and porogen in which polymerisation is performed could be explored to optimise template affinity. It has been hypothesised that for non-covalent MIPs, lower temperatures produce stronger T:FM complexes, which when polymerised, form a larger number of specific binding sites and consequently, less non-specific sites. The porogen has also shown to influence the physical state, of pore structure and size, swellability, durability and morphology. Different porogens, of varying polarity and density, should be investigated. The polymer format employed could also be investigated including precipitate polymers or films. The preparation of BZP films would be beneficial as this would be the first step toward producing a sensing device.

In this study, the rebinding solvent showed to influence template sorption. Different aspects could be investigated, including polarity, aqueous-organic mixtures or the effect of organic modifiers such as acetic acid or surfactants to further optimise binding conditions and template affinity.

A system that is capable of performing in water would also be advantageous, as this would produce a greener and cheaper alternative for rebinding. In addition, it would diversify the applications as the end user distribution could extend to the general public as no formal safety training would be required with respect to hazardous waste. It would also enable the use in aircraft and other locations where hazardous and volatile chemicals are restricted. The semi-covalent polymers were shown to work in a full aqueous system however, this could be explored further by investigating the effect that pH and buffers has on template affinity.

The comparison of the methods used to calculate binding constants needs to be explored further to try and establish the most accurate and reliable for determination. A greater amount of data is required across the whole concentration range to establish and confirm the full nature of the binding characteristics of the

polymers.s

An attempt was made at obtaining the porosity and surface area for the MIPs, however this proved to be complicated due to the sorption and affinity of the polymer for helium. It would be beneficial to analyse all polymers prepared, to provide an insight into the observed trends in imprinting for both the non-covalent and semi-covalent polymers.

Finally, the final application of the polymers is to be incorporated into a detection device that is capable of performing in-field, accurately identifying the presence of BZP in a matrix solution. Within this work, possibilities were examined including fluorescence films however, none of these investigations were extensive and limited to T:M interactions studies. The incorporation of a working BZP polymer into a detection device would be an interesting project with an enormous scope to investigate.

# References

- [1] L. Anderson, R. Muller, G. Vlatakis and K. Mosbach, *Proceedings of the National Academy of Sciences*, 1995, **92**, 4788–4792.
- [2] E. Piletska, M. Romero-Guerra, I. Chianella, K. Karim, A. Turner and S. Piletsky, *Analytica Chimica Acta*, 2005, **542**, 111–117.
- [3] C. Holdsworth, M. Bowyer, C. Lennard and A. McCluskey, *Australian Journal of Chemistry*, 2005, **58**, 315–320.
- [4] S. Piletsky, K. Karim, E. Piletska, A. Turner, C. Day, K. Freebairn and C. Legge, *Analyst*, 2001, **126**, 1826–1830.
- [5] X. Dong, H. Sun, X. Lu, H. Wang, S. Liua and N. Wang, *Analyst*, 2002, **127**, 1427–32.
- [6] N. Greene and K. Shimizu, *Journal of the American Chemical Society*, 2005, **127**, 5695–5700.
- [7] O. Ramström, C. Yu and K. Mosbach, *Journal of Molecular Recognition*, 1996, **9**, 691–696.
- [8] C. Bye, A. D. Munro-Faure, A. W. Peck and P. A. Young, *European Journal of clinical Pharmacology*, 1973, **6**, 163–9.
- [9] H. Campbell, W. Cline, M. Evans, J. Lloyd and A. Peck, *European Journal of clinical Pharmacology*, 1973, **6**, 170–176.
- [10] H. Tsutsumi, M. Katagi, A. Miki, N. Shima, T. Kamata, M. Nishikawa, K. Nakajima and H. Tsuchihashi, *Journal of Chromatography B*, 2005, **819**, 315–22.

## REFERENCES

---

- [11] K. Tekes, L. Tóthfalusi, B. Malomvölgyi, F. Hermán and K. Magyar, *Polish Journal of Pharmacology and Pharmacy*, 1987, **39**, 203–11.
- [12] R. F. Staack, G. Fritschi and H. H. Maurer, *Journal of Chromatography B*, 2002, **773**, 35–46.
- [13] D. J. Pettibone and M. Williams, *Biochemical Pharmacology*, 1984, **33**, 1531–5.
- [14] D. N. Middlemiss and M. D. Tricklebank, *Neuroscience and Biobehavioral Reviews*, 1992, **16**, 75–82.
- [15] A. Johnstone, R. Lea, K. Brennan, S. Schenk, M. Kennedy and P. Fitzmaurice, *Journal of Psychopharmacology*, 2007, **21**, 888.
- [16] P. Gee, S. Richardson, W. Woltersdorf and G. Moore, *The New Zealand Medical Journal*, 2005, **118**, U1784.
- [17] J. L. Herndon, M. E. Pierson and R. A. Glennon, *Pharmacological Biochemical Behaviour*, 1992, **43**, 739–48.
- [18] M. D. Schechter, *Pharmacological Biochemical Behaviour*, 1988, **31**, 817–24.
- [19] M. Wikström, P. Holmgren and J. Ahlner, *Journal of Analytical Toxicology*, 2004, **28**, 67–70.
- [20] NDPSC, 2006, 1–188.
- [21] EACD, *National Drug Policy Ref No:20045663*, 2004, **April**, 1–10.
- [22] R. F. Staack, *Lancet*, 2007, **369**, 1411–3.
- [23] F. Dickey, *Proceedings of the National Academy of Sciences*, 1949, **35**, 227–229.
- [24] T. Takagishi and I. Klotz, *Biopolymers*, 1972, **11**, 483–491.
- [25] G. Wulff and A. Sarhan, *Angewandte Chemie (International Edition in English)*, 1972, **11**, 341–344.
- [26] O. Norrlow, M. Glad and K. Mosbach, *Journal of Chromatography*, 1984, **299**, 29–41.

## REFERENCES

---

- [27] A. Graham, C. Carlson and P. Edmiston, *Analytical Chemistry*, 2002, **74**, 458–467.
- [28] F. Li, J. Li and S. Zhang, *Talanta*, 2008, **74**, 1247–55.
- [29] K. Nilsson, J. Lindell, O. Norrlöw and B. Sellergren, *Journal of Chromatography. A*, 1994, **680**, 57–61.
- [30] G. Wulff, B.-O. Chong and U. Kolb, *Angewandte Chemie International Edition.*, 2006, **45**, 2955–2958.
- [31] N. Perez, M. J. Whitcombe and E. Vulfson, *Journal of Applied Polymer Science*, 2000, **77**, 1851–1859.
- [32] N. Perez, M. J. Whitcombe and E. Vulfson, *Macromolecules*, 2001, **34**, 830–836.
- [33] K. Yoshimatsu, K. Reimhult, A. Krozer, K. Mosbach, K. Sode and L. Ye, *Analytica Chimica Acta*, 2007, **584**, 112–121.
- [34] L. Ye, R. Weiss and K. Mosbach, *Macromolecules*, 2000, **33**, 8239–8245.
- [35] A. Biffis, N. Graham, G. Siedlaczek, S. Stalberg and G. Wulff, *Macromolecular Chemistry and Physics*, 2001, **202**, 163–171.
- [36] P. Curcio, C. Zandanel and A. Wagner, *Macromolecular Bioscience*, 2009, **9**, 596–604.
- [37] D. J. Duffy, K. Das, S. L. Hsu, J. Penelle, V. M. Rotello and H. D. Stidham, *Journal of the American Chemical Society*, 2002, **124**, 8290–8296.
- [38] J. Mathew-Krotz and K. J. Shea, *Journal of the American Chemical Society*, 1996, **118**, 8154–8155.
- [39] M. Quaglia, E. D. Lorenzi, C. Sulitzky, G. Caccialanza and B. Sellergren, *Electrophoresis*, 2003, **24**, 952–957.
- [40] A. Mayes and M. Whitcombe, *Advanced Drug Delivery Reviews*, 2005, **57**, 1742–1778.
- [41] M. Komiyama, T. Takeuchi, T. Mukawa and H. Asanuma, *Molecular Imprinting: From Fundamentals to Applications*, Wiley-VCH, 2003.

## REFERENCES

---

- [42] G. Wulff, W. Vesper, R. Grobe-Einsler and A. Sarhan, *Die Makromolekulare Chemie*, 1977, **178**, 2799–2816.
- [43] G. Wulff and S. Schauhoff, *The Journal of Organic Chemistry*, 1991, **56**, 395–400.
- [44] A. Kugimiya, J. Matsui, H. Abe, M. Aburatani and T. Takeuchi, *Analytica Chimica Acta*, 1998, **365**, 75–79.
- [45] K. Shea and T. Dougherty, *Journal of the American Chemical Society*, 1986, **108**, 1091–1093.
- [46] K. Shea and D. Sasaki, *Journal of the American Chemical Society*, 1989, **111**, 3442–3444.
- [47] K. Shea and D. Sasaki, *Journal of the American Chemical Society*, 1991, **113**, 4109–4120.
- [48] G. Wulff, W. Best and A. Akelah, *Reactive Polymers, Ions Exchangers, Sorbents*, 1984, **2**, 167–174.
- [49] M. Whitcombe, M. Rodriguez, P. Villar and E. Vulfson, *Journal of the American Chemical Society*, 1995, **117**, 7105–7111.
- [50] M. Lubke, M. Whitcombe and E. Vulfson, *Journal of the American Chemical Society*, 1998, **120**, 13342–13348.
- [51] M. A. Khasawneh, P. T. Vallano and V. T. Remcho, *Journal of Chromatography A*, 2001, **922**, 87–97.
- [52] A. Katz and M. Davis, *Nature*, 2000, **403**, 286–289.
- [53] C. Ki, C. Oh, S.-G. Oh and J. Chang, *Journal of the American Chemical Society*, 2002, **124**, 14838–14839.
- [54] M. Petcu, J. Cooney, C. Cook, D. Lauren, P. Schaare and P. Holland, *Analytica Chimica Acta*, 2001, **435**, 49–55.
- [55] V. P. Joshi, M. G. Kulkarni and R. A. Mashelkar, *Journal of Chromatography A*, 1999, **849**, 319 – 330.

## REFERENCES

---

- [56] J. U. Klein, M. J. Whitcombe, F. Mulholland and E. N. Vulfson, *Angewandte Chemie International Edition*, 1999, **38**, 2057–2060.
- [57] N. Kirsch, C. Alexander, M. Lübke, M. Whitcombe and E. Vulfson, *Polymer*, 2000, **41**, 5583–5590.
- [58] N. Kirsch, C. Alexander, S. Davies and M. Whitcombe, *Analytica Chimica Acta*, 2004, **504**, 63–71.
- [59] D. Spivak, *Advanced Drug Delivery Reviews*, 2005, **57**, 1779–1794.
- [60] T. Takeuchi, D. Fukuma and J. Matsui, *Analytical Chemistry*, 1999, **71**, 285–290.
- [61] F. Lanza and B. Sellergren, *Analytical Chemistry*, 1999, **71**, 2092–2096.
- [62] F. Lanza, A. J. Hall, B. Sellergren, A. Bereczki, G. Horvai, S. Bayoudh, P. A. G. Cormack and D. C. Sherrington, *Analytica Chimica Acta*, 2001, **435**, 91 – 106.
- [63] B. Sellergren, M. Lepistoe and K. Mosbach, *Journal of the American Chemical Society*, 1988, **110**, 5853–5860.
- [64] M. Whitcombe, L. Martin and E. Vulfson, *Chromatographia*, 1998, **47**, 457–464.
- [65] J. Svenson, J. G. Karlsson and I. A. Nicholls, *Journal of Chromatography A*, 2004, **1024**, 39–44.
- [66] J. Svenson, N. Zheng and I. A. Nicholls, *Journal of the American Chemical Society*, 2004, **126**, 8554–60.
- [67] J. G. Karlsson, B. Karlsson, L. I. Andersson and I. A. Nicholls, *Analyst*, 2004, **129**, 456–62.
- [68] B. Castro, M. Whitcombe, E. Vulfson, R. Vazquez-Duhalt and E. Bárzana, *Analytica Chimica Acta*, 2001, **435**, 83–90.
- [69] C. Lubke, M. Lubke, M. Whitcombe and E. Vulfson, *Macromolecules*, 2000, **33**, 5098–5105.
- [70] I. Idziak, A. Benrebouh and F. Deschamps, *Analytica Chimica Acta*, 2001, **435**, 137–140.
- [71] B. Brune, J. Koehler, P. Smith and G. Payne, *Langmuir*, 1999, **15**, 3987–3992.

## REFERENCES

---

- [72] H. S. Andersson and I. A. Nicholls, *Bioorganic Chemistry*, 1997, **25**, 203 – 211.
- [73] J. Svenson, H. S. Andersson, S. A. Piletsky and I. A. Nicholls, *Journal of Molecular Recognition*, 1998, **11**, 83–86.
- [74] S. Striegler and E. Tewes, *European Journal of Inorganic Chemistry*, 2002, **2002**, 487–495.
- [75] S. Subrahmanyam, S. Piletsky, E. Piletska, B. Chen, K. Karim and A. Turner, *Biosensors and Bioelectronics*, 2001, **16**, 631–637.
- [76] N. Turner, E. Piletska, K. Karim, M. Whitcombe, M. Malecha, N. Magan, C. Baggiani and S. Piletsky, *Biosensors and Bioelectronics*, 2004, **20**, 1060–1067.
- [77] K. Karim, F. Breton, R. Rouillon, E. V. Piletska, A. Guerreiro, I. Chianella and S. A. Piletsky, *Advanced Drug Delivery Reviews*, 2005, **57**, 1795 – 1808.
- [78] I. Nicholls, H. Andersson, C. Charlton, H. Henschel, B. Karlsson, J. Karlsson, J. O'mahony, A. Rosengren, K. Rosengren and S. Wikman, *Biosensors and Bioelectronics*, 2009, **25**, 543–552.
- [79] G. Wulff, J. Vietmeier and H. Poll, *Die Makromolekulare Chemie*, 1987, **188**, 731–740.
- [80] M. Sibrian-Vazquez and D. A. Spivak, *Journal of the American Chemical Society*, 2004, **126**, 7827–33.
- [81] H. Lin, J. Rick and T. Chou, *Biosensors and Bioelectronics*, 2007, **22**, 3293–3301.
- [82] M. Glad, P. Reinholdsson and K. Mosbach, *Reactive Polymers*, 1995, **25**, 47.54.
- [83] M. Kempe, *Analytical Chemistry*, 1996, **68**, 1948–53.
- [84] M. Sibrian-Vazquez and D. Spivak, *Macromolecules*, 2003, **36**, 5105–5113.
- [85] G. Wulff, R. Kemmerer, J. Vietmeier and H. Poll, *Nouveau Journal de Chimie*, 1982, **6**, 681.
- [86] B. Sellergren, *Die Makromolekulare Chemie*, 1989, **190**, 2703–2711.
- [87] B. Sellergren and K. Shea, *Journal of Chromatography*, 1993, **635**, 31–49.

## REFERENCES

---

- [88] W. Dong, M. Yan, Z. Liu, G. Wu and Y. Li, *Separation and Purification Technology*, 2007, **53**, 183–188.
- [89] M. Kempe and K. Mosbach, *Analytical Letters*, 1991, **24**, 1137 – 1145.
- [90] D. Spivak, M. A. Gilmore and K. J. Shea, *Journal of the American Chemical Society*, 1997, **119**, 4388–4393.
- [91] D. J. O’Shannessy, B. Ekberg and K. Mosbach, *Analytical Biochemistry*, 1989, **177**, 144–9.
- [92] R. J. Umpleby, M. Bode and K. D. Shimizu, *Analyst*, 2000, **125**, 1261–1265.
- [93] R. Umpleby, S. Baxter, Y. Chen, R. Shah and K. Shimizu, *Analytical Chemistry*, 2001, **73**, 4584–4591.
- [94] H. Pan, W. Lee, C. Hung and C. Hwang, *E-Journal of Chemistry*, 2007, **4**, 611–619.
- [95] B. Sellergren, *Journal of Chromatography. A*, 1994, **673**, 133–141.
- [96] O. Bruggemann, R. Freitag, M. Whitcombe and E. Vulfson, *Journal of Chromatography A*, 1997, **781**, 43–53.
- [97] J. Matsui, T. Kato, T. Takeuchi, M. Suzuki, K. Yokoyama, E. Tamiya and I. Karube, *Analytical Chemistry*, 1993, **65**, 2223–2224.
- [98] X. Huang, H. Zou, X. Chen, Q. Luo and L. Kong, *Journal of Chromatography A*, 2003, **984**, 273–282.
- [99] B. Sellergren, *Trends in Analytical Chemistry*, 1999, **16**, 164–174.
- [100] A. Zander, P. Findlay, T. Renner, B. Sellergren and A. Swietlow, *Analytical Chemistry*, 1998, **70**, 3304–3314.
- [101] T. Hjertberg, T. Hargitai and P. Reinholdsson, *Macromolecules*, 1990, **23**, 3080–3087.
- [102] J. Patel, K. Patel and R. Patel, *Colloid & Polymer Science*, 2009, **287**, 89–95.
- [103] B. Corson, W. Heintzelman, L. Schwartzman, H. Tiefenthal, R. Lokken, J. Nickels, G. Atwood and F. Pavlik, *Journal of Organic Chemistry*, 1958, **23**, 544–549.

## REFERENCES

---

- [104] H. Oh, J. Ha, D. Sung and I. Lee, *Journal of Organic Chemistry*, 2004, **69**, 8219–8223.
- [105] F. Breton, R. Rouillon, E. V. Piletska, K. Karim, A. Guerreiro, I. Chianella and S. A. Piletsky, *Biosensors and Bioelectronics*, 2007, **22**, 1948 – 1954.
- [106] D. Pavel, J. Lagowski and C. J. Lepage, *Polymer*, 2006, **47**, 8389 – 8399.
- [107] D. H. Williams, J. P. L. Cox, A. J. Doig, M. Gardner, U. Gerhard, P. T. Kaye, A. R. Lal, I. A. Nicholls, C. J. Salter and R. C. Mitchell, *Journal of the American Chemical Society*, 1991, **113**, 7020–7030.
- [108] I. Nicholls, K. Adbo, H. Andersson, P. Andersson, J. Ankarloo, J. Hedin-Dahlström, P. Jokela, J. Karlsson, L. Olofsson and J. Rosengren, *Analytica Chimica Acta*, 2001, **435**, 9–18.
- [109] L. Wu, K. Zhu, M. Zhao and Y. Li, *Analytica Chimica Acta*, 2005, **549**, 39–44.
- [110] L. Wu and Y. Li, *Journal of Molecular Recognition*, 2004, **17**, 567–574.
- [111] V. Gil and N. Oliveira, *Journal of Chemical Education*, 1990, **67**, 473.
- [112] L. Schwarz, C. Holdsworth, A. McCluskey and M. Bowyer, *Australian Journal of Chemistry*, 2004, **57**, 759–764.
- [113] I. Langmuir, *Journal of the American Chemical Society*, 1916, **38**, 2221–2295.
- [114] N. Kirsch, C. Alexander, S. Davies and M. Whitcombe, *Analytica Chimica Acta*, 2004, **504**, 63–71.
- [115] R. Salvatore, F. Chu, A. Nagle, E. Kapxhiu, R. Cross and K. Jung, *Tetrahedron*, 2002, **58**, 3329–3347.
- [116] P. Villar, M. Whitcombe and E. Vulfson, *Polymer*, 2007, **48**, 1483–1489.
- [117] R. Rajkumar, A. Warsinke, H. Mohwald, F. Scheller and M. Katterle, *Biosensors and Bioelectronics*, 2007, **22**, 3318–3325.